STORE-OPERATED CALCIUM ENTRY IN HUMAN SPERMATOZOA

By

KATHERINE LOUISE NASH

A thesis submitted to

The University of Birmingham

for the degree of

DOCTOR OF PHILOSOPHY

School of Biosciences

College of Life and Environmental Sciences

The University of Birmingham

September 2011

ABSTRACT

The contribution of store-operated calcium entry (SOCE) in the response of human sperm to progesterone, a steroid secreted from the cumulus cells surrounding the oocyte, has not yet been elucidated. The aim of this study was to investigate the presence of SOCE proteins in human sperm and examine the effects of pharmacological modulation of SOCE on the progesterone-induced biphasic intracellular calcium concentration ($[Ca^{2+}]_i$) response. STIM (stromal interacting molecule) and Orai, proteins of the SOCE system were detected in human sperm in a similar location to intracellular Ca^{2+} stores. 2-aminoethyldiphenyl borate (2-APB; SOCE modulator) altered SOCE in human sperm in a bimodal manner as seen in other cell types. Furthermore, 5μM 2-APB potentiated the initial progesterone-induced $[Ca^{2+}]_i$ transient within the neck and midpiece, but not in the flagellum. In the sustained phase of the progesterone-induced $[Ca^{2+}]_i$ response both 5μM 2-APB and 10μM loperamide (another modulator of SOCE) potentiated the $[Ca^{2+}]_i$ response. Higher doses of 2-APB (50-200μM) didn't potentiate the transient $[Ca^{2+}]_i$ and inhibited the sustained response consistent with reported actions on SOCE. Ryanodine receptors were localised to the neck/midpiece region which suggested that they may mobilise intracellular Ca^{2+} stores in response to progesterone, leading to activation of STIM/Orai and initiating SOCE.

ACKNOWLEDGEMENTS

First and foremost I would like to thank my supervisors Steve Publicover and Linda Lefievre for their continued encouragement, support and kindness throughout my PhD studies. Steve I would particularly like to thank you for your patience, understanding and expert advice during my project. Linda I am very proud to say that I feel I have gained a life-long friend in you and I thank you for everything you have done for me.

Secondly, I would like to thank all members of the Publicover research group including Jen Morris, Aduen Morales-Garcia, Sarah Costello, Ruben Peralta and Joao Correria for all the help, advice and laughs along the way. Oh and for listening to me talk about cats, my love of them and constant pursuits to ensure everybody I know has one.

Thirdly, I wish to thank everybody on the 8th floor Biosciences especially Elizabeth Haining, for sharing some hilarious moments and generally helping to keep me sane. I would also like to mention the research staff at the Assisted Conception Unit, Birmingham Women's Hospital and at Birmingham Medical School particularly Jackson Kirkman-Brown, Sarah Conner, Rebecca Frettsome and Thomas Connelly for your intellectual contributions and friendship during my PhD.

I could never have achieved all that I have without the unconditional love and support from my partner Elliot, my mum and my brother William. You have all been great and I love you more than anything in this world.

Last but definitely not least to my three cats Darwin, Sydney and Tazzy for accompanying me during my write-up. Whether that be by cuddling up beside me, chasing my pen as I'm trying

to write or bringing me mouse/frog/bird presents at regular intervals. You were (nearly) always a welcome distraction.

TABLE OF CONTENTS

CHAPTER ONE: INTRODUCTION

LIST OF FIGURES

LIST OF ABBREVIATIONS

AEBSF - 4-(2-aminoethyl)benzenesulfonylfluoride

2-APB - 2-aminoethyldiphenyl borate

AKAP – A-kinase anchor protein

4-AP - 4-aminopyridine

AR – Acrosome reaction

ARC - Arachidonic acid activated channels

ATP - Adenosine triphosphate

Bis-phenol - Bis(2-hydroxy-3-tert-butyl-5-methyl-phenyl) methane

BR – Brain reticulum

BSA – Bovine serum albumin

Ca^{2+} - Calcium ions

$[Ca^{2+}]_i$ – Intracellular calcium concentration

$[Ca^{2+}]_o$ – Extracellular calcium concentration

CAD - CRAC activation domain

cADPR – Cyclic adenosine diphosphate-ribose

cAMP – Cyclic adenosine monophosphate

CASA – Computer assisted sperm analysis

CCE - Capacitative Ca^{2+} entry

CD - Cluster of differentiation

cGMP – Cyclic guanosine monophosphate

CICR – Calcium-induced calcium release

CIF - Calcium influx factor

CNG – Cyclic nucleotide gated

COREC – Centre of Research Ethical Campaign

CRAC – Calcium-release activated calcium

iCRAC – Calcium-release activated calcium current

DNA – Deoxyribonucleic acid

EBSS – Earle's balanced salt solution

EGTA - Ethylene glycol-bis-(2-aminoethyl)-N,N,N', N'-tetraacetic acid

ER – Endoplasmic reticulum

FRET - Forster resonance energy transfer

FRT – Female reproductive tract

FSH - Follicle stimulating hormone

GFP – Green fluorescent protein

GnRH - Gonadotropin releasing hormone

GTP – Guanosine triphosphate

H^+ - Hydrogen ions

HEK-293T – Human embryonic kidney 293 cells expressing the T-antigen of simian virus 40

HEPES - 4-(2-hydroxyethyl)-1-piperazineethanesulfonic acid

HFEA – Human Fertilisation and Embryology Authority

HCO_3^- - Bicarbonate ions

HMW – High molecular weight

Hz – Hertz

I_{CRAC} - Ca^{2+} release activated Ca^{2+} current

IP - Immunoprecipitation

IP_3 - Inositol 1,4,5-trisphosphate

IP_3R - Inositol 1,4,5-trisphosphate receptor

K^+ - Potassium ions

kDa - Kilodalton

LH - Luteinizing hormone

M – Molar

μM - Micromolar

mM – Millimolar

mRNA – Messenger ribonucleic acid

Myc - Myelocytomatosis

nM - Nanomolar

Na^+ - Sodium ions

NC - Nitrocellulose

NCX - Na^+-Ca^{2+} exchanger

NFS – Non-fused sperm

OGB – Oregon green BAPTA-1/AM

PBS – Phosphate buffered saline

PDE – Phosphodiesterase

PFS – Prostasome fused sperm

PHN – Posterior head and neck

Pi – Protease inhibitors

PIP_2 - Phosphatidylinositol- 1,4-bisphosphate

PKA – Protein kinase A

PLC - Phospholipase C

PM – Plasma membrane

PMCA – Plasma membrane Ca^{2+}-ATPase

pS - Picosiemens

PSA – Prostate specific antigen

RNA – Ribonucleic acid

RNE – Redundant nuclear envelope

RT-PCR – Reverse transcription polymerase chain reaction

RyR - Ryanodine receptors

sAC – Soluble adenylyl cyclase

SAM - Sterile-alpha motif

SDS-PAGE- Sodium dodecyl sulphate polyacrylamide gel electrophoresis

SERCA – Sarcoplasmic-endoplasmic Ca^{2+}-ATPase

siRNA – Small interfering ribonucleic acid

SOAR - STIM1 Orai activating region

SOC – Store operated calcium

SOCE - Store operated calcium entry

SPCA - Secretory pathway Ca^{2+}-ATPase

SR – Sarcoplasmic reticulum

STIM – Stromal interacting molecule

TIRF - Total internal reflectance fluorescence

tmACs – Transmembrane adenylyl cyclases

TMB-8 - 8-(NN-diethylamino)octyl-3,4,5-trimethoxybenzoate

TPBS - Triton X-100 phosphate buffered saline

TRPC - Canonical transient receptor potential

TTBS - Tris buffered saline supplemented with 0.1% tween-20

TX-100 – Triton X 100

V - Volts

VOCC – Voltage operated calcium channel

ZP – Zona pellucida

CHAPTER ONE: INTRODUCTION

CHAPTER ONE

INTRODUCTION

1.1 The testis

Spermatozoa are produced in a highly organised and regulated manner within the seminiferous tubules of the testis, the male reproductive organ. The seminiferous tubules provide a favourable, finely regulated environment for the growing cells, only permitting the selective uptake of paracrine factors and preventing immune cell infiltration (Sutovsky and Mandahar, 2006). In addition to sperml production, the testis also produces the necessary hormones for the maintenance of reproductive function, most importantly androgens. Androgens such as testosterone are produced in Leydig cells, which form part of the interstitial tissue situated between the seminiferous tubules along with nerves, blood vessels, white blood cells and lymph vessels (Barratt, 1995).

1.1.1 Architecture of the seminiferous tubules

Extending from the periphery to the lumen of the seminiferous tubule, Sertoli cells are chiefly responsible for maintaining an ideal environment for germ cell differentiation. They are structurally organised into basal and adluminal compartments. The compartments are physiologically separated by cellular barriers, such as tight junctions, that form between the cytoplasmic projections of neighbouring Sertoli cells, developing during puberty to form the

blood-testis barrier (Glover *et al*., 1990). This barrier is vital as at puberty sperm begin to express antigens with the potential to induce an autoimmune response (Barrat, 1995). The basal compartment rests on the boundary tissue in close association with the blood circulation to permit the influx of vital nutrients (Barratt, 1995; Shalet, 2009). Spermatogonia (sperm cell progenitors), are found in this area. As spermatogonia proliferate and differentiate they migrate upwards between Sertoli cells, temporarily disrupting the intercellular junctions. This multiplication and differentiation process, termed spermatogenesis (discussed below), consists of three key stages including mitotic replication to form spermatogonia, meiotic division leading to haploid spermatocyte production and finally a second meiotic division to generate round spermatids. As they leave the compartment, they become embedded in the Sertoli cell before being released into the lumen as spermatozoa (Figure 1.1). The developmental changes from spermatogonia to spermatozoa are completed in 64 days and take place continuously throughout the adult life of the male (Barratt, 1995; Shalet, 2009). This cellular differentiation and proliferation process begins with a small finite number of spermatogonia and leads to a copious number of spermatozoa, >200 million in human and up to 2-3 billion in bull per ejaculate (Sutovsky and Manandhar, 2006).

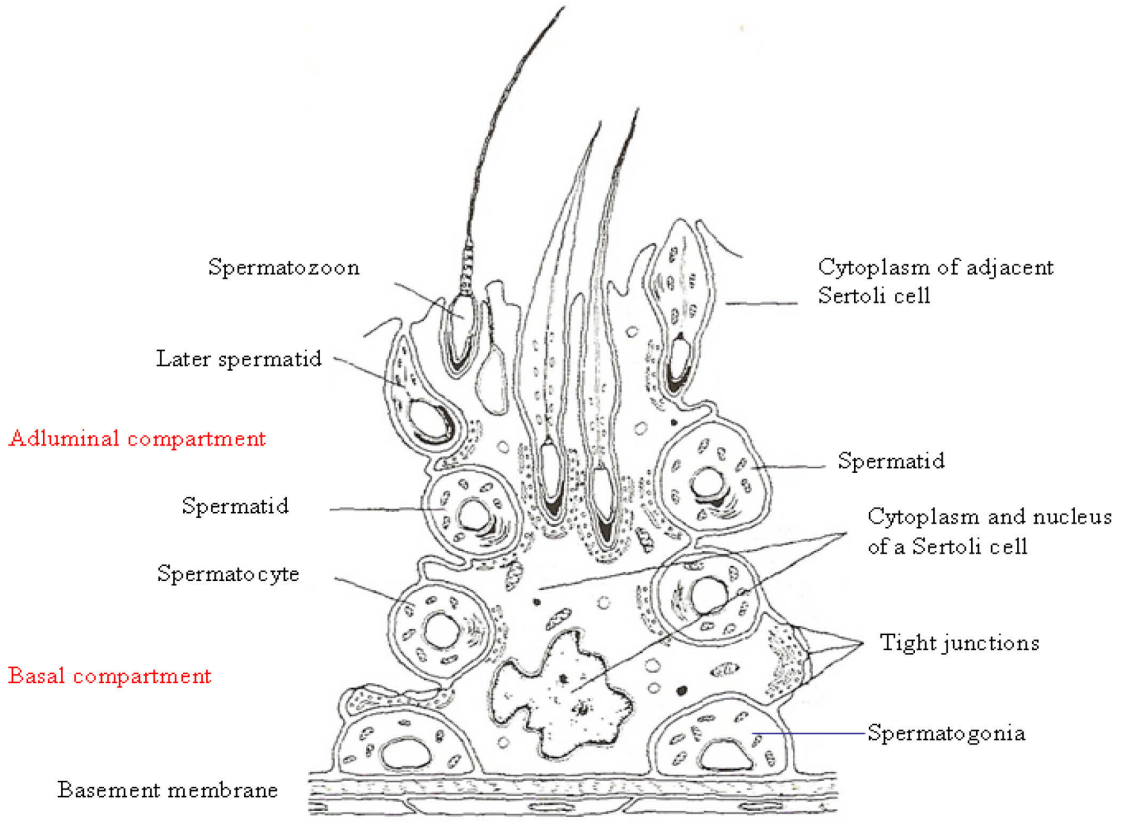

Figure 1.1 Diagram of cross-sectional area of a Sertoli cell displaying the various stages of spermatogenesis. The basal compartment contains spermatogonia which enter spermatogenesis and migrate upwards towards the Sertoli cell lumen, differentiating into haploid spermatocytes, elongating spermatids and finally spermatozoons. Throughout this process, the Sertoili cell acts as a 'nurse' cell, providing a finely regulated environment for optimal sperm production (image adapted from Glover *et al.*, 1990).

1.1.2 Spermatogenesis

Primordial germ cells are incorporated into the region eventually forming the basal compartment of the seminiferous tubules from week four of gestation as they migrate from the endoderm of the yolk sac into the undifferentiated gonad (Shalet, 2009). At birth, these diploid cells become type A spermatogonia, marking the beginning of spermatogenesis, which is arrested at this point until the peri-pubertal period (Sutovsky and Manandhar, 2006).

Type A spermatogonia have the ability to self replicate and following puberty can differentiate into type B spermatogonia at 42 hour intervals (Johnson and Everitt, 1996). Cytoplasmic bridges, forming a syncytium, connect the daughter cells which persist throughout spermatogenesis to generate synchronous development and allow the sharing of mRNA and proteins regardless of genotype (Barratt, 1995; Johnson and Everitt, 1996). The differentiation of type A to type B spermatogonia at puberty is initiated by increased production of the androgen testosterone and is accompanied by testicular growth.

Diploid type B spermatogonia divide mitotically to produce primary spermatocytes. The meiotic phase of spermatogenesis begins when primary spermatocytes duplicate their DNA content and divide to produce haploid secondary spermatocytes. During this division, random segregation of homologous chromosomes and chromosomal crossover (chiasma) ensures each spermatocyte is genetically distinct despite having the same ancestral parent, thus maintaining genetic diversity (Barratt, 1995; Johnson and Everitt, 1996). As meiotic prophase begins the cells start to migrate away from the basement membrane towards the adluminal compartment transiently disrupting junctions between adjacent Sertoli cells. Short lived secondary spermatocytes enter meiosis II forming four haploid spermatids (Figure 1.2).

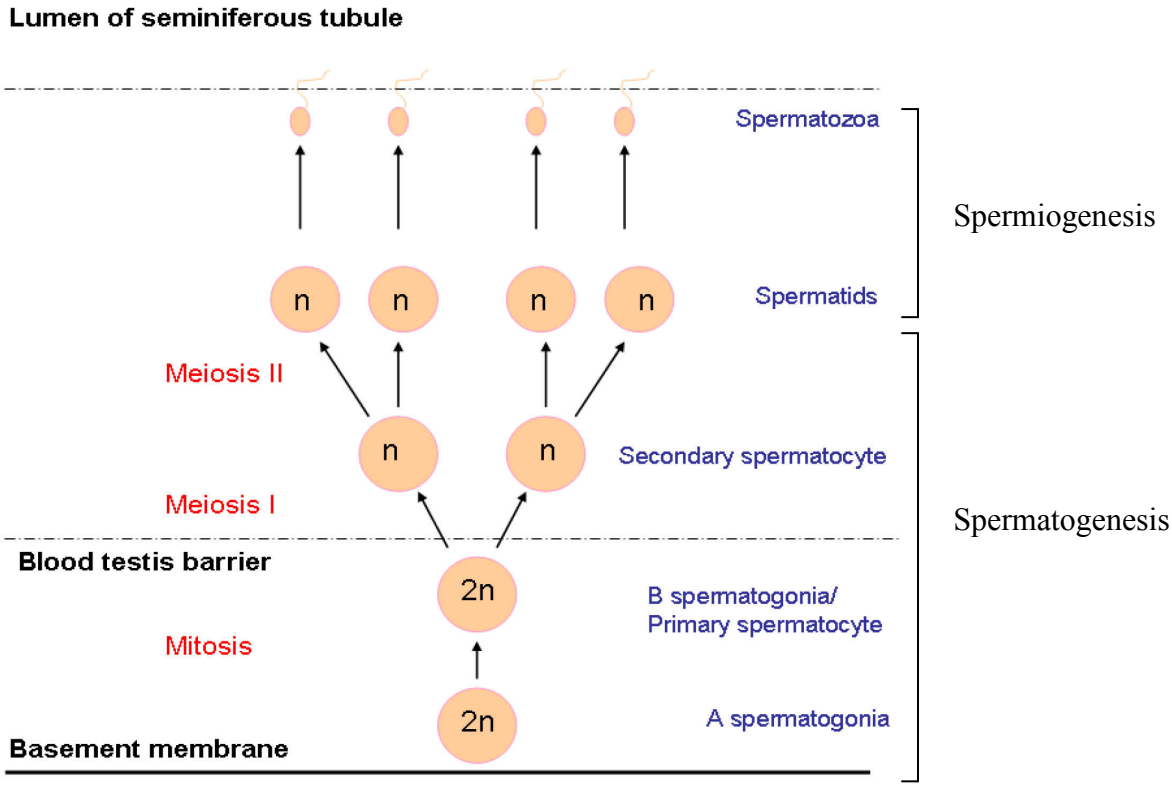

Figure 1.2 Schematic representation of mammalian spermatogenesis and spermiogenesis. Diploid type A spermatogonia can either self-replicate or differentiate into type B spermatogonia and become committed to the spermatogenesis pathway. Type B spermatogonia then meiotically divide into haploid secondary spermatocytes, followed by a second meiotic division to form four haploid spermatids. The process of spermiogenesis initiates tail elongation and transforms round spermatids to morphologically mature spermatozoa.

1.1.3 Spermiogenesis

In humans, spermiogenesis is completed in 22 days and this remodelling process involves the transformation of round spermatids to polarised spermatozoa (Barratt, 1995). Within the nucleus, histones are partially replaced for small basic proteins called protamines (Meistrich *et al.*, 2003). Prior to spermiogenesis, during meiotic events, mRNA transcription and

translation is highly active but protamine packaging inactivates transcription and translation. DNA interacts with protamines in a linear manner, as opposed to being coiled around histones as in somatic cells. This leads to hypercondensation of the sperm nucleus and helps in the formation of a hydrodynamic shape necessary for a motile cell (Brewer *et al.,* 2002; Dadoune, 2003). The Golgi apparatus fuses to form the acrosome, which then migrates and forms a cap on the proximal hemisphere of the sperm head (Sutovsky and Manandhar, 2006). The acrosome, containing acrosin and hyaluronidase, will enable penetration of the sperm through the zona pellucida (a protein capsule surrounding the oocyte). The two centrioles migrate to the opposing cell pole, with one taking a radial position and elongating to form the axoneme of the tail and the second lying at a right angle to form the connecting piece (Sutovsky *et al.,* 1999). The midpiece, containing helically arranged mitochondria, forms around the upper section of the flagellum. Superfluous cytoplasm (up to 70%) is released via the residual body during the final stages of spermiogenesis which is phagocytosed by Sertoli cells following sperm release, leaving only a remnant of cytoplasm in the form of the cytoplasmic droplet encompassing the connecting piece (Barratt, 1995). Once spermiogenesis is completed, the cytoplasmic bridges rupture and sperm are released into the lumen of the seminiferous tubule in a process termed spermiation.

1.2 Hormonal regulation of spermatogenesis

Endocrine control of spermatogenesis is governed by the hypothalamic-pituitary-testicular axis (Shalet, 2009) (Figure 1.3). At puberty, pulses of gonadotropin releasing hormone (GnRH) is secreted by the hypothalamus, stimulating the production of follicle stimulating hormone (FSH) and luteinizing hormone (LH) from the anterior pituitary (McLachlan, 2000).

The importance of the pituitary gland is highlighted by its removal (hypophysectomy) causing the testis to shrink and the arrest of spermatogenesis at the primary spermatocyte stage (Franca *et al.*, 1998). LH binds to receptors on Leydig cells, present in the interstitial tissue, stimulating testosterone production and secretion of between 4-10mg testosterone daily in humans (Johnson and Everitt, 1996). The main site of action for testosterone in the testis is the androgen receptor on the Sertoli cell surface, to support spermatogenesis. FSH binds to receptors located on the basal cell membrane of Sertoli cells stimulating several pathways, most importantly increasing the expression of androgen-receptor proteins thus increasing its responsiveness to testosterone (Baird, 1999). Consequently, FSH and testosterone both act synergistically on the Sertoli cell to support spermatogenesis. Feedback loops acting on the hypothalamus and anterior pituitary modulate GnRH, LH and FSH levels as control mechanisms.

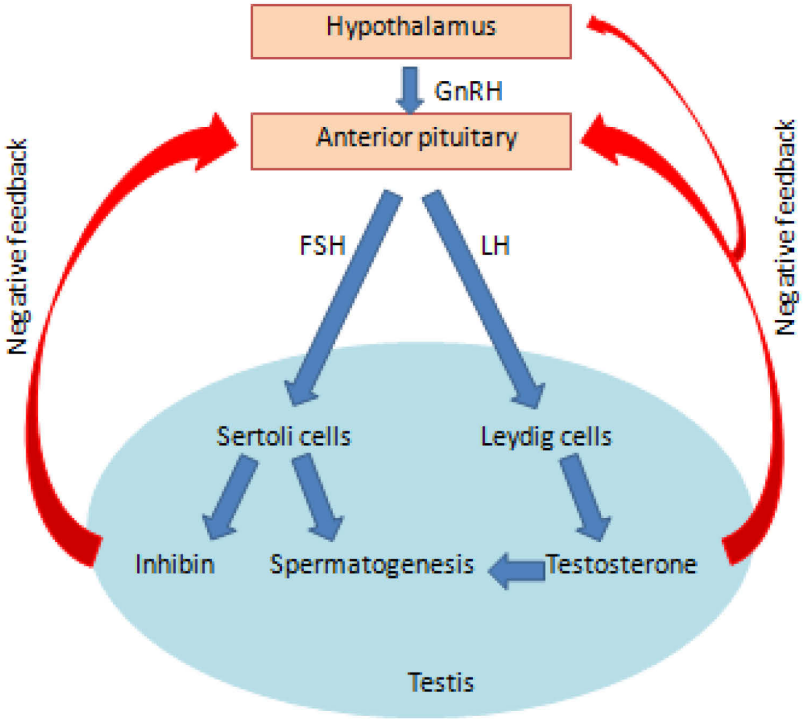

Figure 1.3 Diagram of the hormonal regulation of spermatogenesis. The hypothalamic-pituitary-gonadal axis directs the production of FSH and LH which act on Sertoli cells and Leydig cells respectively to regulate sperm production. Circulating testosterone produced by this process is also converted into dihydrotestosterone, leading to the formation of secondary male characteristics such as facial hair and increased muscle mass.

1.3 Sperm structure

Sperm may be divided into two generalised regions, the head and flagellum (Figure 1.4). Primate, carnivore and ungulate sperm heads are spatula-shaped (spatulate) in comparison with rodent sperm where their sperm heads are hook-shaped (falciform) (Sutovsky and Manandhar, 2006). The head region contains the acrosome, a small amount of cytosol and the hypercondensed nucleus. The nucleus is protected by the rigid perinuclear theca, a cytoskeletal structure comprising of structural proteins connected by disulphide bonds in conjunction with various other protein molecules (Oko, 1995). The perinuclear theca

functions to anchor the acrosome and forms associations with the inner and outer acrosomal membranes to produce the equatorial segment, an area rich in receptor molecules involved in sperm-oolemma binding, such as equatorin (Toshimori *et al.*, 1992).

The flagellum provides the motile force for the cell containing a 9 + 2 microtubular arrangement within the axoneme, as seen in the cilia and flagella of eukaryotic cells (Mitchell, 2007). This 9 + 2 arrangement describes two central microtubules surrounded by nine symmetrically arranged peripheral microtubule doublets, connected together by dynein arms and to the sheath of the central pair by radial spokes. The nine outer doublets are paralleled by nine outer dense fibers that provide flexible, yet firm support for flagella motility (Sutovsky and Manandhar, 2006). The flagellum can be divided into four sections sharing the same axoneme core but differing in extracellular structure, namely the connecting piece, midpiece, principal piece and end piece (Sutovsky and Manandhar, 2006).

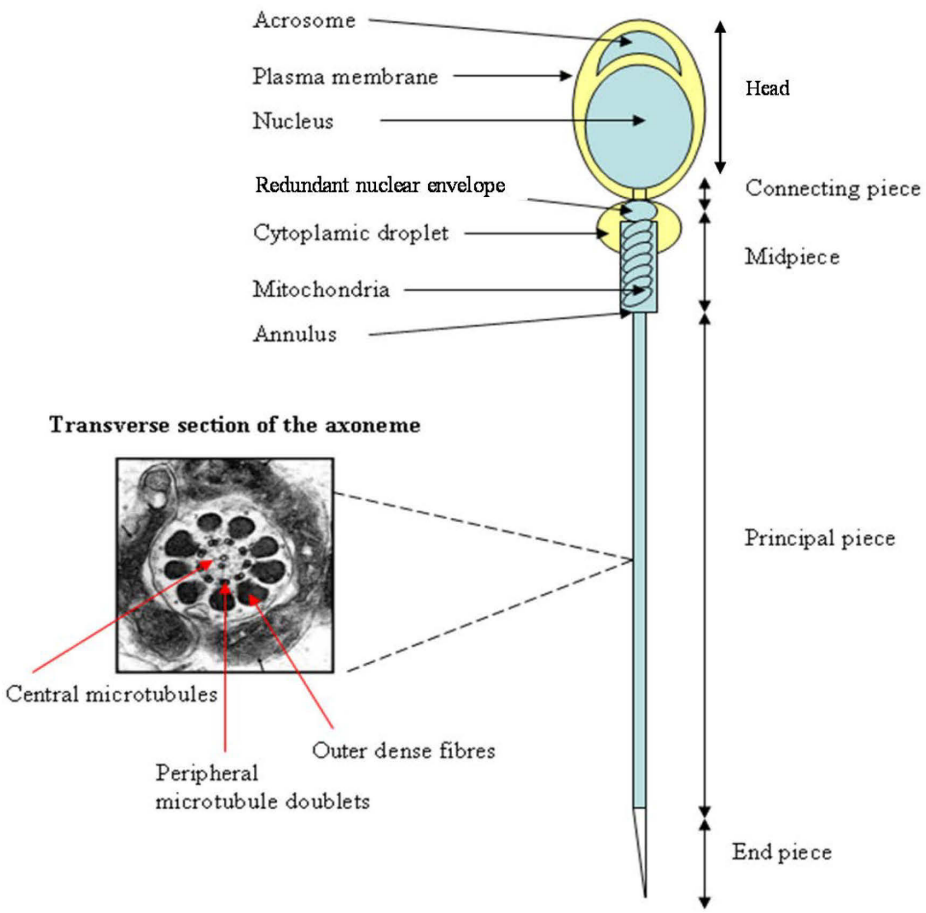

Figure 1.4 Human sperm cell and axoneme structure.The head region contains the large nucleus, acrosomal region and a small amount of cytosol. Joined to the head by the connecting piece, the flagella region stretches from the midpiece to the endpiece, sharing the same axoneme core (as shown) but differing in extracellular structure. Structures such as the redundant nuclear envelope and cytoplasmic droplet are found in the posterior head/midpiece region. (Electron micrograph of transverse axoneme structure from Sathanathan, 1996).

Briefly, in human the connecting piece is the short (0.5µm in length), most proximal portion of the flagellum, which attaches to the implantation fossa of the sperm head via a series of fine proteinaceous filaments (Curry and Watson, 1999). The connecting piece is a continuation of the outer dense fibers from the other flagella segments to form 9 segmented

columns. The centriole, a centrosome remnant, is contained within these 9 columns in a dome shaped structure called the capitulum (Sutovsky and Manandhar, 2006). This centriole lies at right angles to the flagella axis and is important for axoneme construction during spermiogenesis but does not appear essential for the adult spermatozoon.

The midpiece (3.5µm in length for human sperm) connects the distal end of the connecting piece to the start of the principal piece, marked by a circumferential band named the annulus (Turner, 2006). This region is covered by the mitochondrial sheath, consisting of 75-100 helically arranged mitochondria on top of the underlying axoneme. The mitochondrial inner membranes generate energy via ATP production and are suitably positioned around the root of the flagellum to deliver this energy directly to the axoneme for sperm motility (Suarez, 2008).

The principal piece extends between the annulus to the proximal region of the end piece and is the longest tail segment (approximately 55µm in length for human sperm) (Curry and Watson, 1999). It is characterised by a protective fibrous sheath, consisting of two longitudinal columns, arranged in the plane of the central microtubule pair and connected by a series of circumferential ribs (Eddy *et al*., 2003). The fibrous sheath provides mechanical support for the bending flagella as its constituent proteins are rich in disulphide bonds. In addition, more recent studies in mouse have indicated it provides scaffolding for protein kinases involved in capacitation and hyperactivated motility (Eddy *et al.*, 2003). For example, A-kinase anchor proteins (AKAPs) are classified as scaffolding proteins, tethering regulatory subunits of protein kinase A (PKA), phosphodiesterases, protein kinase G and other enzymes to cytoskeletal elements (Moss and Gerton, 2001). Two AKAP isoforms, AKAP 4 (primarily)

and AKAP3 have been localised to this fibrous sheath region (Carrera *et al.*, 1994).

The outer dense fibers terminate at some point during the principal piece whilst the axoneme microtubules continue and terminate within the end piece. The end piece is connected to the distal end of the proximal flagellum, with dynein arms regressing first followed by the central microtubular pair. There is successive termination of the microtubules up to the tip of the flagellum. (Curry and Watson, 1999).

1.4 Sperm transport in the male

Sperm within the lumen of the seminiferous tubule are morphologically fully formed but quiescent. Passage from the tubule to the rete testis is due to smooth muscle contraction from the tubules and entire testicular capsule, along with the flow of testicular fluid produced by the Sertoli cells and rete epithelium (Moore, 1995). Once sperm reach the vasa efferentia, which connect the rete testis to the overlying proximal epididymis, ciliated epithelial cells in this area waft, encourage flow and prevent cellular aggregation that could obstruct testis outflow (Moore, 1995). The proximal epididymis is lined with large, tall, absorptive cells with long microvilli that function to concentrate the sperm 100 fold, via passive fluid reabsorption driven by active sodium and chloride ionic exchange (Johnson and Everitt, 1996; Moore, 1995). Epididymal passage takes an average of 11 days (Rowley *et al.*, 1970), and the epididymis can be separated into three sections the caput, corpus and cauda from the proximal to distal regions. Sperm motility remains low within this region, although the percentage of motile sperm increases during transverse of the tubule (Moore *et al.*, 1983). This is due to time-dependent factors (Jow *et al.*, 1993) and a changing milieu of testicular fluid as

epididymal secretory products such as L-carnitine, glycerophosphorylcholine, lactate, fructose, glycoproteins, dihydrotesterone and sodium, potassium, chloride and bicarbonate ions are introduced (Johnson and Everitt, 1996). The caudal epididymis acts as a sperm reservoir before sperm move to the vas deferens, although the storage capacity is poor in humans. Indeed, due to the flow of epididymal fluid, sperm are frequently voided in urine when not ejaculated (Moore, 1995).

Ejaculation is governed by sympathetic and parasympathetic nerves and results from a coordinated contraction of the smooth muscle surrounding the cauda epididymis and vas deferens (Moore, 1995). During ejaculation sperm are suspended in seminal plasma to produce semen, a total volume of ~3ml in human and up to ~500ml in boar (Moore, 1995). Seminal plasma originates from the accessory sex glands (seminal vesicles, prostate, Cowper and Littre glands) (Figure 1.5). The seminal vesicles are sac like glands that empty upon ejaculation providing the majority of ejaculate volume rich in bicarbonate, prostaglandins, antioxidants, fructose and ascorbic acid (Coffey, 1995). Antioxidants, such as superoxide dismutase, glutathione, catalase and vitamins C and E serve to protect sperm from oxidative stress and subsequent loss of motility (de Lamirande and Gagnon, 1992, 1998).

Approximately 5% of the ejaculate made up from secretions from the Cowper (bulbourethral) and Littre glands. The prostate contributes secretions high in zinc, citric acid, prostate specific antigen (PSA) and choline. PSA helps liquefy the semen following ejaculation as it degrades Semenogelin (I and II) that comprise 20% of the seminal plasma, thus allowing the sperm to swim more freely.

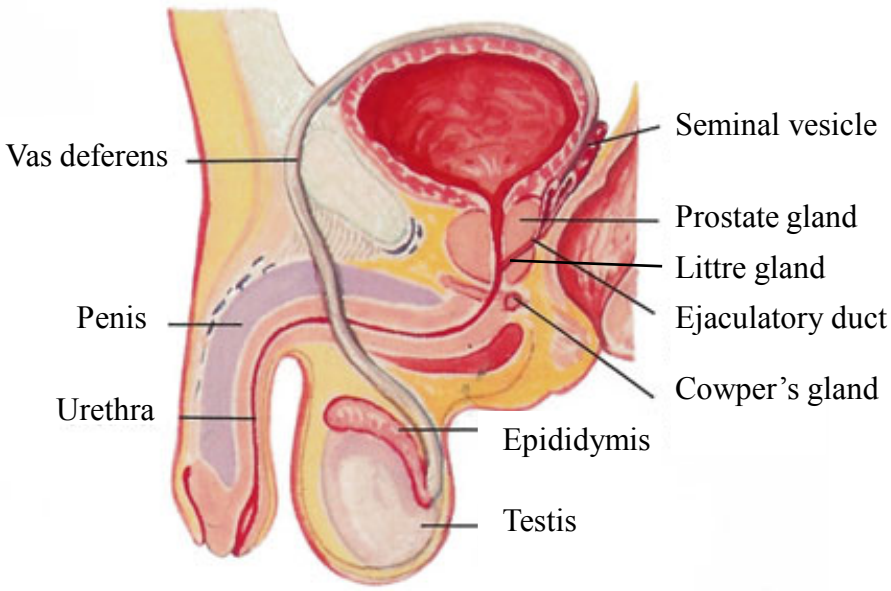

Figure 1.5 Diagram of the male reproductive system**.** Sperm pass from the testis, through the epididymis and vas deferens, until it is mixed with seminal plasma at ejaculation. The seminal plasma consists of secretions from the accessory sex glands, namely the seminal vesicles, prostate and Cowper's gland as seen in the diagram. Diagram adapted from http://www.malefertility.md/male-infertility-causes.html.

A further product derived from epithelial cells lining the prostate, are small membrane-bound vesicles called prostasomes. Although only 40-500nm, proteomic studies have revealed that prostasomes contain over 440 proteins including enzymes and structural proteins such as annexins (Burden *et al.,* 2005; Poliakov *et al.*, 2009). Interestingly, due a high phospholipid content prostasomes are capable of undergoing hydrophobic fusion with sperm, thus transferring their contents to the sperm cell (Ronquist and Brody, 1985). Prostasome/sperm fusion is favoured by an acidic pH and premature fusion is therefore avoided within the alkaline prostatic fluid, until the semen reaches the acidic vaginal environment (Arienti *et al.*, 1997; Carlini *et al.,* 1997; Frenette *et al.,* 2002). Moreover Arienti *et al.* (1997) reported that fluorescently labelled prostasomes were arranged uniformly on the surface of sperm fused at

pH 7.5 in comparison with prostasomes concentrated in the neck/midpiece region of sperm fused at pH 5.0. At this location in the midpiece the delivery of prostasomal products would be optimised for affecting motility. Indeed, studies have shown that the presence of prostasomes has a beneficial effect on sperm motility, increasing the percentage of motile cells in swim-up preparations (see section 2.2.2; Fabiani *et al.,* 1994; Arienti *et al.,* 1999). Other beneficial effects includes the delivery of prostasome-derived cholesterol which acts to limit premature acrosome reaction (AR) by stabilising the acrosomal cap and prostasome fusion initiating a calcium 'burst' to the sperm cell cytoplasm (Cross and Mahasreshti, 1997; Arenti *et al.,* 2004).

1.5 The oocyte

The ovulated oocyte, with a diameter of up to 120μm, is immediately surrounded by a glycoprotein coat synthesized and secreted by the oocyte, the zona pellucida (ZP) (Gosden and Telfer, 1987). Human ZP consists of four ZP proteins as opposed to mouse with only three functional ZP proteins (Lefievre *et al*., 2004). The multifunctional ZP is responsible for displaying species-specific sperm receptors, inducing AR, blocking polyspermy following fertilisation and protecting the zygote in the early stages of development (Gosden and Bownes, 1995). Surrounding the ZP is the cumulus oophorus, a hyaluronan-rich matrix consisting of an inner cell mass (corona radiata) which is continuous with the ZP, followed by the outer cell mass (cumulus) (Figure 1.6). Microvilli from the oocyte surface project a small distance into the ZP which are occasionally met by longer processes extending from the corona that terminate in button like swellings in order to maintain contact with the oocyte

surface (Gosden and Bownes, 1995). Corona cells also contain many gap junctions between themselves and the oocyte in order to permit the movement of factors essential for oocyte growth such as pyruvate or amino acids (Motta *et al.*, 1994, 1995).

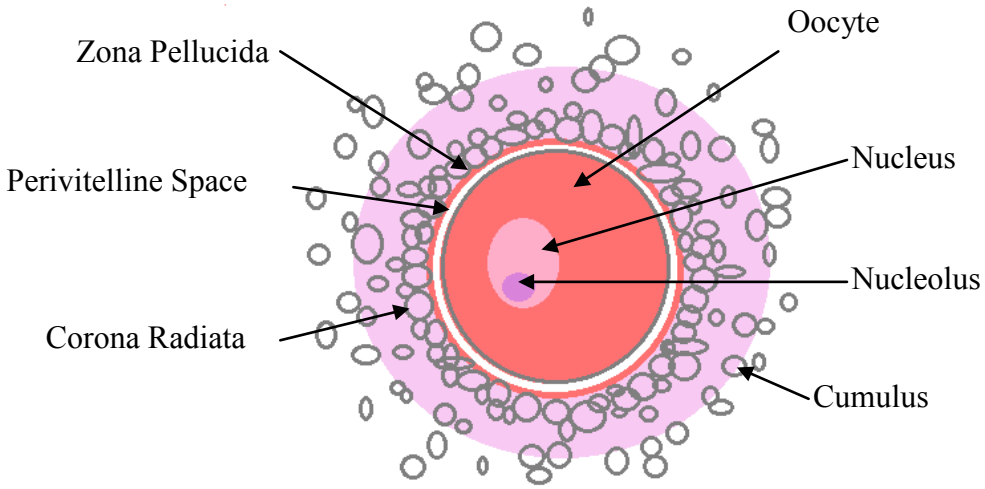

Figure 1.6 Diagram of the cumulus-oocyte complex. The delicate central oocyte containing the genetic material held within the nucleus is protected by the zona pellucida capsule. This is then surrounded by the corona radiata followed by several layers of cumulus cells to form the cumulus-oocyte complex.

1.5.1 The importance of the cumulus and progesterone

Evidence is accumulating that the cumulus plays an important role in filtering healthy from abnormal sperm and that it induces key events in sperm that must occur in order to enable fertilisation. Firstly, the passage of sperm through the cumulus assists in the removal of abnormal sperm via providing a mechanical barrier that has to be penetrated. Leukocytes present amongst the matrix can then phagocytose abnormal cells (Nottola *et al.*, 1998). Within

the outer layers of the cumulus the hormone progesterone is produced during ovulation at concentrations between 1-10μM, which has been reported to regulate sperm motility (Calogero *et al*., 1996; Jaiswal *et al.*, 1999), acrosome reaction (Muratori *et al.*, 2009) and chemotaxis (Teves *et al*., 2006). Therefore, the response of human sperm to progesterone is correlated with fertility with decreased responsiveness seen in sub-fertile patients (Falsetti *et al.*, 1993). The effects of progesterone on human sperm are not mediated via a classical pathway of steroid signalling, typically involving binding to a nuclear receptor to initiate gene transcription. Indeed, as mature sperm are transcriptionally and translationary silent, progesterone therefore exerts its effects via a 'non-genomic' mechanism, which has recently been determined (see section 1.11.3.4).

1.6 Sperm transport in the female

Following coitus in humans, semen is deposited in the anterior vagina near the cervical opening where within a few minutes sperm begin to swim toward the cervical canal (Sobrero and MacLeod, 1962). In comparison, semen is deposited directly into the uterine cavity in pig (Hunter, 1981; Roberts, 1986), or in rodent semen is deposited in the vagina but then the total semen is swept into the uterine cavity within a few minutes (Bedford and Yanagimachi, 1992; Carballada and Esponda, 1997). For humans, speedy transport toward the cervix is needed to help avoid immunological attack toward the 'non-self' sperm and damage due to vaginal acidity. Vaginal pH is normally 5 or lower, but seminal plasma with pH 6.7-7.4 (Roberts, 1986) has the potential to help neutralise the acidic environment (Suarez and Pacey, 2006). Furthermore, seminal plasma contains protective components that coat sperm (Suarez and Oliphant, 1982) and are believed to be gradually shed when sperm leave the seminal plasma

behind (Suarez and Pacey, 2006).

Cervical mucus within the cervical canal acts as a filter, removing less motile or morphologically abnormal sperm (Hanson and Overstreet 1981; Katz *et al.,* 1990, 1997). This filtering system is particularly prevalent at the cervical border where mucus structure is more compact (Yudin *et al.,* 1989). Cervical mucus viscosity is controlled by estrogen concentration, where increased levels lead to a highly hydrated mucus often exceeding 96% water in women (Katz *et al.,* 1997). Moreover, increased mucus hydration is linked to increased sperm penetrability (Morales *et al.,* 1993) and subsequently increased pregnancy rates (Bigelow *et al.,* 2004).

Sperm that successfully traverse the cervix reach the uterus. It has been estimated that a swimming speed of 5mm/min is sufficient for sperm to cross the uterus, which is only a few cm in length, in under 10 minutes (Mortimer and Swan, 1995). However, these observations were conducted in aqueous medium, different to the viscous nature of uterine fluid (Kirkman-Brown and Smith, 2011). Sperm are assisted through this region via contractions of the myometrium during the periovulatory period. These contractions originate in the layer of myometrium directly beneath the endometrium, as opposed to contractions in all layers of myometrium during menses (de Ziegler *et al.*, 2001). Only a few thousand sperm swim through the uterotubal junctions to reach the Fallopian tubes, where they interact with the oviductal epithelium. From here, capacitation and hyperactivation (discussed below) help the sperm reach the tubal ampulla, where a combination of thermotaxis and chemotaxis may help them reach the oocyte (Suarez, 2006).

1.7 Capacitation

Ejaculated sperm are motile and morphologically mature yet still do not have the capability to fertilise an oocyte. Independently, both Chang (1951) and Austin (1951) observed that sperm injected directly into rabbit oviduct following ovulation were unable to fertilise, in comparison with sperm injected a few hours prior to ovulation. Both groups concluded sperm must reside in the female reproductive tract for a period of time before gaining fertilising ability. During the ascent of the female reproductive tract, sperm undergo a series of maturational events collectively termed capacitation, which give sperm the capacity to fertilise the oocyte (Travis and Kopf, 2002). Capacitation includes an increase in plasma membrane fluidity, reorganisation of sperm surface molecules, increased levels of intracellular Ca^{2+} and cyclic adenosine monophosphate (cAMP), membrane hyperpolarisation, intracellular alkalinisation, and increased phosphorylation of some proteins (Tulsiani *et al*., 2007; Barratt and Kirkman-Brown, 2006). This set of modifications is associated with hyperactivated motility and the ability of sperm to undergo an agonist induced (typically progesterone or zona pellucida) acrosome reaction (Yanagimachi, 1994). This process ensures sperm are in the appropriately activated state to bind and penetrate the zona pellucida and fuse with the oocyte.

Sperm capacitation can be separated into early and late events, both of which are mediated by protein kinase A (PKA) (Figure 1.7). Early events occur immediately post-ejaculation and include the activation of sperm motility. Here, bicarbonate ions (HCO_3^-) activate motility through the opening of voltage gated Ca^{2+} channels, CatSper (flagella specific) Ca^{2+} channels and activation of the enzyme soluble adenylyl cyclase (sAC). In contrast to transmembrane adenylyl cyclase (tAC), sAC does not respond to G protein stimulators of transmembrane

cyclases or analogues of GTP and is believed to be the prime HCO_3^- target during sperm capacitation (Chen *et al.*, 2000; Hess *et al.*, 2005). Esposito *et al.* (2004) developed mutant mice deficient for sAC which were infertile and lacked HCO_3- induced capacitation responses. Typically, sAC activation increases intracellular levels of cAMP which activates protein kinase A (PKA) (Gadella and Visconti, 2006; Visconti, 2009), within minutes of HCO_3- exposure (Harrison and Miller, 2000). PKA activation is predicted to cause the serine/threonine phosphorylation of target proteins that activate currently unidentified tyrosine kinases whose targets are primarily located in the flagellum (Lawson *et al.*, 2008; Leclerc *et al.*, 1996; Si and Olds-Clarke, 2000).

It is currently unclear how HCO_3- enters the sperm's intracellular environment although in mouse a Na^+/HCO_3- co-transporter has been implicated (Demarco *et al.*, 2003). Also Wang *et al*. (2003) reported that mutant mice deficient in the Na+/H+ antiporter were infertile, but cAMP analogues restored fertility (Wang *et al.*, 2003). These findings suggest that net neutral proton transport over the plasma membrane is essential for sufficient bicarbonate buffering in order stimulate sAC activity effectively (Gadella and van Gestel, 2004). It has subsequently been hypothesised that there is co-localisation between sAC and Na^+/HCO_3- co-transporters (Demarco *et al.*, 2003).

As opposed to early events, other capacitation associated-processes require longer incubation periods. Most of the data for these slower capacitation processes has been obtained from *in vitro* studies where sperm are incubated in buffers mimicking the glucose and electrolyte content of the oviduct (Visconti *et al.*, 1998; Gadella and Visconti, 2006; Travis and Kopf, 2002). Most importantly, capacitation media must contain serum albumin, Ca^{2+} and HCO_3^-

(Visconti, 2002).

At the level of the plasma membrane, HCO_3^- induces a rapid collapse of the asymmetric phospholipid bilayer in boar (Harrison and Gadella, 2005) and human sperm (de Vries *et al.,* 2003). Normally, components of the phospholipid bilayer include sphingomyelin and phosphatidylcholine reside in the outer surface, with phosphatidylethanolamine and phosphatidylserine confined to the inner surface (Verkleij *et al.*, 1973). However, the introduction of HCO_3^- for as little as 2 minutes, at 15mM, activates phospholipid scramblase leading to the reversible exchange of phospholipids in a non-specific fashion between the phospholipid layers (Gadella and Visconti, 2006). As a result of phospholipid exchange and membrane collapse, serum albumin is able to act as a cholesterol sink, facilitating the removal of cholesterol from the sperm plasma membrane (Cross*,* 1996). Furthermore, serum albumin can be replaced by cholesterol-binding compounds such as high density lipoproteins with the same effect (Therien *et al.*, 1997; Visconti *et al.,* 1999). Alternatively, the addition of cholesterol or cholesterol analogues to the capacitation media halts capacitation (Visconti *et al.*, 1999).

The HCO_3- influx during capacitation also leads to cellular alkalinisation (Parish *et al.*, 1989) and is linked to membrane hyperpolarisation (Zeng *et al.*, 1995). Experiments with bovine sperm incubated in 1% (v/v) CO_2 in air (to induce increased intracellular pH), have been shown to stimulate acrosomal sensitivity and protein phosphorylation thus suggesting alkalisation plays a role in sAC activity (Galantino-Homer *et al.*, 2004). Increased membrane hyperpolarisation is thought to be due to increased potassium (K^+) permeability, with K^+ currents generated by SLO3 channels sensitive to alkalisation and cAMP levels in mouse

sperm (Martinez-Lopez *et al.*, 2009).

Sperm capacitation is also associated with an increase in protein tyrosine phosphorylation, a post-translational modification (Salicioni, 2007). Protein tyrosine phosphorylation is finely controlled through the components of the capacitation medium. Consequently, if you remove either bicarbonate, BSA or Ca^{2+} from the capacitating medium, this prevents an increase in tyrosine phosphorylation (Visconti, 1995; Bedu-Addo *et al.*, 2005). Protein tyrosine phosphorylation has been established to be downstream of the PKA pathway as cAMP-permeable analogues are able to induce the increase in tyrosine phosphorylation in the absence of BSA, HCO_3^- or Ca^{2+} (Visconti, 2009). In addition, mouse sperm that lack sAC do not show changes in tyrosine phosphorylation following incubation in a capacitation supporting media (Esposito *et al.*, 2004).

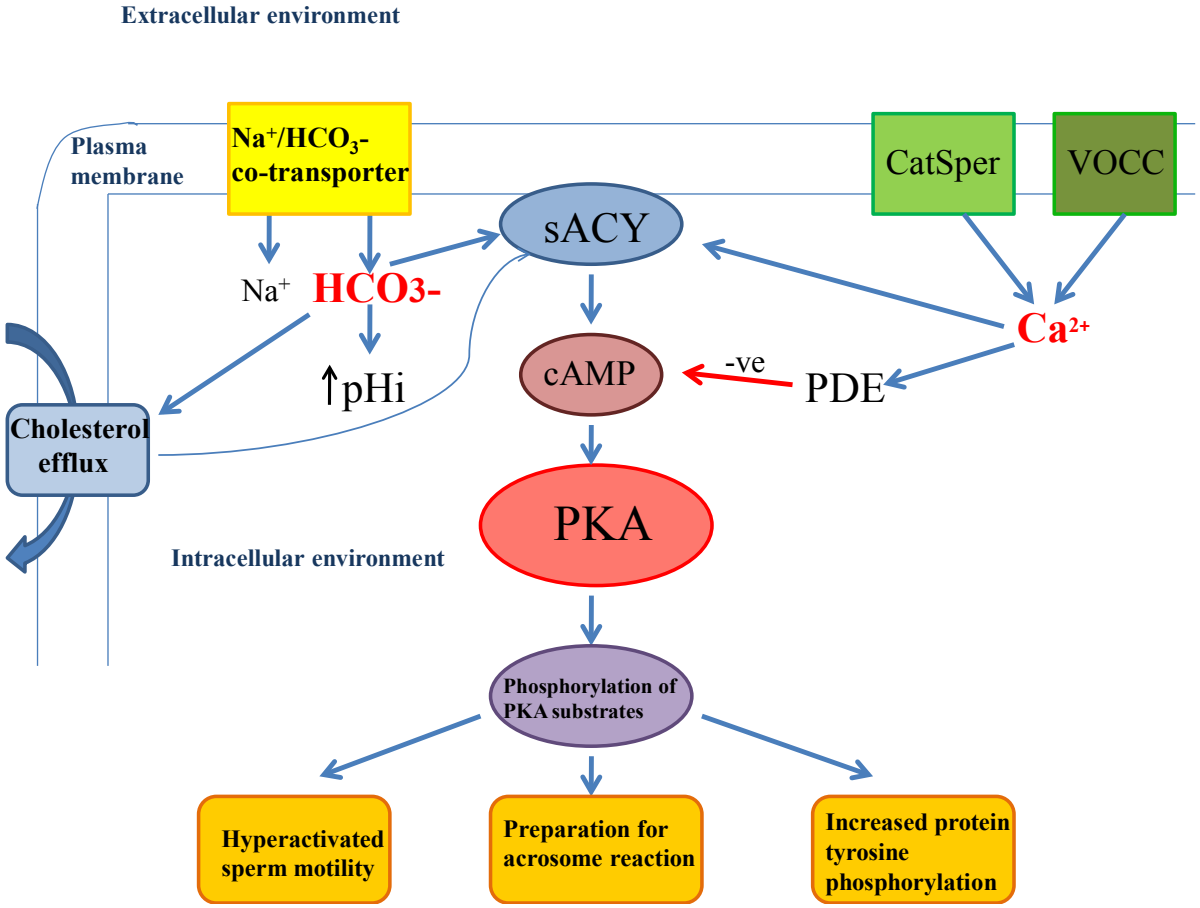

Figure 1.7 Summary of the molecular basis of the events associated with sperm capacitation (adapted from Visconti, 2009). HCO_3- present in capacitating media is transported into the sperm cell via Na^+/HCO_3- co-transporters, initiating cellular alkinisation and cholesterol efflux. Together with the Ca^{2+} influx from activated CatSpers and VOCCs, this leads to an increase in motility. Longer-term effects are mediated by sAC stimulation which leads to an increase in cAMP levels and activates PKA. PKA activation is predicted to initiate the phosphorylation of particular proteins culminating in events associated with capacitation such as hyperactivated motility, preparation for acrosome reaction and an increase in protein tyrosine phosphorylation.

1.8 Motility and hyperactivation

Sperm display two types of motility, activated and hyperactivated. Upon ejaculation sperm motility is activated but influenced by the viscosity of the seminal plasma and certain 'decapacitation' factors such as semenogelin, cholesterol and fertilisation promoting peptide which prevent sperm from initiating capacitation (Burkman, 1995). Typical sperm movements within semen include a relatively straight path, axial rolling, minimal flagella bend amplitude and a lower velocity (Burkman, 1986). Once sperm leave the vaginal pool of seminal plasma, factors originating from epididymal fluid and seminal plasma are lost or redistributed (de Lamirande and Gagnon, 1997) and those with relatively normal morphology and good flagella vigour will show effective progression through the cervical mucus (Katz, Drobnis and Overstreet, 1989). Activated motility is characterised as straight passage with high flagella beat frequency but low bend angle and sperm will remain activated until they reach the uterotubal junction (Figure 1.8).

Hyperactivation is characterised as increased velocity, decreased linearity, increased amplitude of lateral head displacement and whiplash movements of the flagellum (de Lamirande, 1997; Figure 1.8) and coincides with the onset of capacitation. Hyperactivation facilitates sperm progression in the oviduct, dissociation with the oviductal epithelium, through mucoid oviductal secretions and provides the motile thrust needed for zona pellucida penetration (Rathi *et al.*, 2001). Furthermore, there is a strong association between correct and punctual sperm hyperactivation and oocyte penetration leading to successful fertilisation (Suarez, 1992; Stauss *et al.*, 1995).

Hyperactivation is partly due to the cAMP/PKA-dependent tyrosine phosphorylation of flagella proteins such as AKAPs (San Agustin and Witman, 1994). Mice with a targeted deletion for the sperm specific catalytic subunit of PKA are infertile due to poor motility (Skalhegg *et al.*, 2002). However, hyperactivation is mainly mediated by an increase in flagella Ca^{2+} as shown by studies inducing hyperactivation by incubating sperm with Ca^{2+} ionophores A23187 or ionomycin (Suarez *et al.,* 1987, 1992; Xia *et al.*, 2007). The Ca^{2+} influx into the flagella is primarily due to sperm specific CatSper channels (Carlson *et al.*, 2005; Jin *et al.*, 2007) and possibly also voltage operated Ca^{2+} channels (VOCCs) (Arnoult *et al.,* 1996; Ren *et al.,* 2001), both localised to the principal piece of the flagellum (see sections 1.11.3.1 and 1.11.3.4).

In addition to ion channels, an intracellular calcium storage organelle in the base of the head/midpiece region, suggested to be the redundant nuclear envelope (RNE), may provide Ca^{2+} for hyperactivation (Figure 1.8). Pharmacological agents such as thapsigargin and 4-aminopyridine (4-AP), known to release Ca^{2+} from intracellular stores, have been used to demonstrate hyperactivation initiation in bovine, mouse and human sperm the absence of external Ca^{2+} (Suarez and Ho, 2003; Marquez, 2007). In addition, 1,4,5-trisphosphate (IP_3) receptors and Ryanodine receptors (RyR) which gate channels regulating the mobilisation of stored Ca^{2+} and calreticulin, the Ca^{2+} binding protein of reticular stores, have all been localised by antibodies to this area (Ho and Suarez 2001, 2003; Harper *et al.,* 2005). It is not yet understood whether Ca^{2+} for hyperactivation is obtained from CatSpers and the RNE or if the RNE merely modulates hyperactivated motility (Suarez, 2008).

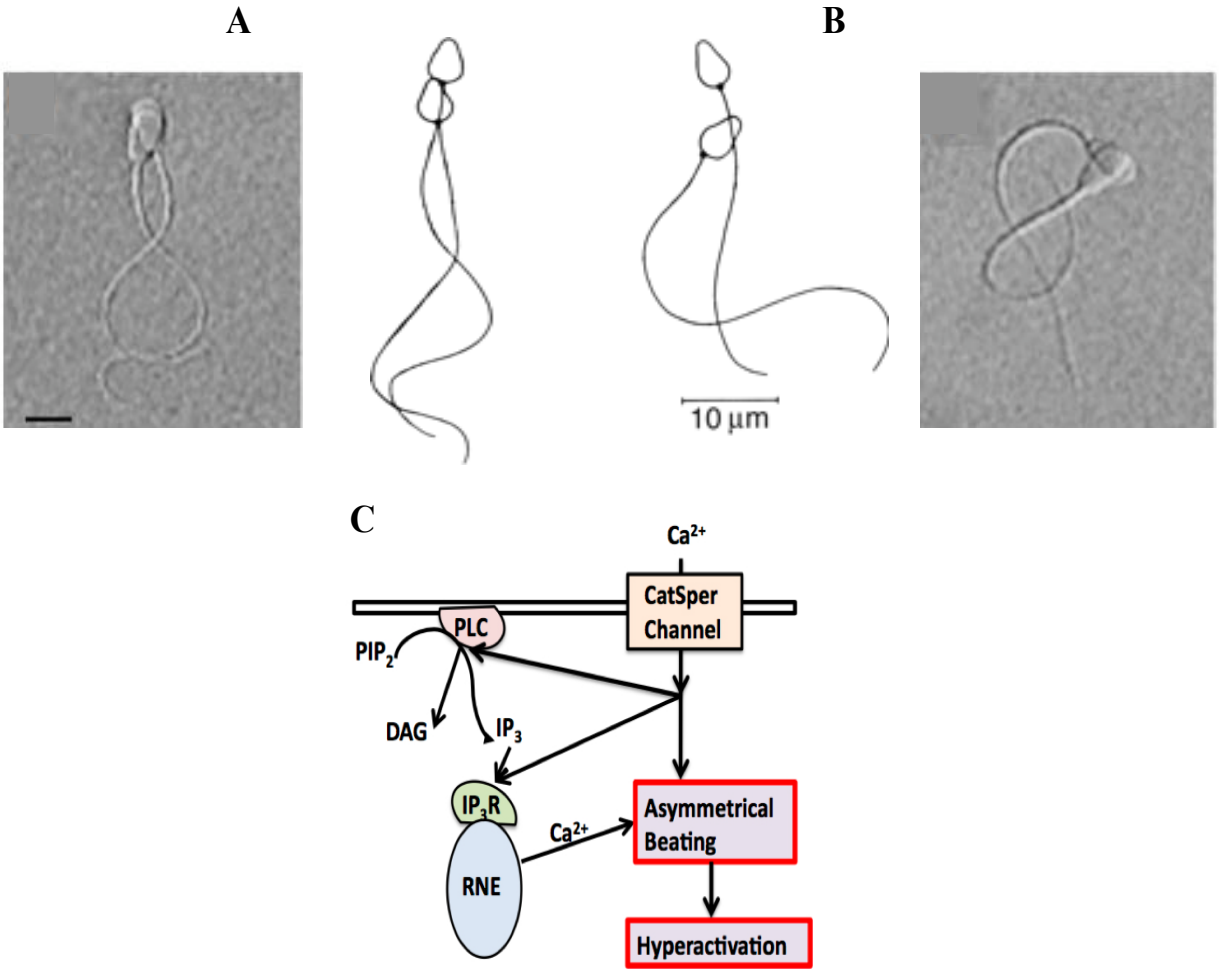

Figure 1.8 Hyperactivation in human sperm. (A) Activated sperm motility and (B) hyperactivated sperm motility (from Suarez, 2008). (C) Mechanism of Ca^{2+} influx into the flagella to control hyperactivation (from http://129.81.170.14/~solson2/Hyperactivation.html).

1.9 Acrosome Reaction

Capacitated sperm are primed and ready to undergo the acrosome reaction. The acrosome reaction involves the fusion at several points between the outer acrosomal membrane and the overlying plasma membrane. This is caused by a substantial $[Ca^{2+}]_i$ elevation culminating in

the irreversible exocytosis of the acrosomal contents to the zona pellucida surface (Bailey and Storey, 1994).

1.9.1 Zona pellucida induced acrosome reaction

The best characterised agonist of the acrosome reaction is the zona pellucida (ZP). Specifically, capacitated sperm bind to ZP3 (one of the four ZP proteins) in a process that is species specific. Sperm-ZP3 binding causes the opening of T-type, low voltage VOCCs (section 1.11.3.1) leading to a transient Ca^{2+} influx, as Ca^{2+} concentrations rise from the nanomolar to the micromolar values within 50 seconds (Arnoult, 1999, O'Toole 2000). This transient is succeeded by a slower and sustained $[Ca^{2+}]_i$ elevation in the continuous presence of ZP3 and is thus described as a biphasic response. Secondly, sperm-ZP3 interaction causes an elevation of intracellular pH, which has been reported via the use of fluorescent indicator dyes (Florman *et al.*, 1989; Rockwell and Storey, 2000). This process is thought to be mediated via a G protein-dependent pathway, as the heteromeric GTP-binding proteins Gi1 and Gi2 are activated in sperm by the ZP (Ward *et al.*, 1994). Furthermore, if G protein stimulation is inhibited by pertussis toxin, the alkalinisation activated by ZP binding does not occur (Florman *et al.,* 1989; Arnoult *et al.,* 1996). Finally, sperm-ZP3 binding also activates phospholipase C (PLC) (Roldan and Murase, 1994; Roldan and Shi, 2007). PLC hydrolyzes phosphatidylinositol- 1,4-bisphosphate (PIP2) to generate inositol- 1,4,5-triphosphate (IP_3) and diacylglycerol. IP_3 can then bind to IP_3 receptors present on the outer acrosomal membrane to mobilise Ca^{2+} from the acrosomal lumen (Walensky and Snyder, 1995).

1.9.2 Progesterone induced acrosome reaction

This phenomenon of Ca^{2+} influx and acrosome reaction caused by sperm-ZP3 binding also occurs upon the exposure of sperm to the steroid hormone progesterone (or its analogue 17 α-OH-progesterone), typically secreted by cumulus cells surrounding the oocyte (Meizel, 1995; Garcia and Meizel, 1999). Bolus application of 3μM progesterone also leads to a rapid transient Ca^{2+} increase resulting in the acrosome reaction (Tesarik and Mendoza 1993; Aitken *et al.,* 1996; Kirkman-Brown *et al.*, 2000), as seen with ZP3. If however, progesterone is applied as a logarithmic gradient, which is more comparable to the in vivo situation, the large initial Ca^{2+} transient typically causing the AR does not occur (Harper *et al.,* 2004). However, slower $[Ca^{2+}]_i$ oscillations can still be observed in up to 50% of the cell population (Bedu-Addo *et al.*, 2007) where they are believed to modulate flagella beat activity as asymmetrical bending of the midpiece occurs during the Ca^{2+} peaks (Harper *et al.,* 2004, 2005). These oscillations are reminiscent of somatic cells once induced to perform cyclic mobilisation of intracellular Ca^{2+} stores (Berridge *et al.*, 1993) and they depend on Ca^{2+} influx to maintain store refilling (Shuttleworth and Mignen, 2003). Also, if extracellular Ca^{2+} was buffered using either 1mM La^{3+} or EGTA-buffered saline, oscillations were generally arrested although a small percentage of cells continued to oscillate. These continuing oscillations were only blocked via the use of tetracaine or TMB-8 (both of which are intracellular Ca^{2+} channel inhibitors) (Harper *et al.*, 2004). Interestingly, these slow oscillations initiated in the sperm neck/midpiece region. In combination with the detection of SPCA1 channels (see section 1.11.4.1) in this area, this further suggests the possibility of a second intracellular Ca^{2+} store, possibly the RNE, separate from that of the acrosome (Harper *et al.*, 2005).

1.10 Fertilisation

Fertilisation defines the point at which sperm and oocyte unite to produce a genetically distinct individual and may be dissected into five stages (Figure 1.9) (Wassarman *et al.*, 2001). Once capacitated sperm are in the vicinity of the oocyte they must firstly traverse the cumulus oophorus, binding to the ZP in a species- specific manner. Secondly these interactions induce the acrosome reaction, a calcium dependent event, culminating in the exocytosis of the sperms acrosomal contents onto the ZP surface. This exposes a new antigenic spectrum on the sperm head surface, including proteins such as IAM38/ZPBP2 which mediate interactions between the sperm and zona glycoproteins (Yu *et al.*, 2006, Sutovsky, 2009). Thirdly, the spermatozoon attempts to penetrate the ZP via a combination of enzymatic digestion using acrosin and mechanical force. Once the sperm reaches the perivitelline space between the ZP coat and the plasma membrane, the fourth step of binding to the plasma membrane can occur. This binding process is thought to be mediated by IZUMO proteins present on the equatorial segment of acrosome-reacted sperm and the tetraspanins CD9 and CD81 present on the plasma membrane of the oocyte, leading to fusion of the egg and sperm (step 5) (Inoue *et al.*, 2005; Le Naour *et al.*, 2000; Rubinstein *et al.*, 2006). Upon successful gamete fusion this initiates egg activation, pronuclear formation and syngamy thus completing the first stages of the creation of a new individual (Evans and Florman, 2011).

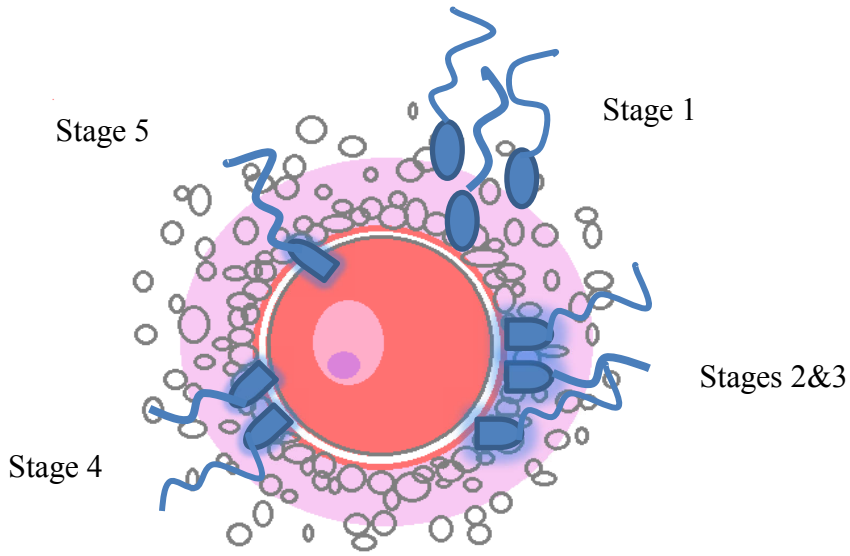

Figure 1.9 Illustration of the five stages of fertilisation. **(1)** Sperm in the vicinity of the oocyte traverse the cumulus oophorus, binding to the ZP in a species- specific manner. **(2)** These interactions induce the sperm to perform the acrosome reaction. **(3)** The spermatozoon then attempts to penetrate the ZP via a combination of enzymatic digestion and mechanical force. **(4)** If successful, the spermatozoon will bind to the plasma membrane leading to **(5)** penetration of sperm into the oocyte and fusion of the gametes. (Sperm are not drawn to scale).

1.11 Calcium (Ca^{2+}) signalling

1.11.1 Ca^{2+} signalling in somatic cells

Within eukaryotic somatic cells, Ca^{2+} is a ubiquitous intracellular second messenger that can change by orders of magnitude in order to activate numerous signal transduction pathways. Typically, the extracellular [Ca^{2+}] is ~1mM, in comparison with a resting cytoplasmic Ca^{2+} concentration ($[Ca^{2+}]_i$) of ~50nM (Collins and Meyer, 2011) and Ca^{2+} storage organelle

concentration of ~400μM. These steep concentration gradients between membranes enable $[Ca^{2+}]_i$ values to increase ten-fold with Ca^{2+} influx into the cell. This resulting increase is sensed and interpreted by the cell with the ability to activate numerous immediate and long-term pathways, such as muscle contraction and gene transcription, respectively (Jimenez-Gonzalez *et al.*, 2006). The versatility of a cell's calcium signalling 'toolkit' with intricate Ca^{2+} flux channels, clearance mechanisms and stores, enables control of the speed, amplitude and spatio-temporal patterning of the calcium signal (Berridge *et al.,* 2000; Jimenez-Gonzalez *et al.*, 2006).

1.11.2 Ca^{2+} signalling in sperm

Sperm are translationally and transcriptionally inactive which means that post-translational modifications control cell activity. One such post-translational modification is the modulation of proteins controlling $[Ca^{2+}]_i$, which plays a major role in many important sperm events including motility, acrosome reaction, chemotaxis, and is associated with capacitation events as discussed in section 1.7 (Carlson *et al.*, 2003; Kirkman-Brown *et al.*, 2003). Due to the multifunctional role of Ca^{2+} signalling in a highly specialised sperm cell there must be a range of Ca^{2+} conducting channels and stores to ensure perfectly timed $[Ca^{2+}]$ signals, such as oscillation and waves, are activated discretely (Jimenez-Gonzalez *et al.*, 2006). Before examining the specialised mechanisms of Ca^{2+} signalling in sperm it is important to outline and explain the Ca^{2+} mechanisms from somatic cells to provide an explanatory overview. Subsequently, each of the following sections is comprised of Ca^{2+} mechanisms in somatic cells followed by those in sperm (Figure 1.12).

1.11.3 Ca^{2+} channels at the plasmalemma

Studies aimed at examining Ca^{2+} flux at the plasmalemma have found four potential channel types, including voltage operated Ca^{2+} channels (VOCCs), store operated Ca^{2+} channels (SOCs), cyclic nucleotide-gated (CNG) channels, in addition to CatSpers which are unique to sperm. Activation of these channels, causes an extracellular Ca^{2+} influx resulting in increased cytoplasmic $[Ca^{2+}]_i$ displayed as a Ca^{2+} spike (Jimenez-Gonzalez *et al.*, 2006).

1.11.3.1 Voltage operated calcium channels (VOCCs)

VOCCs are a family of channel forming transmembrane proteins, mediating Ca^{2+} entry into cells in response to depolarisation across the plasma membrane (Catteral, 2000). They are formed from several subunits, with the 190-250 kDa α1 subunit forming the ion conducting pore. Ten distinct α1 subunits have been identified, separated into three subtypes of Cav1, Cav2 and Cav3. Electrophysical studies have defined different currents passing through these channels as L-, N- P- Q- R- and T-types (Catteral, 2000). Cav1 α1 subunits are responsible for L-type Ca^{2+} currents involved in physiological processes such as muscle contraction and gene transcription. Cav2 α1 subunits conduct N, P, Q and R-type Ca^{2+} currents primarily resulting in rapid synaptic transmission. Finally, Cav3 α1 subunits conduct T-type Ca^{2+} currents which are low voltage activated (depolarisation at voltages >-60mV) and are activated and inactivated more rapidly than other Ca^{2+} channel types (Catteral 2000). The heterogeneous nature of VOCCs ensures a variety of Ca^{2+} entry pathways can be activated in response to membrane depolarisation, which can continue on to have different cellular effects (Catteral 2000).

VOCCs have been detected within immature and mature sperm cells in both human and rodent (Arnoult *et al*., 1996). The primary role for VOCCs in sperm is predicted to involve regulation of the bicarbonate cAMP signal. Studies in mouse sperm have demonstrated that depolarisation-evoked Ca^{2+} entry is amplified by HCO_3^- via a PKA-dependent mechanism and is potentiated by the cAMP analogue cAMP-AM (Wennemuth *et al*., 2003). Patch clamping of immature human and rodent sperm has shown that these cells display T-type Ca^{2+} currents, being low-voltage activated and fast-inactivating, enabling tight controls on $[Ca^{2+}]_i$ (Arnoult *et al.,* 1996; Jagannathan *et al.*, 2002). In support of this, immunostaining in human sperm with isoform specific antibodies have localised α 1H [Cav3.2] to the principal piece of the tail and to the posterior region of the sperm head and α1I [Cav3.3] has been localised to the midpiece (Serrano *et al.*, 2004). Also, transcripts for VOCC isoforms α1C [Cav1.2], α1B [Cav2.2], α1E [Cav2.3], α1G [Cav3.1], α 1H [Cav3.2] and α1I [Cav3.3] have all been detected in motile human sperm (Park *et al.,* 2003).

1.11.3.2 Store operated Ca^{2+} channels (SOCs)

$[Ca^{2+}]_i$ can be elevated by either Ca^{2+} entry across the plasmalemma or Ca^{2+} release from internal stores. In many cases, these two processes are coupled together in order to replenish stores and mediate long-term cytosolic Ca^{2+} signals (Putney *et al.*, 2001). This intracellular store depletion and refilling process is termed store operated Ca^{2+} entry (SOCE) or capacitative Ca^{2+} entry (CCE) and is mediated by SOCs within the plasma membrane. The depletion of an intracellular Ca^{2+} store (typically the ER) triggers the opening of SOCs at the plasma membrane. In somatic cells, SOCE can be initiated via agonists that stimulate the

release of Ca^{2+} from intracellular stores such as IP_3, thapsigargin and incubation in Ca^{2+} free media (Harper *et al*., 2004; Berridge *et al.,* 2000). The best characterised SOC current is the Ca^{2+} release activated Ca^{2+} current (I_{CRAC}), which passes through the CRAC channel. CRAC is described as a non-voltage gated, highly Ca^{2+} selective low conductance channel (Smyth *et al.*, 2006; Parekh *et al.*, 1997, 2005).

Paramount to the theory of SOC activation is the requirement for a communicative pathway between the Ca^{2+} store and the CRAC channels. The identity of CRAC was previously thought to be transient receptor potential channels (TRP) in particular the canonical TRP (TRPC) (Padinjat and Andrews, 2004). However since 2005 studies have demonstrated the involvement of two transmembrane protein groups; stromal interacting molecules (STIM) and Orai, residing in the endoplasmic reticular membrane and plasma membrane respectively (Liou *et al.*, 2005; Feske *et al*., 2006), with crosstalk that enables them to orchestrate successful SOCE.

1.11.3.2.1 Stromal interacting molecule (STIM)

STIM is a single-pass transmembrane protein typically located in the endoplasmic reticulum (ER) of resting somatic cells. Drosophila and *C. elegans* have one Stim protein, but amphibians, birds and mammals have two STIM homologues, suggesting gene duplication at the invertebrate-vertebrate transition about 500 million years ago (Cahalan, 2009; Cai, 2007). The N-terminus of STIM1 lies in the ER lumen, adjacent to a single EF-hand Ca^{2+} binding motif that acts as a luminal Ca^{2+} sensor (Liou *et al.,* 2005; Zhang, 2005, reviewed by Frischauf, 2008). The N-terminus and EF-hand are connected to the transmembrane region

via a sterile-alpha motif (SAM) containing two N-linked glycosylation sites (see Figure 1.10). The opposing C-terminus stretches into the cytoplasm with two coiled-coil regions overlapping with an erzin-radixin-moesin (ERM)-like domain, followed by glutamate-, serine/proline-, serine/threonine- and lysine-rich regions (Frischauf, 2008). This area in Drosophila (and *C.elegans*) differs significantly from mammalian cells, most notably lacking the serine/proline and lysine-rich regions (Cahalan, 2009). STIM2 shares 61% sequence identity with STIM1 and the Drosophila homologue stim, has 31% identity and 60% sequence similarity to STIM1 (Cahalan, 2009).

Stim was originally identified quite recently via a large scale RNAi screen in Drosophila D2 cells, with an aim to target proteins possibly involved in SOC entry (Roos *et al.*, 2005). A parallel study also identified the mammalian isoforms STIM1 and STIM2 from HeLa cells (Liou *et al.*, 2005). Both groups used thapsigargin (sarcoplasmic-endoplasmic reticulum Ca^{2+}-ATPase (SERCA) blocker) to deplete the ER Ca^{2+} store content, as Ca^{2+} leaks out passively. Hits were defined by decreased SOC entry and confirmed in single cells by Ca^{2+} imaging and whole cell recording (Cahalan, 2009). In addition, the use of knock out mice for STIM1 and STIM2 demonstrated reduced capacitive Ca^{2+} entry (Liou *et al.*, 2005).

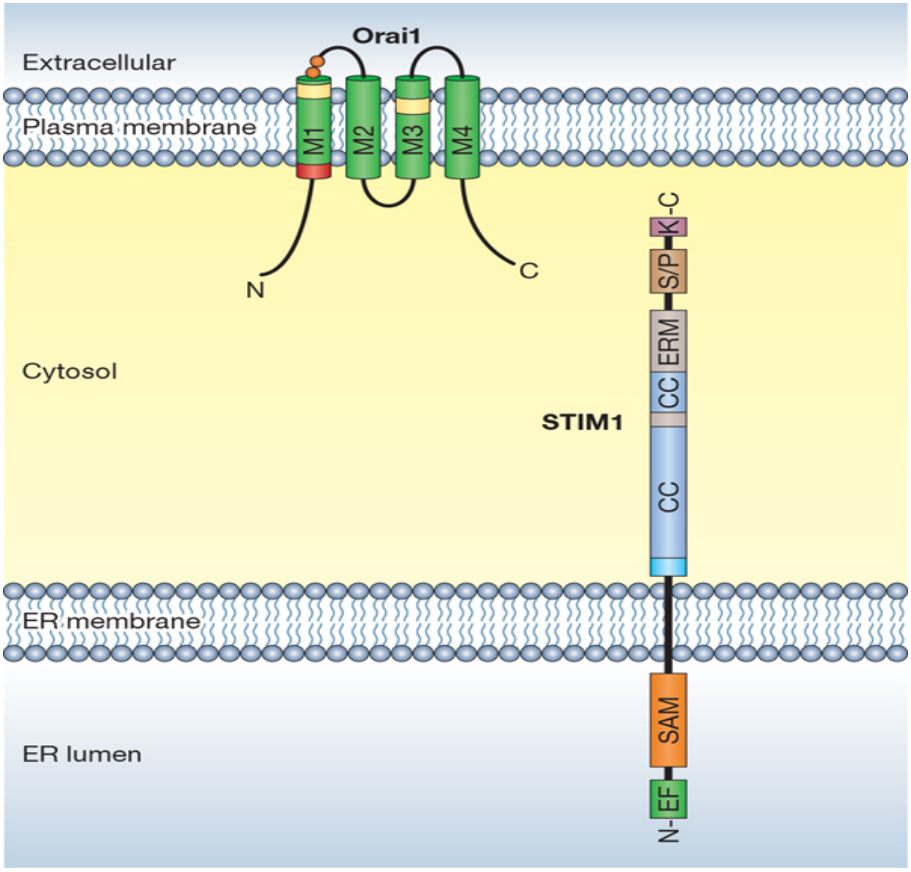

Figure 1.10 Illustration of STIM1 and Orai1 proteins (from Lewis *et al.*, 2007). STIM1 exists as a single-pass transmembrane protein typically located spanning the ER membrane in somatic human cells. A negatively charged EF hand acts as a luminal calcium sensor close to the N-terminus, next to the SAM domain which contributes to oligomerisation. In the opposing segment stretching into the cytosol, two coiled coil (CC) regions are joined to an acidic stretch comprising of the ezrin-radixin-moesin (ERM)-like domain through to the C-terminus. This acidic stretch is the most variable region of the protein with the serine-proline (S/P) rich section being altered to a proline-histidine rich region in STIM2, which otherwise shares 61% sequence identity with STIM1. All three Orai proteins are comprised of four transmembrane segments residing in the plasma membrane. Only the N-terminus of Orai 1 comprises of a proline/arginine rich region. All three Orai isoforms contain a CC region within their C-terminus, although their exact organisation differs between the isoforms.

A role for STIM as a Ca^{2+} sensor was first suggested due to its EF-hand Ca^{2+} binding motif. Further experiments using EF-hand mutants (to prevent Ca^{2+} binding) led to Ca^{2+} influx and CRAC channel activation, but without depletion of the ER Ca^{2+} store (Zhang *et al.*, 2005; Liou *et al.*, 2005). This ability of the EF-hand mutants to bypass the requirement for Ca^{2+}

store depletion convincingly demonstrated that the Ca^{2+} unbound state of STIM leads to CRAC channel activation (Cahalan, 2009).

Following Ca^{2+} store depletion and dissociation of Ca^{2+} from the EF hand, this initiates unfolding of the adjacent SAM domains and the subsequent oligomerisation of STIM proteins (Stathopulos *et al*., 2008, 2009; Cahalan, 2009). Chemically induced oligomerisation of STIM1 also resulted in translocation and activation of CRAC channels, without ER Ca^{2+} store depletion. However, the marked redistribution of STIM1 following Ca^{2+} store depletion was not accompanied by any obvious changes in bulk ER structure (Liou *et al.*, 2005; Zhang *et al.*, 2005). Forster resonance energy transfer (FRET) measurements determined that oligomerisation of STIM triggers translocation toward predetermined foci in the peripheral ER at junctions where close contact with the overlying plasma membrane can be formed Liou *et al.*, 2007; Muik *et al.*, 2008). STIM then conveys the message that the ER has been depleted and triggers SOCE, but does not form part of the CRAC channel itself (Cahalan, 2009). This process is spatially reproducible and rapidly reversible following signal termination and Ca^{2+} store refilling (Liou *et al.*, 2007; Smyth *et al.*, 2008).

1.11.3.2.2 Orai

The second component of this pathway has been identified as the transmembrane protein Orai. Orai (meaning the gates of heaven) was also originally identified using RNAi screening, with one group identifying mutations in Orai1 that lead to severe combined immune deficiency (SCID) (Feske *et al.*, 2006). Present in three isoforms within mammalian systems (Orai1-3), Orai1 unlike STIM1 is believed to solely reside within the plasma membrane

(Feske *et al.*, 2006). All three isoforms are predicted to contain four transmembrane segments and form Ca^{2+} selective plasma membrane channels. The N-terminus contains a proline/arginine-rich region and stretches into the cytoplasm along with the C-terminus (see Figure 1.10). There is also an N-glycosylation site within the extracellular loop between transmembrane segments 3 and 4 (Frischauf, 2008).

Evidence suggests that Orai1 proteins form the CRAC channel itself when co-expressed with STIM1. STIM1 has been demonstrated to couple functionally to all three Orai homologues in expression systems, to form very large CRAC-like currents (Mercer *et al.*, 2006; Lis *et al.*, 2007; DeHaven *et al.*, 2007). This was discovered by duplicating the unique biophysical fingerprint of the CRAC channel in patch clamp studies, which was then amplified 10-100-fold when STIM and Orai were over-expressed together in heterologous cells (Zhang *et al.*, 2006; Mercer *et al.*, 2006). Orai1 subunits were confirmed to form the CRAC channel pore, as point mutations of a key glutamate residue in the loop between transmembrane segments, caused a marked alteration of ion selectivity (Prakriya *et al.*, 2006; Vig *et al.*, 2006, Yeromin *et al.,* 2006).

Following Ca^{2+} store depletion, STIM1 organises Orai subunits into adjacent plasma membrane clusters (Penna *et al.*, 2008; Luik *et al.*, 2006; Xu *et al*., 2006), with Ca^{2+} influx through CRAC channels occurring precisely at these points (Luik *et al*., 2006). Total internal reflectance fluorescence (TIRF) microscopy has been used to pinpoint yellow fluorescent (YFP)-tagged STIM1 clusters to within 100-200nm of the cell surface (Liou *et al.,* 2005, 2007; Baba *et al*., 2006; Wu *et al*., 2006). Specifically, the cytosolic C-terminus of STIM

functions as the effector domain to open Orai across a 10-25nm ER-PM gap (Muik *et al.*, 2008; Calloway *et al.*, 2009). The precise region of STIM1 responsible for Orai recruitment and activation has been determined, known as both the CRAC activation domain (CAD) and STIM1 Orai activating region (SOAR) (Park *et al*., 2009 and Yuan *et al*., 2009 respectively). CAD/SOAR consists of STIM1 amino acid region 344-442 which is the minimal sequence required to fully activate Orai1 by binding to the N- and C-termini. This acts in combination with STIM1 amino acid region 450-485 to regulate the strength of the interaction (Yuan *et al*., 2009). CAD/SOAR regions have been demonstrated to directly activate CRAC independent of ER Ca^{2+} release and without the need of other molecules (Park *et al*., 2009). This conformational coupling mechanism strongly opposes a previously hypothesised diffusible messenger system which relies on the synthesis of a Ca^{2+} influx factor (CIF). CIF is produced by the ER in response to Ca^{2+} store depletion which acts to diffuse the 10-25nm ER-PM gap, synthesising $iPLA_2\beta$, culminating in the production of liposolids to activate CRAC (Bolotina, 2008), but its presence was proven unnecessary by these recent results. Additionally, all previous studies involving truncated STIM1 leading to inhibition of CRAC channel activation were due to disruptions within this essential amino acid region (Huang *et al.,* 2006; Baba *et al.,* 2006; Li *et al.,* 2007).

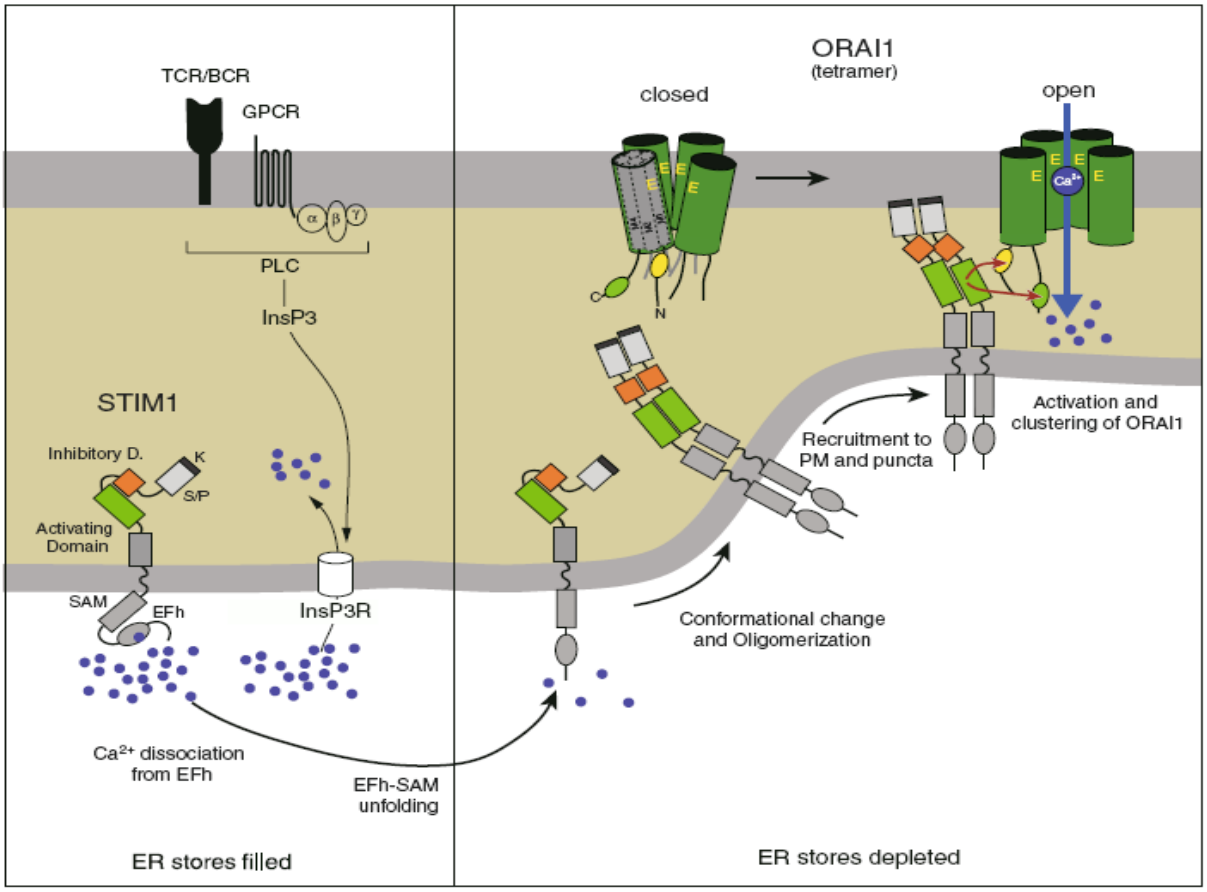

Figure 1.112 Diagram of STIM1 activating Orai1 during SOCE. Left panel shows EF hand of STIM1 bound to Ca^{2+} within an intracellular Ca^{2+} store. Depletion of Ca^{2+} triggers multimerisation as the EF hand and SAM regions unfold and STIM1 translocates to areas in the ER within close proximity of the plasma membrane (right panel). STIM1 binding organises Orai subunits into adjacent plasma membrane clusters, with Ca^{2+} influx through CRAC channels occurring precisely at these points**.** Diagram from Feske, 2009.

Within human sperm, SOCE may be responsible for extending transient $[Ca^{2+}]_i$ oscillations caused by agonist induced store mobilisation, such as a progesterone gradient (Harper *et al.,* 2004). TRPC channels and several mRNAs for TRPC1-7 have been found in mouse spermatogenic cells and TRPC1, 3 and 6 proteins in mature mouse sperm have been reported by Trevino *et al.* (2001). Studies using human sperm have also localised TRPC to the sperm head and flagellum (Castellano *et al.,* 2003). However, the more recent studies suggesting CRAC channels are also formed from subunits of Orai proteins (as discussed above) although

the presence of Orai and its Ca^{2+} store counterpart STIM have not yet been investigated in sperm.

1.11.3.3 Cyclic nucleotide-gated (CNG) channels

CNG channels are activated by the direct binding of the second messengers cAMP and/or cGMP, with a greater affinity for cGMP (Biel, 2008). This transmembrane tetrameric complex encodes changes in cAMP/cGMP concentrations into changes in membrane potential thus providing an entry pathway for Ca^{2+} to flood into the cell. Structurally, CNG channels belong to the superfamily of pore-loop cation channels having six α-helical segments (S1-S6) in the transmembrane core with an ion-conducting pore loop between S5 and S6 (Biel, 2008). CNG channels are well known for their central signal transduction roles in olfactory neurons and retinal photoreceptors and less so in other tissues such as brain, kidney and testis (Kaupp and Seifert, 2002).

Cyclic nucleotide signalling is imperative to normal sperm function, primarily due to the cAMP/ sAC/ PKA pathway essential for events such as capacitation as discussed in section 1.7. The cGMP pathway has also been reported to be involved in chemotaxis and flagella movement of marine invertebrate sperm (Revelli *et al.*, 2002). However, cGMP, its associated phosphodiesterases (PDEs, particularly PDE5) and protein kinase G (PKG), are notably low or absent in mammalian sperm (Lefievre *et al.*, 2000).

1.11.3.4 CatSpers

pH-sensitive CatSpers are expressed exclusively in sperm. Located in the principal piece of the flagellum, they are ideally placed for their involvement in motility regulation and chemotaxis. Structurally, they are similar to CNG channels, containing six transmembrane segments with a central Ca^{2+} selective pore. Four subunits have been identified; CatSper 1 (Ren *et al.*, 2001), CatSper 2 (Quill *et al.*, 2001), CatSper 3 and CatSper 4 (Lobley *et al*., 2003). In mature sperm, CatSper1 and CatSper2 have been localised to the principal piece of the flagellum, suggesting a role for CatSpers in motility. Transcripts of CatSper genes were detected at a greater frequency in human semen samples with high motility as opposed to those of low motility (Li *et al.,* 2007) and three brothers homozygous for a deletion on chromosome 15 that encoded part of CatSper2 were infertile (Avidan *et al.,* 2003). Furthermore, male mice that are null mutants for CatSper-1, -2, -3, -4 are motile, but their sperm are unable to become hyperactivated and are therefore infertile (Ren *et al.*, 2001; Quill *et al.*, 2003; Jin *et al.*, 2007; Qi *et al.,* 2007). Interestingly, two recent studies have found a role for CatSpers as the non-genomic progesterone receptor for sperm. By utilising novel patch clamp techniques for mature sperm, both groups concluded that nanomolar progesterone concentrations and alkaline pH potentiates a rapid Ca^{2+} influx through CatSper channels (Lishko *et al.,* 2011; Strunker *et al.,* 2011). The exclusivity of CatSpers to sperm coupled with its structural differences with genomic progesterone receptors poses an interesting option for the future development of male oral contraceptives.

1.11.4 Calcium clearance mechanisms

Ca^{2+} clearance mechanisms are essential in order to return to resting $[Ca^{2+}]_i$ levels following Ca^{2+} influx and are maintained by a combination of Ca^{2+}-ATPases, Na^{+}- Ca^{2+} exchangers and mitochondrial uniporters. These Ca^{2+} channels and exchangers have been demonstrated to be important in Ca^{2+} removal to the extracellular environment, or into intracellular stores (Berridge *et al.*, 2000; Wennemuth *et al.*, 2003).

1.11.4.1 Ca^{2+}-ATPases

Three types of Ca^{2+}-ATPases have been identified, including the sarcoplasmic endoplasmic Ca^{2+}-ATPase (SERCA), the secretory pathway Ca^{2+}-ATPase (SPCA) and the plasma membrane Ca^{2+}-ATPase (PMCA) (Michelangeli *et al*., 2005). These three channels show 30% sequence homology (Gunteski-Hamblin *et al*., 1992), all belong to the P-type ATPase family and transport ions through their channels by becoming transiently phosphorylated (de Meis and Vianna, 1979). SPCA distribution is more ubiquitous than its SERCA relative although not every organism contains both, for example *Arabidopsis thaliana* lacks an SPCA homolog and *Saccharomyces cerevisiae* lacks a SERCA homolog (Wuytack *et al*., 2003). However, it does appear that every eukaryote contains at least one type of Ca^{2+}-ATPase.

PMCAs are the largest and fastest of the three Ca^{2+}ATPases, present in four isoforms (PMCA1-4) and about 12 splice variants (Carafoli and Brini, 2000). PMCA1 and 4 are ubiquitously distributed throughout many somatic cells, indicating a housekeeping role in addition to more specific pathways. PMCA has been detected using Western blotting and

immunofluorescence labeling within rat spermatids and mouse spermatozoa (Berrios *et al*., 1998; Wennemuth *et al*., 2003). In mouse sperm, PMCA (specifically the PMCA4 isoform) has been localised to the principal piece of the flagellum (Wennemuth *et al.*, 2003; Okunade *et al.*, 2004), suggesting a role in motility. The development of PMCA4 knock-out mice have supported these findings as they have seemingly normal spermatogenesis, but were infertile due to the inability of the sperm to hyperactivate (Prasad *et al.*, 2004; Okunade *et al.*, 2004).

The presence of SERCA in sperm is currently unclear. Groups such as Rossato *et al.* (2001), demonstrated that 10-100nM concentrations of thapsigargin (classified as a SERCA inhibitor) initiated Ca^{2+} oscillations, culminating in the acrosome reaction. However, Western blots probed with SERCA-specific antibodies proved fruitless by our group (Harper *et al.*, 2005). In addition, we demonstrated that thapsigargin was required in the 1-10 μM range to produce Ca^{2+} oscillations (Harper *et al.*, 2005), concentrations that result in non-specific SERCA inhibition (Wictome *et al.*, 1992). However, a possible role of SERCA during spermatogenesis has been speculated (Jimenez-Gonzalez *et al.*, 2006).

Within somatic cells, SPCA is typically located on the Golgi body or secretory vesicles and two isoforms have been identified, SPCA1 and SPCA2. Interestingly, sperm possess neither of these organelles yet RT-PCR studies have identified mRNA for SPCA1 in rat spermatids (Wootton *et al.,* 2004) and Western blotting has detected SPCA1 in mature human spermatozoa (Harper *et al.,* 2005). The latter study also localised SPCA1 to anterior mid-piece and posterior region of the head. Furthermore, using the pharmacological agent Bis(2-hydroxy-3-tert-butyl-5-methyl-phenyl) methane (bis-phenol; a SERCA and SPCA inhibitor

(Kirkman-Brown *et al.*, 1994; Harper *et al.*, 2005)) our group were able to induce Ca^{2+} mobilisation in sperm and also stop progesterone-induced Ca^{2+} oscillations (Harper *et al.*, 2005). Therefore SPCA localisation and the ceasing of progesterone-induced Ca^{2+} oscillations using an SPCA inhibitor, further reflects the possibility for the RNE acting as a Ca^{2+} store within this region (Ho and Suarez, 2003).

1.11.4.2 Na^{+}-Ca^{2+} exchanger (NCX)

The two types of the Na^{+}-Ca^{2+} exchanger (NCX) are NCX and K+ dependent NCX (NCKX). NCX is a passive ion transport system that operates by utilising the electrochemical gradient produced as $3Na^{+}$ ions pass through the channel to remove $1Ca^{2+}$ ion into the extracellular environment or intracellular stores (Reeves and Hale, 1984, Jimenez-Gonzalez *et al.,* 2006). NCX activity is essential in cardiac muscle for example, as it is the primary pathway of Ca^{2+} removal from ventricular myocytes (Weber *et al*., 2002). NCX is also able to operate in reverse mode to assist Ca^{2+} influx (Jimenez-Gonzalez *et al.,* 2006; Baartscheer *et al*., 2011) and therefore contribute to Ca^{2+} homeostasis.

Briefly, NCX has been identified in rodent, bovine and sea urchin sperm with localisation studies pinpointing to the flagellum (Bradley *et al.*, 1980; Rufo *et al.,* 1984; Su *et al.*, 2002). However the role of NCX appears to be reduced post-ejaculation as for bovine sperm NCX is inhibited by seminal proteins (Rufo *et al.*, 1984).

1.11.4.3 Mitochondrial uniporter

Mitochondria are tubular organelles that accumulate Ca^{2+} under normal physiological conditions (Jimenez-Gonzalez *et al.,* 2006). Encompassed by a double membrane, the outer mitochondrial membrane is permeable to ions and small proteins with a molecular weight of less than 10kDa, whilst the ion impermeable inner mitochondrial membrane forms folds (called cristae) into the internal space (Bianchi *et al*., 2004). The area between the two membranes is utilised by respiratory chain complexes leading to the production of an electrochemical gradient of approximately 180mV, thus initiating a large driving force for Ca^{2+} into the organelle (Bianchi *et al*., 2004) and enabling mitochondria to act as a Ca^{2+} buffer. Ca^{2+} moves down this electrochemical gradient independent of other ions with no co-transport or exchange systems and is thus called the mitochondrial uniporter.

Mitochondrial Ca^{2+} uptake is essential for mitochondrial homeostasis via the activation of enzyme complexes such as pyruvate and isocitrate dehydrogenase (McCormack *et al*., 1990). Also, mitochondria help to generate and shape $[Ca^{2+}]_i$ signals either by polarised cells having mitochondria unequally distributed providing particular areas with a finely tuneable Ca^{2+} buffer or by coupling mitochondria with other intracellular Ca^{2+} stores or channels in order to regulate Ca^{2+} levels (Jouaville *et al*., 1998). In addition, mitochondria are able to induce cell apoptosis via the release of cytochrome C into the cell cytoplasm (Gunter *et al.*, 2000).

Mitochondria are located within the midpiece region of sperm where they form an important Ca^{2+} buffer. Studies have shown that mitochondria can accumulate Ca^{2+} into the matrix space (Storey and Keyhani, 1973; Babcock *et al.*, 1975), but that this accumulation varies between species and stage of development (Vijayaraghavan and Hoskins, 1990; Wennemuth *et al*., 2003). Moreover, mitochondrial uncoupling via application of 0.1-1.5 mM 2,4-dinitrophenol does not affect intracellular store mobilisation whilst human sperm are responding to progesterone (Harper *et al.*, 2004). Therefore mitochondria are involved in $[Ca^{2+}]_i$ homeostasis in sperm but to a limited degree (Jimenez-Gonzalez *et al.*, 2006).

1.11.5 Mobilisation of stored Ca^{2+}

Most cells contain intracellular organelles with the capacity to store Ca^{2+} such as the endoplasmic reticulum, sarcoplasmic reticulum, mitochondria and the nuclear envelope. The ability of cells to store Ca^{2+} is essential as high $[Ca^{2+}]_i$ can be cytotoxic and the release of stored Ca^{2+} can be used to amplify incoming Ca^{2+} signals. Two channels with the capability of regulating the mobilisation of stored Ca^{2+} are the inositol 1,4,5-trisphosphate receptor (IP_3R) and the ryanodine receptor (RyR).

In human sperm, there is evidence for at least two intracellular Ca^{2+} stores. Firstly, the acrosome stores Ca^{2+} and displays IP_3Rs on the outer acrosomal surface. Mobilisation of Ca^{2+} from this store is essential in exocytosis of the acrosomal contents to the zona pellucida surface (Bailey and Storey, 1994). Secondly, there is a Ca^{2+} store in the sperm neck/midpiece region although its identity remains controversial. The RNE is a likely candidate and/or the

cytoplasmic droplet situated around the sperm neck (Naaby Hansen *et al*., 2001; Harper *et al*., 2004, 2005). Other studies indicate the mitochondria, as similarly to somatic cells, sperm mitochondria can accumulate Ca^{2+} (Wennemuth *et a*l., 2003).

1.11.5.1 Inositol 1,4,5-trisphosphate receptors (IP_3Rs)

Inositol 1,4,5-trisphosphate (IP_3) is a ubiquitous water soluble second messenger formed via the hydrolysis of phosphatidylinositol 4,5-bisphosphate (PIP_2). IP_3Rs are activated by IP_3 engagement culminating in Ca^{2+} release to the intracellular environment (Michelangeli *et al.*, 1995, Bootman *et al.,* 2001). Three isoforms of the tetrameric IP_3R channel have been identified namely IP_3R1, 2 and 3 sharing over 74% sequence homology in humans (Taylor *et al*., 1999), but differing in their affinities for IP_3 (Iwai *et al.,* 2007).

All three IP_3R mRNA isoforms (IP3R1-3) have been detected in rat sperm, although expression patterns vary during spermatogenesis (Tovey *et al.,* 1997). Isoform specific IP_3R antibodies have detected IP_3R1 in human sperm, localised to the anterior acrosome (Ho and Suarez, 2003; Kuroda *et al.*, 1999). In correlation with this location, after the acrosome reaction has occurred IP_3R labelling is substantially decreased or lost (Tomes *et al.*, 1996, Kuroda *et al.*, 1999). However, further studies in bovine sperm have also localised IP_3R1 to the RNE (Ho and Suarez, 2001). Interestingly, anti-IP3 staining can also be seen in the RNE for about half of human spermatozoa even though <90% of cells are also stained in the acrosomal region (Naaby-Hansen *et al.*, 2001). Therefore, the literature currently indicates

that two IP_3R controlled Ca^{2+} stores are present within sperm, reinforced by studies showing the presence of calreticulin (a Ca^{2+} binding protein) in correlating areas.

1.11.5.2 Ryanodine receptors (RyRs)

The second possible channel responsible for the mobilisation of intracellular Ca^{2+} stores is the RyR. RyR's are intracellular Ca^{2+} channels involved in controlling Ca^{2+} induced Ca^{2+} release (CICR) and are named due to their binding ability to the plant alkaloid ryanodine. The three RyR genes encode 3 different RyR protein isoforms sharing evolutionally origin, 66-70% amino acid homology and homotetrameric structural similarities (each consisting of four 560 kDa polypeptide subunits) (Eu *et al.*, 1999). The three isoforms RyR1, RyR2 and RyR3 were primarily discovered in skeletal, cardiac and brain tissues respectively, but their existence is now documented to be far more widespread, although not as ubiquitous as their structural counterpart the IP_3R (Otsu *et al*., 1990; Xu *et al*., 1993; Trevino *et al*., 1998).

The presence of RyR in sperm is controversial. Initial data obtained by RNAse protection analysis and *in situ* hybridisation, suggested that RyR1 and RyR3 mRNA were present in areas of seminiferous epithelium abundant in spermatocytes and spermatids in mice (Giannini *et al.*, 1995). Tevino *et al.* (1998) confirmed these findings with immunocytochemical studies using specific antibodies to all three isoforms, detecting RyR1 and RyR3 proteins during spermatogenesis and also detecting RyR3 in mature mouse sperm. Chirella *et al.* (2004) confirmed the presence of RyR1 in spermatogonia, spermatocytes and spermatids by using Western blot and RT-PCR but did not detect RyR3 at the protein level (only mRNA in a

mixed population of germ cells). Also, no RyR presence at any stage of bovine sperm development was detected using similar immunocytochemical methods or labelling with a fluorescent ryanodine analogue BIODIY-FL-X (Ho and Suarez, 2001). In contrast, staining was observed in mouse sperm primarily in the distal two-thirds of the sperm head, the tip of the sperm head, connecting body and proximal flagellum (Trevino *et al.*, 1998) and BIODIPY-FL-X staining was also reported in the sperm neck region of human sperm (Harper *et al.*, 2004). Currently, only RyR3 has been identified in mature sperm of any species (Trevino *et al.*, 1998). However, detection by immunocytochemical and pharmacological methods for RyR3 in human sperm is especially difficult due to a lack of specific antibody probes and its unresponsiveness to caffeine stimuli (Hakamata *et al.*, 1994). Also, epididymal sperm from RyR3 knock-out mice were shown to hyperactivate, implying functional RyR3 is not an essential prerequisite for hyperactivation (Ho and Suarez, 2003). In contrast, RyR1 knock-out proved fatal at gestation preventing the significance of RyR1 in hyperactivation being discovered (Ho and Suarez, 2001).

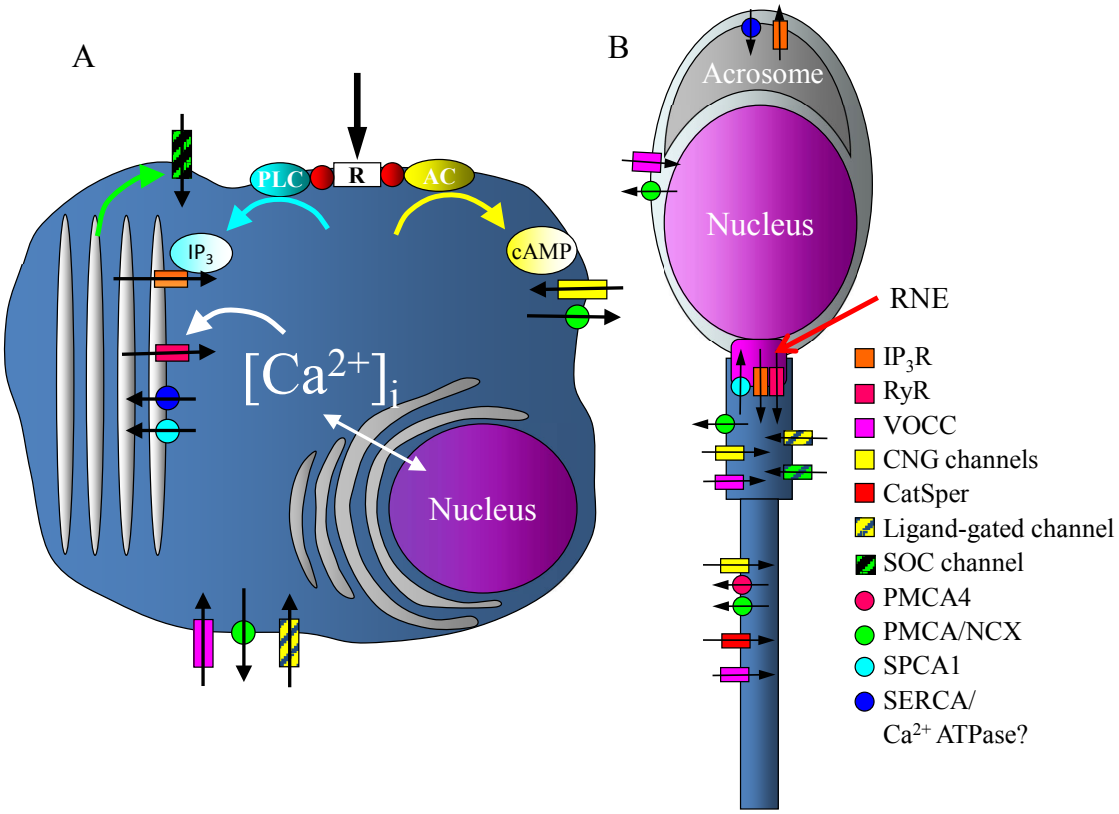

Figure 1.12 Diagrams of the Ca^{2+} influx and efflux channels present in (A) somatic cells and (B) sperm cells (adapted from Bedu-Addo *et al*., 2008).

RESEARCH AIMS

The aims of this research thesis were to:

Confirm a SOCE system operates in capacitated human sperm.

Investigate the presence and localisation of proteins of the SOCE system, namely STIM and Orai and to examine if punctate structures can be observed when intracellular Ca^{2+} stores are depleted.

Study the effects of pharmacological modulation on SOCE using different doses of 2-APB on the progesterone-induced biphasic $[Ca^{2+}]_i$ response, in discreet areas of the cell.

Investigate if 10μM loperamide, a further modulator of SOCE, has any effects on the progesterone-induced biphasic $[Ca^{2+}]_i$ response.

Analyse the presence of RyRs in human sperm, to help determine if they may contribute to the SOCE system.

CHAPTER TWO: MATERIALS AND METHODS

2.1 Materials

Protein G Plus/Protein A Agarose suspension, 4-(2-aminoethyl)benzenesulfonylfluoride (AEBSF) hydrochloride and 2-aminoethoxydiphenyl borate (2-APB) were all purchased from Calbiochem (distributed by Merck Biosciences, Beeston, Nottingham, UK). Oregon Green 488 BAPTA-1/AM and Fura-2 AM were supplied by Molecular Probes (distributed by Invitrogen, Paisley, UK) and complete protease inhibitor cocktail tablets (PI) from Roche Diagnostics (Lewes, East Sussex, UK). Poly-D-lysine, poly-L-lysine and pluronic F-127 were purchased from Invitrogen (Paisley, UK), who also supplied NuPAGE 3-8% Tris-Acetate gels and NuPAGE antioxidant. Nitrocellulose (NC) membranes and were purchased from GE healthcare UK (St. Giles, Bucks, UK) and were blocked from non-specific binding using ProtoBlock System Kit from National Diagnostics (distributed by Geneflow Ltd, Fradley, Staffordshire, UK). Chemiluminescence was produced using Lumi-GLO, an enhanced chemiluminescence kit from Insight Biotechnology (Wembley, Middlesex, UK). Slides were fixed using fluorescence mounting medium from Dako Cytomation (Ely, Cambridgeshire, UK). 5ml round-bottom, 15ml and 50ml tubes were supplied by Falcon (Becton Dickinson, USA).

Anti-RyR1 (2142) antibodies and anti-RyR2 (1093) antibodies were a kind gift from Professor Tony Lai (Wales Heart Institute, Cardiff, UK) as were the GFP–tagged STIM1, MYC–tagged Orai1, GFP-tagged CD9, MYC-tagged SHIP1 and pApuro DNA from Dr. Michael Tomlinson (University of Birmingham, UK). The RyR positive controls of skeletal

and brain sarcoplasmic reticulum homogenates (SR and BR respectively) in addition to anti-SPCA1 (LTQQ) and Bis(2-hydroxy-3-tert-butyl-5-methyl-phenyl) methane (bis-phenol) were generously donated by Dr. Frank Michelangeli (University of Birmingham, UK). Other antibodies used including streptavidin donkey anti-rabbit and streptavidin conjugated TEXAS-RED were purchased from Jackson Immunoresearch Laboratories (Stratech Scientific, Soham, Cambridgeshire, UK). The anti-rabbit IgG (Dylight (R) 800 conjugate) used in conjunction with the Odyssey system was purchased from Cell Signaling Technology (Boston, USA). Anti-Orai1-3 and anti-STIM1-2 antibodies along with corresponding blocking peptides were purchased from ProSci incorporated (distributed by Axxora, Bingham, UK). In addition, a further anti-Orai1 antibody (O8264) was purchased from Sigma (Poole, Dorset, UK). The MYC antibody was from Upstate Biotechnology. All other chemicals including thapsigargin, progesterone, digitonin, EGTA, FITC-conjugated Pisum sativum and the green fluorescent protein (GFP) antibody were purchased from Sigma (Poole, Dorset, UK).

Cook (Queensland, Australia) supplied Sydney IVF fertilization medium. Dulbecco's modified Eagle's medium (DMEM) and penicillin/streptomycin/glutamine were purchased from PAA laboratories (Somerset, UK). All other media's including Earle's balanced salt solution (EBSS) and low Ca^{2+} EGTA-buffered EBSS (~$3x10^{-7}$M Ca^{2+}) were prepared in the laboratory (see appendix I) and were supplemented immediately prior to use with 0.3% (w/v) fatty acid free bovine serum albumin (BSA) obtained from JRH Biosciences (Andover, UK).

2.2 Preparation of human sperm

Human semen samples were provided by research donors via masturbation after a minimal two days sexual abstinence at either the Birmingham Women's hospital (Human Fertilisation and Embryology Authority (HFEA) centre 0119) or at the Biosciences department of the University of Birmingham (life and health sciences ethical review committee ERC 07-009), in accordance with the HFEA Code of Practice (version 7). All donors gave informed written consent under the Central Office for Research Ethics Committees (COREC) ethical approval.

2.2.1 Sperm preparation using a Percoll gradient

Human sperm were liquefied for at least 30 minutes at 37°C and 5% CO_2 and 1-1.5mls were layered onto a Percoll gradient, as described previously in Lefievre *et al*. (2007). The gradient consisted of two 1ml Percoll fractions (80% and 40%) made isotonic with M medium (137mM NaCl, 2.5mM KCl, 20mM HEPES, 10mM glucose). Centrifugation at 600 gravitational acceleration (g) for 20 minutes caused separation of sperm from seminal plasma and into two subsets according to density (Figure 2.1). Typically, morphologically normal sperm are found below the 80% Percoll fraction, whereas abnormal or immature sperm vary in density and are therefore found at the 40/80% interface (Huszar and Vigue, 1993; Sbracia *et al*., 1996). Following Percoll separation, the resulting 40% and 80% sperm fractions were counted using an improved Neubauer hemocytometer (as according to the World Health Organisation methods, 1999) to evaluate sperm concentration and washed once by centrifugation (2000g, 5 minutes) with phosphate buffered saline (PBS).

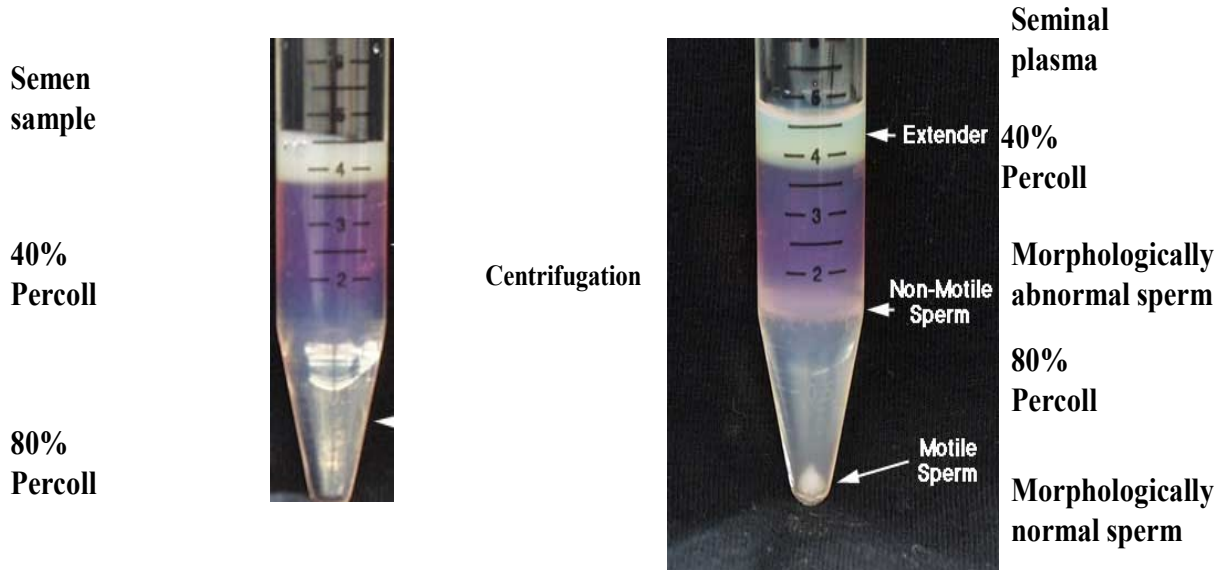

Figure 2.1 Separation of sperm from semen using a discontinuous Percoll density gradient. Modified from www.ansci.wisc.edu/jjp1/ansci_repro/lab/lab11/lab11_2003/percoll3.html.

2.2.2 Preparation of human sperm using the swim-up technique

Alternatively, for $[Ca^{2+}]_i$ imaging and fluorimetry experiments, following semen liquefaction, motile sperm were collected using a swim-up technique (Mortimer, 1994; Harper *et al.*, 2003, Nash *et al.*, 2010). 0.3ml semen samples were pipetted into round-bottom tubes, beneath 1ml EBSS supplemented with 0.3% BSA (pH 7.3-7.4) and incubated at an angle of 45 º for 1 hour, at 37ºC, 5% CO_2 (FFigure 2.2). Motile cells were collected from the top 0.7ml of the tubes and sperm concentration was again determined using an improved Neubauer hemocytometer. Sperm concentrations were readjusted to 6 x 10^6 sperm/ml with EBSS/0.3% BSA and were left to capacitate for 6 hours at 37ºC, 5% CO_2, prior to imaging experiments (Kirkman-Brown *et al*., 2000).

2.3 Immunocytochemistry and confocal microscopy

For this section and sections 2.4, 2.5, 2.6 and 2.7, all semen samples were prepared using the Percoll separation technique.

2.3.1 RyR, STIM and Orai immunocytochemistry

For RyR, STIM or Orai immunodetection, PBS washed human sperm were readjusted to 25 x 10^6 sperm/ml in PBS and 25µl aliquots were dispersed onto glass slides pre-coated with poly-L-lysine (to promote adhesion), followed by air drying. Cells were fixed with 4% (v/v) formaldehyde solution for 6 minutes. Formaldehyde was then removed via three PBS washes. Slides were subsequently incubated for 15 minutes with PBS supplemented with 0.2% (v/v) Triton X-100 (0.2% TPBS) to permeabilise cells and then washed for 5 minutes with 0.1% (v/v) Triton X-100 (0.1% TPBS). Non-specific binding was minimised by incubating cells with 10% goat serum diluted in 0.1% TPBS for 1 hour at room temperature. Cells were incubated overnight at 4˚C with either the primary polyclonal antibodies specific for RyR1 or RyR2 (1/25), or primary polyclonal antibodies specific for the STIM (1/25) or Orai isoforms (1/10). Following overnight incubation, the slides were extensively washed with PBS/0.1%TPBS. To amplify detection we used the secondary antibody biotin-SP anti-rabbit (1/200) for 1 hour. Antibody staining was made visible by a 1 hour incubation with streptavidin conjugated TEXAS RED (1/360). FITC was avoided to minimise any effects of mitochondrial autofluorescence at this wavelength. Again, the slides were washed extensively in PBS and mounted using prolong anti-fade mounting medium. Control slides were produced using the same method as described above but omitting the primary antibody incubation step to evaluate non-specific binding.

2.3.2 Isolation of cytoplasmic droplets

Sperm obtained from the 40/80% Percoll interface were washed in PBS and stored at 4°C overnight (Roberts *et al.*, 1976). To detach the droplets from sperm, the suspension was homogenised by passage (five times) through a 25 gauge needle resuspended in 0.25M sucrose solution made in PBS (Oko *et al.*, 1993). The suspension was centrifuged at 100g for 10 min at 4°C. Supernatant containing the droplets were poured over dry glass wool, loosely packed into two 10ml columns (Roberts *et al.*, 1976). Columns were washed with PBS. The first 6ml filtrate was centrifuged at 25,000g, for 10 min, at 4°C to pellet the droplets.

2.2.3 STIM1 translocation

STIM1 translocation following intracellular Ca^{2+} store depletion was examined using the method described above with the following modifications; PBS washed human sperm were readjusted to 50 x 10^6/ml in PBS and 15µM bis-phenol, or nothing (controls) were added to the cell suspensions for 8 minutes at this point. Following a 5 minute centrifugation at 2000g, cells were the fixed in 1.5ml microtubes using 4% formaldehyde, for 6 minutes. Cells were again centrifuged, resuspended in PBS and smeared onto poly-L-lysine treated slides as above. Cells were permeabilised and probed with anti-STIM1 antibodies as above. The acrosomal status of cells treated with or without 15µM bis-phenol were assessed using FITC-conjugated Pisum Sativum Agglutinin, added at 50µg/ml to the Streptavidin conjugated TEXAS RED.

Images were acquired using an imaging system controlled by Openlab (version 3.1.7, Improvision, Coventry, UK) with a Hammamatsu Orca Camera attached to a Nikon TE2000 microscope. Fluorescence and phase contrast images were taken at X 60 magnification using an oil Plan Fluor DIC H lens. These experiments were conducted at room temperature unless stated otherwise. In addition, confocal microscopy was performed using either a Zeiss 510 laser-scanning confocal microscope (Zeiss, Welwyn Garden City, UK) and processed using the Zeiss LSM Image Examiner software or a Leica DMIRE2 inverted microscope (Leica Microsystems, Milton Keynes, UK) using the software TCS SP2 in order to view staining in more detail.

2.3.4 Image analysis

STIM1 movement following Ca^{2+} store depletion was assessed using AQM software. Regions of interest were drawn around three separate sperm regions including the acrosome, posterior head and neck (PHN) and midpiece. The average fluorescence intensity for each region was acquired for a minimum of 20 cells over at least 5 fields of view per slide. Raw values were imported into Microsoft Excel and the percentage fluorescence for each area of each individual cell was calculated. Average fluorescence intensities for each region were calculated and comparisons of STIM1 distribution were made between cells with intracellular store depletion using bis-phenol and negative controls.

2.4 Western blotting of STIM and Orai

Washed sperm were resuspended at 2 x 10^6 in 20µl PBS supplemented with 1% Triton X-100. Samples were centrifuged at 2000g for 5 minutes and supernatant transferred to a fresh 1.5ml microtube. 20µl 1x SDS-PAGE (sodium dodecyl sulphate polyacrylamide gel electrophoresis) sample buffer was added to the insoluble fraction and 4µl 5x SDS-PAGE sample buffer was added to the soluble fraction. Alternatively for the Orai1 Western blot (using the Sigma anti-Orai1 antibody), ~500 x 10^6 sperm were solubilised using IP buffer (see immunoprecipitation below) followed by brief sonication. For both methods samples were then incubated at 95°C for 5 minutes and separated on SDS-PAGE gels under reducing conditions. SDS is an anionic detergent which acts by denaturing any secondary and non-disulphide linked tertiary protein structures and imparting a negative charge to a protein in relation to its mass. SDS-PAGE then allows for sample fractionation in relation to protein size as the negatively charged proteins are attracted to the anode (Crambach and Rodbard, 1971). STIM1 and STIM2 with an estimated molecular weight 77-96 kDa, were separated on a 10% gel (Manji *et al.*, 2000). Alternatively, Orai 1-3 with an estimated molecular weight of 33-35 kDa were separated using a 15% gel, as migration speed through the gel is directly related to protein size (Lis *et al.,* 2007). Proteins were electrotransferred onto nitrocellulose (NC) membranes for 1 hour at 100V. Non-specific binding sites were blocked with ProtoBlock System Kit prepared as according to instructions, for 1 hour. Following a brief TTBS (tris buffered saline; 150mM NaCl, 20mM Tris-HCl (pH 7.8) supplemented with 0.1% Tween-20) wash, NC membranes were incubated with either anti-STIM1, anti-STIM2 (both at 1/1000 in TTBS), anti-Orai1, anti-Orai2 or anti-Orai3 (all at 1/250 in TTBS) overnight with gentle agitation. After

extensive washing with high salt TTBS (TBS: 0.5M NaCl, 20mM Tris-HCl (pH 7.8) supplemented with 0.1% Tween-20), membranes were incubated for a further hour with the corresponding peroxidase-conjugated affinipure donkey anti-rabbit IgG (1/10000) and positive bands were detected by chemiluminescence. Finally, silver staining of NC membranes were preformed to ensure equal protein loading (Jacobson and Karsnas, 1990). Alternatively, following incubation with the primary antibody, membranes were prepared for use with the Odyssey Infrared Imaging System (LI-COR). This method involved a 1 hour incubation with an alternative secondary antibody; anti-rabbit IgG (Dylight) (1/20,000 in TTBS), extensive washing with TTBS and bands were detected using near-infrared (NIR) fluorescence as opposed to chemiluminescence.

Where possible, antibodies were preadsorbed with or without their corresponding blocking peptides to determine antibody specificity. To prepare antibodies with blocking peptides, blocking peptides were added in excess (1mg antibody: 5mg blocking peptide) for two hours at room temperature with constant rotation to allow blocking to occur. Experiments using peptide-preadsorbed and non-preadsorbed antibodies were performed in parallel.

2.5 Immunoprecipitation

2.5.1 Immunoprecipitation of RyRs

For RyR immunoprecipitation (IP), washed human sperm (~500 x 10^6 per condition) were solublised using IP buffer (150mM NaCl, 20mM Tris, pH 7.4, 2mM DTT, 1% Triton X-100) and briefly sonicated. IP buffer also contained protease inhibitors (PI) consisting of 10% PI cocktail and 1mM AEBSF hydrochloride (PI/AEBSF), which were also added at further intervals throughout the experiment in an effort to decrease protein degradation. Samples were then incubated at 4°C for 1 hour with constant mixing.

Solubilised proteins were collected via a 15 minute centrifugation at 18,000g and 4°C, to pellet insoluble proteins. Two pre-clearing steps involving 2 x 30 minute incubations with 30µl protein G plus/A agarose beads were implemented to minimise none specific binding with the beads in later steps. The incubations were performed at 4°C with centrifugation at 2500g for 5 mins to remove beads after use. Anti-RyR antibodies (10µg) and fresh PI/AEBSF were added and the suspension was nutated overnight at 4°C. The following morning protein G plus/A agarose beads (10µl per µg primary antibody) were added in addition to fresh PI/AEBSF and the suspension was nutated for 2 hours at 4°C. Immunocomplexes were precipitated using centrifugation at 2500g for 4 min and washed 3 times with IP buffer and then twice with PBS. The Protein G plus/A agarose beads were removed by re-suspension in 1x SDS-PAGE sample buffer.

2.5.2 Immunoprecipitation of STIM and Orai

STIM1 and Orai1 were immunoprecipitated as above with the following modifications; 1µg of either STIM1 or Orai1 antibodies were used to pre-coat 20µl of protein G plus/A agarose beads (33% slurry suspension) and nutated overnight in 750µl IP buffer. Sperm were solublised using IP buffer followed by sonication and only one pre-clearing step with 20µl protein G plus/A agarose beads for one hour was used. Sperm lysates were then centrifuged at 11000g for 10 minutes and supernatant transferred to fresh 1.5ml microtubes. The pre-coated protein G plus/A agarose beads were washed three times with IP buffer and the remaining supernatant was aspirated away. Equal volumes of sperm protein lysate were added to the antibody coated protein G plus/A agarose beads and nutated for 90 minutes.

All samples were incubated at 70°C for 10 minutes and protein detection was performed via Western blotting as above for STIM and Orai proteins but with the following modifications for RyR detection. Samples were run on a 3-8% tris-acetate Nupage gel, with anti-oxidant added to the electrophoresis buffer (1/400). The transfers onto NC membranes were performed using transfer buffer preferable for high molecular weight proteins (20% v/v methanol, 0.1% w/v SDS, 380mM glycine and 50mM Tris) and were performed overnight using a cooling system at 4°C, at 1.2 A (constant current). Finally, we used high salt TTBS washes (see appendix I), in an effort to further decrease background staining. The same primary and secondary antibodies were used as for Western blotting.

2.6 Calcium phosphate transfection of HEK-293T cells

The HEK-293T [HEK (human embryonic kidney) – 293 cells expressing the large T-antigen of SV40 (simian virus 40)] cell line was cultured in Dulbecco's modified Eagle's medium (DMEM) supplemented with 10% heat-inactivated fetal bovine serum (FBS), 100 U/ml penicillin, 100µg/ml streptomycin and 0.292 mg/ml glutamine, at 37°C in a humidified 5% CO_2 incubator. 24 hours prior to transfection, cells were plated at a density of 3 x 10^6 per 10cm plate (Protty *et al.*, 2009). Expression constructs for GFP (green fluorescent protein) – tagged STIM1 and MYC–tagged Orai1 in addition to the positive controls GFP-tagged CD9 and MYC-tagged SHIP1 and negative control pApuro DNA, were transiently transfected into HEK-293T cells using the calcium phosphate protocol (Kingston *et al.*, 2001). Briefly, 5µg of each construct was mixed with 450µl dH_20, 63µl 2M calcium chloride in a 5 ml tube, followed by the drop-wise addition of 500µl 2x HEPES buffered saline [HBS (2.0g/L dextrose, 10.g/L HEPES, 0.74g/L KCl, 16g/L NaCl, 0.27g/L $Na_2HPO_4.2H_2O$)] and left to precipitate for 5-15 minutes. Using a 1ml pipette, air was bubbled through the solution for 10 seconds then added to the various plates of HEK-293T cells. The media was replaced on the next day and cells were harvested by scraping into 1ml PBS 48 hours post-transfection. Pelleted cells were then lysed with 1% Triton x-100. Transfection efficiency is typically within the region of 50-80% (Gavrilescu and Van Etten, 2007).

To confirm successful transfections, proteins were separated by Western blotting (as above) using SDS-PAGE gels under reducing conditions. NC membranes were probed with either anti-STIM1 (1/1000), anti-GFP (control, 1/1000), anti-Orai1 (1/200, Sigma) or anti-MYC (control, 1/1000) and nutated overnight. Following three TTBS washing steps, membranes

were incubated for a further hour with the corresponding secondary antibodies. For anti-STIM1, anti-Orai1 and anti-MYC this was peroxidase-conjugated affinipure donkey anti-mouse IgG (1/10,000) and for anti-GFP this was peroxidase-conjugated affinipure donkey anti-rabbit IgG (1/10,000).

2.7 Single cell imaging

For this section and sections 2.9 and 2.10, all semen samples were prepared using the swim-up separation technique. Following capacitation for 6 hours at 6 x 10^6 sperm/ml, human sperm concentration was reduced to 4 x 10^6 sperm/ml again using EBSS supplemented with 0.3% BSA. 200 µl aliquots of cells were then loaded with 12µm Oregon Green BAPTA-1/AM (0.6% DMSO, 0.12% pluronic F-127) for 30 minutes. Following this incubation, the entire aliquot was transferred to a perfusable imaging chamber for 30 minutes, at 37ºC and 5% CO_2. The lower surface of the chamber was formed by a coverslip pre-coated with 1% poly-D-Lysine which was used to attach cells. The imaging chamber was connected to a Nikon TE300 inverted fluorescence microscope, fitted with a Cairn Opto LED light source (Cairn Research, Kent, UK). The chamber was first perfused with fresh medium to remove excess dye and unattached sperm. Following a control period of 3-5 minutes media could be changed and pharmacological agents added by replacing saline in the perfusion header (Nash *et al.*, 2010). During experiments temperature was kept at a consistent 25+/-1ºC with a constant flow of medium at approximately 0.4 ml/minute (Figure 2.2). Images were captured every 10 seconds using a 40x objective and a Q Imaging Rolera-XR cooled CCD camera or

an Andor Ixon 897 EMCCD camera controlled by a PC running iQ software (Andor Technology, Belfast, UK).

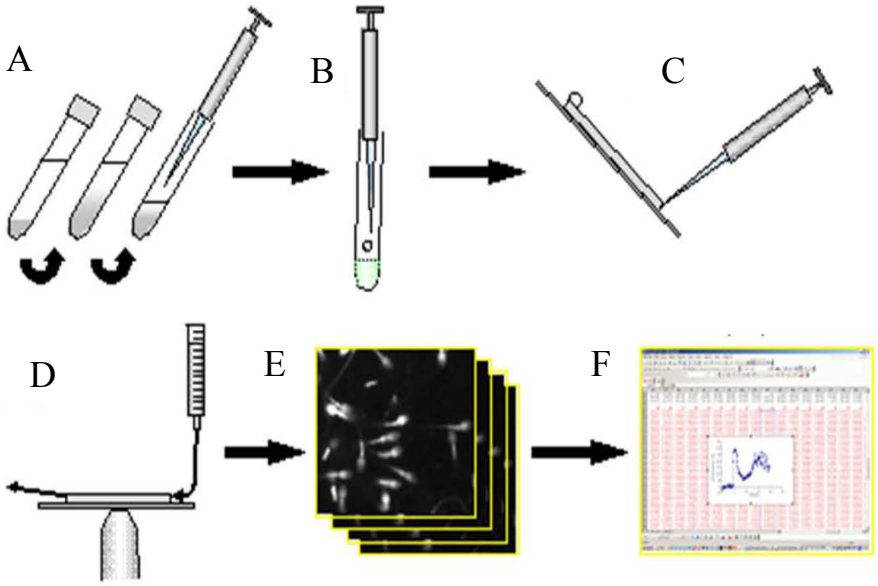

Figure 2.2 Illustration of the key steps involved in Ca^{2+} imaging for sperm. **(A)** Semen is layered below sEBSS for 1 hour at a 45° angle. Motile cells transverse the tube towards the surface and are removed. **(B)** Following a 5-6 hour incubation, cells are incubated with Oregon Green 488 BAPTA-1/AM and then **(C)** transferred to an imaging chamber. **(D)** The chamber is connected to a microscope and perfused with media containing various pharmacological agents. **(E)** Time lapse images are captured and **(F)** data is processed offline in excel.

2.7.1 Data processing

Data were processed offline using AQM software as described in Kirkman-Brown *et al.* (2000) and Nash *et al.* (2010). A region of interest (ROI) was drawn around the posterior head region of individual sperm and average fluorescence intensities per pixel were obtained as opposed to per cell, to enable analysis of $[Ca^{2+}]_i$ in discreet areas of the cell. A free area of

background was also selected to enable automatic background subtraction by the software. Cells were excluded if they were not adhered correctly and thus migrated away from the ROI during the recording, or if they were dying (displayed as a gradual loss of fluorescence during the control period). These raw values were imported into Microsoft Excel and normalized using the equation $R = [(F - F_{rest}) / F_{rest}] \times 100\%$, where R is normalized fluorescence intensity, F is fluorescence intensity at a time *t* and F_{rest} is the mean of at least 10 determinations of F obtained during the control period.

For each time point the mean value of R for all cells in the experiment (R_{tot}) was calculated to provide the mean normalised head fluorescence and then plotted on a time-fluorescence intensity graph (Figure 2.2). The amplitude of the progesterone $[Ca^{2+}]_i$ transient was calculated by taking the average the three points spanning the peak of the R_{tot} trace. Amplitude of the sustained component of the $[Ca^{2+}]_i$ response to progesterone was calculated by taking the average of 3 consecutive points 4 min after application of progesterone. In experiments where cells were exposed first to 2-APB or loperamide and then to progesterone, the data were first processed as described above but the incremental increase in fluorescence induced by progesterone was determined by defining a second 'control' period composed of the four images captured immediately before application of progesterone. The progesterone-induced fluorescence increment was then calculated by subtracting values of R (or R_{tot}) during the 'APB control' from those recorded at the peak of the progesterone-induced $[Ca^{2+}]_i$ transient or during the sustained phase of the response. Microsoft Excel was used to perform paired or unpaired *t* tests on normalised fluorescence values as appropriate. Statistical significance was set at $P<0.05$.

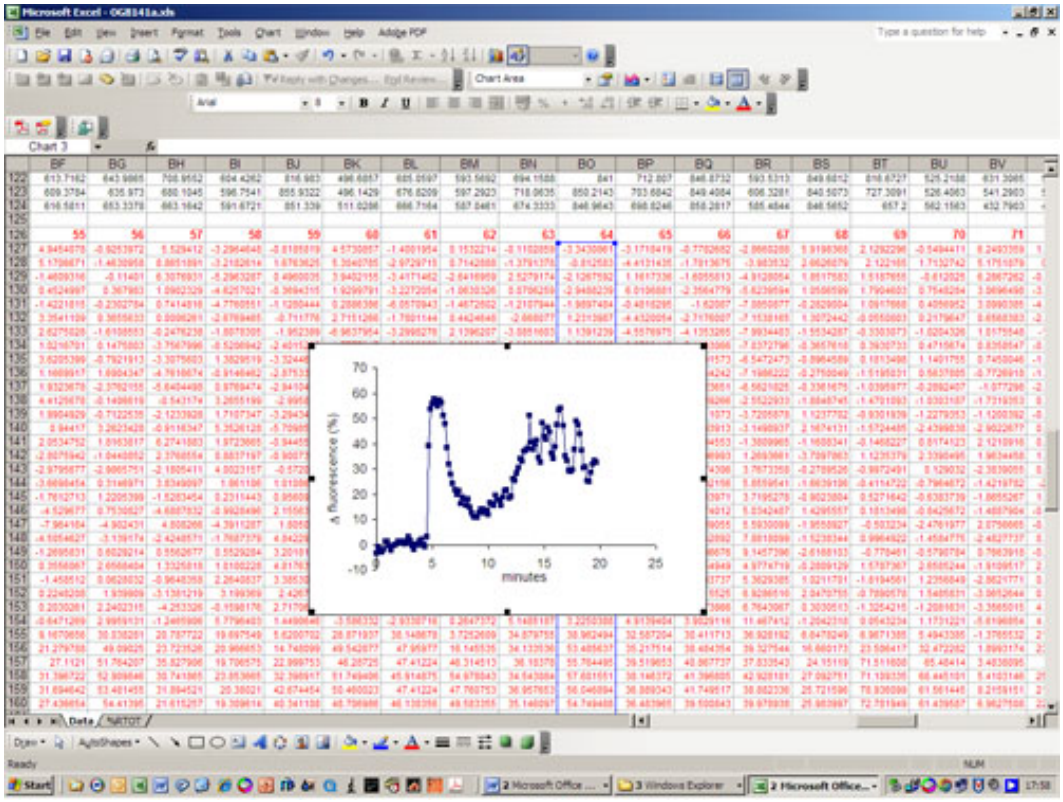

Figure 2.3 Analysis of a single sperm cell exposed to progesterone and graphical representation of the data using Excel. Figures in black are the time series of fluorescence data, arranged vertically. Figures in red (below) are normalized data obtained using the equation mentioned above for all cells. The graph shows a normalised time fluorescence intensity graph for cell 64 in this experiment. With progesterone stimulation at 5 minutes, a transient rise in fluorescence followed by a slow rise and series of small oscillations can be observed.

2.8 Fluorimetry

Following capacitation for 6 hours, 2ml aliquots at 6 x 10^6 sperm/ml were loaded with Fura-2 AM in 10% Pluronic F-127 (1μM final extracellular concentration) for 12 minutes at 37°, 5% CO_2. Samples were then centrifuged at 300g for 5 minutes and resuspended in 2ml fresh sEBSS for a further 18 minutes at 37°, 5% CO_2 for dye de-esterification. Experiments were conducted in a 2.5ml quartz cuvette warmed to 37° and magnetically stirred to ensure rapid distribution of any agents added. An initial minimum control period of 200s was observed at the start of experiments to ensure a resting $[Ca^{2+}]_i$ was maintained. Fluorimetry was performed using a Perkin-Elmer LS50B luminescence spectrometer running Fl-Winlab version 2.01 with an excitation wavelength pair of 340/380 nm and emission held at 510 nm. Slit width was set at 15nm with a sampling rate of 12.5Hz. Calibration of $[Ca^{2+}]_i$ was determined at the end of each experiment using 20μM digitonin to initiate a maximal response followed by 47uM (pH7.4) of the Ca^{2+} chelator EGTA, thus providing a minimal response (Bedu-Addo *et al*., 2005, Harper *et al*., 2006). We assumed a K_d of 285 nM for fura-2 at 37°C (Groden *et al*., 1991).

2.8.1 Data processing

Resting $[Ca^{2+}]_i$ was calculated as the average for the 100s period preceding any 2-APB or progesterone addition. For each trace the transient response was measured by first identifying the absolute maximum value during the transient and then averaging the data for a 4s period

spanning this point. Amplitude of the transient was taken as the difference between the calculated peak $[Ca^{2+}]_i$ and resting $[Ca^{2+}]_i$.

2.9 Computer assisted semen analysis (CASA)

Sperm motility parameters were assessed using computer assisted semen analysis (CASA) (Hamilton Thorne running IVOS v.10). Capacitated cells at 6 x 10^6/ml were centrifuged at 300g and resuspended in either sEBSS 0.3% BSA with the concentration adjusted to 10 x 10^6/ml. 100µl aliquots were treated with or without agonist stimulants and 5µl sperm suspension aliquots were introduced to either side of a 20-µm depth sperm analysis chamber (2X-CEL, Hamilton Thorne Biosciences). Experiments were performed at 37°C with CASA slides pre-warmed. Hyperactivated sperm were defined were defined by track velocity (VCL) >100µm/s, linearity (LIN) <65µm/s and lateral head displacement (ALD) >7.5µm/s.

2.9.1 Data processing

Percentages of different motility patterns were automatically registered by the CASA machine while performing the experiments. Changes in motility parameters due to different treatments were compared in Microsoft excel using paired t-tests. Statistical significance was set at $P<0.05$.

CHAPTER THREE: STORE-OPERATED CALCIUM ENTRY AND THE EXPRESSION OF STIM AND ORAI PROTEINS IN HUMAN SPERM.

3.1 Abstract

STIM transmembrane proteins act as Ca^{2+} sensors typically residing in the ER of somatic cells. Upon store depletion and dissociation of Ca^{2+} from the EF hand, STIM oligomerises and translocates toward predetermined foci in the ER juxtaposed to the plasma membrane. Orai proteins are recruited to these pre-determined points on the plasmalemma where they are stimulated by activation domains on STIM to mediate store-operated Ca^{2+} entry (SOCE). These clusters of STIM and Orai at the plasma membrane can be visualised as punctate structures. SOCE systems in human sperm were thought to be mediated by canonical transient receptor potential (TRPC) channels; however the identification and characterisation of STIM and Orai proteins has called for a re-evaluation of SOCE systems in human sperm. Western blotting and immunoprecipitation has confirmed the presence of STIM1, STIM2, Orai1, Orai2 and (possibly) Orai 3 in human sperm. Immunofluorescence labelled the midpiece/neck region for all four proteins and over the acrosome for Orai1, consistent with areas of known intracellular Ca^{2+} stores. No bulk movement of STIM1 following induced SOCE using 15μM bis-phenol (an SPCA inhibitor) was observed, as STIM and Orai proteins generally both localise to similar regions within the midpiece/neck. It is therefore likely that upon store depletion STIM1 multimerises and then forms associations with Orai proteins in the overlying plasma membrane. Punctate-like structures could be seen in human sperm but were not further induced by Ca^{2+} store depletion, possibly due to the size constraints of the cell and/or microscopic resolution. In summary, human sperm express STIM and Orai proteins at known sites of Ca^{2+} storage, although they do not show all of the characteristic traits of STIM and Orai overexpression as seen in other cell types.

3.2 Introduction

An approach to studying SOCE in sperm has been to monitor cytoplasmic/intracellular calcium concentrations ($[Ca^{2+}]_i$) via the use of fluorescent Ca^{2+} indicator dyes, using fluorimetric measurements from cell populations or, more recently Ca^{2+} imaging of single cells (see Nash *et al.*, 2010 for overview). Blackmore (1993) utilised fluorimetry to investigate the effect of thapsigargin, a SERCA inhibitor, which can passively release Ca^{2+} from intracellular stores. In response to thapsigargin he observed a sustained $[Ca^{2+}]_i$ increase due to Ca^{2+} entry from the extracellular environment. Further experiments involving incubation in an EGTA-buffered media (to chelate extracellular Ca^{2+}) showed no increased $[Ca^{2+}]_i$ with thapsigargin treatment, until Ca^{2+} was reintroduced into the media and then a sustained rise in $[Ca^{2+}]_i$ was recorded. Studies by other groups have also noted that sperm cells bathed in EGTA-buffered media exhibited a small transient rise in intracellular Ca^{2+} when thapsigargin was applied indicating stored calcium was being released (Rossato *et al.,* 2001; Williams and Ford, 2003). However, the high doses of thapsigargin used in such experiments (5-30μM) have been questioned as they are 10-300 times the dose required for complete SERCA block (O'Toole *et al*., 2000; Williams and Ford, 2003; Harper *et al*., 2005). An alternative drug; Bis(2-hydroxy-3-tert-butyl-5-methyl-phenyl) methane (bis-phenol) which acts as an SPCA inhibitor, has yielded similar results at mobilising Ca^{2+} stores but at SPCA-selective concentrations (Harper *et al*., 2005). These results suggest that sperm possess an intracellular Ca^{2+} store and that although mobilisation may not always be detectable, it is sufficient to induce SOCE. Also SOCE has been reported in the sperm of other species namely mouse (O'Toole *et al.*, 2000), sheep (Dragileva *et al.*, 1999), and sea urchin (Gonzalez-Martinez *et al.*, 2004, Ardón *et al.*, 2009).

As discussed previously (section 1.11.3), TRPC have been suggested to form SOC channels in somatic cells and various isoforms have been detected in mouse sperm, localised over the anterior head region (Trevino *et al.*, 2001; Jungnickel *et al.*, 2001; Castellano *et al.,* 2003; Stamboulian *et al.*, 2005). However, the discovery of STIM and Orai in 2005 and 2006 respectively (Liou *et al.*, 2005; Feske *et al*., 2006), has called for re-evaluation of SOCE systems present in human sperm. The transmembrane protein STIM1 acts as a Ca^{2+} sensor typically residing in the ER of somatic cells, monitoring Ca^{2+} via an EF-hand in the lumen of the storage organelle. Upon store depletion, STIM proteins oligomerise and translocate toward predetermined foci in the ER juxtaposed to the plasma membrane (Liou *et al.,* 2005). Orai proteins are then 'recruited' to these pre-determined points on the plasmalemma where they are activated by the SOAR domain on STIM to form CRAC channels, permitting the entry of iCRAC (Feske *et al.*, 2006; Yuan *et al*., 2009). The resulting Ca^{2+} influx is involved in several cellular processes in somatic cells including cell differentiation and growth and is implicated in events such as hyperactivation and chemotaxis in sperm (Yoshida *et al*., 2003; Harper *et al*., 2004; Fischer, 2007). The refilling of intracellular Ca^{2+} stores terminates the Ca^{2+} influx, causing STIM and Orai proteins to return to their resting conformations.

Interestingly, STIM1 has been demonstrated to form distinct 'puncta' or 'hotspots' at the plasma membrane following Ca^{2+} store depletion, which does not coincide with any bulk ER movement (see Figure 3.1). This was shown by both light and then electron microscopy, with puncta displaying surface areas ranging 1-10μm (Liou *et al.*, 2005; Mercer *et al.,* 2006; Zhang *et al.*, 2005; Baba *et al.*, 2006). This phenomenon is due to STIM proteins normally forming a

dimer stabilised by C-terminal coiled-coil interactions that can heteromultimerise when ER Ca^{2+} stores are filled (Cahalan, 2009; Penna *et al*., 2008). However when stores are depleted, further oligomerisation occurs within seconds, initiating the translocation of STIM toward ER-plasma membrane junctions in clusters (Liou *et al.*, 2005; Muik *et al.*, 2008). The formation of punctuate structures following Ca^{2+} store depletion is therefore a functionally significant process that should be examined in human sperm.

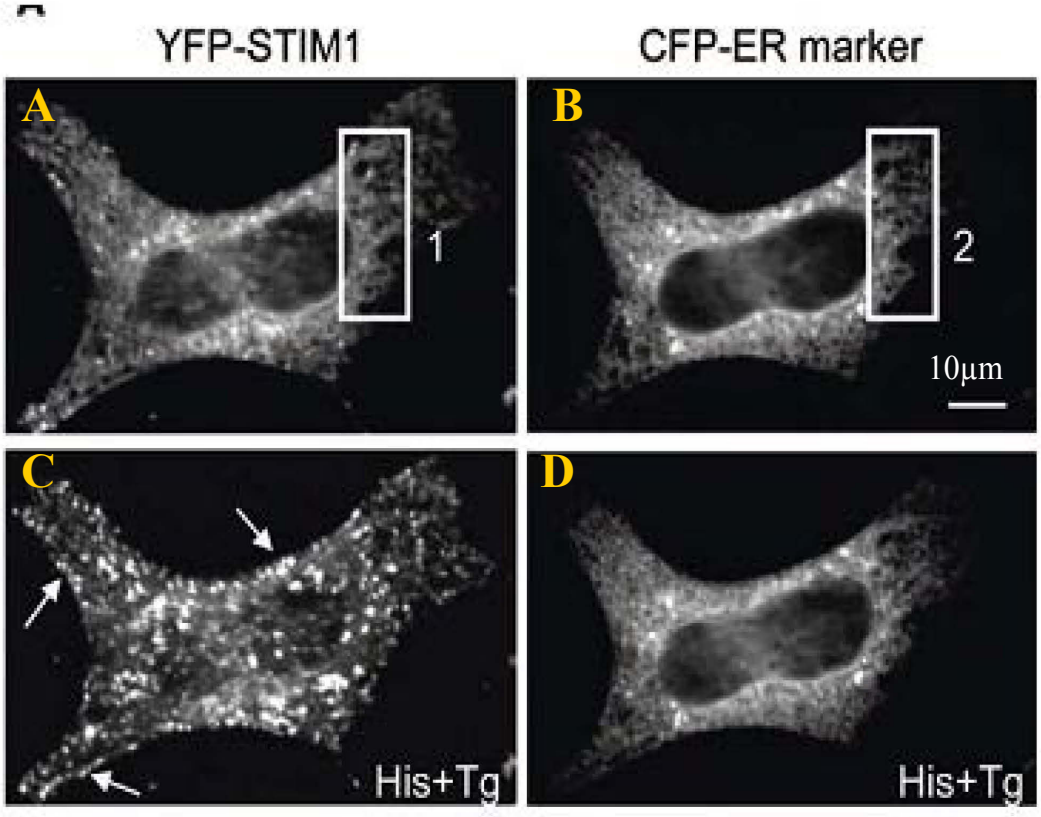

Figure 3.1 HeLa cells co-transfected with YFP-STIM1 and a CFP-ER marker. YFP-STIM1 redistributes into punctuate structures (arrows) following Ca^{2+} store depletion using thapsigargin (A, C). There is no change in ER distribution following Ca^{2+} store depletion (B, D). Images from Liou *et al.* (2005).

Chapter Aims

The aims for this chapter were to firstly confirm that a SOCE system operates in capacitated human sperm, using single cell Ca^{2+} imaging techniques to examine the effects of 15μM bis-phenol treatment on resting cells and on cells where intracellular Ca^{2+} stores have been depleted. Following this, was to investigate the presence and localisation of STIM and Orai proteins using Western blotting, immunoprecipitation and immunocytochemical techniques. Additionally, we also wanted to examine the formation of punctate structures following Ca^{2+} store depletion.

3.3 Results

3.3.1 Bis-phenol induces SOCE.

We utilised Ca^{2+} imaging techniques to confirm that pharmacological treatment of human sperm was able to induce SOCE. 15μM bis-phenol (SPCA inhibitor) caused a sustained increase in fluorescence within 4 minutes (bis-phenol R_{tot}= 48.7±3.4%, n=17; Figure 3.2A). In more than a quarter of cells (26.4±4.2%, 5 experiments, 250 cells) this sustained $[Ca^{2+}]_i$ elevation was preceded by a clear $[Ca^{2+}]_i$ transient, consistent with mobilisation of a small Ca^{2+} store followed by activation of store-operated Ca^{2+} influx (Figure3.2A). To confirm that this effect of SPCA inhibition reflected an increase in Ca^{2+} flux at the plasma membrane, we repeated this procedure on cells bathed with EGTA-buffered saline ($[Ca^{2+}]$ ≈$3*10^{-7}$M). As described previously, superfusion with EGTA-buffered medium causes a marked fall in $[Ca^{2+}]_i$ (Harper *et al.*, 2004; Bedu-Addo *et al*., 2007). Application of bis-phenol (15μM) after exposure to EGTA-buffered saline for approximately 4 minutes had a negligible effect upon $[Ca^{2+}]_i$, (some cells showing a small transient elevation). However, upon introduction of sEBSS (1.8mM Ca^{2+}, containing 15μM bis-phenol) to the imaging chamber there was a large, sustained increase in $[Ca^{2+}]_i$, consistent with activation of SOCE (Figure 3.2B).

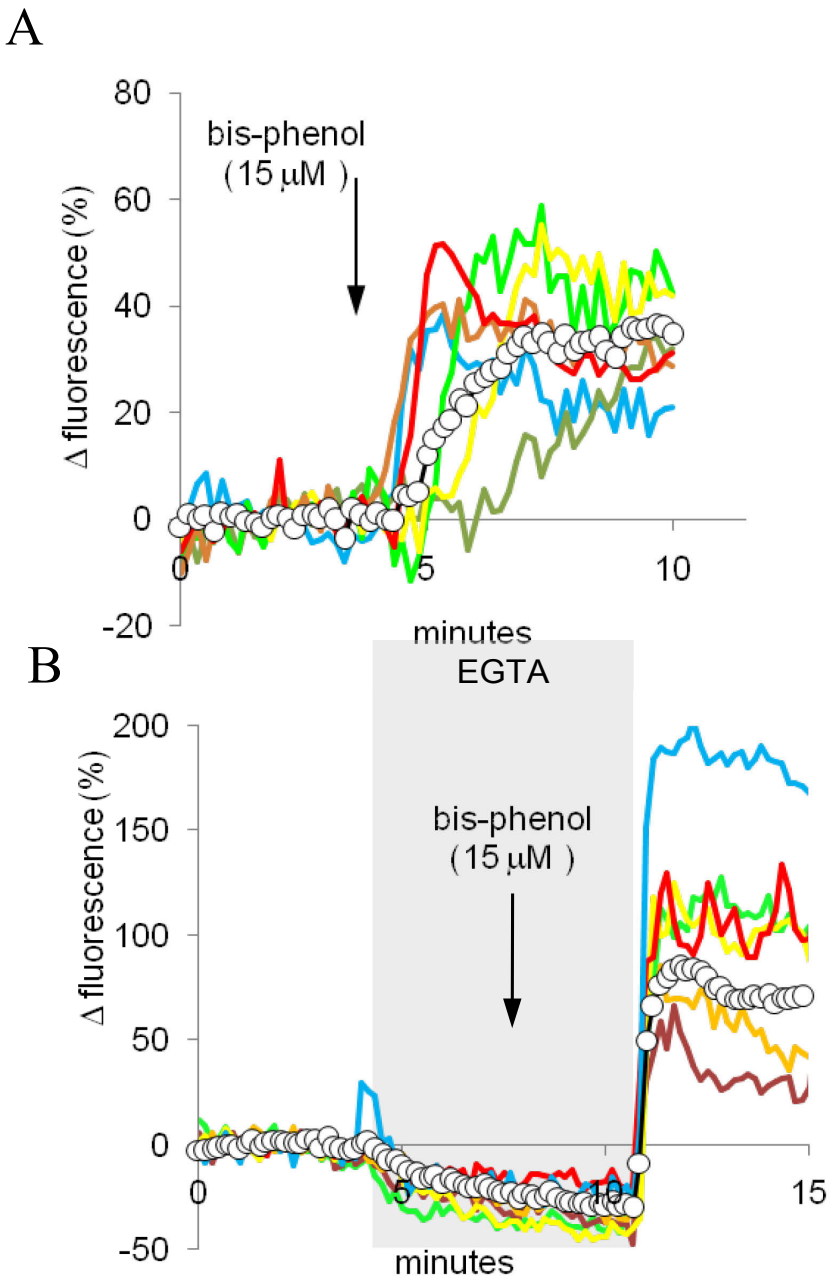

Figure 3.2 Effects of bis-phenol on resting $[Ca^{2+}]i$ and on cells induced to perform SOCE. **(A)** Capacitated sperm were perfused with sEBSS and 15µM bis-phenol was added to the perfusion media from 4 minutes (arrow). **(B)** Alternatively, cells were perfused with sEBSS which was switched to EGTA-buffered sEBSS ($3x10^{-7}$M Ca^{2+}, shown by grey shading) at 4 minutes. Mid-way through this period 15µM bis-phenol was added (arrow). Reintroduction of standard sEBSS to the chamber caused $[Ca^{2+}]_i$ to return to levels above the control. Individual cell traces are shown by coloured lines. Experimental averages (R_{tot}) are shown by white circles.

3.3.2 Detection and distribution of STIM and Orai in human sperm.

Preliminary data for our STIM and Orai detection studies via Western blotting has shown that Orai1 and Orai2 are detected at low levels in human sperm at their appropriate molecular weight (~35 kDa), within the TX-100 insoluble fraction (Figure 3.3). A clear band for Orai3 (~33 kDa) wass detected, again in the insoluble fraction. For Western blotting, Orai 1-3 were separated using a 15% gel and STIM1-2 with a higher estimated molecular weight (77-96 kDa) were separated on a 10% gel (Manji *et al.*, 2000), as migration speed through the gel is directly related to protein size (Lis *et al.,* 2007). STIM1 was detected between 77-90 kDa, but it is present in low levels in comparison with STIM2, both of which were detected in total sperm. Separating sperm into TX-100 soluble and TX-100 insoluble sperm fractions was conducted to assist in determining the localisation of the STIM and Orai proteins within sperm.

HEK-293T cells were transfected with STIM-GFP and Orai-MYC constructs in order to develop positive controls for further experiments (Figure 3.4). Since these constructs had not been used before, CD9-GFP and SHIP-Myc positive controls were included in the experiment. Whole cell lysates were Western blotted for STIM1, Orai1, GFP and Myc. STIM1 blotting demonstrated the expected bands between 103-115 kDa, corresponding to the molecular weight of STIM1 (77-90 kDa) plus GFP (25 kDa). STIM1 was not detected in the mock transfection (pApuro) or the CD9 control. In contrast, GFP blotting identified bands corresponding to GFP-tagged STIM1 and CD9 which is predicted at 50 kDa. Again, no bands were detected in the mock transfection, confirming specificity of the STIM1 and CD9 bands. Also, Orai1 blotting demonstrated the expected bands between 36-40 kDa corresponding to

the molecular weight of Orai1 (35 kDa) plus Myc (1.2 kDa). Again, Orai1 was not detected in the mock transfection or the MYC tagged SHIP control. In contrast, MYC blotting identified bands corresponding to MYC-tagged Orai1 and MYC which is predicted at 30 kDa. Again, no bands were detected in the mock transfection, confirming specificity of the Orai1 and MYC bands.

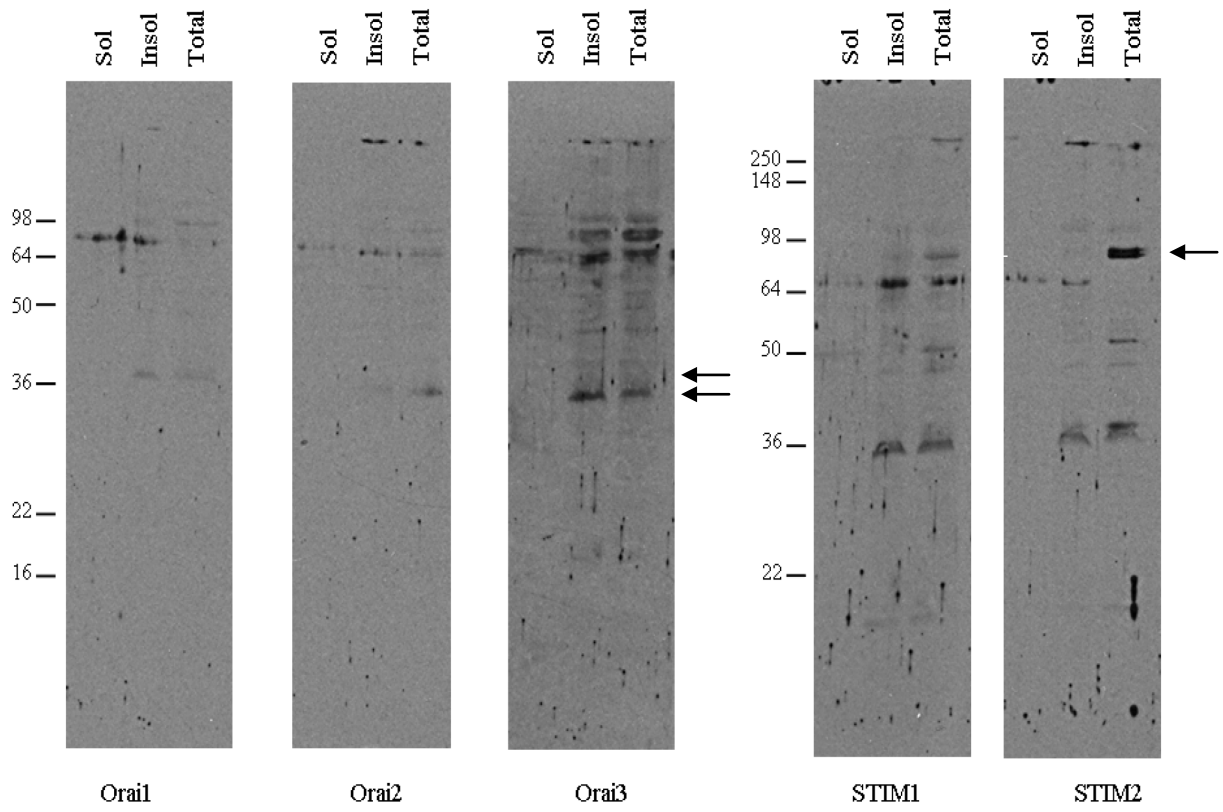

Figure 3.3 Orai and STIM proteins can be detected in human sperm**.** Total sperm (Total), TX-100 soluble (Sol) and TX-100 particulate (Insol) sperm fractions were subjected to either 15% SDS-PAGE for Orai or to 10% SDS-PAGE for STIM detection and probed with anti-Orai1-3 and anti-STIM1-2 antibodies respectively from ProSci incorporatedBands at the correct molecular weights are marked by the arrows.

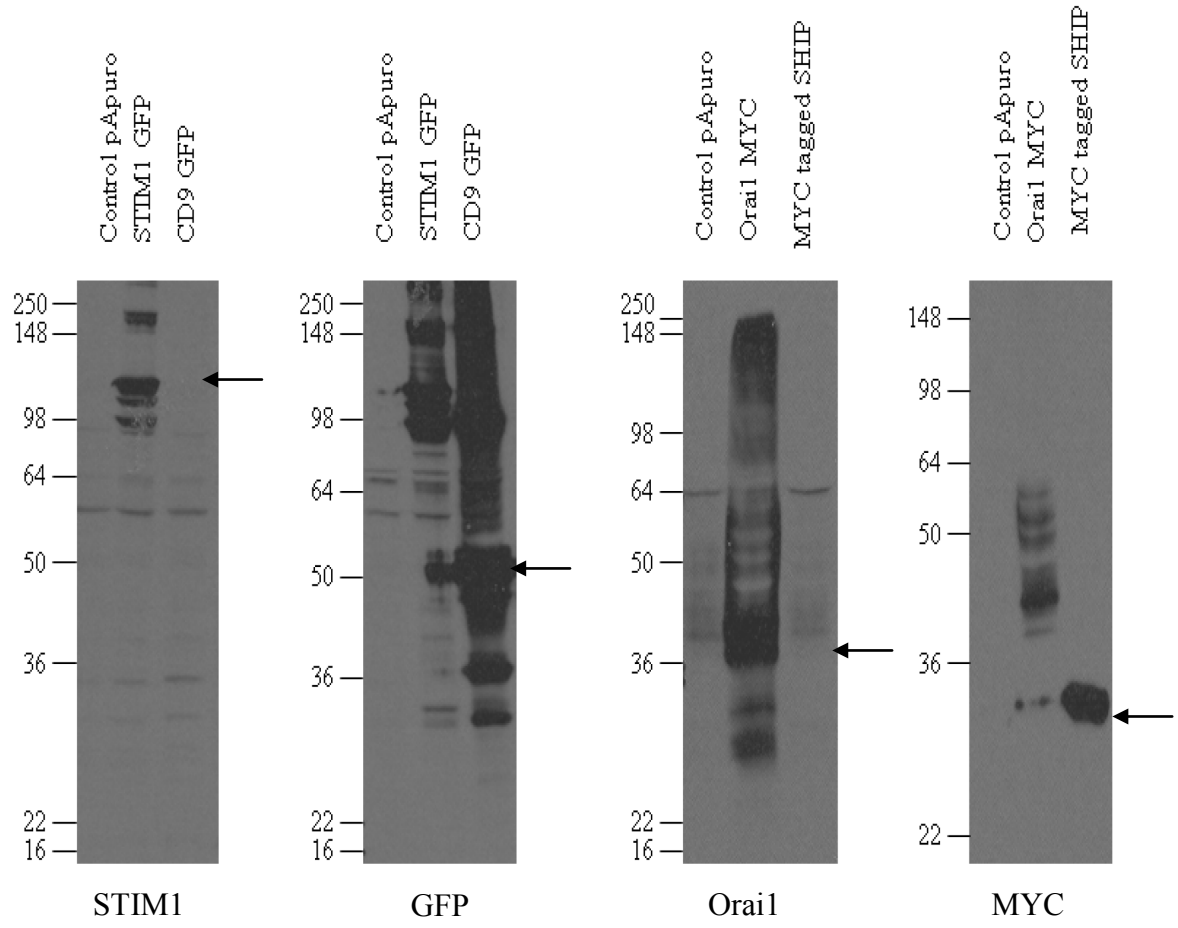

Figure 3.4 Orai1 and STIM1 transfections in HEK-293T cells. Lysed HEK-293T cells transfected with either an empty vector control (pApuro), STIM1-GFP, or CD9-GFP and were subjected to 10% SDS-PAGE, transferred to nitrocellulose and incubated with either anti-STIM1 (ProSci) or anti-GFP (Sigma). Also, lysed HEK-293T cells transfected with empty vector control (pApuro), Orai1-MYC or MYC tagged SHIP were subjected to 15% SDS-PAGE, transferred to nitrocellulose and incubated with either anti-Orai1 (ProSci) or anti-MYC (Upstate Biotechnology). Bands at the correct molecular weights are marked by the arrows.

Blocking peptides provided by ProSci were used in the following experiments to examine the specificity of the Orai and STIM antibodies used. They consist of the peptides used to immunise the animals that produced the antibody. Therefore, pre-adsorbtion of the antibody with an excess of its target peptide inhibits binding with the protein of interest and any subsequent binding is therefore non-specific. The effectiveness of the blocking peptides for the antibodies we used has previously been described (Feske *et al.*, 2006; Zhang *et al.*, 2006; Soboloff *et al.*, 2006).

Orai1 was detected by Western blotting of sperm lysate (of ~500 x 10^6 sperm), at the appropriate molecular weight of 35 kDa, when probing using the Sigma anti-Orai1 antibody (O8264) (Figure 3.5). This band corresponds with the Orai-Myc positive control and the heavy staining with this antibody between 35 and 50 kDa, probably reflects glycosylation (Gwack *et al.*, 2007). Prior to this, we attempted to detect Orai1 using far fewer sperm (2 x 10^6), followed by Western blotting and probing using the anti-Orai1 antibody produced by ProSci (4041) but only a weak band could be seen (Figures 3.3, 3.6A). Immunocytochemistry revealed that anti-Orai1 (ProSci) labels the midpiece and acrosomal regions in addition to weaker fluorescence observed on the principal piece of the flagellum (Figure 3.6B), although labelling was less intense in comparison with Orai2 and Orai3. Blocking peptides successfully reduced labelling within the midpiece and acrosomal regions (Figure 3.6D). In negative controls where no primary antibody was included we observed no significant fluorescence (Figure 3.6F).

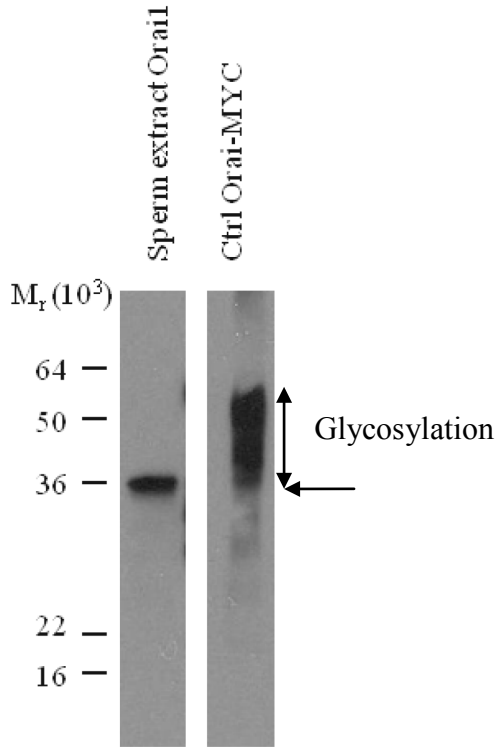

Figure 3.5 Expression of Orai1 in human sperm. ~500 x 10^6 human sperm lysed in IP buffer, as described in materials and methods, were subjected to 15% SDS-PAGE and detected using anti-Orai1 (Sigma). Positive controls were produced from HEK-293T cells transfected with Orai1-MYC. The band at the correct molecular weight is marked by the arrow.

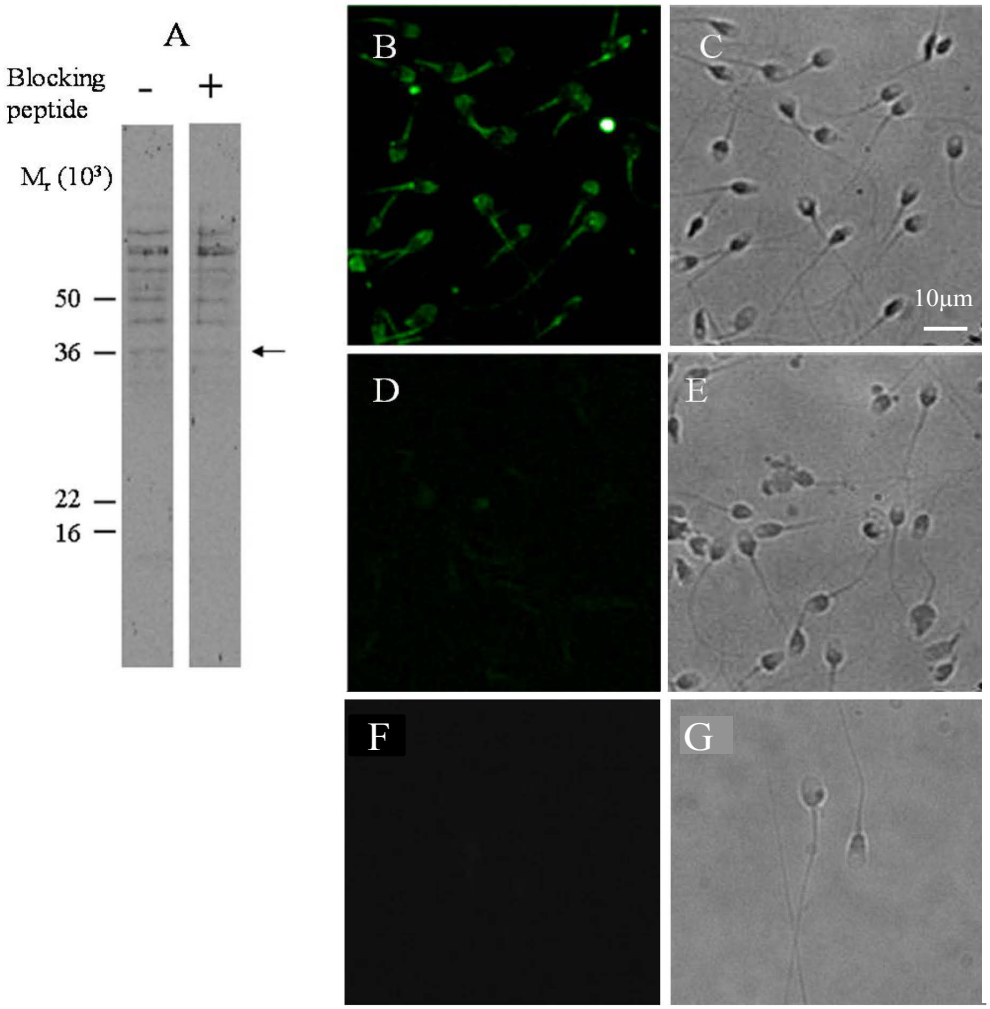

Figure 3.6 Expression of Orai1 in human sperm. **(A)** Total sperm extract subjected to 15% SDS-PAGE, transferred to nitrocellulose and incubated with anti-ORAI1 (-) or anti-ORAI1 preadsorbed with its corresponding blocking peptide (+). **(B-E)** Formaldehyde-fixed sperm were incubated with anti-Orai1 as described in Materials and Methods. Slides were incubated with anti-Orai1 (ProSci) **(B)** or pre-adsorbed with corresponding blocking peptide **(D)**. **(F)** Cells were prepared as in (A) but anti-Orai1 was omitted to provide a negative control. **(C, E, G)** Corresponding phase-contrast images.

Antibodies to Orai2 (ProSci 4111) detected a clear band from total sperm extract (2 x 10^6) at 36 kDa (Figure 3.7A). The predicted mass for Orai2 is ~29 kDa, but when glycosylated, Orai proteins can migrate at higher than predicted molecular mass on SDS-PAGE gels. Corresponding blocking peptides for anti-Orai2 specifically reduced band intensity at ~36 kDa to very low levels. When examining Orai2 labelling via immunocytochemistry, the midpiece and principal piece were clearly stained, with weaker staining observed over the acrosome and equatorial segments (Figure 3.7B). Specific detection was abolished anti-Orai2 with the corresponding blocking peptide but this led to non-specific labelling of the equatorial segment, which was not apparent with unblocked antibody (Figure 3.7D). In negative controls, where no primary antibody was included, we observed no significant fluorescence (Figure 3.6F).

For Orai3, although we observed a band around the appropriate molecular weight (33 kDa) by Western blotting of total sperm extract (2 x 10^6), a number of further bands at higher and lower (Figure 3.3, 3.8A) molecular weights could be seen (using ProSci 4215). Even on the manufacturer's website when probing rat spleen lysate, the Orai3 band is not particularly clear. Also, pre-adsorbtion of the antibody with its corresponding blocking peptide failed to alter the pattern of detection on the blot (Figure 3.8A). However, using immunocytochemistry, Orai3 primarily labelled the anterior midpiece and sperm neck region and this was abolished with the corresponding blocking peptide (Figure 3.8B, D).

In standard Western blots of sperm lysate (Figures 3.3 and 3.9A) using antibodies to STIM1 from ProSci (4119) and BD Biosciences (610954), we only detected a weak band. However, immunoprecipitation with the ProSci antibody revealed a clear band at ~95 kDa (Figure 3.9B), consistent with reports that glycosylation causes STIM1 to migrate at >90 kDa rather than the predicted molecular weight of 77 kDa (Manji *et al.*, 2000). Furthermore, this band was not observed in the negative control IP (normal rabbit IgG) but was clearly detected in the STIM1-GFP positive control at ~115 kDa (90 kDa STIM1 + 25 kDa GFP tag). Immunocytochemistry pinpointed anti-STIM1 labelling primarily to the sperm neck region which often appeared as a bright spot and to the midpiece where staining often appeared as two parallel streaks (Figure 3.9C). Preadsorbtion with blocking peptides reduced labelling to negligible levels (Figure 3.9E).

STIM2 was strongly detected via Western blotting of whole sperm lysates (using ProSci 4123) as an intense doublet at 77-96 kDa and weaker bands at 45 kDa and 30 kDa (Figures 3.3, 3.10A). These bands were reduced to negligible levels using the corresponding blocking peptide (Figure 3.10A). Immunocytochemistry for anti-STIM2, labelled the entire flagellum showing a stronger signal in the midpiece and in <10% of cells we observed acrosomal staining (Figure 3.10B). Corresponding blocking peptides prevented labelling in these regions but, as with Orai2, we observed fluorescence at the equatorial segments, which was not apparent in unblocked preparations (Figure 3.10D).

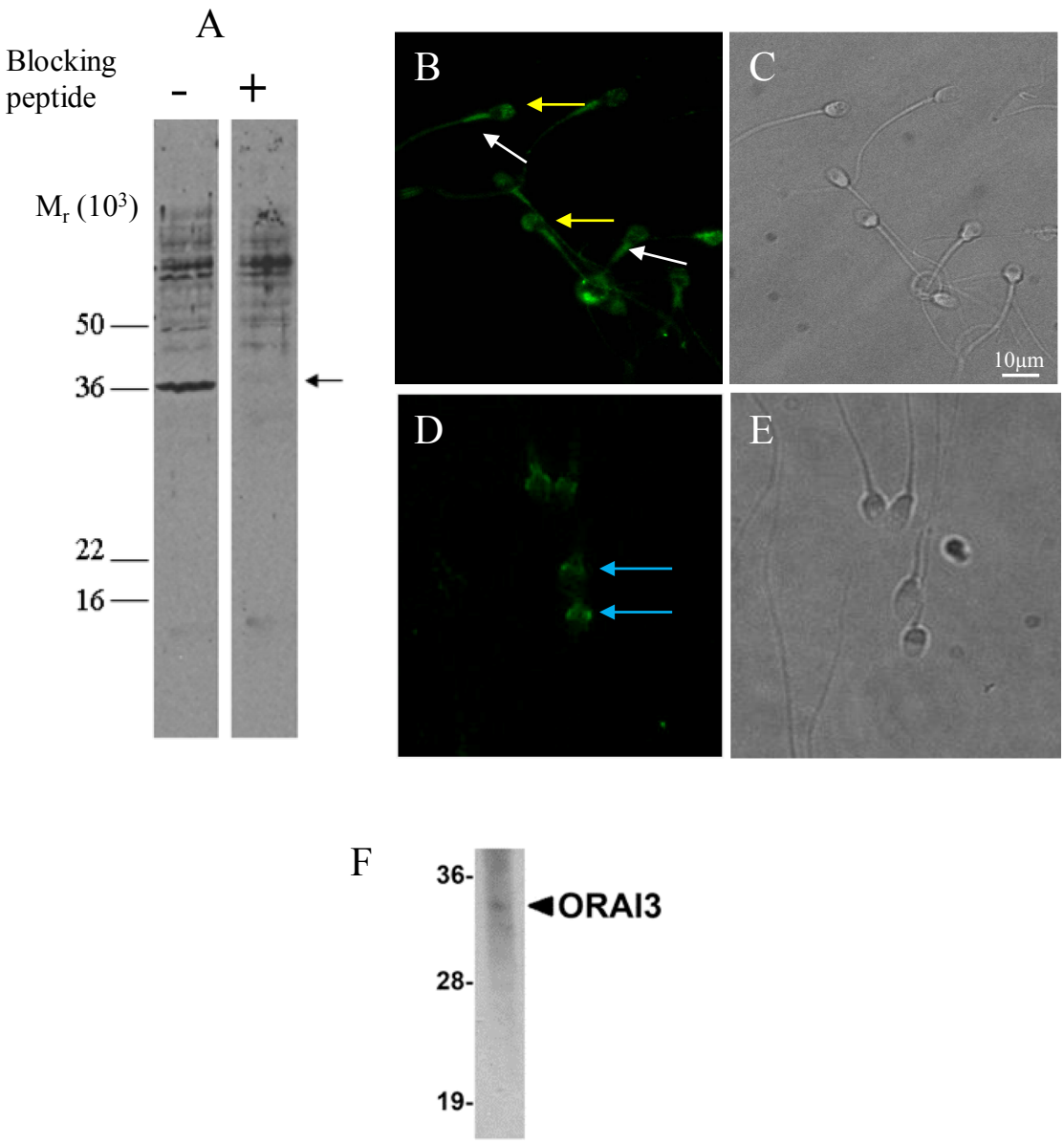

Figure 3.7 Expression of Orai2 in human sperm**. (A)** Total sperm extract subjected to 15% SDS-PAGE, transferred to nitrocellulose and incubated with anti-Orai2 (-) or anti-Orai2 preadsorbed with its corresponding blocking peptide (+). **(B-E)** Formaldehyde-fixed sperm were incubated with anti-Orai2 as described in Materials and Methods. Slides were incubated with anti-Orai2 **(B)**, pre-adsorbed with corresponding blocking peptide **(D)**. **(C, E)** Corresponding phase-contrast images. **(F)** Orai3 monoclonal antibody staining example from ProSci website. http://www.prosci-inc.com/ORAI3-Monoclonal-Antibody-c-PM-4911.

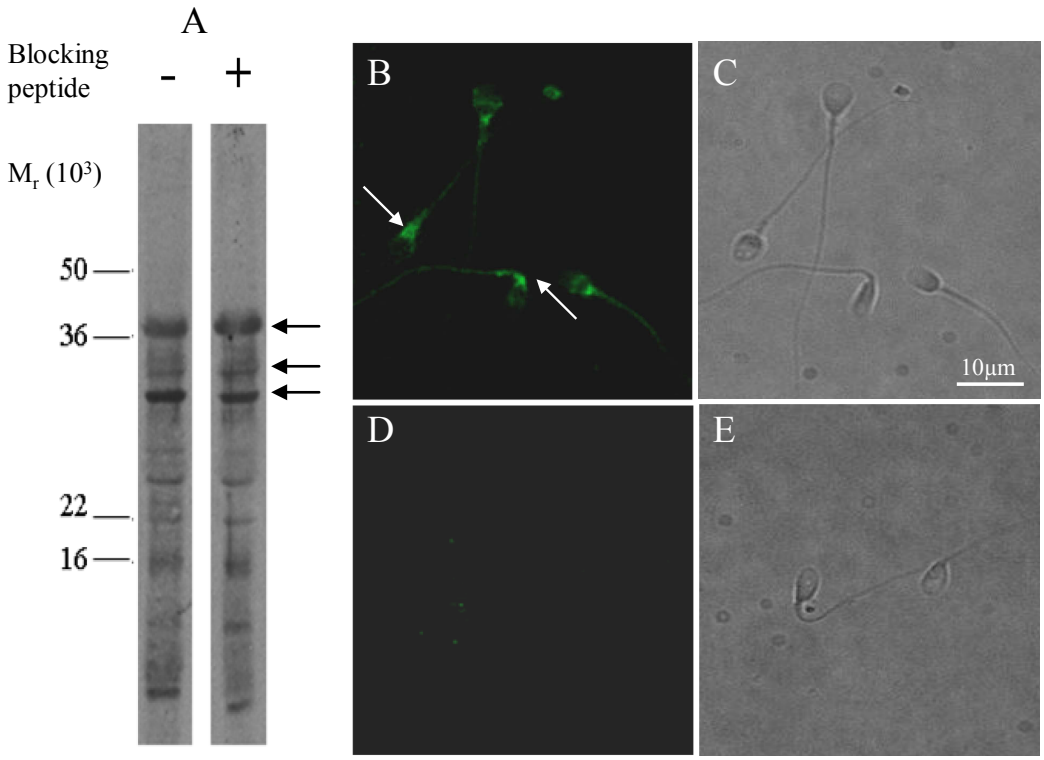

Figure 3.8 Expression of Orai3 in human sperm**. (A)** Total sperm extract subjected to 15% SDS-PAGE, transferred to nitrocellulose and incubated with anti-Orai3 (-) or anti-Orai3 preadsorbed with its corresponding blocking peptide (+) (all ProSci). **(B-E)** Formaldehyde-fixed sperm were incubated with anti-Orai3 as described in Materials and Methods. Slides were incubated with anti-Orai3 **(B)**, pre-adsorbed with corresponding blocking peptide **(D)**. **(C, E)** Corresponding phase-contrast images.

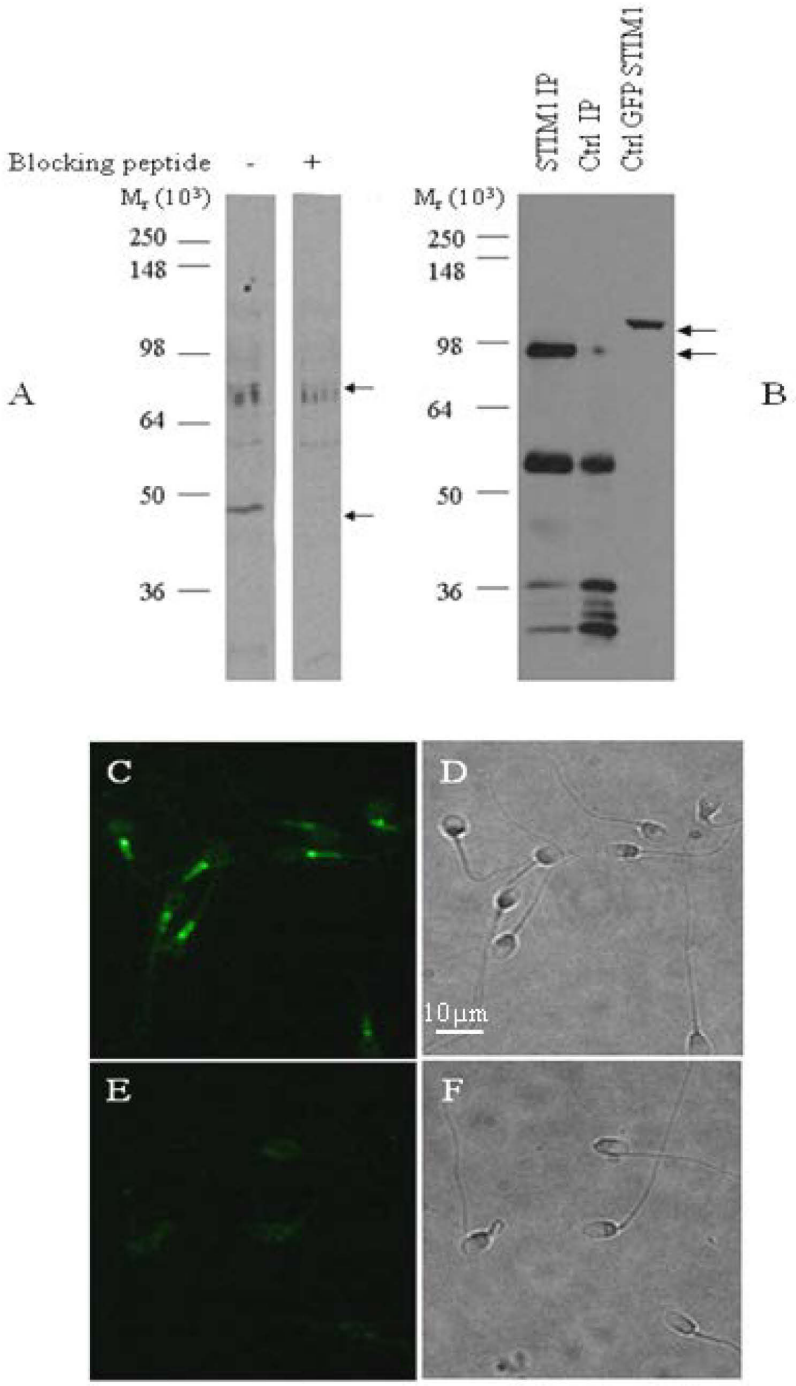

Figure 3.9 Expression of STIM1 in human sperm**. (A)** Total sperm extract subjected to 10% SDS-PAGE, transferred to nitrocellulose and incubated with anti-STIM1 (-) or anti-STIM1 preadsorbed with its corresponding blocking peptide (+). **(B)** ~500 x 10^6 human sperm lysed in IP buffer as described in materials and methods, immunoprecipitated and subjected to 10% SDS-PAGE. Bands were detected using anti-STIM1 (ProSci). Positive controls were produced from HEK-293T cells transfected with STIM1-GFP. The bands at the correct molecular weights are marked by the arrows. **(C-F)** Formaldehyde-fixed sperm were incubated with anti-STIM1 as described in Materials and Methods. Slides were incubated with anti-STIM1 **(C)**, pre-adsorbed with corresponding blocking peptide **(E). (D, F)** Corresponding phase-contrast images.

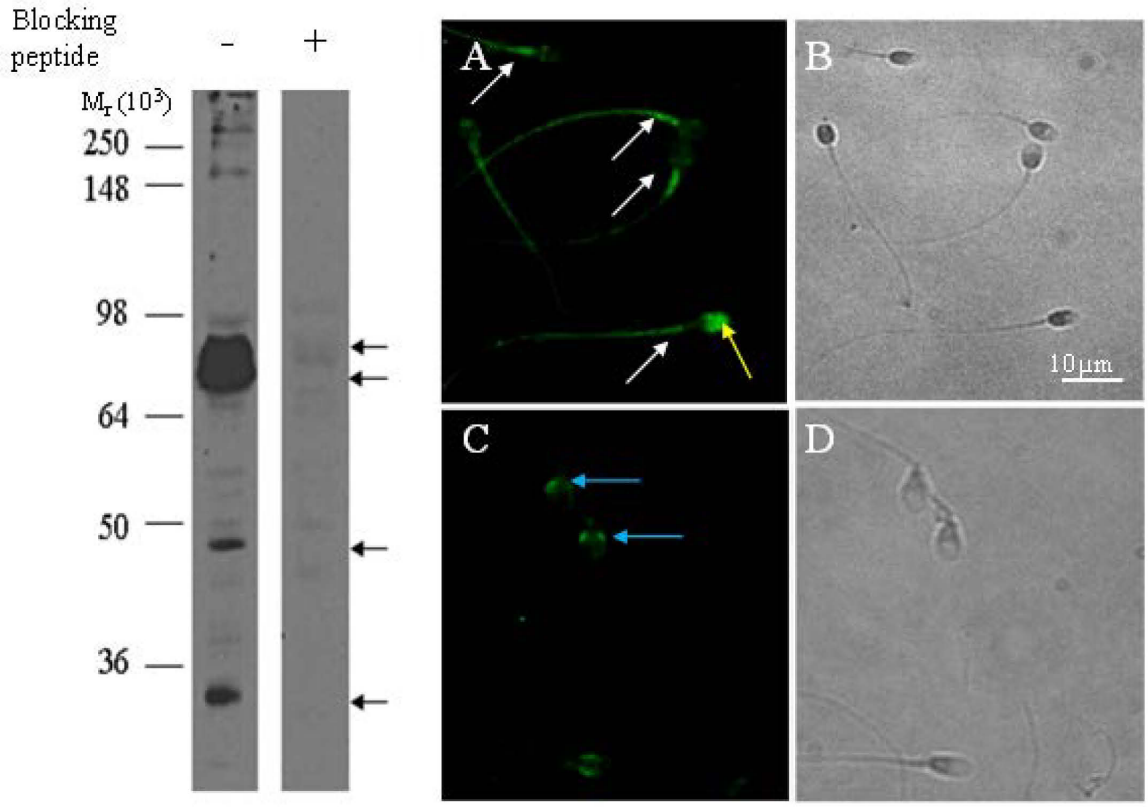

Figure 3.10 Expression of STIM2 in human sperm. **(A)** Total sperm extract subjectedmitted to 10% SDS-PAGE, transferred to nitrocellulose and incubated with anti-STIM2 (-) or anti-STIM2 preadsorbed with its corresponding blocking peptide (+) (all ProSci). **(B-E)** Formaldehyde-fixed sperm were incubated with anti-STIM2 as described in Materials and Methods. Slides were incubated with anti-STIM2 **(B)**, pre-adsorbed with corresponding blocking peptide **(D)**. **(C, E)** Corresponding phase-contrast images.

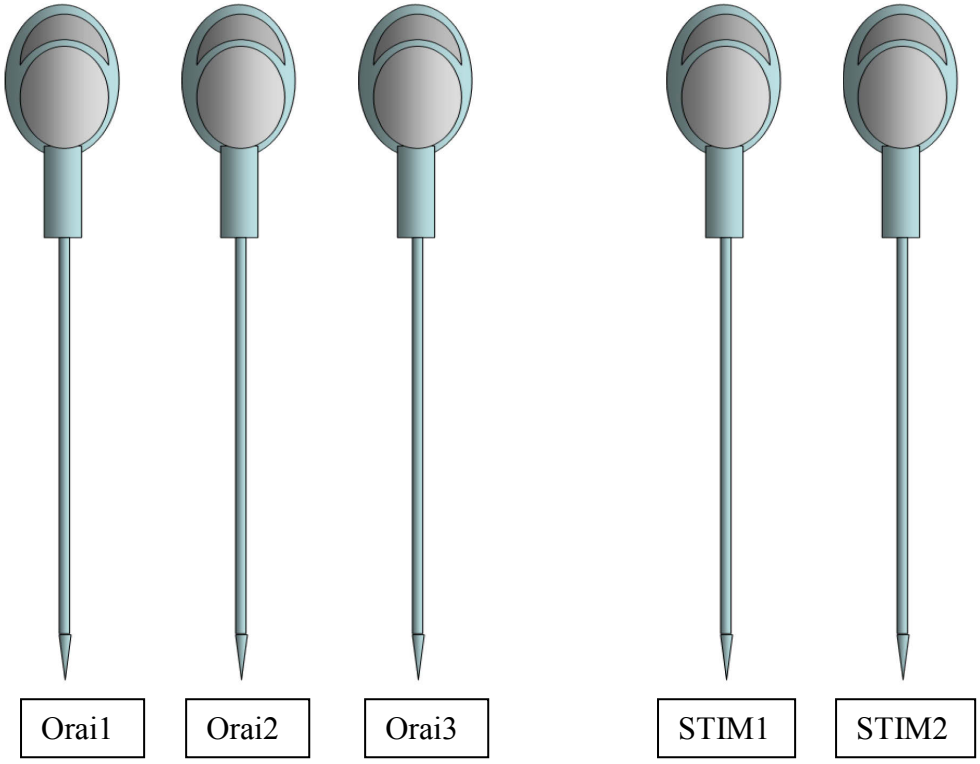

Figure 3.11 Summary diagram of the expression of Orai and STIM proteins in human sperm as according to immunocytochemistry. All STIM and Orai isoforms primarily stain in the midpiece/sperm neck region, an area of intracellular Ca^{2+} storeage. Lighter staining across the acrosome for Orai1 and Orai2 can be observed and a generalised staining pattern is seen for STIM2.

3.3.3 Lack of punctate structures in human sperm.

Following intracellular Ca^{2+} store depletion, STIM1 has been demonstrated to translocate and form punctate structures (Liou *et al.*, 2005). After activation of SOCE (via exposure of sperm to 15μM bis-phenol) we stained for STIM1 and assessed fluorescence in four areas, namely acrosome, post-acrosome head, midpiece and flagellum and expressed this as a percentage of total fluorescence to analyse movement of STIM1. In control cells, prepared under capacitating, 60-70% of total fluorescence was always within the midpiece (Figure 3.12A) which correlates with our initial immunocytochemistry staining results (Figure 3.9). Following SOCE, the percentage of fluorescence originating from the midpiece remained unchanged ($P>0.05$; 3 experiments, 170 cells; Figure 3.12A). Assessment of acrosomal status in cells stimulated with this protocol showed an increase in the proportion of reacted cells from 11% to almost 40%, as has been described previously (Meizel and Turner 1993; Dragileva *et al.*, 1999), but there was no reduction in the small proportion of fluorescence detected in the acrosomal region, consistent with the restriction of specific staining to the midpiece. In control preparations we observed approximately 50% of cells with 'spot' like staining within the midpiece of ~100nM diameter (Figure 3.12B). Treatment of cells with (15μM bis-phenol) caused no significant change in the proportion of cells with this appearance ($P=0.32$, 200 cells; chi-square).

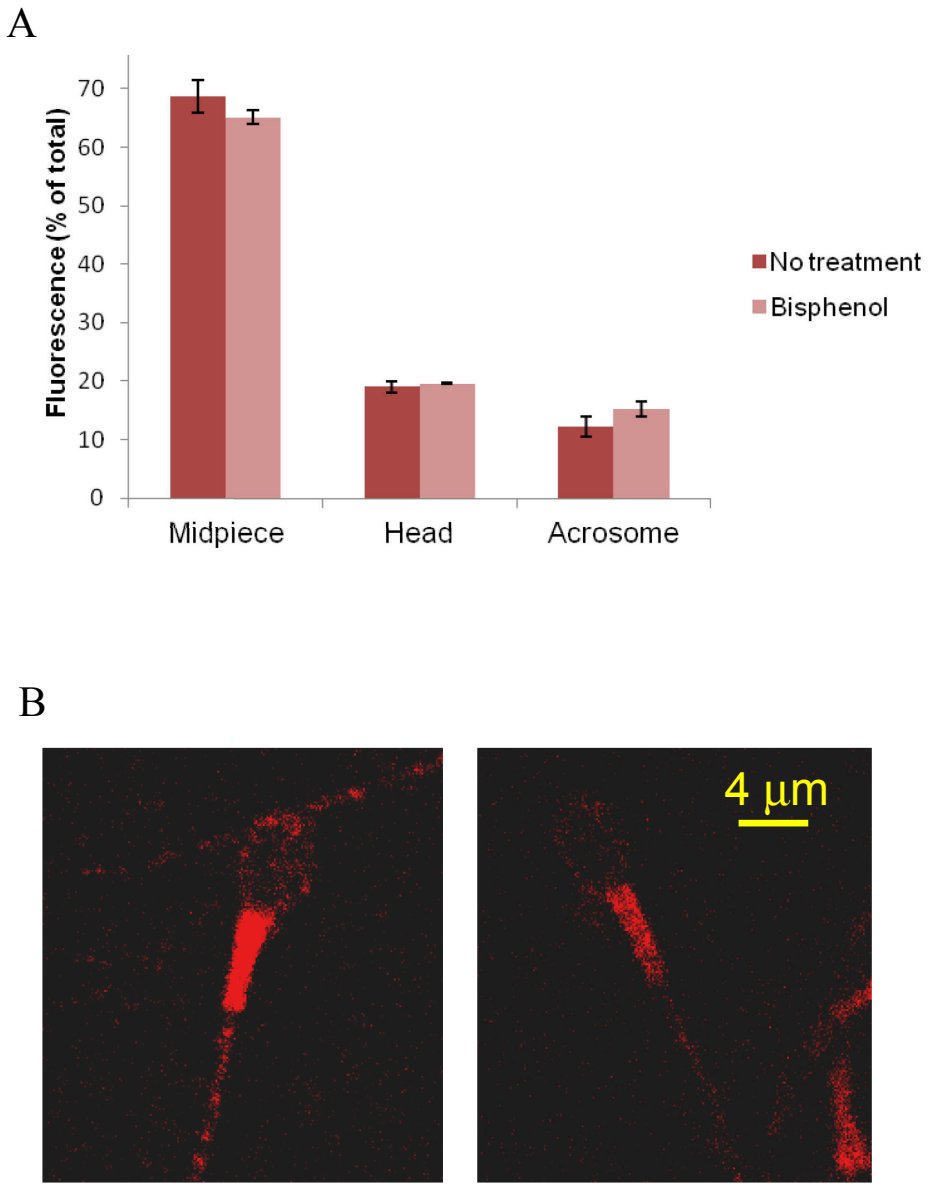

Figure 3.12 Distribution of punctate structures in human sperm. **(A)** Bars represent intensity of immunofluorescence staining of STIM1 in either the sperm midpiece, posterior head or acrosome (as a percentage of total fluorescence) under control conditions (dark bars) and after incubation for 12 minutes with 15µM bis-phenol (light bars). Each bar shows mean ±SEM of fluorescence in 170 cells from 3 experiments. **(B)** Confocal microscopy of human sperm immunofluorescently stained for STIM1 displayed two patterns of staining in the midpiece. Midpiece staining appeared equally distributed (left) or punctate (right).

3.4 Discussion

SOCE involves the mobilisation of stored Ca^{2+}, leading to activation of Ca^{2+} influx through store operated Ca^{2+} channels, at the plasma membrane. SOCE has been demonstrated in mammalian and sea urchin sperm following Ca^{2+} store mobilisation (Blackmore 1993, Dragileva *et al.*, 1999; O'Toole *et al.*, 2000; Williams and Ford, 2003; Espino *et al.*, 2009; Ardón *et al.*, 2004) and in our results (Figure 3.2). We have detected both isoforms of STIM, and all three Orai isoforms within human sperm using a range of Western blotting, immunoprecipitation and immunolocalisation techniques (Figures 3.3-3.10), although results for Orai3 were ambiguous (Figure 3.8). Furthermore, blocking peptides reduced or abolished the signal in Western blotting and immunolocalisation studies.

Western blotting for Orai1 suggests that it is unglycosylated in sperm as a clear band at ~35 kDa can be seen, as opposed to the glycosylated Orai1 seen in our positive control (recombinant Orai expressed in HEK-293T cells) (Figure 3.5). Orai1 contains an N-glycosylation motif situated in its extracellular loop between transmembrane segments 3 and 4 and Gwack *et al.* (2007) have demonstrated that mutations in this motif, preventing N-glycosylation of Orai1, do not lead to loss of function and is therefore not essential *in vitro*. They also report that in HEK-293T cells expressing Orai1, prevention of glycosylation (by treatment with tunicamycin, which inhibits the first step of glycosylation) altered the band appearance on SDS gels from a 'fuzzy' band with a molecular weight of ~45 kDa to a clearer band closer to the predicted molecular weight of 35 kDa, as observed here.

All three Orai isoforms are expressed in a wide range of human tissue at the mRNA level from kidney to lung, although Orai1 is predicted to be the most important of the Orai family Gwack *et al.*, 2007). For example, siRNA directed against Orai1 decreased SOCE in HEK-293T cells where as siRNA against Orai2 and Orai3 had little effect (Gwack *et al.*, 2007). However, Orai2 and Orai3 have been shown to partially replace Orai1 in Orai1 mutant HEK-293T cells to help restore SOCE (Mercer *et al.*, 2006). Furthermore, as all three Orai isoforms are localised to the plasma membrane and when overexpressed Orai1 can co-immunoprecipitate with Orai2 and Orai3, it is predicted that in vivo both Orai2 and Orai3 are able to multimerise with Orai1 to form Ca^{2+} conducting channels (Gwack *et al.*, 2007).

Co-immunoprecipitation studies into Drosophila Schneider 2 (S2) cells using cross-linking agents have suggested that Orai1 is predominantly a dimer in resting conditions, which then forms a tetrameric structure following STIM activation (Penna *et al*., 2008). Recent studies into arachidonic acid activated channels (ARC), have shown a different stoichiometry for Orai, with the ARC pore composed of a heteropentameric assembly of three Orai1 subunits and two Orai3 subunits (Mignen *et al.*, 2009). Thererfore it would be interesting to determine the Orai stoichiometry when in combination with STIM in human sperm. In our hands and in the hands of other research groups (e.g. Gwack *et al*., 2007), co-immunoprecipitation studies between STIM and Orai were unsuccessful. This may be due to low affinity rapidly dissociating interactions between STIM and Orai in human sperm, especially when put into context with the rapid Ca^{2+} transients and oscillations observed in human sperm throughout this study.

Both STIM1 and STIM2 have been detected in human sperm (Figures 3.9 and 3.10). The two STIM isoforms show a two-fold difference in their Ca^{2+} sensitivities. STIM2 translocation begins when ER luminal Ca^{2+} drops below approximately 400μM, but the less sensitive STIM1 requires luminal Ca^{2+} to fall below 200μM for translocation (Brandman *et al.,* 2007). STIM2 therefore responds to the Ca^{2+} deficit caused by weaker stimuli and has a lower potency in activating Orai subunits, suggesting a role in Ca^{2+} homeostasis (Brandman *et al*., 2007; Parvez *et al*., 2008). These studies correlate with our immunocytochemistry studies whereby STIM2 appears to have a more generalised distribution than STIM1 (Figures 3.9C and 3.10B) and perhaps acts as a basal $[Ca^{2+}]_i$ regulator. In addition, it has been recently shown in HEK-293T cells that a second population of STIM2 (in addition STIM2 residing in the ER), can be detected as a cytoplasmic protein. Here it can interact with Orai1 to mediate basal $[Ca^{2+}]_i$ levels independent of stored Ca^{2+} mobilisation (Graham *et al*., 2011). Interestingly, we observe STIM2 within our Western blots as a doublet which may represent the two STIM2 subsets. This theory is also consistent with our immunocytochemistry studies for Orai showing weak staining observed in areas of the cell, such as the principal piece of the flagellum, where no Ca^{2+} stores are found (Figures 3.6B, 3.7B, 3.8B).

Immunocytochemistry for STIM and Orai has revealed bright staining consistent with areas of Ca^{2+} storage, at the midpiece and acrosomal regions (Costello *et al.,* 2009) (Figures 3.6-3.11). Therefore, STIM and Orai proteins are ideally positioned within human sperm to conduct SOCE. This system may be responsible for extending sustained $[Ca^{2+}]_i$ oscillations caused by agonist induced store mobilisation, such as a progesterone gradient (Harper *et al.*, 2004), as discussed in chapter 5. Indeed STIM1 has been shown to mediate Ca^{2+} entry during sustained Ca^{2+} oscillations in other cell types (Bird *et al*., 2009). Furthermore, in sperm the positioning

of SOCE systems may be ideally placed to help regulate motility as when examining the peaks in Ca^{2+} oscillations induced by progesterone, they have been shown to correlate with asymmetrical bending of the midpiece and an increased excursion of the flagellum (Harper *et al*, 2004; Bedu-Addo *et al.*, 2005; Machado-Oliverira *et al.,* 2008). In addition, the application of 4-aminopyridine (to induce hyperactivation; Gunter *et al.*, 2004) causes mobilisation of Ca^{2+} stores within the midpiece accompanied by asymmetric flagella beating (Costello, S. unpublished data).

In somatic cells following Ca^{2+} depletion, STIM1 accumulates at specific predetermined foci in the peripheral ER, where close contact with the overlying plasma membrane can be formed (Liou *et al*., 2007; Muik *et al*, 2008) and can be visualised by the formation of puncta-like structures. We did not observe any bulk movement of STIM1 proteins following induced SOCE (Figure 3.12A) and immunocytochemical studies have shown similar localisation of STIM and Orai isoforms (Figure 3.11). This indicates that they are potentially capable of immediate action as in muscle cells (Launikonis and Rios, 2007; Shin and Muallem, 2008) with SOCE inducing STIM1 oligomerisation which then forms associations with Orai proteins in the overlying plasma membrane. Indeed, the separation between plasmalemma and intracellular membranes in sperm cells is probably ≤30 nM (Morozumi *et al*., 2006; Zanetti and Mayorga, 2009) and the diameter of the midpiece about 1µm, such that migration of STIM may not be required for STIM-Orai interaction. This hypothesis correlates with studies looking at STIM1 associations with microtubules in somatic cells. STIM1 and STIM2 have been shown to be binding partners of the microtubule plus-end-tracking protein EB1 (Grigoriev *et al.*, 2008). Here store depletion disrupts microtubular association and STIM1 switches to its local plasma membrane Orai binding partner. Microtubules within human

sperm begin within the connecting piece and transverse the length of the midpiece and flagellum. Subsequently, STIM1 could bind to microtubules within the midpiece area and interact with localised plasma membrane Orai channels. This also agrees with the localisation of Orai 1, 2 and 3 to the midpiece region (Figures 3.6-3.8) and allows a fast return for STIM1 to the Ca^{2+} store following refilling.

SOCE does not appear to induce the formation of punctate structures in human sperm (Figure 3.12B). However, studies of punctate structures report diameters of 1-10µm per spot (Liou *et al.*, 2005; Mercer *et al.,* 2006; Zhang *et al.*, 2005; Baba *et al.*, 2006). The dimensions of a human sperm head is only 5µm by 3µm, therefore Orai and STIM may not be able form the large multimers as apparent when STIM and Orai is overexpressed in other cell types (Liou *et al.*, 2005). Also, STIM oligomerises within seconds of store depletion and only co-localises with Orai for a short period of time, therefore these short interactions may have been disrupted and lost during the sperm fixing procedure (Deng *et al*., 2009).

In summary, human sperm have been shown to perform SOCE in response to the depletion of stored Ca^{2+} which may be mediated by the STIM-Orai system. Both STIM isoforms and Orai1 and Orai2 have been detected, although the presence of Orai3 remains ambiguous. STIM1 does not appear to translocate and form the large punctate structures in response to intracellular store depletion, as seen when STIM and Orai are overexpressed in other cellular systems. This is most probably due to the size constraints and highly specialised nature of the cell, requiring immediate Ca^{2+} regulation mechanisms.

CHAPTER FOUR: PHARMACOLOGICAL MODULATION OF STORE-OPERATED CALCIUM ENTRY IN HUMAN SPERM USING 2-APB.

4.1 Abstract

Previously in chapter 3, we have reported that STIM and Orai, proteins of the SOCE system, can be detected in human sperm and are primarily localised to areas of intracellular Ca^{2+} stores. The best characterised modulator of SOCE is the pharmacological agent 2-aminoethyldiphenyl borate (2-APB). 2-APB was initially thought to be an IP_3R antagonist, although this was later disproved and its bimodal roles as both a SOCE stimulator and inhibitor were established. At low concentrations (typically <20μM) 2-APB stimulates SOCE, conversely at higher concentrations (>30μM) it inhibits SOCE, although this varies according to the Orai isoforms expressed. In this section we aimed to determine if 2-APB was able to modulate SOCE in human sperm in the same manner. By using single cell Ca^{2+} imaging and fluorimetry, we show that 2-APB elevates resting $[Ca^{2+}]_i$ in a dose-independent manner. This phenomenon of 2-APB activating membrane Ca^{2+} channels independently of Ca^{2+} store mobilisation has been described previously and may be due to Ca^{2+} entry mediated by Orai3 alone or in areas where Orai is co-expressed with STIM2. Bathing cells in EGTA-buffered media to deplete Ca^{2+} stores and applying 5μM 2-APB enabled a transient that activated immediately upon the reintroduction of Ca^{2+}, indicating sensitisation of the SOCE system by 2-APB. We also report that the application of high dose 2-APB (≥50μM) on cells performing bis-phenol induced SOCE, had inhibitory effects on SOCE, which acted in a reversible manner. 2-APB has been reported to have stimulatory effects on TRPV3, however we failed to detect the presence of TRPV3 in Western blots. Therefore, this data suggests that 2-APB acts on SOCE channels in human sperm in a complex bimodal manner as previously seen in other cell types transfected STIM and Orai proteins.

4.2 Introduction

We have shown in chapter 3 that STIM and Orai, proteins of the SOCE system could be detected in human sperm and are primarily localised to areas of known intracellular Ca^{2+} stores. One of the best characterised and extensively used modulators of SOCE is the pharmacological agent 2-aminoethyldiphenyl borate (2-APB). 2-APB was initially thought to be a membrane-permeant inhibitor of the IP_3R, consequently reports of 2-APB inhibiting SOCE were thought to be evidence of direct IP_3R activation of CRAC channels (Ma *et al.*, 2000; discussed in DeHaven *et al.*, 2008). More recent studies have shown evidence to the contrary with inhibitive actions of 2-APB on SOCE independent of IP_3Rs (Braun *et al.,* 2001; Prakriya and Lewis, 2001; Ma *et al.*, 2001; Bird and Putney, 2006). For example, Braun *et al.* (2001) used patch clamping of rat basophilic leukaemia cells (RBL-2H3 ml) to demonstrate 2-APB blocked I_{CRAC}, whilst having no effect on Trp-3 channels, arachidonic acid-activated, L-type Ca^{2+} channels and IP_3Rs. Also, SOCE has been shown to occur in cell lines devoid of IP_3Rs (Sugawara *et al.*, 1997). Furthermore, within human sperm, progesterone induced Ca^{2+} oscillations, believed to be due to SOCE, are insensitive to the inhibition of IP_3 generation or IP_3Rs (Harper *et al.,* 2004).

2-APB has bimodal actions and investigations in cells transfected with STIM have shown that at low concentrations (typically <20μM) 2-APB stimulates SOCE, conversely at higher concentrations (>30μM) (DeHaven *et al.,* 2008) it inhibits SOCE, although this varies according to the Orai isoforms expressed (Lis *et al.*, 2007). It is also clear from the literature on 2-APB as a modulator of SOCE that its actions are complex and the mechanisms behind its actions are not fully understood (Wang *et al*., 2009, DeHaven *et al*., 2008). At low doses, it

has been shown 2-APB acts to rapidly potentiate STIM and Orai interactions by locking the C-terminus (probably the CAD/SOAR region) of STIM with Orai1, to enable channel coupling (Wang *et al.*, 2009). 2-APB therefore appears to help bypass the typical oligomerisation and re-organisation of STIM prior to Orai activation and sensitises Orai1 for the impending I_{CRAC}. However, at higher concentrations 2-APB has an inhibitory effect on SOCE, except on Orai3 mediated SOCE (Lis *et al.*, 2007; Wang *et al.*, 2009). It is hypothesised that 2-APB binds to similar sites on all Orai isoforms, but on Orai3 it substitutes STIM interactions and stimulates I_{CRAC} directly altering channel properties by increasing their pore size, regardless of dosage (Schindl *et al.*, 2008; Wang *et al.*, 2009). Subsequently, we wanted to investigate whether stimulatory and inhibitory concentrations of 2-APB had any effects on the response of SOCE in sperm.

Chapter Aims

The aims of this chapter were to firstly investigate if 2-APB can modulate basal $[Ca^{2+}]_i$. Following this we then wanted to examine if 2-APB can modulate $[Ca^{2+}]_i$ of sperm induced to perform SOCE, similar to the bimodal effects observed in cells transfected with STIM and Orai proteins.

4.3 Results

4.3.1 2-APB elevates resting $[Ca^{2+}]_i$ in human sperm.

2-APB is the best characterised modulator of SOCE and when applied to resting sperm populations at a concentration of 5μM we observed a small slowly-developing rise which appeared to stabilise at a new level within approximately 100 seconds (Figure 4.1A). This response was visible in ~75% of single cell traces as a sustained $[Ca^{2+}]_i$ elevation or sometimes a transient rise. The mean increase in R_{tot} 3 minutes after application of 2-APB was 14.8 ±1.8% (n=14). Exposure of cells to higher (typically inhibitory) doses of 2-APB had similar effects on resting cells as for treatment with 5μM 2-APB (Figure 4.1B, P>0.5; paired t-test, n=4), indicating no dose related response. Furthermore, a similar phenomenon of dose-insensitivity was observed when $[Ca^{2+}]_i$ of resting cells treated with various doses of 2-APB was measured fluorimetrically, using fura-2 loaded cells (Figure 4.1C). Where cells were bathed in a Ca^{2+} free/EGTA-buffered media for 3 minutes prior to 2-APB application, this abolished the stimulatory effect of 2-APB. In fact, a recognisable fall in $[Ca^{2+}]_i$ can be seen upon application of the 5μM 2-APB (Figure 4.1D). Exposure of cells to higher doses of 2-APB (up to 100 μM) had similar effects to 5μM (P>0.5; paired t-test, n=4).

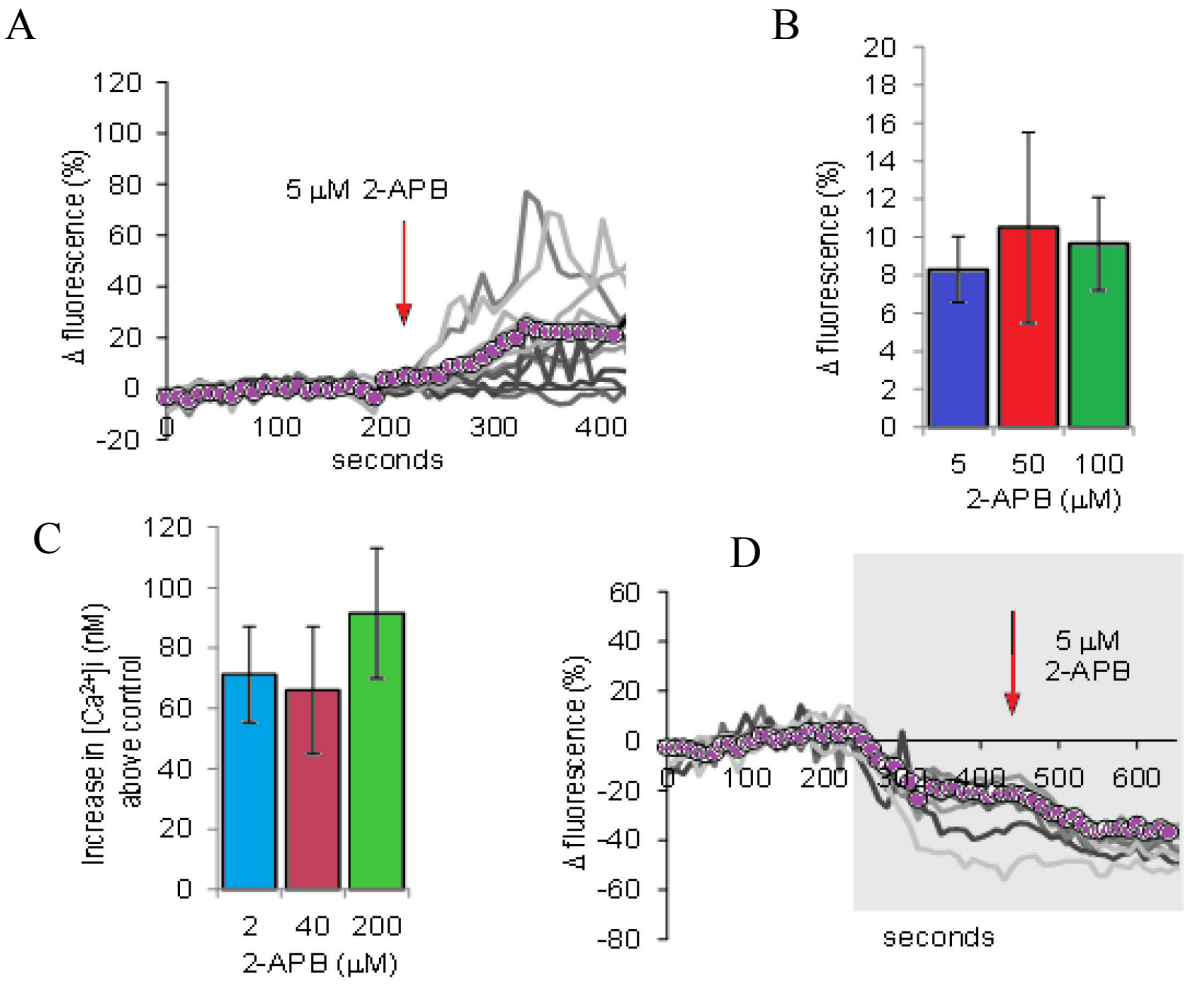

Figure 4.1 Effects of 2-APB on resting $[Ca^{2+}]_i$. **(A)** Capacitated sperm were perfused with sEBSS and 5µM 2-APB was added to the perfusion media at 220 seconds (arrow). Individual cell traces are shown by grey lines. Experimental averages (R_{tot}) are shown by purple circles. **(B)** Bars show the increase in R_{tot} 3 minutes following 2-APB application and are the mean +/- SEM of sets of four experiments, in which aliquots from the same sample were treated with 5, 50 or 100µM 2-APB. **(C)** Bars show the mean increment in $[Ca^{2+}]_i$ in 2, 40 or 200µM 2-APB treated cells in comparison with controls, measured fluorimetrically using fura-2. **(D)** Effect of 5 µM 2-APB on resting $[Ca^{2+}]_i$ in low-Ca^{2+} saline. Capacitated sperm were perfused with EGTA-buffered saline ($3x10^{-7}$M $[Ca^{2+}]$, shown by grey shading) then exposed to 5µM 2-APB (arrow). Again, individual cell traces are shown by grey lines and experimental averages (R_{tot}) are shown by purple circles.

4.3.2 5μM 2-APB pre-treatment potentiates SOCE in human sperm.

In order to examine the effects of 2-APB on SOCE we needed to deplete intracellular Ca^{2+} stores and initiate SOCE. Superfusion with EGTA-buffered medium causes a marked fall in $[Ca^{2+}]_i$ ($[Ca^{2+}]_o$ ~$3x10^{-7}$M Ca^{2+}), leading to Ca^{2+} store depletion (Harper *et al.*, 2004; Bedu-Addo *et al*., 2007). We exposed cells for 400 seconds with the EGTA-buffered media until $[Ca^{2+}]_i$ stabilised with all cells showing a decrease in fluorescence of 20-40% during the first 150 seconds (Figure 4.2A). When Ca^{2+} was re-introduced by altering the media to sEBSS, mean fluorescence and therefore $[Ca^{2+}]_i$ recovered to control levels over 100-150 seconds. In parallel experiments we introduced 5μM 2-APB midway through the 400 second treatment with EGTA-buffered media (Figure 4.2B). This had no immediate effect on $[Ca^{2+}]_i$ in most cells, the only discernible response being a small additional fall in $[Ca^{2+}]_i$ in some sperm (as seen in Figure 4.1D). However, in every experiment, when Ca^{2+} was returned to the perfusing media we observed a marked increase in the proportion of cells in which recovery was immediate (82+/-17%, n=5, 327 cells; compared to controls 34±17%, n=5, 305 cells; $P<0.015$, paired t-test). Indeed, when comparing the mean responses (R_{tot}) from parallel control and 5μM 2-APB (Figure 4.2C), the difference between the two traces indicated pre-treatment with 5μM 2-APB enabled a transient that activated immediately upon the reintroduction of Ca^{2+}. This transient peaked within 10 seconds and decayed over the following 90 seconds. This effect was most noticeable at 5μM 2-APB with responses at 50 and 100μM having similar kinetics but a smaller amplitude (Figure 4.2D). Therefore, store depletion by extracellular EGTA is sufficient to activate SOCE in a large proportion of cells and this effect is potentiated by 5μM 2-APB.

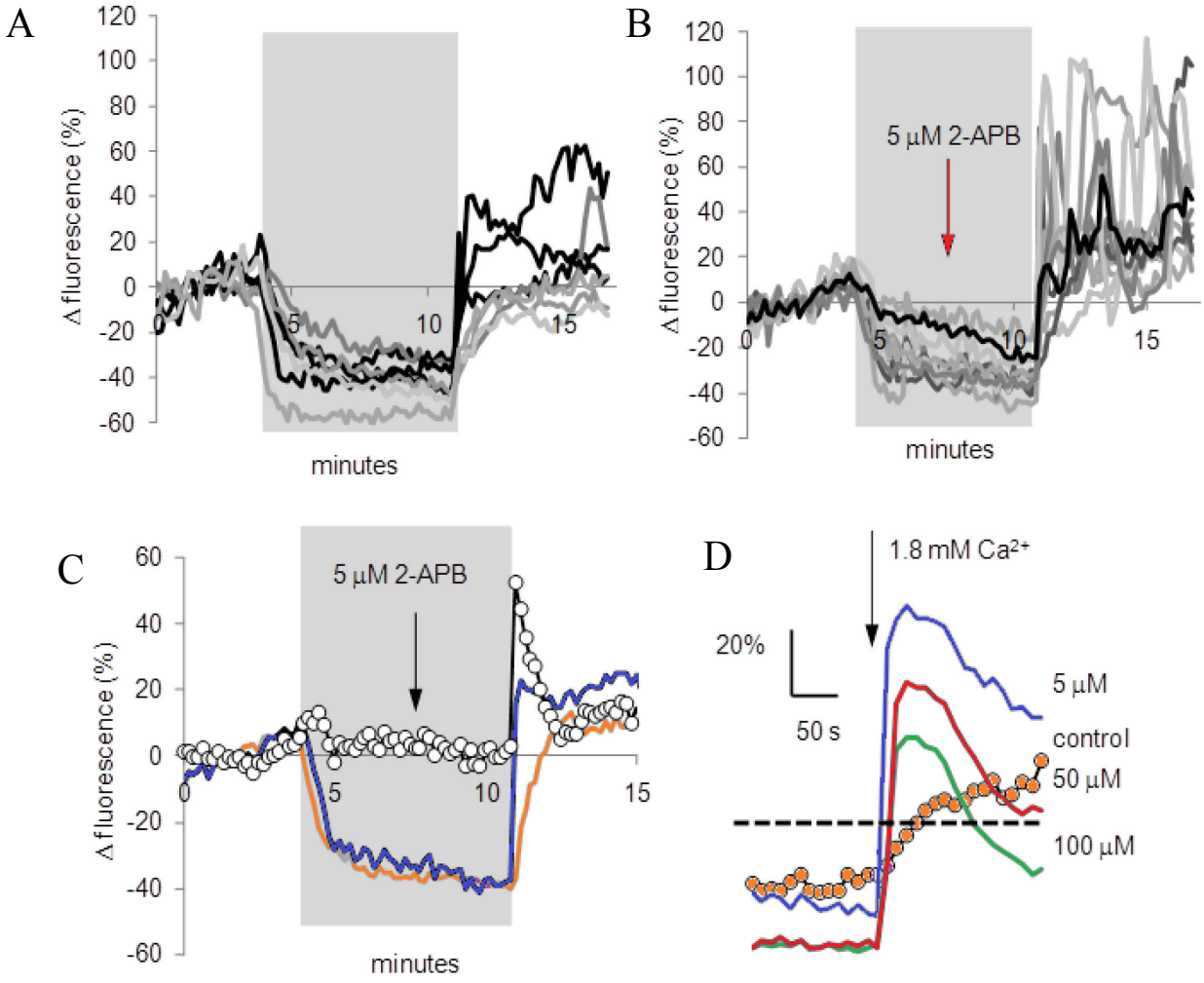

Figure 4.2 Depletion of stored Ca^{2+} reveals an effect of 2-APB. **(A)** Capacitated sperm were perfused with EGTA-buffered saline ($3x10^{-7}$M $[Ca^{2+}]$, shown by grey shading) causing a sustained fall in $[Ca^{2+}]_i$. Reintroduction of standard sEBSS to the chamber caused $[Ca^{2+}]_i$ to return to control levels. **(B)** Cells were perfused with EGTA-buffered saline as in (A) except 5µM 2-APB was added mid-way through this period (as shown by red arrow). **(C)** Mean responses (R_{tot}) taken from A (control – orange trace) and B (5µM 2-APB treatment – blue trace) reveal a difference in kinetics following sEBSS reintroduction (as shown by circles trace). **(D)** 2-APB pre-treatment reveals a dose-dependent response when media is changed from EGTA-buffered saline to standard EBSS. Traces show mean responses (R_{tot}) carried out either in control conditions or with pre-treatment with 5, 50 or 100µM 2-APB as marked (n=4). Dashed line shows control fluorescence prior to exposure to EGTA-buffered saline.

4.3.3 Inhibitory 2-APB concentrations reduce bis-phenol induced SOCE.

In support of these previous findings, we examined the effect of high dose 2-APB on the Ca^{2+} influx initiated by 15μM bis-phenol. In 6 out of 7 experiments 50μM 2-APB caused a clear reduction of the bis-phenol-induced enhancement of $[Ca^{2+}]_i$. Some recovery of $[Ca^{2+}]_i$ occurred during exposure to 2-APB and inhibition reversed upon washout of the drug (Figure 4.3B). This effect was not observed when applying 5μM 2-APB (Figure 4.3A).

4.3.4 TRPV3 is not detectable in human sperm

Stimulatory 2-APB concentrations (i.e. <20μM), in addition to increasing I_{CRAC} carried by Orai1 and Orai2, have been reported to have stimulatory effects on one of the transient receptor potential cation channels (subfamily V), namely TRPV3 (Chung *et al*., 2004; Hu *et al*., 2009). Western blotting failed to detect expression of TRPV3 in human sperm, as opposed to detecting a band at the appropriate molecular weight prepared from human keratinocytes, where TRPV3 is known to be expressed (Figure 4.4, Peier *et al*., 2002; Chung *et al*., 2004). In addition, staining of this band was blocked by preadsorption of the antibody with the immunogenic peptide

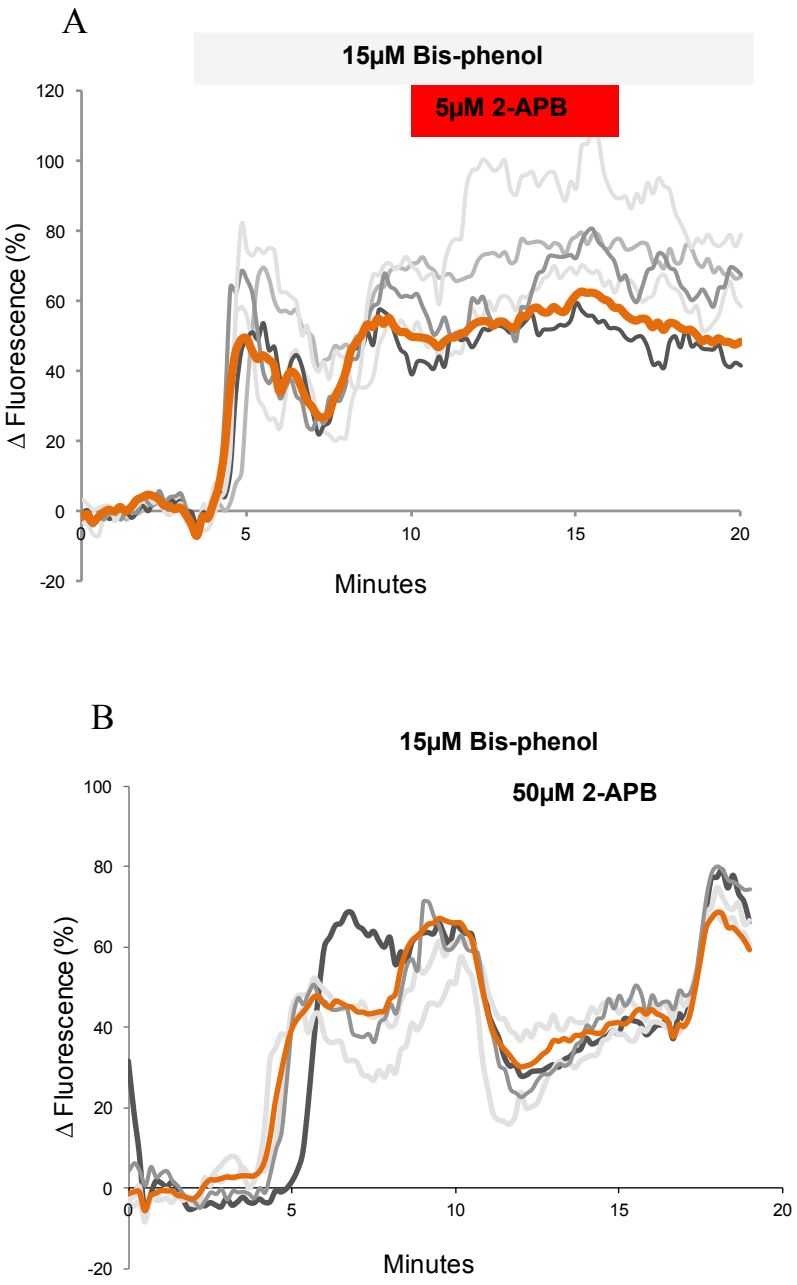

Figure 4.3 2-APB modulates bis-phenol induced SOCE**. (A)** Capacitated sperm were perfused with sEBSS and 15µM bis-phenol was added to the perfusion media at 4 minutes (grey bar). 5µM 2-APB was also added to the perfusion media at 10.5 minutes (red bar). Example individual cell traces are shown by grey lines. Experimental averages (R_{tot}) are shown by orange traces. **(B)** Experiment was performed the same as in (A), except the concentration of 2-APB was increased to 50µM.

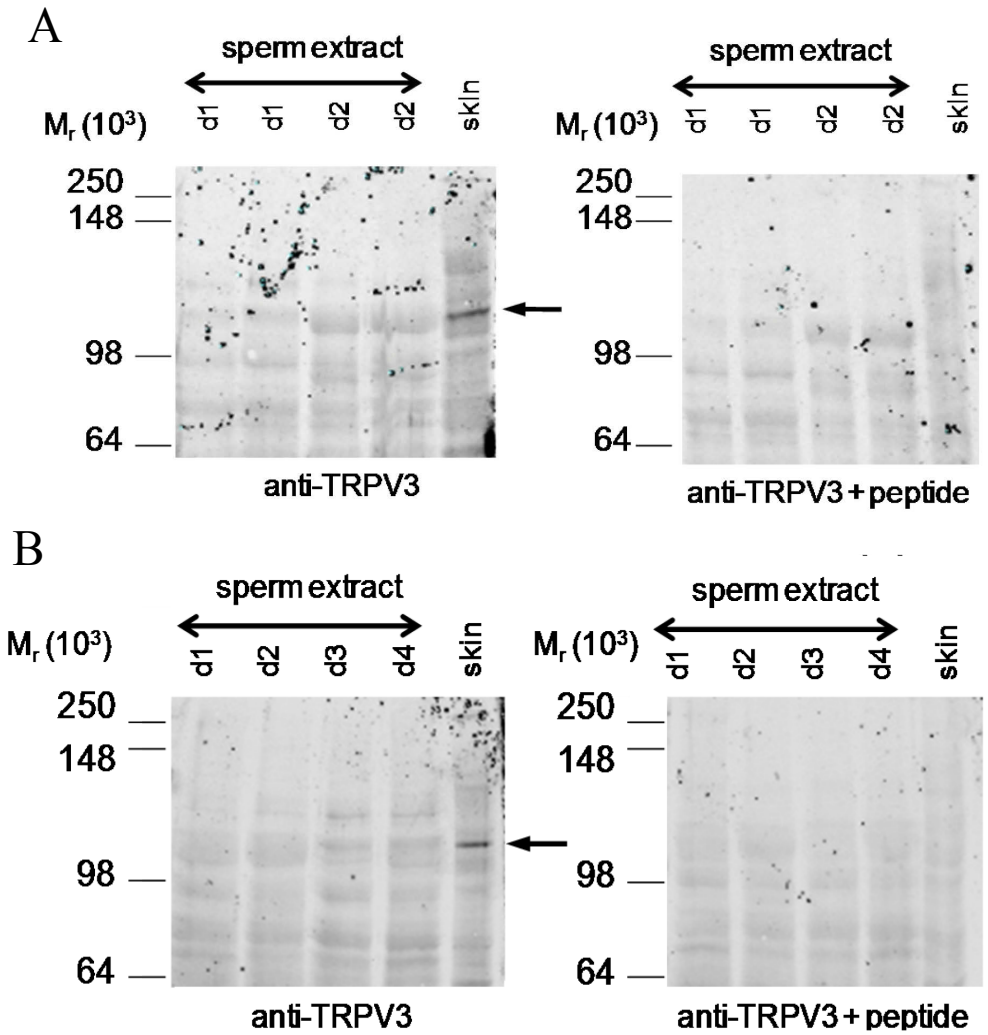

Figure 4.4 TRPV3 is not detected in human sperm. **(A)** Left panel (lanes 1-4) show immunoblot for TRPV3 with sperm preparations from two different donors (d1 and d2). Lane 5 shows positive control of human keratinocyte proteins (arrow). Right panel shows identical blot, carried out in parallel, except the TRPV3 antibody was preadsorbed with its corresponding antigenic peptide. Positive control band has been lost. **(B)** Identical experiments as to in (A) except using four different donors (d1-d4).

4.4 Discussion

2-APB was initially thought to be an IP_3R antagonist, although this was later disproved and its bimodal roles as both a SOCE stimulator and inhibitor were established (Ma *et al.*, 2000, 2001). Due to the confirmation of SOCE systems and the detection of STIM and Orai proteins in chapter 3, we investigated the effects of 2-APB on SOCE in human sperm. 2-APB at both low and high doses induced an elevation of $[Ca^{2+}]_i$ without the requirement for Ca^{2+} store mobilisation (Figures 4.1A, B, C). This elevation was not apparent in EGTA-buffered preparations and is therefore dependent on the presence of extracellular Ca^{2+} (Figure 4.1D). The ability of 2-APB to activate membrane Ca^{2+} channels independently of Ca^{2+} store mobilisation has been described previously, but only in cells expressing Orai3 alone (and to a lesser extent Orai1 alone) and in cells where Orai1 is co-expressed with STIM2 (Schindl *et al*., 2008; Peinelt *et al*., 2008; DeHaven *et al.,* 2008; Wang *et al*., 2009). This increase in $[Ca^{2+}]_i$ could be seen in these cell types even when applying typically inhibitory (30-50μM) doses of 2-APB (Wang *et al*., 2009; Figure 4.5). For Orai3, it is predicted that 2-APB binds directly to Orai3 mimicking STIM interactions and stimulating I_{CRAC} independent of dosage, as siRNA targeted against STIM1 did not alter 2-APB induced Orai3 stimulation (Schindl *et al*., 2008). For STIM2, a cytosolic form of STIM2 has been recently shown to combine with Orai1 in order to mediate basal $[Ca^{2+}]_i$ without the requirement for store depletion (Graham *et al.*, 2011). In chapter 3, we have established the presence of STIM2 and (probably) Orai3. Subsequently the increases we observe in resting sperm populations following 2-APB application may well be due to Orai3 activity and STIM2 mediated basal Ca^{2+} regulation.

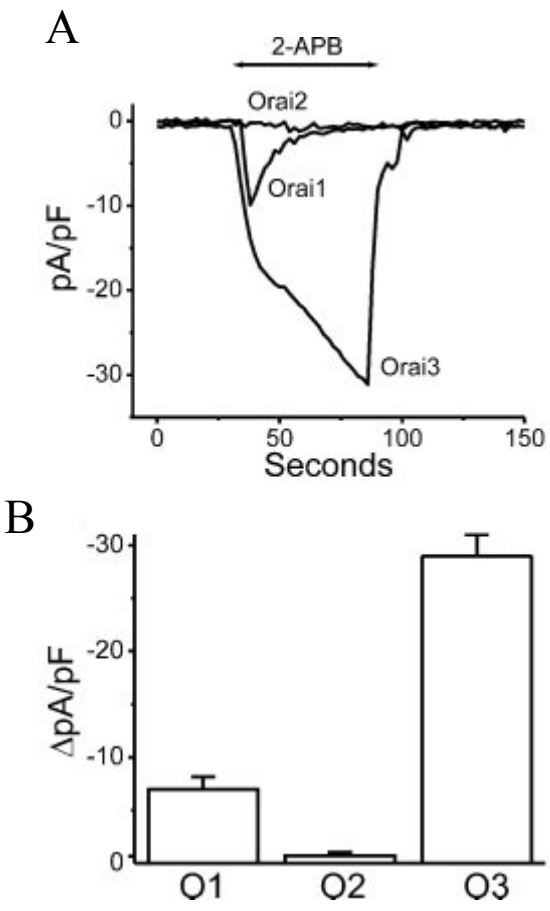

Figure 4.5 (A) Whole-cell currents recorded from HEK-293 cells expressing Orai1, Orai2 or Orai3 showing the potentiation of Orai3 by a typically inhibitory 2-APB dose (50μM). **(B)** Bars show the change in iCRAC following the application of 50μM 2-APB on HEK-293 cells expressing Orai1 (O1), Orai2 (O2), or Orai3 (O3). Figure from DeHaven *et al*. (2008).

We have again confirmed that a SOCE system operates in human sperm; as seen from switching EGTA-buffered media, to a Ca^{2+} containing sEBSS media and observing a rapid rise back to control $[Ca^{2+}]_i$ levels (Figure 4.2). It has been demonstrated that low dose 2-APB can stimulate SOCE by essentially priming STIM and Orai for SOCE (Wang *et al*., 2009). Alternatively, 2-APB may have effects on increasing the pore size of CRAC, thus increasing maximal I_{CRAC} (DeHaven *et al.,* 2008). Interestingly, the application of 5μM 2-APB during the EGTA-buffered phase in these experiments enabled faster recovery back to and in excess

of control levels (Figures 4.2A, B, C). It is therefore suggested that low dose 2-APB enables quicker activation of SOCE due to either STIM/Orai sensitisation and/or increased CRAC pore size leading to increased levels of I_{CRAC}.

Further evidence for 2-APB effecting a SOCE system in human sperm is demonstrated by Figure 4.3. When sperm were exposed to 15μM bis-phenol in order to mobilise stored Ca^{2+} and activate SOCE, the application of 50μM 2-APB reversibly inhibited this process (Figure 4.3B). Similar results have been reported by other groups in HEK-293 cells with STIM1 overexpression (DeHaven *et al*., 2008). This effect was not observed when applying 5μM 2-APB (Figure 4.3A). However, these results were variable and on a few occasions we observed potentiation as opposed to inhibition when applying 50μM 2-APB, suggesting heterogeneity of the Orai isoforms forming the CRAC channels between preparations.

Studies have shown low micromolar 2-APB doses are able to activate TRPV3 (Chung *et al*., 2004). Other human TRPV's are non-responsive or require doses 100-fold greater (Hu *et al*., 2004; Juvin *et al*., 2007; Neeper *et al*., 2007). Although functional TRPV1 has been detected in boar sperm (Maccarrone *et al*., 2005), we found no reports in the literature of TRPV3 present in human sperm and were unable to detect it via Western blotting. This was in comparison with clear detection in human keratinocytes used as a positive control. Therefore the 2-APB induced modification of SOCE in human sperm is unlikely to be due to interactions with TRPV proteins.

The detection of STIM and Orai proteins in chapter three indicates that they may be responsible for mediating the SOCE system in human sperm. In this chapter we have shown that SOCE can be pharmacologically mediated by the best characterised SOCE modulator 2-APB, which typically exerts its effects through STIM and Orai proteins. Furthermore, we have provided evidence that the actions of low dose 2-APB are unlikely to be due to TRPV3 as we cannot detect this protein in human sperm. Therefore, here we provide further evidence that the SOCE system in human sperm is controlled by the interactions of STIM and Orai proteins.

CHAPTER FIVE: PHARMACOLOGICAL MODULATION OF THE PROGESTERONE INDUCED BIPHASIC [CA^{2+}] RESPONSE IN HUMAN SPERM USING 2-APB.

5.1 Abstract

Progesterone, a product of the cumulus surrounding the oocyte exerts its effects via a non-genomic mechanism to influence hyperactivation, acrosome reaction, chemotaxis and capacitation in human sperm. Bolus application of progesterone results in a biphasic Ca^{2+} response with a rapid $[Ca^{2+}]_i$ transient, followed by a sustained elevation. Recent reports have determined that a major component of the transient response is due to the direct activation of CatSper channels by progesterone. However, inhibition of CatSper currents only partially inhibits the progesterone-induced $[Ca^{2+}]_i$ transient, suggesting a second mode of Ca^{2+} entry during this phase. In addition, SOCE has been linked to the sustained phase of the progesterone response, as the mobilisation of an intracellular Ca^{2+} store has been shown to occur during this period. In previous chapters we have detected and localised SOCE proteins to regions of intracellular Ca^{2+} stores and we have shown that SOCE in human sperm can be altered by the best characterised SOCE modulator 2-APB. Hence our aim for this chapter was to determine if pharmacological modulation of SOCE had any effects during the biphasic $[Ca^{2+}]_i$ response to progesterone application. By using single cell Ca^{2+} imaging we show that 5μM 2-APB potentiated the progesterone-induced $[Ca^{2+}]_i$ transient at the sperm posterior head and neck (PHN) and midpiece but not at the flagellum. This data suggests 2-APB sensitive SOC channels located in the PHN and midpiece regions contribute to the initial $[Ca^{2+}]_i$ transient induced by progesterone. When examining the sustained phase, 2-APB pre-treatment potentiated the $[Ca^{2+}]_i$ observed in the midpiece but had negligible effects in the PHN. Higher doses of 2-APB (50-100μM) did not potentiate the $[Ca^{2+}]_i$ transient and inhibited the sustained response, consistent with the reported effects of high-dose 2-APB on SOCE. We

therefore propose that the activation of SOCE may contribute to both the initial $[Ca^{2+}]_i$ transient and sustained phase induced by progesterone on human sperm.

5.2 Introduction

Once semen is deposited in the anterior vagina, sperm cells leave the seminal plasma and are regulated and influenced by the cells and secretions of the female reproductive tract (FRT) and cumulus-oocyte complex. Progesterone is the best characterised endogenous regulator of sperm activity, present throughout the FRT with levels peaking at 1-10µM concentrations in the cumulus, a mass of granulosa cells encompassing the oocyte where progesterone is actively synthesised (Osman *et al.*, 1989; Munuce *et al*., 2006; Correia and Kirkman-Brown, 2007). Groups have demonstrated that progesterone can influence several sperm functions including hyperactivation (Calogero *et al*. 1999; Jaiswal *et al*, 1999), acrosome reaction (Muratori *et al.*, 2009), chemotaxis (Teves *et al*., 2006) and capacitation (Yamano *et al.*, 2004). Consequently, the response of human sperm to progesterone is correlated with fertility with decreased responsiveness seen in sub-fertile patients (Falsetti *et al.*, 1993).

The effects of progesterone on human sperm are not mediated via a classical pathway of steroid signalling, typically involving binding to a nuclear receptor to initiate gene transcription. Indeed, neither transcription nor translation is believed to occur in mature sperm and progesterone therefore exerts its effects via a 'non-genomic' mechanism, to instigate a rapid Ca^{2+} influx into the cell cytoplasm in less than one second (Blackmore *et al*., 1990; Baldi *et al*., 2009). Bolus application of 0.3nM-3µM progesterone leads to a rapid transient Ca^{2+} increase followed by a sustained elevation (also known as the plateau phase) (Blackmore, 1993; Meizel, 1995).

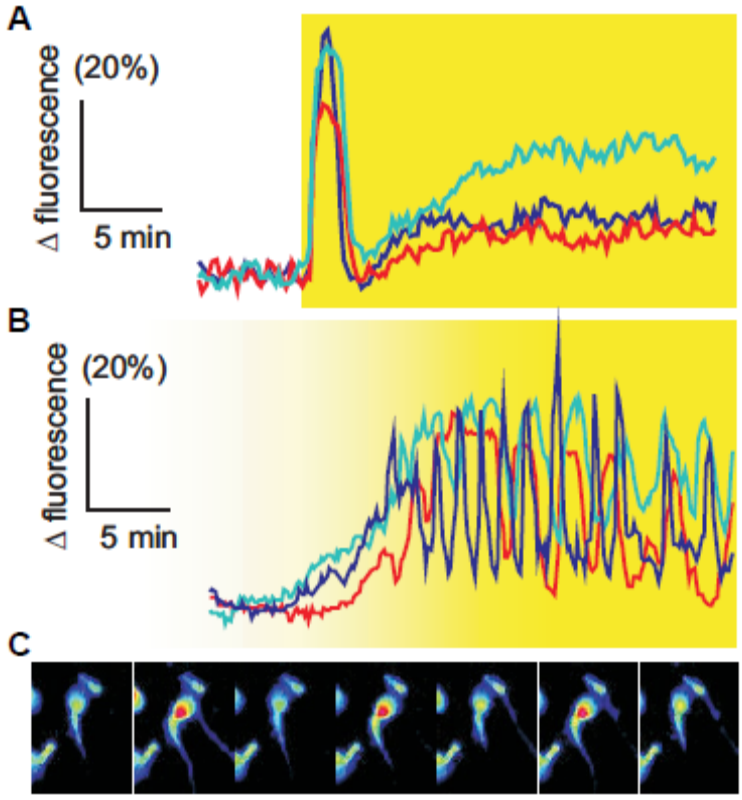

Figure 5.1 The influence of progesterone on human sperm applied as either a 3.1µM bolus dose or as a 0.3-1µM logarithmic gradient (from Bedu-Addo *et al.,* 2008). **(A)** When applied as bolus dose, a biphasic elevation can be observed. **(B)** This is opposed to the oscillations seen with the application of a progesterone gradient. **(C)** Pseudo-coloured imagery can be used to demonstrate sperm cells producing Ca^{2+} oscillations (with high $[Ca^{2+}]_i$ shown by warm colours).

Recently, two groups utilised a novel patch clamp technique for mature sperm to demonstrate that a major component of the transient response is due to the direct activation of CatSper channels by progesterone (Lishko *et al.*, 2011; Strunker *et al.*, 2011). The opening of these CatSper channels potentiates a rapid influx of Ca^{2+} into the principal piece of the flagellum to trigger hyperactivation. In addition, CatSpers are ideally positioned to aid chemotactic turns (Qi *et al.,* 2007). However, the use of the T-type channel blocker NNC55-0396 abolished CatSper currents in whole-cell clamped human sperm (Lishko *et al.,* 2011; Strunker *et al.,*

2011) but only partially inhibited the progesterone-induced $[Ca^{2+}]_i$ transient even when applied at concentrations well in excess of the saturating dose (Strunker *et al*., 2011; Lefievre, unpublished data). Furthermore, we have observed that the progesterone-induced Ca^{2+} transient phase can be pharmacologically dissected into an 'early' component (almost certainly CatSper activation) and a second, 'late' component (Kirkman-Brown *et al*., 2000), Therefore, it appears that progesterone activates a second Ca^{2+} signalling response in human sperm, either downstream of or in parallel to its action on CatSper.

The identity of this second component of the Ca^{2+} signal is unknown, but may be derived from the mobilisation of intracellular Ca^{2+} stores culminating in SOCE (also known as capacitative Ca^{2+} entry (CCE)). If progesterone is applied as a logarithmic gradient (as opposed to a bolus dose), which is more comparable to the *in vivo* situation, the large initial Ca^{2+} transient does not occur (Harper *et al.,* 2004). However, slower $[Ca^{2+}]_i$ oscillations can still be observed in up to 50% of the cell population (Bedu-Addo *et al.*, 2007, Figure 5.1). These regular oscillations in addition to the oscillations observed in the plateau phase following a Ca^{2+} transient have been shown to be initiated by progesterone mobilising an intracellular Ca^{2+} store present in the sperm neck region (Harper *et al.,* 2004). These oscillations are reminiscent of somatic cells induced to perform cyclic mobilisation of intracellular Ca^{2+} stores (Berridge *et al.*, 1993) and they depend on Ca^{2+} influx to maintain store refilling (Shuttleworth and Mignen, 2003). In addition, SOCE in sperm has been reported in other species namely mouse (O'Toole *et al.*, 2000), sheep (Dragileva *et al.*, 1999), and sea urchins (Gonzalez-Martinez *et al.*, 2004, Ardón *et al.*, 2004). In most cases the initial $[Ca^{2+}]_i$ transient caused by mobilisation of stored Ca^{2+} was negligible compared to the subsequent prolonged elevation, suggesting that the Ca^{2+} content of the store, though a crucial

'trigger', was small but sufficient to initiate SOCE (Blackmore, 1993; Dragileva *et al*., 1999; Williams & Ford, 2003).

We have previously detected and localised SOCE proteins namely Orai1-2 and STIM1-3 primarily to the regions of intracellular Ca^{2+} stores (chapter 3). We have also shown that SOCE in human sperm can be altered by the best characterised SOCE modulator 2-APB (chapter 4). Therefore, we wanted to determine whether pharmacological modulation of SOCE had any effects during the biphasic $[Ca^{2+}]_i$ response to progesterone application. This enables us to further determine if SOCE has a role in the progesterone response.

Chapter Aims

The aims of this chapter were to investigate if both stimulatory (2-5μM) and inhibitory (50-200μM) 2-APB doses had any effects on the biphasic Ca^{2+} response to progesterone application. Furthermore, we wanted to dissect these responses and examine if there were any differences in the $[Ca^{2+}]_i$ response in the midpiece and flagellum as opposed to the typical region of interest, the posterior head and neck (PHN).

5.3 Results

5.3.1 2-APB enhances the progesterone-induced $[Ca^{2+}]_i$ transient in the PHN.

A biphasic $[Ca^{2+}]_i$ response can be seen in >90% of human sperm cells treated with a 3µM dose of progesterone (Figure 5.2A) (Kirkman-Brown *et al*., 2000). Low dose (5µM) 2-APB acts on SOCE to stimulate increased activity of CRAC channels and consequently increases I_{CRAC} (DeHaven *et al*., 2008). Pre-treating our fixed sperm populations with 5µM 2-APB prior to progesterone exposure, increased the amplitude of the initial $[Ca^{2+}]_i$ at the posterior head and neck region (PHN) by 58±13% in comparison with parallel controls (p=0.0001, n=20, paired t-test; Figures 5.2B, C, D). These results were confirmed using fluorometry, whereby cell suspensions loaded with fura2 (as opposed to Oregon Green 488 BAPTA-1/AM (OGB) in Ca^{2+} imaging) gave similar results. 2µM 2-APB increased the amplitude of the transient from 137±28 nM to 289 ±42 nM (P=0.0005; n=14).

From analysing the kinetics of the mean responses (R_{tot}) of these Ca^{2+} imaging experiments, there was no difference in the rise time of the $[Ca^{2+}]_i$ transient (from initiation to maximum, control=36.6±2.8 seconds; 2-APB pre-treated =37.0±2.9 seconds; P=0.80, paired t-test, n=16). However, there were differences in the decay phase (from peak to the inflexion at the end of the falling phase) which was slightly increased in preparations pre-treated with 5µM 2-APB (from 107±7 seconds to 119±7 seconds, P=0.03, paired t-test, n=16). In addition, pre-treatment with higher doses of 2-APB (50µM and 100µM) also caused an enhancement of the

$[Ca^{2+}]_i$ transient amplitude, but the effect was smaller (Figure 5.2D) and at 100µM was not significant (P>0.25 compared to non-pre-treated preparations, paired t-test, n=4).

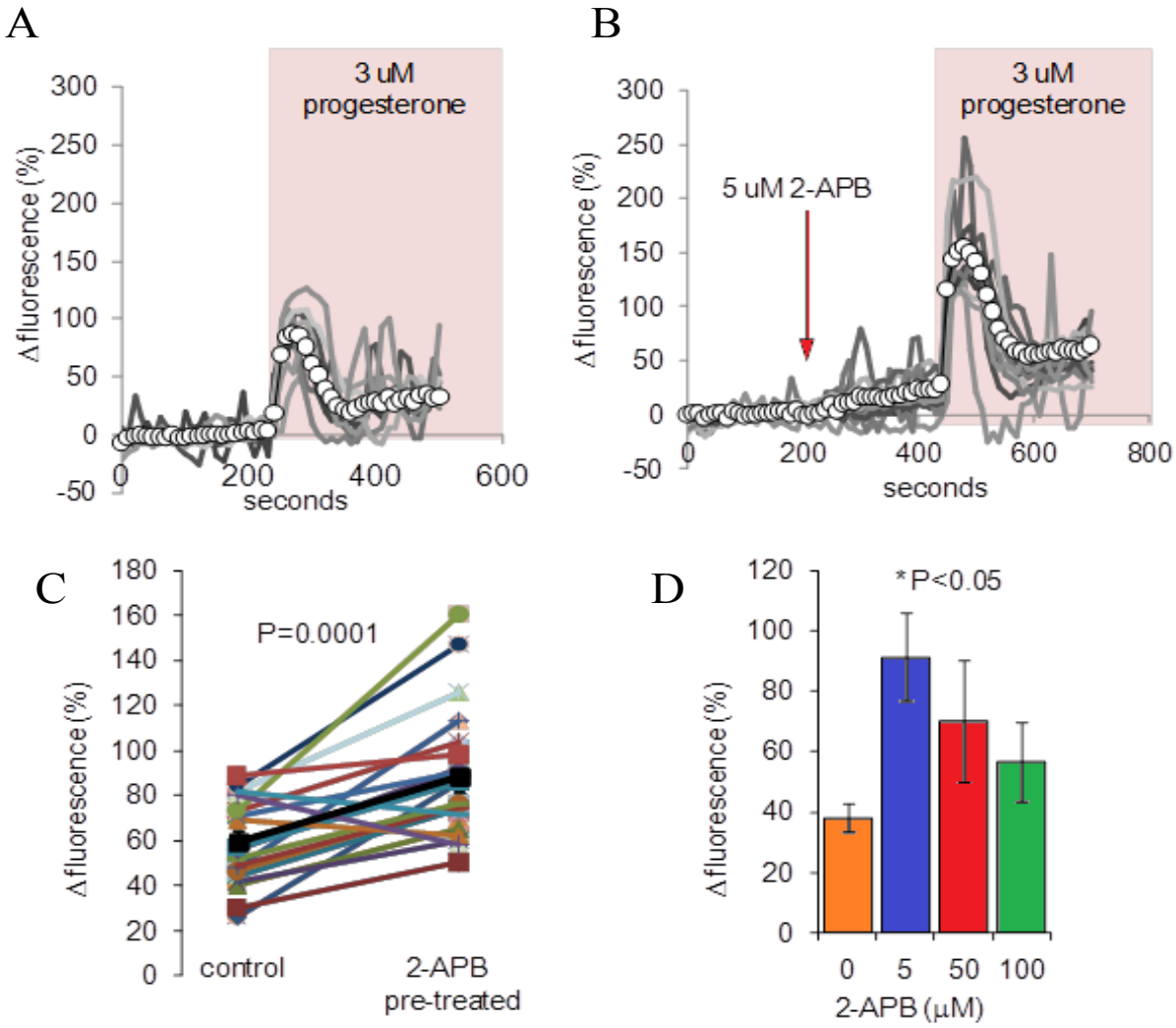

Figure 5.2 2-APB potentiates the progesterone-induced $[Ca^{2+}]_i$ transient. **(A)** Capacitated sperm are treated with 3µM progesterone (shown by shading) which causes an $[Ca^{2+}]_i$ transient. **(B)** Cells were treated with 3µM progesterone as in (A) except 5µM 2-APB was added prior to progesterone application (arrow). Individual cell traces can are shown by grey lines and experimental averages (R_{tot}) are shown by white circles. **(C)** Summary of results from 20 pairs of experiments with control (left) and 5µM 2-APB pre-treated (right). Each point shows mean response (R_{tot}) at peak of progesterone transient. Mean is shown by black trace. **(D)** Bars show the mean effect of various 2-APB concentrations on the peak amplitude of the progesterone transient (n=4).

5.3.2 Transient responses to progesterone in the midpiece and flagellum.

Typically, OGB-loaded human sperm fluoresce at the PHN region (Nash *et al.*, 2010) and is most likely the main region detected in fluorimetric population recordings. However, it has recently been determined that the primary site of action for progesterone is the CatSper channel located on the principal piece of the flagellum (Lishko *et al*., 2011; Strunker *et al*., 2011). Therefore, we compared the effects of 2-APB pre-treatment on progesterone-stimulated $[Ca^{2+}]_i$ responses in the PHN, with those in the midpiece and flagellum (Figure 5.3A).

Firstly, from examining the same experiments but focusing on the midpiece region, exposure to progesterone also caused a transient $[Ca^{2+}]_i$ rise. However, this rise was typically ~25% smaller in comparison to the PHN ($p<0.002$, n=10), although both time to peak and decay duration of R_{tot} were similar ($P>0.05$, Figures 5.3, B). In parallel experiments, but where cells were pre-treated with 5μM 2-APB prior to progesterone application, the response in the midpiece was enhanced similar to that of the PHN (Figure 5.3B, C; p=0.002 compared to parallel controls, n=10).

Secondly, we analysed $[Ca^{2+}]_i$ in the principal piece of the flagellum from five pairs of experiments (control and 5μM 2-APB pre-treated). The difficulty in this analysis is that typically only human sperm heads are fixed to the poly-D coated slides and subsequently there is often flagella movement during the experiment. Therefore, we only used cells where the flagella $[Ca^{2+}]_i$ could be accurately assessed i.e. where the principal piece was visible and

in focus throughout the experiment. Notably, the duration of $[Ca^{2+}]_i$ response in the principal piece was 73±7.5 seconds, significantly shorter than in the PHN region in the same cells (143±8.4 seconds; $P<0.0005$, Figure 5.5A). However, the amplitude (normalised to pre-stimulus fluorescence) was significantly larger ($P=0.0004$, n=43, Figures 5.5A). Interestingly, pre-treatment with 2-APB did not increase the amplitude of the progesterone transient in the principal piece (131±12% in controls, n=43; 115±11% after pre-treatment, n=57, $P>0.3$; Figure 5.4B) but the ratio of transient amplitude PHN to amplitude of the principal piece in the same cell increased from 0.79±0.07 in control cells to 1.52±0.21 in cells pre-treated with 5μM 2-APB ($P=0.00011$; Figure 5.5C).

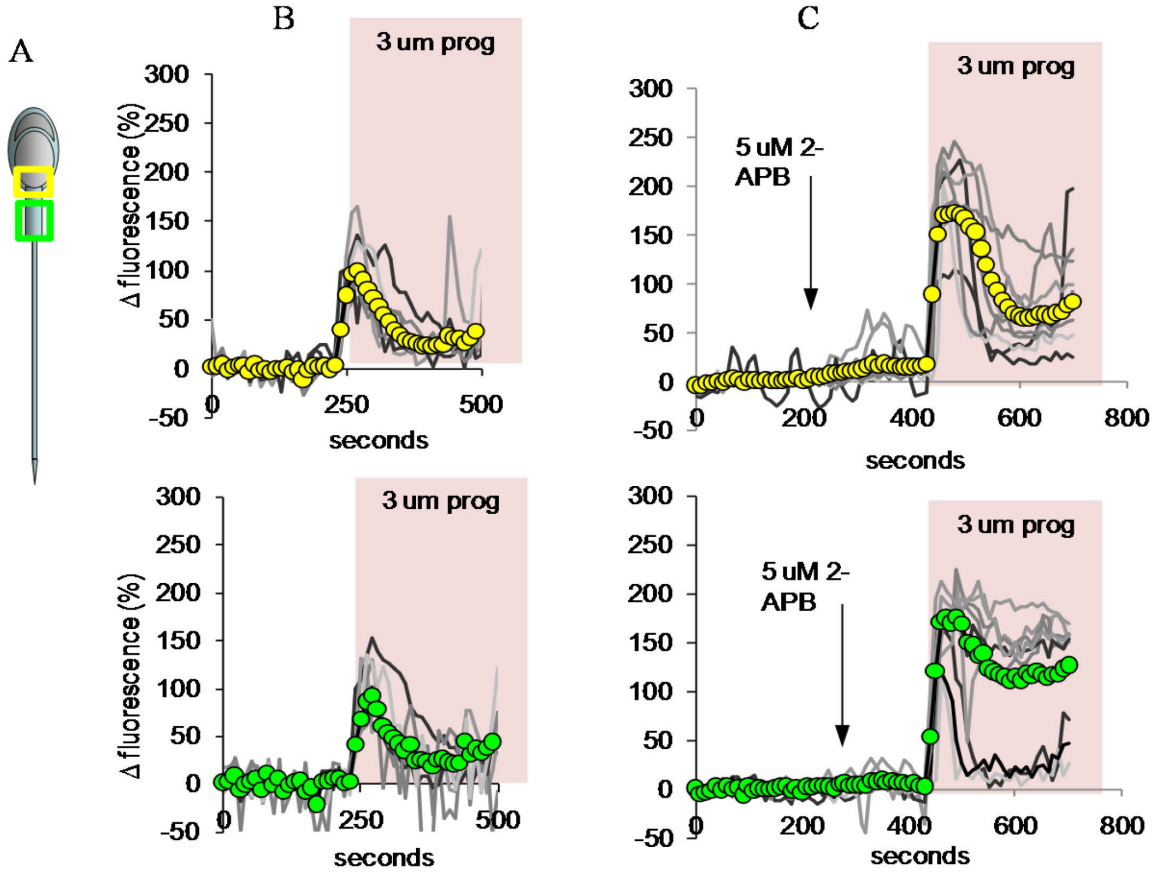

Figure 5.3 5µM 2-APB enhances the sustained phase of the $[Ca^{2+}]_i$ progesterone response in the midpiece region. **(A)** Diagram to show regions of interest with posterior head and neck (PHN) in labelled in yellow, midpiece in green and principal piece of flagellum in red. **(B)** $[Ca^{2+}]_i$ transient caused by progesterone application (shown by shading) at the PHN region (top panel) and midpiece (bottom panel). **(C)** Parallel experiments to (B), except cells are pre-treated with 5µM 2-APB. Individual cell traces can are shown by lines and experimental averages (R_{tot}) are shown by circles.

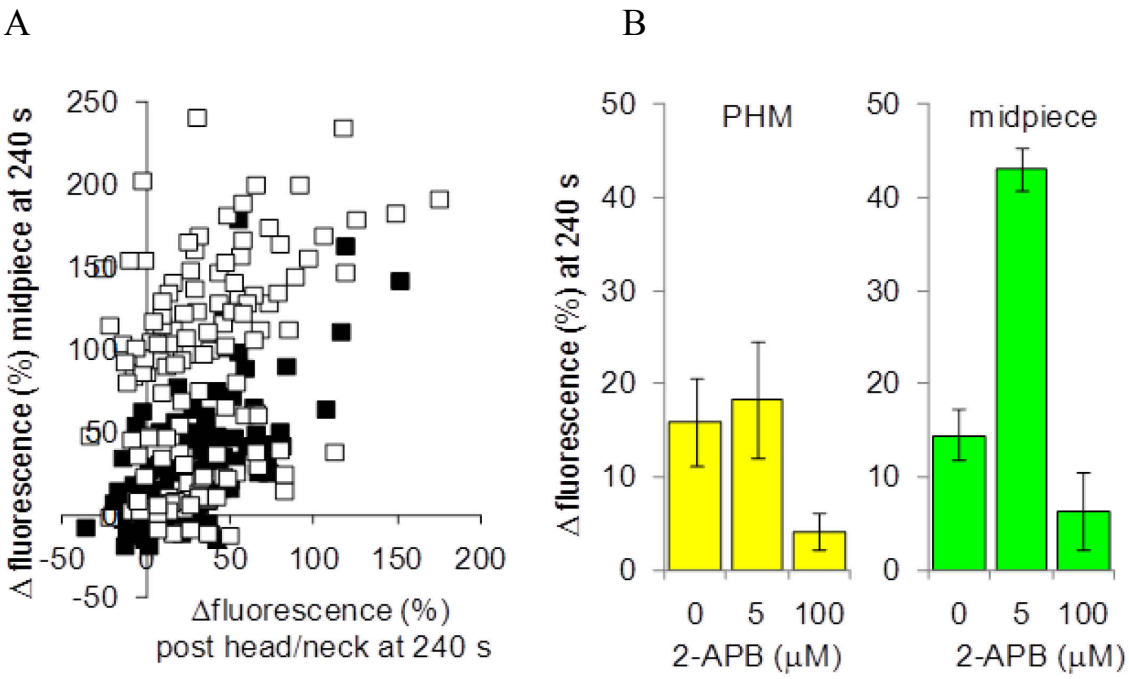

Figure 5.4 2-APB acts in a dose-dependent manner to modulate the sustained response in the midpiece, but not in the PHN. **(A)** Scattergram shows the sustained response (240 seconds after progesterone application) in PHN and midpiece from control (black squares) and 2-APB pre-treated (white squares) cells (both show >130 cells from 4 experiments. **(B)** Dose-dependence effect of 2-APB pre-treatment on the sustained phase of the progesterone response (240 seconds after progesterone application). PHN is represented by the yellow bars and midpiece is represented by the green bars from four sets of parallel control and 2-APB (5 and 100μM pre-treated experiments. Each bar shows mean±SEM.

5.3.3 5μM 2-APB alters the plateau phase of progesterone induced $[Ca^{2+}]_i$ transients.

To investigate the effect of 2-APB on the plateau phase we examined the difference between the mean response (R_{tot}) recorded immediately prior to the application of progesterone and the R_{tot} four minutes later. When examining this difference at the PHN region there was sometimes an increase with 2-APB treatment but this was inconsistent (control=18±5%, 2-APB pre-treated=20±6%) and not significant (P=0.66, paired t-test, n=11; Figures 5.3C, 5.4B). However when examining the midpiece, 2-APB pre-treatment strongly enhanced $[Ca^{2+}]_i$ in the sustained elevation phase (from 16±4% to 52±12%, P=0.004; Figures 5.3C, 5.4B). Interestingly, in Figure 5.3C two populations of cells can be observed, one being strongly enhanced by 2-APB treatment, the other returning almost to control levels.

Figure 5.4A shows the relationship between the sustained response amplitudes in the PHN and the midpiece in individual cells. Under control conditions there is a close correspondence between the sustained responses in these two regions of the sperm (black squares; y=0.75x + 6.5; R^2=0.41) but in 2-APB-pretreated cells there are two populations of sustained responses, one resembling that seen in control cells and the other showing an 'active' sustained response in the midpiece, consistent with the two types of midpiece responses noticeable in Figure 5.3C. On the basis of frequency distributions for amplitude at 240 s we defined 'active' sustained responses as those of ≥80%. 2-APB increased the incidence of these 'active' responses from 10% (13/136) in control cells to 51% (69/136) in 5μM 2-APB pre-treated cells ($P<10^{-12}$, chi-square). In 4 sets of experiments we compared the effect on the sustained $[Ca^{2+}]_i$

of 2-APB at concentrations of 5μM and 100μM. At both the PHN and midpiece there was a clear inhibition of the $[Ca^{2+}]_i$ elevation recorded 240 s after progesterone application with 100μM 2-APB pre-treatment (Figure 5.4B).

When analysing the progesterone response of single cell traces from the PHN and midpiece of 5μM 2-APB pre-treated cells we observed a delay between the $[Ca^{2+}]_i$ increase in the PHN and the midpiece. In the cell population whereby 2-APB pre-treatment does not initiate an increase in amplitude of sustained phase in the midpiece, the elevation mirrored that of in the PHN but just of lower amplitude (Figure 5.6A). However, when 2-APB pre-treatment did initiate an increase in amplitude of the sustained phase at the midpiece, we often observed an inflection in the rising phase of the $[Ca^{2+}]_i$ increase (Figure 5.6B, arrow) and occasionally a delay in onset compared to the PHN (33.8±6.3% of cells, n=6). Subtraction of the response recorded at the PHN from that in the midpiece revealed a sustained $[Ca^{2+}]_i$ increase which became detectable 10-30s after application of progesterone (Figures 5.6B, C). Examination of midpiece traces from cells in parallel control (non 2-APB pre-treated) experiments showed a similar delay in the sustained response but the frequency of occurrence was much lower (7.6±2.8% of cells; P=0.01, paired t-test).

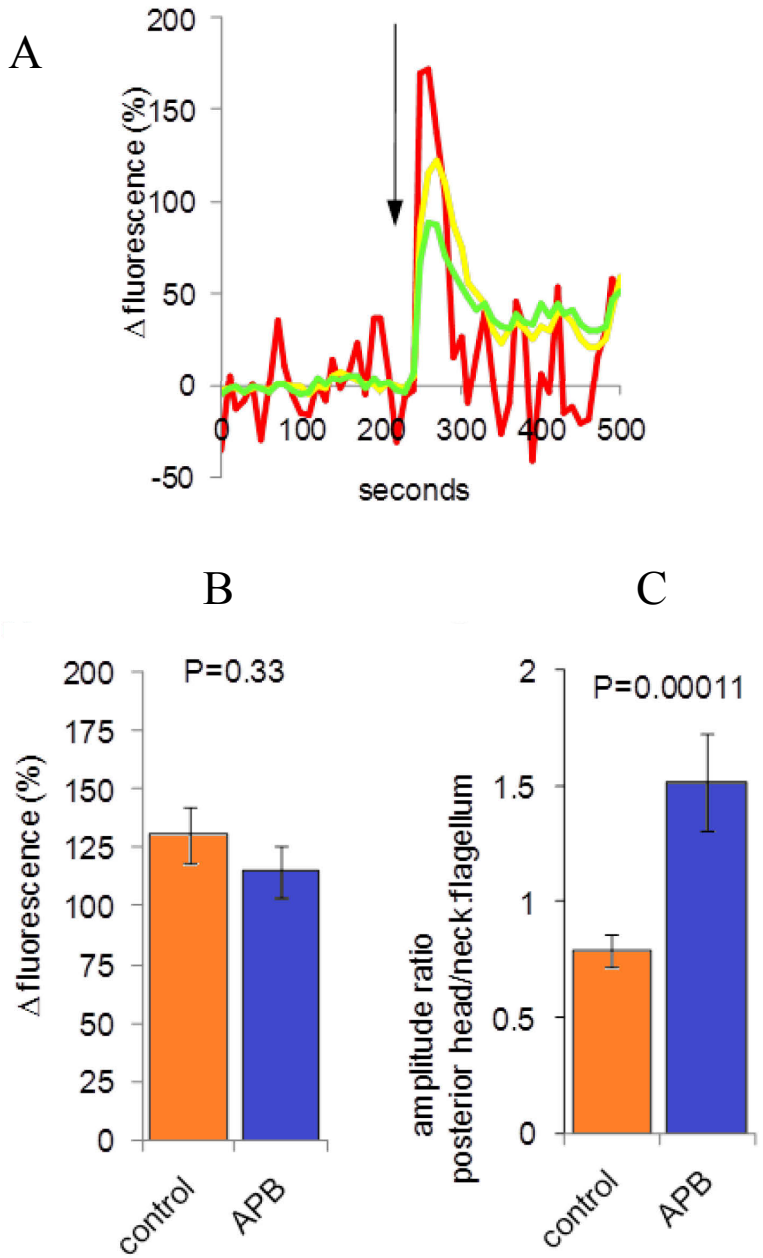

Figure 5.5 5µM 2-APB pre-treatment does not enhance flagella $[Ca^{2+}]_i$ following progesterone application. **(A)** $[Ca^{2+}]_i$ transient caused by progesterone application (arrow) at the PHN region (yellow), midpiece (green) and principal piece of flagellum (red). Each trace shows the mean response from the same 9 cells. **(B)** Bars show the amplitude of peak progesterone induced $[Ca^{2+}]_i$ transient in the principal piece of the flagellum, in control conditions (orange bar, n=43) and following 5µM 2-APB pre-treatment (blue bar, n=57). **(C)** Bars show the ratio of amplitude of peak progesterone induced $[Ca^{2+}]_i$ transient in the PHN and principal piece, in control conditions (orange bar, n=43) and following 5µM 2-APB pre-treatment (blue bar, n=57).

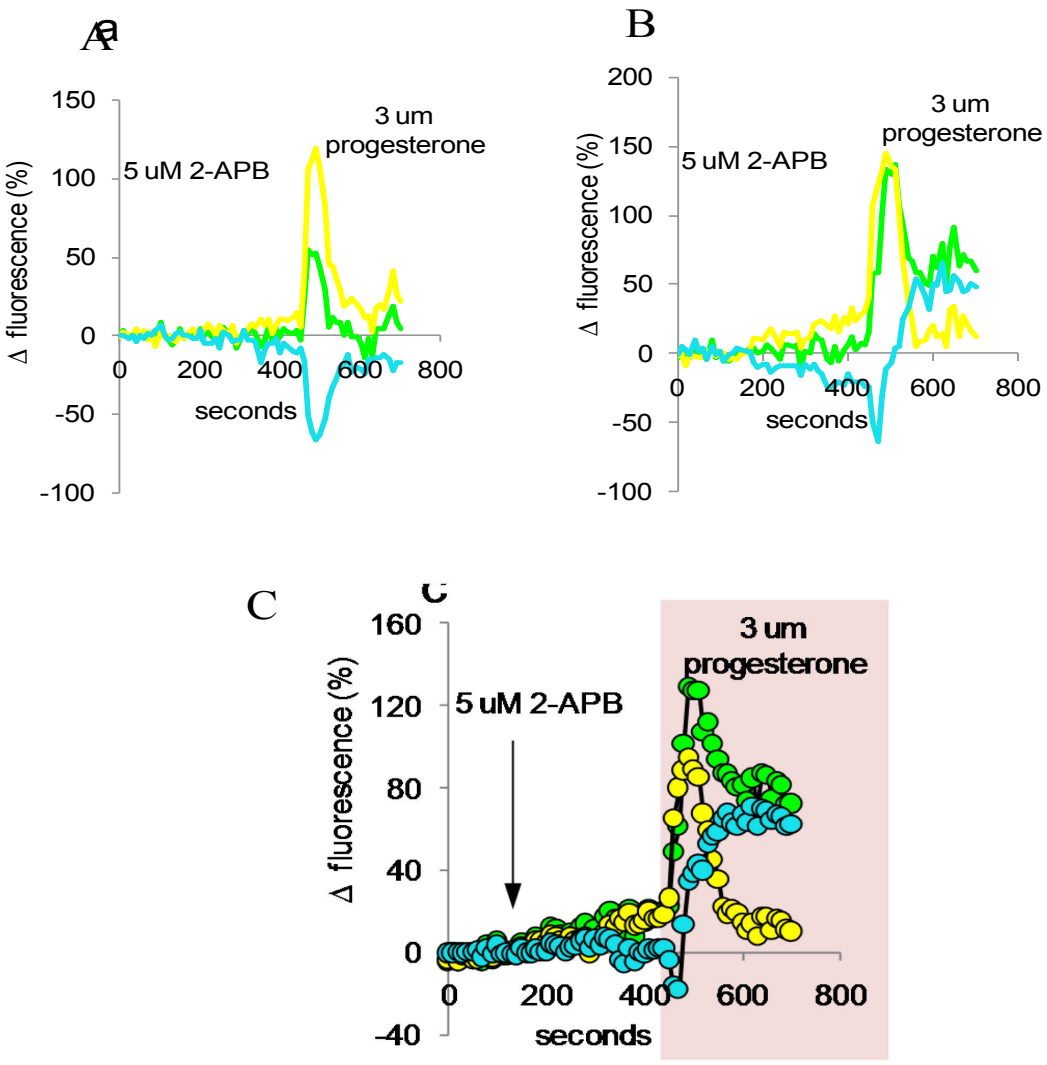

Figure 5.6 5µM 2-APB pre-treatment alters the sustained phase of $[Ca^{2+}]_i$ progesterone response in the midpiece. **(A)(B)**; Progesterone-stimulated $[Ca^{2+}]_i$ elevation in the PHN (yellow trace) and midpiece (green trace) of two 2-APB pre-treated cells from the same experiment. Application of 5µM 2-APB is shown by arrow and application of 3µM progesterone is shown by shading. Blue traces shows difference between midpiece and PHN responses. In 'A' $[Ca^{2+}]_i$ in the midpiece (green trace) during the transient is modest and $[Ca^{2+}]_i$ returns to control levels, as opposed to in 'B' whereby a large elevation in $[Ca^{2+}]_i$ can be seen during the transient followed by a plateau. In 'B' there is a visible inflection during the rising phase of the transient (arrow) and a late rise in the difference (blue) trace. **(C)** Shows the mean responses (R_{tot}) from 35 cells in the same experiment.

5.3.4 Examining the progesterone $[Ca^{2+}]_i$ response using an increased frame rate.

In three experiments we attempted to see this delay more clearly by using an increased frame rate (10 Hz). Our results are consistent with the recent reports that progesterone directly activates CatSper channels (Lishko *et al.*, 2011; Strunker *et al.*, 2011), as the $[Ca^{2+}]_i$ response in the principal piece preceded that in the PHN region by 1.6 ±0.2 s (n=29; $P<10^{-8}$) (Figure 5.7A). At first, the initial Ca^{2+} transient kinetics in the midpiece appeared synchronous with those in the PHN. However, in cells showing an increase in $[Ca^{2+}]_i$ at the midpiece in the sustained phase, there was often a clear inflexion in the rising phase after 10-30 seconds, thus indicating a second Ca^{2+} mobilisation event (Figure 5.7B).

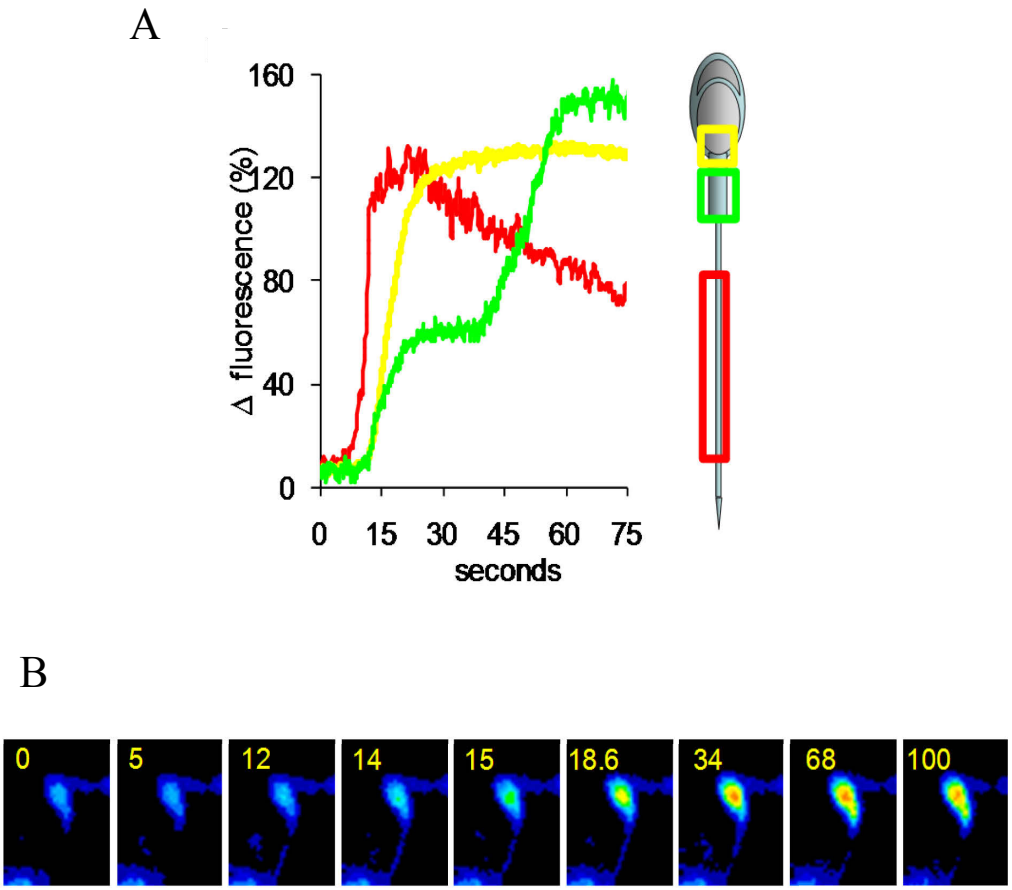

Figure 5.7 Examining the 5µM 2-APB pre-treated progesterone biphasic $[Ca^{2+}]_i$ response at 10 Hz. **(A)** Progesterone-stimulated $[Ca^{2+}]_i$ elevation in the flagellum (red trace), PHN (yellow trace) and midpiece (green trace) of a 5µM 2-APB pre-treated cell imaged at 10 Hz. The flagellar response slightly precedes responses in the other two compartments and the rising phase of the midpiece response shows a clear inflexion ≈25s after onset. **(B)** Pseudo-coloured imagery to demonstrate initial progesterone-stimulated $[Ca^{2+}]_i$ elevation in the PHN followed by the midpiece later (with high $[Ca^{2+}]_i$ shown by warm colours).

5.4 Discussion

Recently, Lishko *et al.* (2011) and Strunker *et al.* (2011) determined that the primary site of action for progesterone is at the CatSper channels located in the principal piece of the flagellum. However, this response could not be completely inhibited by agents such as NNC55-0396, which did abolish CatSper currents in whole-cell clamped human sperm. Therefore, this strongly suggests other components are involved in the progesterone induced $[Ca^{2+}]_i$ biphasic response. We have shown that 2-APB acts in a dose dependent manner to effect the progesterone induced $[Ca^{2+}]_i$ transient (Figures 5.2A-D). Low doses had the strongest affect, as opposed to high doses that had negligible effects on the transient. This complex dose-dependence is characteristic of the action of 2-APB on cells expressing the STIM and Orai mediated SOCE system (DeHaven *et al*., 2008).

Analysis of discrete sections of human sperm revealed different effects on the Ca^{2+} transient following progesterone application. Under control conditions, a transient response was seen at both the PHN and midpiece, although the response in the midpiece was significantly smaller (Figure 5.3B, C). In the principal piece of the flagellum, the transient was larger but briefer than in other sections (Figure 5.5A). Pre-treatment with 5μM 2-APB significantly potentiated the transients recorded in the PHN and midpiece, but not in the principal piece (Figure 5.3B, C and 5.5B, C). Therefore it appears the $[Ca^{2+}]_i$ rise in the flagellum following progesterone application is not altered by 2-APB. This correlates with STIM and Orai distribution in human sperm, whereby only small amounts of STIM2 and no other STIM/Orai proteins are found in this area (Figure 3.10) and there are no known Ca^{2+} storage organelles. In addition, this indicates that the increases in transient $[Ca^{2+}]_i$ seen in the PHN and midpiece following

progesterone treatment are not merely due to Ca^{2+} entry through CatSper channels in the flagellum, followed by passive diffusion.

Studies have shown that the sustained (often oscillatory) phase of the progesterone induced $[Ca^{2+}]_i$ transient may be due to mobilisation of Ca^{2+} from intracellular stores (Harper *et al*., 2004). When examining the sustained $[Ca^{2+}]_i$ elevation (measured 4 minutes after progesterone application), this was significantly enhanced in the midpiece by 5μM 2-APB pre-treatment, in comparison to the PHN (Figures 5.3, 5.4, 5.6). Therefore, we hypothesise that low-dose 2-APB has two effects; they activate SOCs in the neck instantly (similar to skeletal cells (Launikonis and Rios, 2007, Stiber *et al*., 2008)), whilst in the midpiece there is a late activation of SOCs occurring after Ca^{2+} store mobilisation. This hypothesis is supported by the data collected using an increased image acquisition rate (>1 Hz, Figure 5.7A). Here the progesterone-induced $[Ca^{2+}]_i$ transient in the flagellar principal piece occur 1-2 seconds prior to those occurring in the midpiece and PHN. This is consistent with previous observations that progesterone directly and immediately activates CatSper channels (Strunker *et al*., 2011; Lishko *et al*., 2011). This rise in flagella $[Ca^{2+}]_i$ induces mobilisation of Ca^{2+} from the intracellular Ca^{2+} stores at the neck and midpiece (Figure 5.7A). This mobilisation may be negligible but sufficient to activate SOCs which amplifies and prolongs the $[Ca^{2+}]_i$ signal, an effect that is potentiated by 2-APB. This is consistent with previous reports of a small initial $[Ca^{2+}]_i$ triggering SOCE (Blackmore, 1993; Dragileva *et al*., 1999; Williams & Ford, 2003) and previous studies showing an effect of progesterone on the mobilisation of intracellular Ca^{2+} stores (Harper *et al*., 2004; Publicover *et al*., 2007).

In summary, the potentiation of 2-APB pre-treatment on the progesterone-induced $[Ca^{2+}]_i$ transient at the sperm posterior head and neck (PHN) and midpiece but not at the flagellum, suggests a role for SOCE in the progesterone $[Ca^{2+}]_i$ transient. This also confirms CatSper channels in the flagellum are not potentiated by 2-APB, as expected, and that SOCE does not appear to occur in the flagellum consistent with the fact that there are no intracellular Ca^{2+} stores in this region. The sustained phase is also potentiated by 2-APB pre-treatment particularly at the midpiece indicating 2-APB sensitive SOCE systems in this area. This data correlates with the localisation of STIM and Orai proteins of the SOCE system primarily to the neck/midpiece regions in chapter 3. Furthermore, higher doses of 2-APB (50-100μM) did not potentiate the $[Ca^{2+}]_i$ transient and inhibited the sustained response, consistent with the reported effects of high-dose 2-APB on SOCE (DeHaven *et al*., 2008) and on SOCE traces in human sperm seen in chapter 4. We therefore propose that the activity of SOCE may contribute to both the initial $[Ca^{2+}]_i$ transient and sustained phase induced by progesterone on human sperm.

CHAPTER SIX: PHARMACOLOGICAL MODULATION OF SOCE AND THE PROGESTERONE INDUCED BIPHASIC [CA^{2+}] RESPONSE IN HUMAN SPERM USING LOPERAMIDE

6.1 Abstract

Loperamide, used in the pharmacological industry as an anti-diarrhoea medication has been shown to stimulate SOCE in cell types such as NIH 3T3 fibroblasts and astrocytoma 1321N cells with or without intracellular Ca^{2+} storage depletion. Due to the detection of STIM and Orai proteins (chapter 3) and the findings that SOCE is probably mediated by the STIM/Orai pathway which can be modulated by 2-APB (chapter 4), we wanted to investigate the modulation of SOCE by loperamide. Secondly, we wanted to investigate the effects of loperamide on the biphasic progesterone induced $[Ca^{2+}]_i$ response and examine if this had any impact on hyperactivation. We show that in human sperm 10μM loperamide caused an increase in resting $[Ca^{2+}]_i$ in more than 65% of cells. It is suggested that this may be due to activation of a small population of SOC channels that modulate basal $[Ca^{2+}]_i$ levels without prior Ca^{2+} store depletion. Pre-treatment with 10μM loperamide did not significantly enhance the amplitude of the progesterone-induced $[Ca^{2+}]_i$ transient although it did significantly increase the duration. Similarly to 5μM 2-APB pre-treated cells, the sustained component of the response to progesterone was significantly enhanced by loperamide pre-treatment. However, unlike 2-APB this effect of loperamide was similar in the sperm PHN region and in the midpiece, indicating slightly different targets for the two drugs. Using CASA we show that treatment with 10μM loperamide prior to progesterone application significantly enhanced the proportion of hyperactivated cells. These results therefore suggest that SOCE may contribute to both the initial $[Ca^{2+}]_i$ transient and sustained phase induced by progesterone on human sperm which can be modulated by loperamide.

6.2 Introduction

Marketed as Imodium, loperamide is a well known and widely used anti-diarrhoeal medication (Awouters *et al*., 1983; Shriver *et al*., 1981). Its primary mechanism of action, at nanomolar doses, is to block opioid receptors in the gastrointestinal tract to inhibit peristaltic contractions (Shriver *et al*., 1981). However, at micromolar concentrations, loperamide has been shown to stimulate SOCE channels in a dose-dependent manner following the depletion of intracellular Ca^{2+} stores (Daly *et al.*, 1995; Harper *et al*., 1997). Daly and Harper (2000), examined loperamide concentrations of 1-30μM and reported non-specific effects on VOCCs and potent calmodulin antagonist actions at higher doses. The mechanism of Loperamideis currently undetermined, although it is hypothesised that loperamide allosterically increases conduction through SOC channels (Harper and Daly, 1999). Typically, loperamide does not affect resting $[Ca^{2+}]_i$, however an increase in basal $[Ca^{2+}]_i$ levels has been reported in undifferentiated HL60 cells and astrocytoma 1321N cells, both of which were dependent on extracellular Ca^{2+} (Harper *et al*., 1997). These findings are thought to be due to a lower threshold for the initiation of SOCE in these cells types.

Bolus application of 0.3nM-3μM progesterone, secreted from the cumulus cells surrounding the oocyte leads to a rapid transient Ca^{2+} increase followed by a sustained elevation (also known as the plateau phase) (Blackmore, 1993; Meizel, 1995). The initial transient has been reported to be primarily due to the direct activation of CatSper channels by progesterone (Lishko *et al.*, 2011; Strunker *et al.*, 2011). However, as the T-type channel blocker NNC55-

0396 abolished CatSper currents in whole-cell clamped human sperm (Lishko *et al.,* 2011; Strunker *et al.,* 2011) but only partially inhibited the progesterone-induced $[Ca^{2+}]_i$ transient, this has indicated that other Ca^{2+} channels may play a role in the progesterone induced $[Ca^{2+}]_i$ response. In chapter 4 we have shown that 2-APB can modulate SOCE and in chapter 5 we have demonstrated that it can also affect the amplitude of the initial progesterone induced $[Ca^{2+}]_i$ transient and plateau phase. Subsequently we wanted to investigate if loperamide, a different SOCE modulator, has similar properties.

Chapter aims

The aims of this chapter were to determine if loperamide has an effect on resting $[Ca^{2+}]_i$ as seen with other cell types and as reported in chapter 3 with low-dose 2-APB on human sperm. Secondly, we wanted to investigate the effects of loperamide on the biphasic progesterone induced $[Ca^{2+}]_i$ response and examine if this had any impact on hyperactivation.

6.3 Results

6.3.1 Loperamide directly activates Ca^{2+} influx in human sperm

Loperamide has been shown to stimulate SOCE channels following the depletion of intracellular Ca^{2+} stores and even in resting cells (Daly *et al.*, 1995; Harper *et al*., 1997). The optimum concentration to initiate SOCE but minimise non-specific actions was reported at 10μM (Daly and Harper, 2000). Here, 10μM loperamide caused an increase in resting $[Ca^{2+}]_i$ in 66 ±7% of cells (8 experiments, 519 cells), occurring as either as a plateau/ramp (Figure 6.1A) or as a transient increase in $[Ca^{2+}]_i$ of up to 5 minutes in duration. The mean increase in fluorescence (R_{tot}) 90 seconds after application of 10μM loperamide was 22.1 ±4.7%, increasing to 30.1±7.7% after 3 min (6 experiments; 424 cells). When 10μM loperamide was applied to cells which had been perfused for 3 minutes with EGTA-buffered saline ($3x10^{-7}$M Ca^{2+}), there was no increase in fluorescence but there was a small fall in $[Ca^{2+}]_i$ (Figure 6.1B).

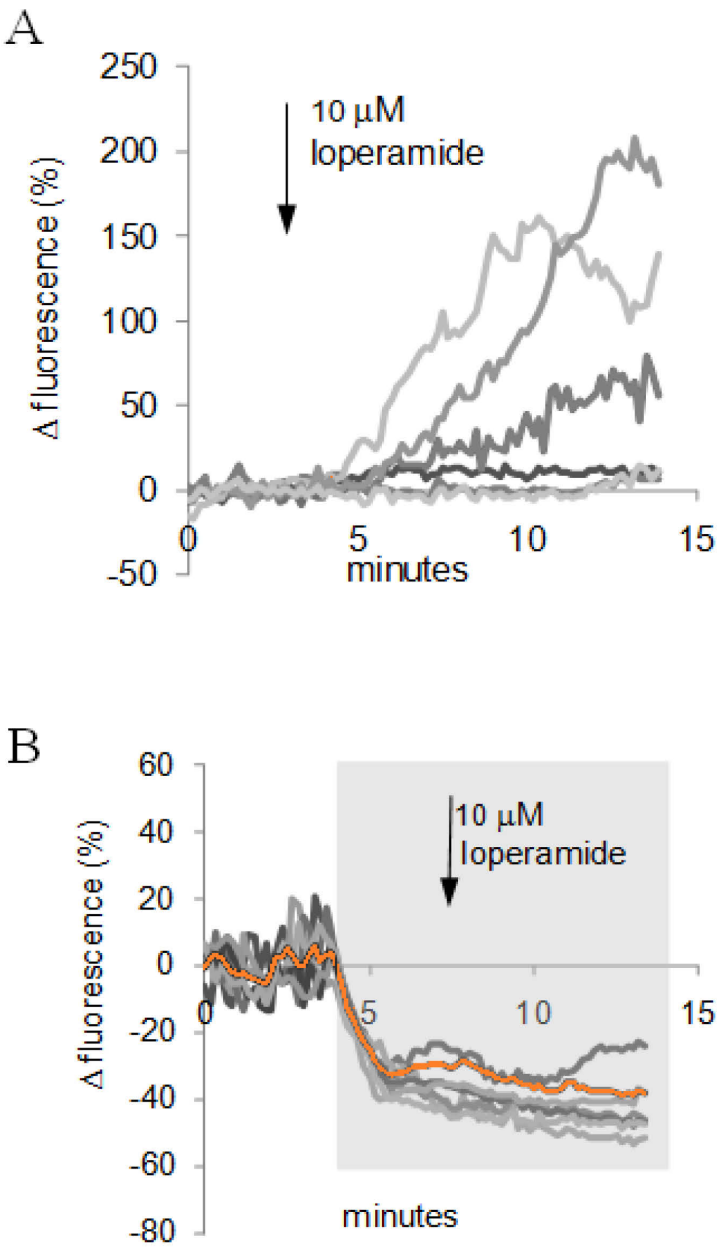

Figure 6.1 Effect of loperamide on $[Ca^{2+}]_i$ in human sperm. **(A)** Capacitated sperm were perfused with sEBSS and 10µM loperamide was added to the perfusion media from 6 minutes (arrow). Grey traces show example responses from 6 individual cells. **(B)** Effect of 10µM loperamide on resting $[Ca^{2+}]_i$ is reversed in low-Ca^{2+} saline. Cells were perfused with EGTA-buffered saline ($3x10^{-7}$M Ca^{2+}, shown by grey shading) then exposed to 10µM loperamide (arrow). The stimulatory effect of loperamide was abolished and in many cells there was a clear enhancement of the EGTA-induced fall in $[Ca^{2+}]_i$. Orange trace shows mean normalised fluorescence (R_{tot}) for this experiment. Grey traces show example responses from individual cells.

6.3.2 Loperamide potentiates the response of human sperm to progesterone.

In 7 out of 11 experiments, pre-treatment with 10μM loperamide enhanced the amplitude of the progesterone-induced $[Ca^{2+}]_i$ transient but this effect was inconsistent and was not statistically significant (P=0.38, paired t-test). More strikingly, in 11 paired experiments (control and pre-treatment experiments using the same sample) 10μM loperamide increased the duration of the progesterone-induced $[Ca^{2+}]_i$ transient (initiation to end of falling phase measured on the mean $[R_{tot}]$ trace) from 150±8 to 284±30 seconds (P=0.00035, paired t test; Figure 6.2B). In a small number of cells (10-20%) the transient peak persisted for ≥100 seconds before $[Ca^{2+}]_i$ began to fall (Figure 6.2A yellow and red traces) and in more than 50% of cells the initial $[Ca^{2+}]_i$ transient was followed by a second large plateau or a series of large $[Ca^{2+}]_i$ oscillations (Figure 6.2A). Similarly to 2-APB pre-treated cells (Figure 5.3), the sustained component of the response to progesterone (increment in R_{tot} 4 minutes after progesterone application) was enhanced by loperamide pre-treatment ($P<0.05$; paired t; n=9; Figure 6.2C). However, unlike 2-APB this effect of loperamide was similar in the sperm PHN region and in the midpiece (Figure 6.3).

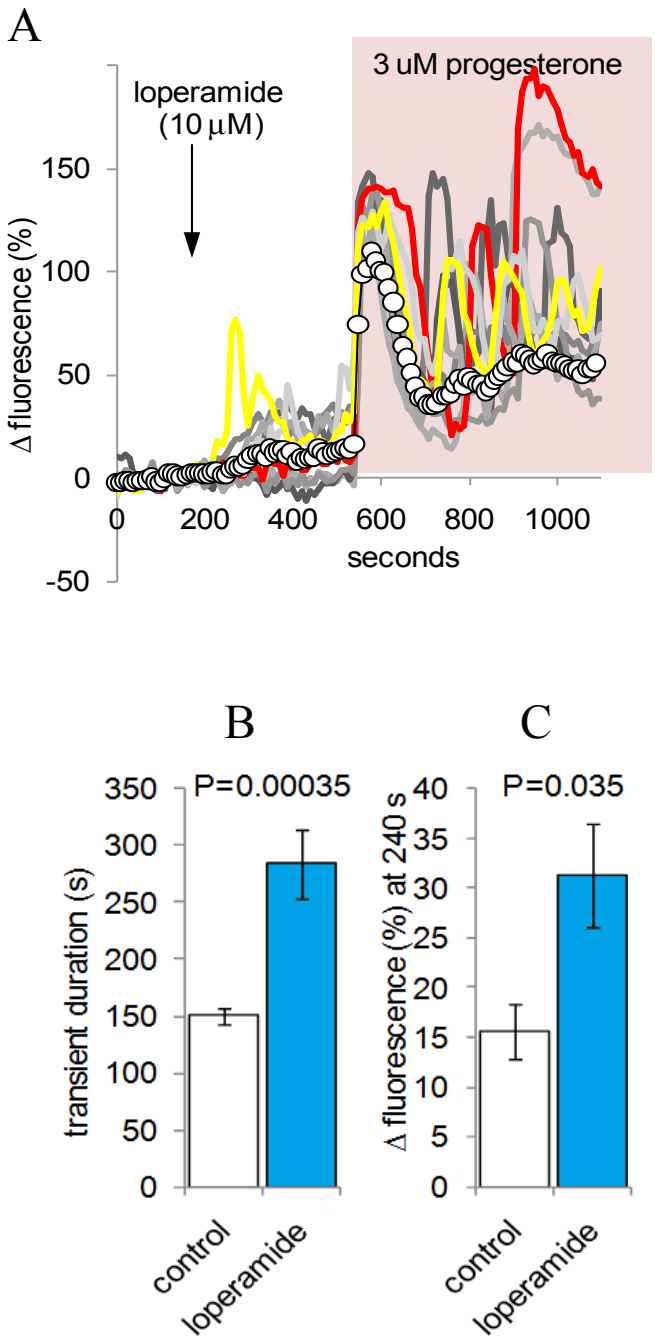

Figure 6.2 Loperamide potentiates the response of human sperm to progesterone. **(A)** Capacitated sperm were perfused with sEBSS and 10µM loperamide was added to the perfusion media from 180 seconds (arrow), followed by 3µM progesterone at 550 seconds (shading). Traces shows 9 individual cell responses and the mean (R_{tot} ○-○) for all cells in the experiment. **(B)** Duration of the progesterone-induced $[Ca^{2+}]_i$ transient was increased over that in parallel controls. Bars show mean±SEM of 11 paired experiments. **(C)** Mean progesterone-induced increase in fluorescence (R_{tot}) 240 seconds after progesterone application was increased over that in parallel controls. Bars show mean±SEM of 9 paired experiments.

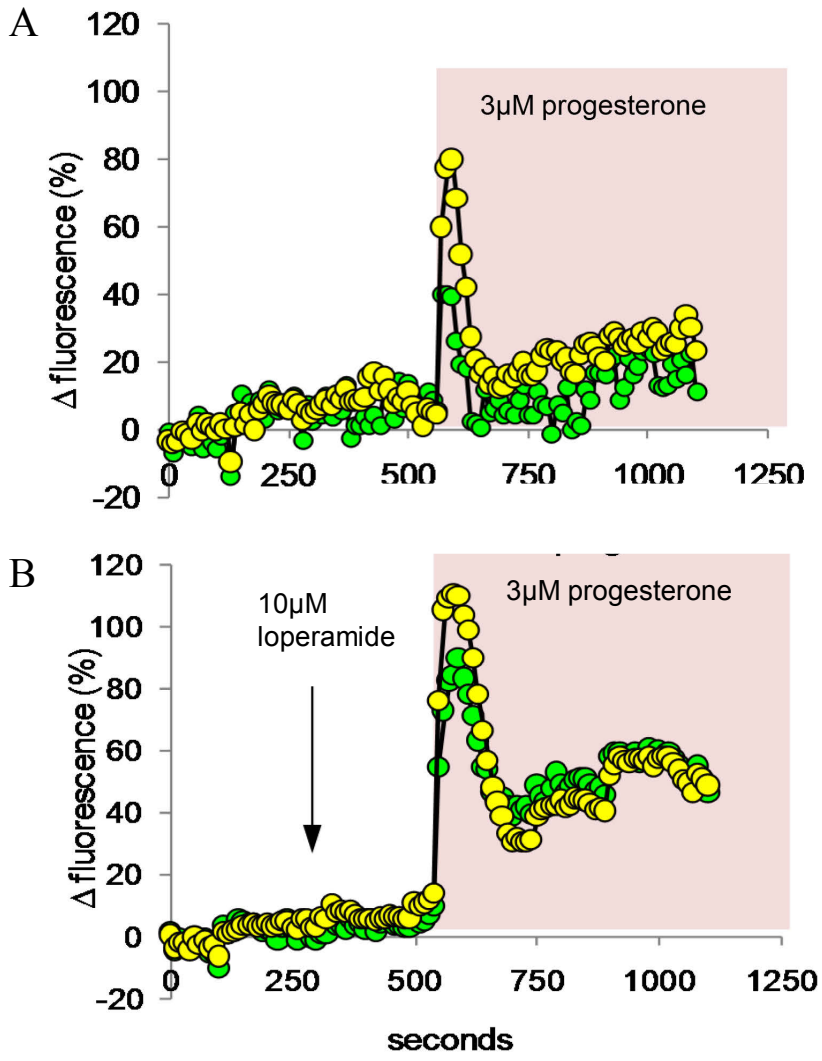

Figure 6.3 Effects of Loperamide pre-treatment on the progesterone response at the sperm posterior head and neck (PHN) and midpiece. Traces show mean normalised fluorescence (R_{tot}) in the PHN (yellow circles) and in the midpiece (green circles). **(A)** Shows control conditions (mean of 19 cells) and **(B)** after pre-treatment with 10μM loperamide (mean of 33 cells).

6.3.3 Loperamide potentiates progesterone-induced hyperactivation of motility.

Stimulation of human sperm with progesterone induces a burst of hyperactivation (Gakamsky *et al.*, 2009; Kilic *et al.*, 2009), apparently associated with the progesterone transient. Since loperamide causes both elongation of the progesterone-induced $[Ca^{2+}]_i$ transient and enhancement of the subsequent plateau phase, we investigated the effects of loperamide pre-treatment on hyperactivation. When cells were exposed either to 3µM progesterone alone or 10µM loperamide alone before introduction into the observation chamber, assessment by CASA showed no significant increase over parallel controls ($P>0.05$; paired, n=7) in the proportion of cells classified as hyperactivated (Figure 6.4; Mortimer, 1994). However, if cells were exposed to loperamide for 200 seconds prior to progesterone application, then there was a significant enhancement in the proportion of hyperactivated cells compared to the control or to either progesterone or loperamide alone ($p<0.025$; paired t, n=7).

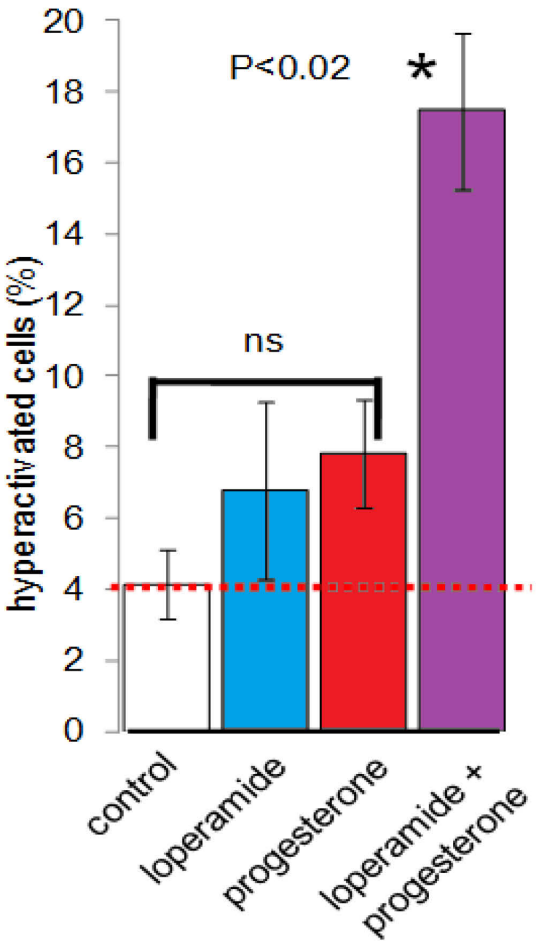

Figure 6.4 Effects of loperamide and progesterone on sperm hyperactivation. Bars show mean (±SEM) percentage hyperactivated cells following treatment with 10µM loperamide, 3µM progesterone, 10µM loperamide + 3µM progesterone, or control populations from 7 experiments as assessed by CASA.

6.4 Discussion

Due to the detection of STIM and Orai proteins (chapter 3) and that SOCE is probably mediated by the STIM/Orai pathway which can be modulated by 2-APB (chapter 4) we wanted to investigate further known modulators of SOCE. Loperamide, used in the pharmacological industry as an anti-diarrhoea medication has been shown to stimulate SOCE in cell types such as NIH 3T3 fibroblasts and astrocytoma 1321N cells with or without intracellular Ca^{2+} storage depletion (Harper *et al*., 1997). The application of 10μM loperamide to resting human sperm caused an increase in $[Ca^{2+}]_i$ in over 65% of cells. It is hypothesised that the increase in $[Ca^{2+}]_i$ in astrocytoma 1231N cells following the application of 30μM loperamide (without stored Ca^{2+} depletion) is a result of a small basal population of activated SOC channels (Harper *et al*., 1997). This correlates with data in chapter 3 (Figures 3.10, 3.11) whereby the distribution of STIM2 and Orai1 is more generalised than other components and these proteins can be observed and a cytosolic form of STIM2 has been shown to combine with Orai1 in order to mediate basal $[Ca^{2+}]_i$ (Graham *et al*, 2011). Loperamide may be activating these basal Ca^{2+} regulation mechanisms when applied without prior Ca^{2+} store depletion.

When examining the affects of loperamide pre-treatment on the progesterone-induced biphasic $[Ca^{2+}]_i$ response, we did not observe a significant increase in the transient amplitude as with low-dose 2-APB (Figure 6.3A, compared to Figure 5.2). We did however observe an increase in amplitude and duration of the plateau phase and recorded oscillations in >50% of cells (Figures 6.2A, 6.2C, 6.3B). This plateau phase of the response to progesterone (including Ca^{2+} oscillations) is thought to involve mobilisation of an intracellular Ca^{2+} store

present in the sperm neck region (Harper *et al.,* 2004). This therefore suggests that loperamide potentiates SOC channels active in the plateau phase of the response. There was no difference between responses in the midpiece region and the PHN. This contrasts with the effect of 5μM 2-APB treatment (Figure 5.3C) whereby the $[Ca^{2+}]_i$ of the midpiece varied from that of the PHN in the biphasic progesterone response. This may indicate slightly different targets for the two pharmacological agents, possibly having different affinities for the different STIM and Orai proteins present.

The application of progesterone to free swimming sperm has been reported to initiate a burst of transitional or hyperactivated motility, associated with the Ca^{2+} transient (Gakamsky *et al*., 2009; Kilic *et al*., 2009). This brief effect is difficult to capture using computer-assisted semen analysis (CASA) due to the lag time in between applying the progesterone, inserting the sample into the CASA chamber, selecting fields of view and analysing responses. However, in samples whereby cells were pre-treated with loperamide prior to progesterone application, there was a significant increase in the proportion of hyperactivated cells, indicating that enhancement of the plateau phase positively modifies motility in human sperm as recently suggested by Park *et al*. (2011).

In summary, loperamide pre-treatment on the progesterone-induced $[Ca^{2+}]_i$ response appears to exert the majority of its effects in the sustained phase, at both the midpiece and PHN equally. This data correlates with the localisation of STIM and Orai proteins of the SOCE system primarily to the neck/midpiece regions in chapter 3. Furthermore, as loperamide alters the proportion of cells undergoing hyperactivation following progesterone treatment this may

suggest SOCs may be a useful pharmacological target in the treatment of sub-fertile patients who have low sperm motility.

CHAPTER SEVEN: THE EXPRESSION OF RYANODINE RECEPTORS (RYR) IN HUMAN SPERM

7.1 Abstract

The inositol 1,4,5-trisphosphate receptor (IP_3R) and the ryanodine receptor (RyR) are found in the membranes of intracellular Ca^{2+} storage organelles of somatic cells, regulating the mobilisation of stored Ca^{2+}. SOCE is typically mediated via an IP_3R pathway, however in human sperm the cyclic mobilisation of stored Ca^{2+} initiated by a logarithmic progesterone gradient was insensitive to IP_3 or IP_3R inhibition, but was sensitive to RyR manipulation. Furthermore, recent investigations into membrane-bound vesicles, called prostasomes, have also suggested the involvement of RyRs in the plateau phase of the biphasic $[Ca^{2+}]_i$ response induced by bolus progesterone application, which is believed to be regulated by SOCE. Subsequently, our main aim for this chapter was to establish whether RyRs can be detected in human sperm and if they are localised to areas of intracellular Ca^{2+} stores where they may form part of the SOCE system. We detected bands at the appropriate molecular weights (~560 kDa) for RyR1 and RyR2 using immunoprecipitation. Immunocytochemistry shows anti-RyR1 and RyR2 antibodies primarily stain within the sperm neck/midpiece region for both mature and immature subsets of human sperm, co-localising with SPCA1 at areas of known intracellular Ca^{2+} stores. Brighter staining for RyRs was observed in immature human sperm and from cytoplasmic droplets (remnants of the germ cell cytoplasm) indicating a possible developmental role and/or the presence of prostasomes within our cytoplasmic droplet preparations. Difficulties in detecting RyRs may be due to their high conductance levels meaning minimal RyRs may satisfy the Ca^{2+} influxes required to initiate and maintain SOCE. Our results therefore probably suggest that RyRs are present in human sperm and consequently may have a role in mobilising intracellular Ca^{2+} stores during SOCE, which can then be replenished by SPCA1 activity.

7.2 Introduction

Two possible channels with the capability of regulating the mobilisation of stored Ca^{2+} are the IP_3R and the RyR. In somatic cells, these channels transverse the membranes of intracellular Ca^{2+} stores, namely the endoplasmic and sarcoplasmic reticulums and amplify signals generated via Ca^{2+} store mobilisation. IP_3Rs are activated by IP_3 engagement culminating in Ca^{2+} release to the intracellular environment (Michelangeli *et al.*, 1995). Typically in SOCE, intracellular Ca^{2+} store release is mediated via an IP_3R pathway and IP_3 has been localised to both the acrosomal and sperm neck regions in human sperm, sites of intracellular Ca^{2+} stores (Kuroda *et al.*, 1999; Ho and Suarez, 2003; Naaby-Hansen *et al.*, 2001). However, Ca^{2+} oscillations induced by a logarithmic progesterone gradient initiated in the sperm neck/midpiece region and were mediated by the cyclic mobilisation of stored Ca^{2+}, were insensitive to IP_3 or IP_3R inhibition but were sensitive to RyR manipulation (Harper *et al.*, 2004). For example, tetracaine (RyR inhibitor) prevented oscillations, in comparison with caffeine and low dose ryanodine (RyR agonist) which induced oscillations to become greater and more defined in a dose-dependent manner (Harper *et al.*, 2004). Furthermore, SOCE has been shown to occur in cell lines devoid of IP_3Rs (Sugawara *et al.*, 1997).

BIODIPY-FL-X ryanodine (a fluorescent ryanodine analogue) has been shown to stain the sperm neck region (Harper *et al.*, 2004). Furthermore work by our group sequencing S-nitrosylated proteins from NO-exposed human sperm, identified the presence of RyR2 (Lefievre *et al.*, 2007). Also, exposure of human sperm to NO donors caused the mobilisation

of stored Ca^{2+} by protein S-nitrosylation (Machado-Oliveira *et al.*, 2008), consistent with the known susceptibility of RyR for modification by NO, due to a large number of sulphydryls (Otsu *et al.,* 1990; Eu *et al.*, 1999). Despite this, the presence of RyRs in human sperm remains controversial as, RyRs have not been detected in bovine sperm using BIODIPY-FL-X ryanodine and only RyR3 has been detected in mature rodent sperm (Trevino *et al.*, 1998).

Recent investigations into membrane-bound vesicles called prostasomes (see section 1.4) have suggested the involvement of RyRs in the progesterone induced $[Ca^{2+}]_i$ biphasic response (Park *et al*., 2011). RyRs are activated by cyclic adenosine diphosphoribose (cADPR) which is produced by a mammalian enzyme CD38 (a type of adenosine diphosphate ribosyl cyclase (ADPR-cyclase)) from nicotinamide adenine dinucleotide (NAD) (Lee, 2006). Upon pH-dependent fusion of prostasomes to the midpiece region of human sperm, Park *et al.* (2011) reported the transfer of CD38 proteins and consequently increased CD38 activity in prostasome-fused sperm (PFS) compared to non-fused sperm (NFS). Furthermore, they showed that PFS produced cADPR in response to progesterone exposure, as opposed to NFS which did not. They particularly examined the plateau phase of the biphasic $[Ca^{2+}]_i$ response, thought to be due to SOCE. They found that use of a cADPR inhibitor (8-bromo-cADPR) reduced the amplitude of the plateau phase, as did other RyR inhibitors including a high concentration of ryanodine and high concentrations of the SOCE inhibitor 2-APB. They concluded from their results that the plateau phase of the progesterone induced biphasic $[Ca^{2+}]_i$ response was due to Ca^{2+} store mobilisation through the activation of RyR by cADPR. Subsequently, it is important to establish whether RyR can be detected in mature human sperm, where they may have a role in SOCE.

Chapter Aims

The aims of this chapter were to investigate the presence of RyR1 and RyR2 in human sperm using Western blotting and immunoprecipitation (IP). Furthermore, we wanted to examine the cellular localisation of RyRs in human sperm to determine if their localisation correlates with intracellular Ca^{2+} stores and thus may be involved in SOCE.

7.3 Results

7.3.1 The detection of RyRs in human sperm by Western blotting and IP.

The detection of RyRs in human sperm via Western blotting proved problematic. RyRs are high molecular weight (HMW) proteins at 560 kDa (Eu *et al.*, 1999) and Western blotting for HMW proteins requires a modified protocol, which typically causes higher levels of background staining. In addition, repeats were inconsistent and due to the high amounts of protein being loaded, smears were common. Subsequently, we used IP as a method of investigation. IP allows the concentration of target proteins more than 250 fold and therefore aids the identification of rare proteins usually found in very small quantities (Gundersen and Shapiro, 1984). IP involves isolating the target antigen from a complex solution using an antibody specific for that antigen, in our case RyR1 or RyR2. This method has been successful for a range of other sperm proteins such as SERCA 2 (Lawson *et al*., 2007) and AKAP3 (Bajpai *et al*., 2006). IP using anti-RyR1 and anti-RyR2 antibodies for human sperm lysates shows bands at levels consistent with the sarcoplasmic reticulum (SR) and brain reticulum (BR positive controls at ~ 560 kDa (RyR1 and RyR2 controls respectively) (Figure 7.1A, B; shown by arrows). We have not attempted detection of RyR3 in human sperm primarily due to a lack of specific antibody probes and its unresponsiveness to pharmacological stimuli (Hakamata *et al.*, 1994). Also, epididymal sperm from RyR3 knock-out mice were shown to hyperactivate, implying functional RyR3 is not an essential prerequisite for hyperactivation (Ho and Suarez, 2003).

Within our electrophoresis gels we often observed degradation products for the SR control lane, especially if we overexposed the film (Figure 7.1C). Interestingly, the protein degradation patterns observed for the RyR1 IP (shown by arrows) correlate with these degradation products seen in the overexposed SR lane. This may be due to the high molecular weight RyR tetramer breaking down during the experimental procedure. To illustrate the sensitive nature of RyRs, if we incubated an aliquot of our SR control alongside the RyR1 IP (to mimic experimental conditions), the band intensity was substantially reduced, in comparison with a fresh SR sample taken from storage at -80°C less than one hour prior to gel electrophoresis (Figure 7.1D). These results demonstrate the fragility and sensitivity of RyRs to experimental conditions and highlights why the detection of RyR in human sperm may have been elusive in previous studies by other groups.

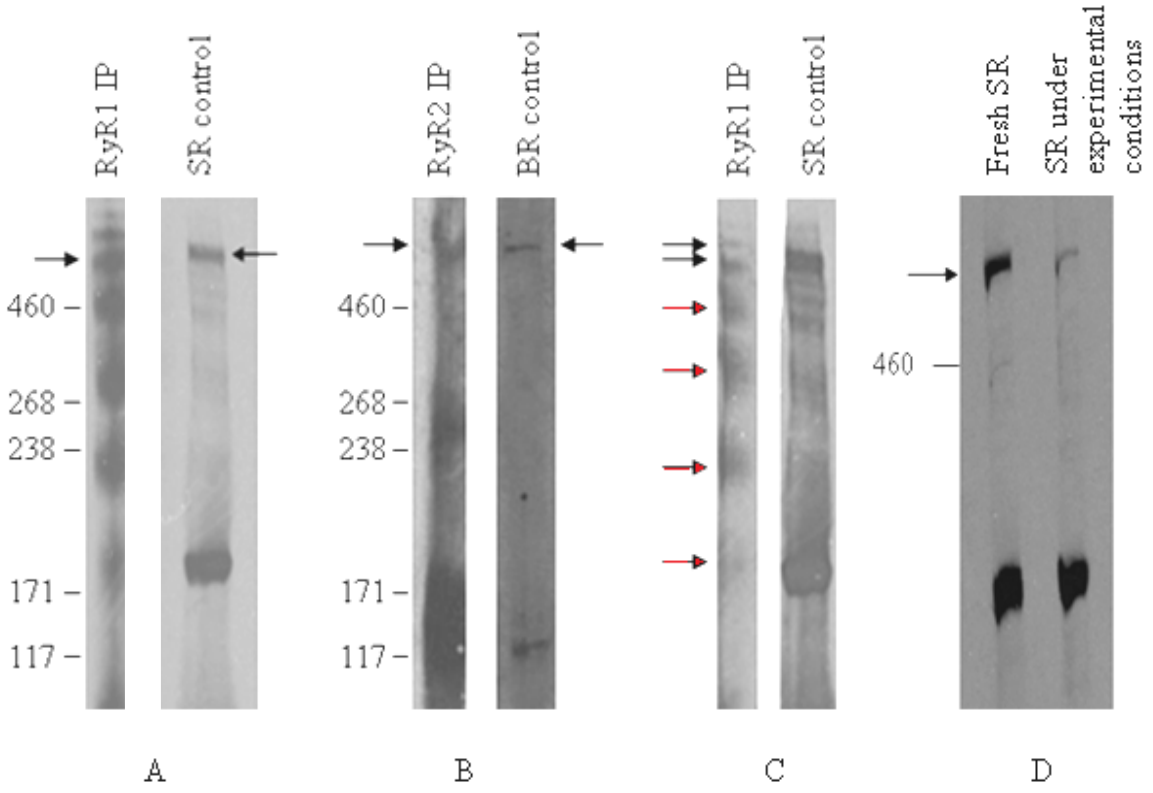

Figure 7.1 RyR detection in human sperm using immunoprecipitation. Sperm lysates were immunoprecipitated using either RyR1 (**A**) or RyR2 (**B**) antibodies and proteins were separated by 3-8% tris-acetate Nupage gels for detection. Bands at the correct molecular weights are marked by the arrows. (**C**) Protein degradation patterns for RyR1 IP lanes and overexposed SR control lanes were shown (red arrows). SR within 1 hour of defrosting from incubation at -80°C (fresh SR) or SR exposed to the experimental conditions needed for IP (SR under experimental conditions) were separated by 3-8% tris-acetate Nupage gels for detection (**D**).

7.3.2 Immunolocalisation of RyRs in human sperm and cytoplasmic droplets.

A 40/80% Percoll gradient separates sperm according to density. Typically, morphologically normal or mature sperm are found below the 80% Percoll fraction due to a higher density reflecting completed cytoplasmic extrusion during spermiogenesis (Huszar and Vigue, 1993). Alternatively, abnormal or immature sperm usually have a lower density and are therefore found at the 40/80% interface (known as the 40% fraction) (Sbracia *et al*., 1996). Anti-RyR1 and RyR2 antibodies primarily stain within the sperm neck/midpiece region for both mature and immature subsets of human sperm (Figures 7.2A, C and 7.3 A, C). Greater staining was often observed towards the sperm neck region (e.g. Figure 7.2A, lower arrow) as opposed to the annulus (e.g. Figure 7.2A, upper arrow). This localisation correlates with the presence of a Ca^{2+} store within this region such as the redundant nuclear envelope (RNE) (Ho and Suarez, 2003).

Cytoplasmic droplets are remnants of the germ cell cytoplasm (containing expelled organelles such as ER) that remain tethered at the neck region of the elongating spermatid, most of which is liable to phagocytosis by Sertoli cells during spermiogenesis (Cooper, 2004). Interestingly, there was a higher degree of RyR staining in cells recovered from the 40% fraction and from isolated cytoplasmic droplets, as opposed to the 80% fraction, especially in individual cells where a larger cytoplasmic droplet/ excess residual cytoplasm could be visualised (e.g. compare Figures 7.3A with 7.3C and 7.4). This may therefore indicate that the

levels of RyRs vary during sperm development are higher in immature sperm and those retaining these droplets.

Confocal microscopy also pinpointed both the RyR1 and RyR2 to the same sperm/neck midpiece region (Figure 7.5 A, B). Interestingly, they are found in the same area as SPCA1 (Figure 7.5C), a Ca^{2+}ATPase that functions to pump excess cytoplasmic Ca^{2+} back into intracellular stores or the extracellular environment (Harper *et al*., 2003).

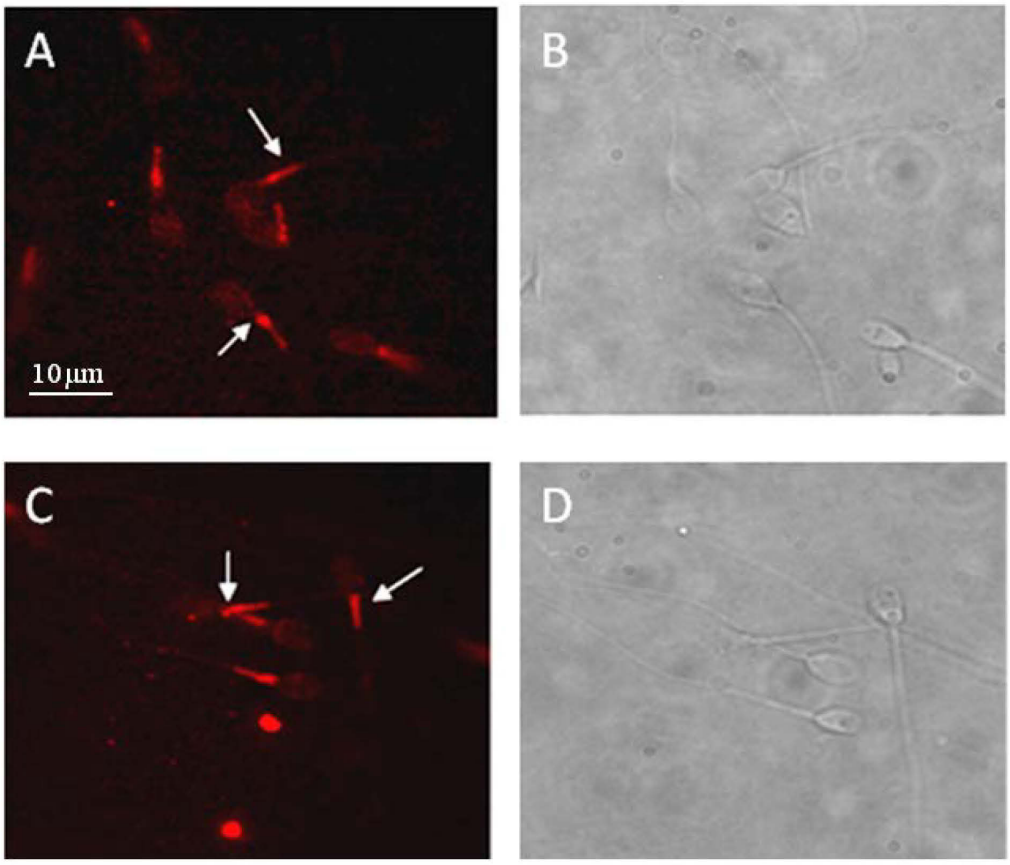

Figure 7.2 Localisation of RyR1 in human sperm**. (A-D)** Formaldehyde-fixed sperm were incubated with anti-RyR1 as described in materials and methods. **(A)** Sperm obtained from the 80% Percoll fraction and **(C)** from the 40% Percoll fraction. **(B, D)** Corresponding phase contrast images of these fields of view.

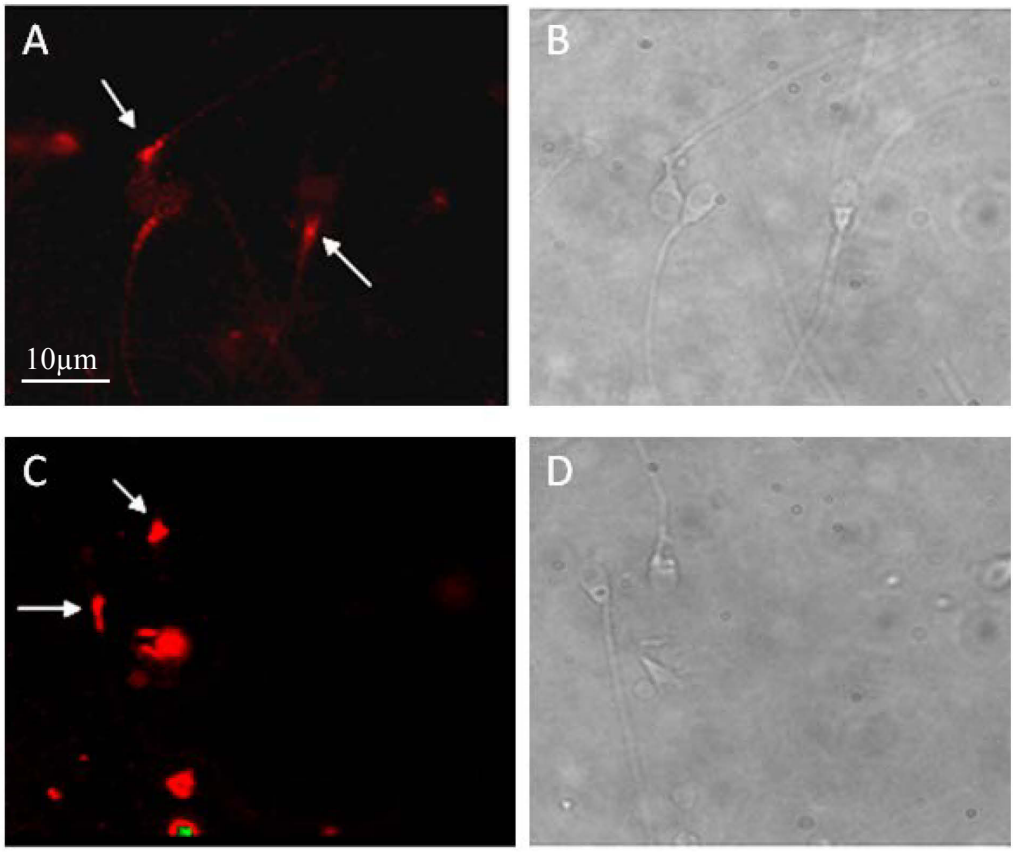

Figure 7.3 Localisation of RyR2 in human sperm. **(A-D)** Formaldehyde-fixed sperm were incubated with anti-RyR2 as described in materials and methods. **(A)** Sperm obtained from the 80% Percoll fraction and **(C)** from the 40% Percoll fraction. **(B, D)** Corresponding phase contrast images of these fields of view.

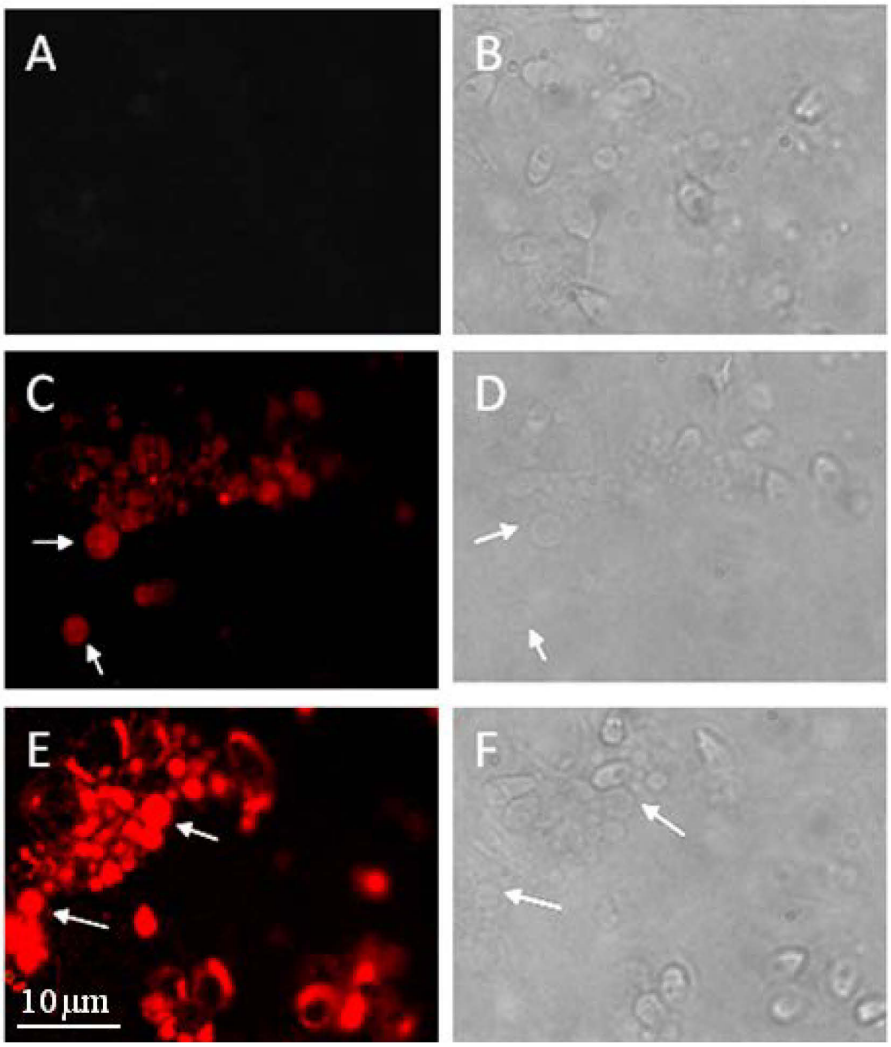

Figure 7.4 Localisation of RyRs in cytoplasmic droplets from human sperm. Human sperm obtained from the 40% Percoll fraction were homogenised and cytoplasmic droplets removed using dry glass wool as described in the materials and methods section. Formaldehyde-fixed cytoplasmic droplets were incubated with anti-RyR1 **(C)** or anti-RyR2 **(E). (A)** Shows cytoplasmic droplet preparation with primary antibodies omitted for negative control. **(B, D, F)** Corresponding phase contrast images of these fields of view.

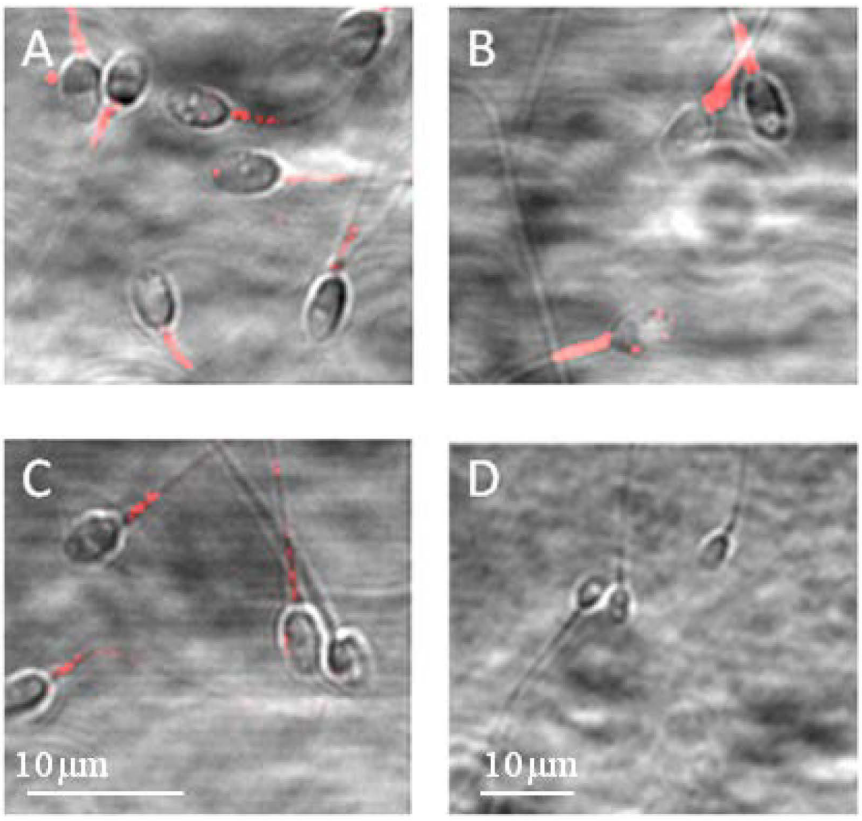

Figure 7.5 Localisation of RyRs and SPCA1 in human sperm using confocal microscopy. Human sperm obtained from the 80% Percoll fraction were incubated with **(A)** anti-RyR1**, (B)** anti-RyR2 or **(C)** anti-SPCA1 (x40 objective). **(D)** Shows sperm prepared the same but with primary antibodies omitted for negative control (x20 objective).

7.4 Discussion

Anti-RyR1 and anti-RyR2 antibodies have been shown to stain primarily around the sperm neck/midpiece region (Figures 7.2, 7.3 and 7.5), consistent with staining observed using BIODIPY-FL-X ryanodine (Harper *et al*., 2004). This localisation corresponds with evidence, such as calreticulin and SPCA1 detection in the same vicinity, for a Ca^{2+} storage organelle in the neck/midpiece region of human sperm (Suarez, 2008; Harper *et al.*, 2005). Using IP we detected bands correlating with the approximate molecular weights for RyR1 and RyR2 (560 kDa) as demonstrated by the SR and BR positive controls (Figure 7.1). Unfortunately, when bands excised from a silver stained RyR1 IP gel were examined by mass spectrometry, we were unable to detect RyR1.. Therefore, from our studies it appears very likely that RyRs are present, but it is proving difficult to confirm.

The difficulty in detecting RyRs by mass spectrometry may be explained by the following reasoning; The Ca^{2+} conductance of RyRs (>100 pS) is particularly high in comparison with other Ca^{2+} permeable channels such as voltage-gated L-type Ca^{2+} channels (~20 pS; Zalk *et al.*, 2007). Therefore, it may be presumed that the specific localisation of minimal RyRs may satisfy the Ca^{2+} influxes required to initiate and maintain cyclic Ca^{2+} mobilisation (Gianni *et al.,* 1995). RyRs may therefore be present, but in very low abundance. Furthermore, as shown by Figure 7.4D, RyRs are sensitive to degradation, so the few RyRs present may be broken down due to experimental conditions.

When conducting immunolocalisation studies for RyR1 and RyR2 we often observed brighter fluorescence staining for anti-RyR2 probed cells. In addition, it was RyR2 detected by mass

spectrometry in human sperm in Lefievre *et al*. (2007). Furthermore, when examining sperm motility via CASA, Park *et al.* (2011) found that there was only a detrimental effect on sperm motility following progesterone application, when sperm cells were fused with prostasomes deficient in RyR2. From this data and our own results, this suggests that RyR2 may be the more functionally important isoform present in human sperm.

Interestingly, higher RyR labelling was observed in immature sperm, compared to mature sperm. Immature sperm by definition are more likely to possess a larger cytoplasmic droplet or excess residual cytoplasm as cytoplasmic droplets are remnants of the germ cell cytoplasm. When we isolated cytoplasmic droplets and labelled with anti-RyR antibodies, clear staining could be observed across the whole structure (Figure 7.4). The increased presence of RyRs within cytoplasmic droplets may indicate a developmental role, with the majority of RyRs subsequently removed during shedding of excess cytoplasm, as only a few are required for mature sperm. For example, Chiarella *et al.* (2004), showed that blockage of RyR using high doses of ryanodine (300μM for 1 hour) reduces spermatogonial proliferation and induces meiosis *in vitro* organ cultures of testis from 7-day old mice. Also, RyR expression is thought to vary at various points during development (Gianni *et al.*, 1995). This may therefore account for the brighter staining in cytoplasmic droplets.

In discussing the expression of RyRs in sperm it is important to remember the potential importance of prostasomes, vesicles derived from epithelial cells lining the prostate that are believed to fuse with sperm post ejaculation (Burden *et al.,* 2005; Poliakov *et al.*, 2009). The potential importance of prostasomes for 'delivery' of $[Ca^{2+}]_i$ signalling tools to human sperm

has only recently become apparent (Park *et al*., 2011). PFS have been demonstrated to have higher levels of RyRs in contrast to NFS (Park *et al*., 2011). Though we did not specifically fuse sperm with prostasomes, the presence of SPCA1 in the majority of cells (Harper *et al*., 2005; Figure 7.5C), which was only detected in <10% of NFS (Park *et al*., 2011) suggests that many of the sperm used in these studies are prostasome-fused. It is also possible that we may have isolated some prostasomes within our cytoplasmic droplet preparations. The size of prostasomes (40-500 nm) is much less than that of the cytoplasmic droplets studied here, which are typically ≥2μM diameter, but prostasome-droplet fusion may have occurred contributing to the high levels of RyRs observed.

SPCA1 has been detected within the midpiece area of human sperm (Figure 7.5C, Harper *et al*., 2005; Park *et al*., 2011). Typically, SPCA1 sits in the plasma membrane of internal Ca^{2+} storage organelles and acts as a Ca^{2+} pump to replenish Ca^{2+} stores. It is often coupled with RyRs in order to form organelles that are activated by calcium-induced calcium release (CICR). Pharmacological manipulation of SPCA1 using the SPCA inhibitor bis-phenol reduces the progesterone induced $[Ca^{2+}]_i$ plateau phase in PFS (Park *et al*., 2011) and we have shown in earlier chapter 3 that it can be used to modulate SOCE (Figures 3.2A, B). Furthermore, Bafilomycin A1, which inhibits Ca^{2+} accumulation in acidic organelles (Docampo and Moreno, 1999) also reduced the progesterone induced $[Ca^{2+}]_i$ plateau phase. Subsequently, these results suggest that the intracellular Ca^{2+} store mobilised in SOCE by progesterone operates by opening RyR-gated channels and is replenished by SPCA1.

The cellular location of RyRs in human sperm is suspected to be within the RNE. In somatic cells, RyRs typically reside within the ER, but this cellular structure is removed during spermiogenesis in human sperm into the cytoplasmic droplet (reviewed in Costello *et al*., 2009). It is suggested that the RNE contains ER remnants, as this membrane is continuous with the ER in the immature cell. This hypothesis correlates with a study dating back to 1978 examining ER regression during spermiogenesis in rat (Clermont *et al.*, 1978). In this study it was concluded that the breakdown of the membranous component of the ER is synchronous with the time point at which material is added to the flagellum and sperm neck region. Subsequently, the protein content of the endoplasmic reticulum is released into the cytoplasm next to the axoneme where it has the capability of condensing and precipitating into new structures (Clermont *et al.*, 1978). Therefore, it is feasible that the RNE contains ER remnants and associated RyRs, thus making it able to serve as an intracellular Ca^{2+} store.

Interestingly, the presence of a RNE is a common element to many species of mammalian sperm such as the mouse, hamster, monkey, bat, bull and human (Toshimori *et al.*, 1985; Franklin *et al.,* 1968; Oko *et al.,* 1976). Unlike other redundant organelles it is not removed during spermiogenesis, suggesting it may have a functional role. Immunogold labelling of transmission electron micrographs has revealed two compartments within the RNE including one full of nuclear pores and the second containing extensive membranous structures with enlarged cisternae (Ho and Suarez, 2003). Interestingly, the presence of IP_3R and calreticulin at the neck region of bovine and hamster sperm has been localised to the area of membranous structures within the RNE. Furthermore, studies have demonstrated the capacity for nuclear envelopes to perform as Ca^{2+} stores in other cells, such as hepatocytes and starfish oocytes (Gerasimenko *et al.*, 1995; Santella *et al.*, 1997). Ho and Suarez (2003) also noted that the

RNE is distributed asymmetrically around the flagella base and thus is able to release more Ca^{2+} to one side of the axoneme where it is needed to produce asymmetrical flagella beats. Therefore, it is possible that the RNE in the neck region of mammalian sperm could serve as a Ca^{2+} store and may be involved in regulating sperm motility.

During this chapter we have therefore provided more evidence to support the presence of RyRs in human sperm. Immunolocalisation of RyRs to the PHN/midpiece region where they are found in a similar location to SPCA1 and SOCE proteins suggesting they may have a role in mobilising intracellular Ca^{2+} stores during SOCE. However, more research is required on this area of study especially with the recent report that prostasomes deliver of $[Ca^{2+}]_i$ signalling tools to human sperm, which we had not accounted for previously.

CHAPTER EIGHT: GENERAL DISCUSSION

GENERAL DISCUSSION

Within eukaryotic somatic cells, Ca^{2+} is a ubiquitous intracellular second messenger that can change by orders of magnitude in order to activate numerous signal transduction pathways, culminating in responses from muscle contraction to gene transcription (Berridge *et al.*, 2000). The versatility of the calcium signalling 'toolkit' of a cell with intricate Ca^{2+} flux channels, clearance mechanisms and stores, enables control of the speed, amplitude and spatio-temporal patterning of the calcium signal (Berridge *et al* 2000; Jimenez-Gonzalez *et al.*, 2006). Spermatozoa are translationally and transcriptionally inactive which means that post-translational modifications, such as regulation of protein function by the modulation of $[Ca^{2+}]_i$, are vital for cell activity and are involved in key events including chemotaxis, motility, acrosome reaction and capacitation (Carlson *et al.*, 2003; Kirkman-Brown *et al.*, 2003). The main aim of this study was to investigate SOCE, which involves Ca^{2+} release from internal stores, leading to Ca^{2+} entry across the plasmalemma. This process enables replenishment of intracellular Ca^{2+} stores and the mediation of long-term cytosolic Ca^{2+} signals (Putney *et al.*, 2001).

We have confirmed that SOCE does occur in human sperm as previously reported for human (Blackmore, 1993; Rossato *et al*., 2001; Williams and Ford 2003; Harper *et al*., 2004) as well as sperm for other species (Dragileva *et al.*, 1999; O'Toole *et al.*, 2000; Gonzalez-Martinez *et al.*, 2004, Ardón *et al.*, 2009). Furthermore we have shown that the SOCE trace could be

modulated by application of the best characterised modulator of SOCE, 2-APB. 2-APB potentiated SOCE in human sperm (when intracellular Ca^{2+} stores were depleted) at low doses (5μM) and had inhibitory effects at high doses (>50μM). This mirrors the complex bimodal actions of 2-APB, as previously reported for other cell types (DeHaven *et al*., 2008; Wang *et al*., 2009).

Our investigation of the biphasic $[Ca^{2+}]_i$ response initiated by the application of 3μM progesterone, showed that this response can be modulated by pharmacological agents that modify SOCE. It has been suggested that the initial transient is primarily due to the direct activation of CatSper channels located in the principal piece of the flagellum by progesterone (Lishko *et al.*, 2011; Strunker *et al.*, 2011). However, as channel blockers abolished CatSper currents in whole-cell clamped human sperm but only partially inhibited the progesterone-induced $[Ca^{2+}]_i$ transient, this has indicated that other Ca^{2+} channels may play a role in the progesterone induced $[Ca^{2+}]_i$ response (Lishko *et al.,* 2011; Strunker *et al.,* 2011). We have determined using single cell imaging and fluorimetry that pre-treatment of human sperm with 5μM 2-APB prior to progesterone exposure significantly increases the amplitude of the initial Ca^{2+} transient at the PHN and midpiece. This therefore indicates that 2-APB sensitive SOC channels located in the PHN and midpiece regions contribute to and amplify the initial $[Ca^{2+}]_i$ transient induced by activation of CatSper channels in the flagellum, allowing the signal to propagate rapidly into the neck and head of the cell. 2-APB pre-treatment did not influence the transient observed in the principal piece of the flagellum, consistent with the studies reporting the Ca^{2+} influx here is solely regulated by CatSpers, which are not potentiated by 2-APB (Strunker *et al*., 2011; Lishko *et al*., 2011).

The plateau phase of the biphasic Ca^{2+} response to progesterone has been shown to be due to progesterone mobilising an intracellular Ca^{2+} store present in the sperm neck region, often leading to Ca^{2+} oscillations (Harper *et al.,* 2004). Subsequently, we investigated the effects of our SOCE modifying pharmacological agent 5μM 2-APB, on this section of the progesterone-induced biphasic $[Ca^{2+}]_i$ response. Within the PHN we saw an increased amplitude with 5μM 2-APB pre-treatment but this was inconsistent and not significant. However within the midpiece region we observed a population of cells where 5μM 2-APB pre-treatment strongly enhanced $[Ca^{2+}]_i$ in the sustained elevation phase. Interestingly, when we observed this enhanced sustained elevation in the midpiece we often noticed an inflexion in the rising phase of the Ca^{2+} transient for the midpiece, indicating a late Ca^{2+} mobilising event which occurs 10-20 seconds after the initial propagation of the $[Ca^{2+}]_i$ transient into the sperm neck and head. These results therefore indicate that the sustained response to progesterone can also be potentiated by 5μM 2-APB acting on SOCE systems at the midpiece and possibly the PHN regions (summarised in Figure 8.1).

Using an increased image acquisition rate (>1 Hz) we have revealed that the progesterone-induced $[Ca^{2+}]_i$ transient in the flagellar principal piece occurs 1-2 seconds prior to those occurring in the midpiece and PHN. This is consistent with previous observations that progesterone directly and immediately activates CatSper channels (Strunker *et al*., 2011; Lishko *et al*., 2011). We propose the rise in flagella $[Ca^{2+}]_i$ then induces mobilisation of Ca^{2+} from the intracellular Ca^{2+} stores at the PHN and midpiece, which are initiated shortly after the flagella $[Ca^{2+}]_i$ increase. This mobilisation may be negligible but sufficient to activate SOCs, especially when sensitised via 5μM 2-APB, which amplifies and prolongs the $[Ca^{2+}]_i$ signal.

We also examined the effects of loperamide, as a further pharmacological tool which has been shown to potentiate SOCE (Daly *et al.*, 1995; Harper *et al*., 1997). 10μM loperamide increased basal $[Ca^{2+}]_i$ in >65% of cells even without intracellular Ca^{2+} store depletion but it did not significantly potentiate the initial progesterone induced Ca^{2+} transient. Loperamide did however potentiate the sustained phase of the progesterone transient increasing the amplitude and duration of $[Ca^{2+}]_i$ in the PHN and midpiece, with Ca^{2+} oscillations recorded in >50% of cells. This therefore may indicate slightly different cellular targets between loperamide and 2-APB. It is predicted that loperamide allosterically increases conduction through SOC channels (Daly and Harper, 1999) as opposed to low-dose 2-APB which effectively sensitises the components of the SOCE system and may directly alter the pore size of Orai3 (Schindl *et al*., 2008; Wang *et al*., 2009). This coupled with the heterogeneous nature of human sperm populations may explain why these pharmacological agents have slightly different physiological effects on the progesterone induced Ca^{2+} response.

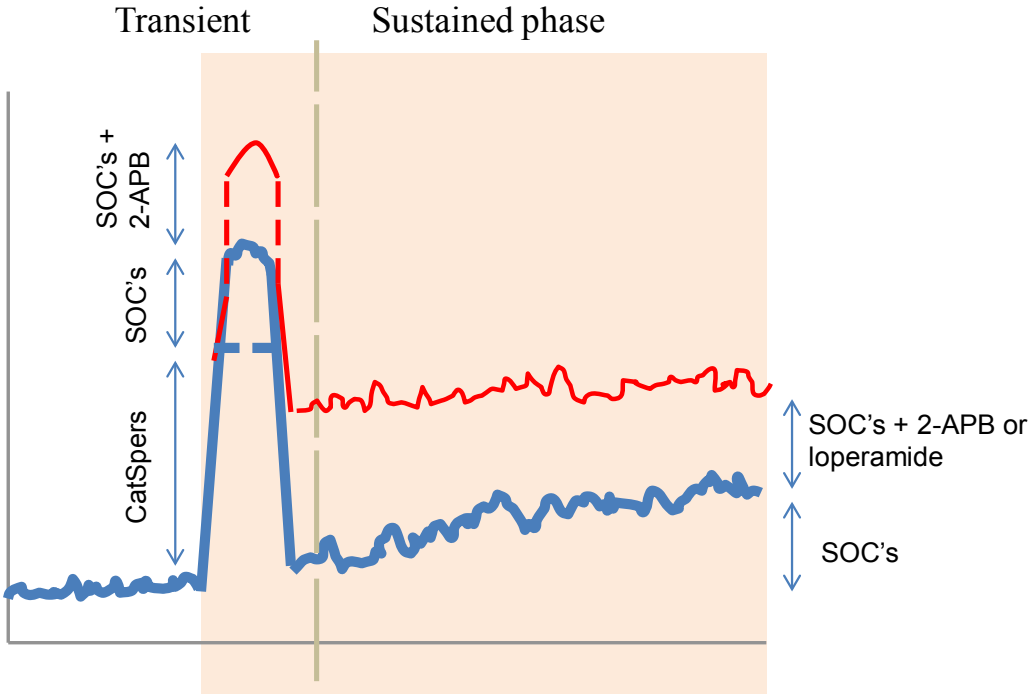

Figure 8.1 Illustration of the proposed contribution of SOCE to the progesterone response. Within the initial Ca^{2+} transient CatSpers are responsible for the initial Ca^{2+} influx, which is amplified and propagated by Ca^{2+} influx though SOCs. SOCE here can be potentiated by low dose 2-APB. The sustained phase is primarily due to progesterone mobilising an intracellular Ca^{2+} store leading to SOCE in the midpiece which can be potentiated by 5µM 2-APB and loperamide.

The Ca^{2+} oscillations observed in the plateau phase of the biphasic Ca^{2+} response have been compared against flagella beat. Harper *et al*. (2004) found that the oscillatory peaks were synchronised with flagella bending and lateral head movement suggesting these oscillations regulate motility. Subsequently we wanted to investigate the physiological responses of our SOCE potentiating agent loperamide that primarily appeared to effect the plateau phase. The initial application of progesterone to free swimming sperm has been reported to initiate a burst of translational or hyperactivated motility, associated with the Ca^{2+} transient (Gakamsky *et al*., 2009; Kilic *et al*., 2009). In samples whereby cells were pre-treated with 10µM

loperamide prior to progesterone application, there was a significant increase in the proportion of hyperactivated cells, indicating that enhancement of the plateau phase positively modifies motility in human sperm as recently suggested by Park *et al*. (2011).

The discovery of the stromal interacting molecule (STIM) and Orai in 2005 and 2006 respectively, called for re-evaluation of SOCE systems present in human sperm (Liou *et al.*, 2005; Feske *et al*., 2006). We detected STIM1, STIM2, Orai1 and Orai2 in human sperm. Furthermore, immunofluorescence labels the midpiece/ neck region for all four proteins and over the acrosome for Orai1, consistent with areas of intracellular Ca^{2+} stores. In somatic cells, STIM and Orai have been shown to reside in the endoplasmic reticulum and overlying plasma membrane respectively (Liou *et al*., 2005; Feske *et al*., 2006), but the majority of this cellular structure is removed during spermiogenesis in human sperm into the cytoplasmic droplet (reviewed in Costello *et al*., 2009). The identity of the intracellular Ca^{2+} store located within the PNH/midpiece region in human sperm is not yet clear although the redundant nuclear envelope is a strong contender (Ho and Suarez, 2003). It is suggested that the RNE contains ER remnants, as this membrane is continuous with the ER in the immature cell. This hypothesis correlates with a study dating back to 1978 examining ER regression during spermiogenesis in rat (Clermont *et al.*, 1978). They conclude that the breakdown of the membranous component of the ER is synchronous with the time point at which material is added to the flagellum and sperm neck region. Subsequently, the protein content of the endoplasmic reticulum is released into the cytoplasm next to the axoneme where it has the capability of condensing and precipitating into new structures. Therefore, it is feasible that the RNE contains ER remnants, thus making it able to serve as an intracellular Ca^{2+} store.

Within our single cell Ca^{2+} imaging results we observed an increase in $[Ca^{2+}]_i$ with both the application of 5-100μM 2-APB and 10μM loperamide on resting human sperm, independent of store mobilisation. This effect has been reported previously in cells expressing Orai3, or in cells where Orai was co-expressed with STIM2 (DeHaven *et al*., 2008; Peinelt *et al*., 2008; Zhang *et al*., 2008; Motiani *et al*., 2010). Our results for the expression of Orai3 were ambiguous, although from our immunocytochemistry results we did observe strong staining for STIM2 with a generalised distribution even along the flagellum where no intracellular Ca^{2+} stores are present. Interestingly, STIM2 has been shown to respond to Ca^{2+} deficits caused by weaker stimuli and has a higher potency in activating Orai subunits (Brandman *et al*., 2007; Parvez *et al*., 2008). In addition, a cytoplasmic subset of STIM2 (pre-STIM2) which retains its 101 amino acid localisation signal, has been reported to interact with Orai1 to mediate basal $[Ca^{2+}]_i$ levels, independent of stored Ca^{2+} mobilisation (Graham *et al*., 2011). On our Western blots, STIM2 appears as a clear doublet showing two proteins at a similar molecular weight, leading us to speculate that they may therefore represent the two STIM2 populations. Subsequently, it is suggested that the STIM2 and Orai1 proteins seen throughout the cell may be regulating basal $[Ca^{2+}]_i$ concentrations, independently of store mobilisation and can be potentiated by the application of 2-APB and loperamide.

Two possible channels with the capability of regulating the mobilisation of stored Ca^{2+} prior to SOC activation are the inositol 1,4,5-trisphosphate receptor (IP_3R) and the ryanodine receptor (RyR). Ca^{2+} oscillations induced by a logarithmic progesterone gradient were insensitive to IP_3 or IP_3R inhibition but were sensitive to RyR manipulation (Harper *et al.*, 2004). In addition, investigations into prostasome-fused human sperm concluded that the plateau phase of the progesterone induced biphasic $[Ca^{2+}]_i$ response was due to Ca^{2+} store

mobilisation through the activation of RyR by cADPR (Park *et al*., 2011). We detected proteins at the appropriate molecular weights for RyRs via Western blottingand localised RyRs to the sperm neck region via immunocytochemistry, consistent with staining observed using BIODIPY-FL-X ryanodine (Harper *et al*., 2004). This also corresponds with evidence for a Ca^{2+} storage organelle in the neck/midpiece region of human sperm as does the detection of SPCA1 in this region as shown in this study and others (Harper *et al*., 2005). Subsequently we have formed a theoretical model system whereby within the progesterone response, Ca^{2+} store mobilisation is triggered through the activation of RyR by cADPR and/or Ca^{2+} increases derived from CatSpers at the flagellum. This depletion of stored Ca^{2+} is sensed by STIM1 which oligomerises and associated with Orai in the overlying plasma membrane to form CRAC channels. The resulting Ca^{2+} influx can prolong Ca^{2+} signalling events and/or be used to refill intracellular stores via activity of the Ca^{2+} pump SPCA1 (Figure 8.2).

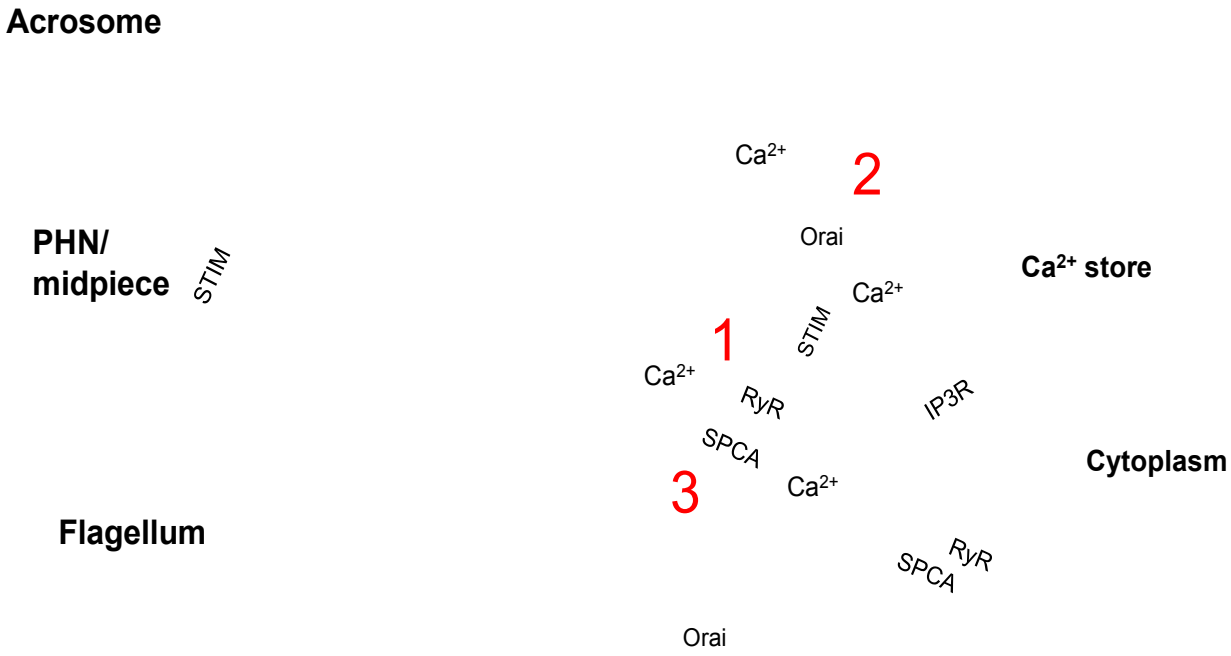

Figure 8.2 Illustration of the events regulating Ca^{2+} at the PHN/midpiece region as found by this study. (1) Ca^{2+} efflux from intracellular Ca^{2+} stores through RyRs due to the gating of cADPR and/or cyclic mobilisation of Ca^{2+}. (2) The Ca^{2+} depletion in the intracellular store initiates oligomerisation of STIM which then interacts with Orai at the overlying plasma membrane to form CRAC channels, permitting Ca^{2+} influx. The influx of Ca^{2+} into the cytoplasm stimulates the uptake of Ca^{2+} back into the stores by SPCA1, returning intracellular Ca^{2+} stores back to normal.

8.2 FUTURE WORK

In addition to loperamide and 2-APB, futher modulators of SOCE have been identified. Gadolinium (Gd^{3+}) is an effective blocker of store-operated currents in cells transfected with Orai subunits at 1-5 μM Gd^{3+} (DeHaven *et al*., 2009). Preliminary results indicate that 1μM Gd^{3+} applied to human sperm cells previously exposed to 15 μM bis-phenol has little effect on inhibiting SOCE already activated. However, 10-100 μM Gd^{3+} appears to cause dose-dependent reduction of the bis-phenol-induced elevation of $[Ca^{2+}]_i$ above control levels. Unfortunately, high dose Gd^{3+} exerts non-specific effects on other Ca^{2+} channels. Our main problem appears to be the precipitation of Gd^{3+} in EBSS upon preparation, which may mean higher doses are required to get active concentrations into the cells. We are therefore continuing to investigate alternative media's in order to produce accurate Gd^{3+} concentrations. Other promising SOCE modulators include the imidazoles SKF96365 and verapamil. Preliminary investigations into the SOCE inhibitor SKF96365 have been inconclusive. It is clear to us that the SOCE system in human sperm does not completely mirror that of somatic cells and therefore we are careful to interpret our results and make early assumptions. Therefore investigations into SKF96365 require further repetitions to reach an accurate assessment of whether it indeed modulates SOCE in human sperm.

The presence of RyR in sperm also requires further investigation. Due to the size and scarcity of RyR in human sperm, they are difficult to detect via immunoprecipitation and Western blotting. Subsequently, a next step would be to examine the pharmacological manipulation of RyRs using Ca^{2+} imaging techniques. Harper *et al*. (2004) and Park *et al*. (2011) have investigated RyR manipulation with high dose ryanodine and caffine in resting cells and during the sustained phase of the progesterone induced biphasic $[Ca^{2+}]_i$ response, but it would be interesting to examine the effects of

RyR manipulation on the transient phase. Furthermore, it would be useful to investigate the effects of cADPR on the biphasic progesterone response especially in light of the contributions of prostasome-fusion (Park *et al*., 2011). In addition, a more detailed and targeted investigation into the detection of RyRs using mass spectrometry would be interesting, as RyR peptides have been detected previously in human sperm (Lefievre *et al*., 2007).

Feske *et al.* (2006) discovered Orai1 due to a missense mutation in this protein, present in two sufferers of hereditary severe combined immunodeficiency syndrome. This mutation led to a reduction in SOCE and therefore reduced T-cell gene transcription mediated by a calcium-regulated transcription factor NFAT (Feske *et al*., 2001, 2005, 2006). Since this discovery, Orai proteins have been linked to a range of other pathological conditions including hypertension (Giachini *et al.*, 2009), type-2 diabetes (Zbidi *et al.,* 2009) and breast cancer (Motiani *et al*., 2010). This recent study into breast cancer cell lines revealed pathological links between breast cancer cell line sensitivity to estrogen and the STIM/Orai stoichiometry used. When this information is coupled with the results of this study, it would therefore be interesting to investigate the precise STIM/Orai stoichiometry in human sperm and the degree of heterogeneity, with initial comparisons between the sperm of fertile and sub-fertile patients to define any relationships with pathological conditions. This would require the use of methods such as whole sperm patch clamping as successfully utilised in the recent CatSper studies by Strunker *et al*. (2011) and Lishko *et al*. (2011).

Furthermore, as seen in chapter 6, whereby agonists of SOCE enhanced the proportion of hyperactivated cells following progesterone treatment, SOCs may therefore be attractive

candidates for novel pharmacological agents targeted at tackling infertility due to poor motility. Currently, intracytoplasmic cytoplasmic sperm injection (ICSI) is the major 'treatment' for poor motility, a costly, invasive procedure with possible increased health risks to the offspring (Karpman *et al*., 2005). Subsequently an orally or topically delivered pharmacological agent to increase sperm motility may prove very useful.

APPENDIX I

MEDIA

Supplemented Earle's Balanced Salt Solution (sEBSS)

Sodium Dihydrogen Phosphate 0.122g/l (1.0167 mM)

Potassium Chloride 0.4g/l (5.4 mM)

Magnesium Sulphate.$7H_2O$ 0.2g/l (0.811 mM)

Dextrose Anhydrous 1.0g/l (5.5mM)

Sodium Pyruvate 0.3g/l (2.5mM)

DL-Lactic Acid, Sodium 4.68g/l (19.0 mM)

Calcium Chloride.$2H_2O$ 0.264g/l (1.8 mM)

Sodium Bicarbonate 2.2g/l (25.0 mM)

Sodium Chloride ~6.8g/l (116.4 mM)

Sodium chloride was added to sEBSS until osmolarity was 285-295 mOsm, which was checked using an Advanced Micro Osmometer (Vitech Scientific Ltd, West Sussex, UK). The osmometer was pre-calibrated using a 50 mOsm/Kg H_2O and an 850 mOsm/Kg H_2O calibration standard. sEBSS pH was adjusted to 7.3-7.4 with 1M HCL and 1M NaOH and stored as 100ml volumes in glass bottles at 4°C until use. 0.3% bovine serum albumin (BSA) was added on day of experiment.

EGTA-buffered (Ca^{2+} free) sEBSS

Sodium Phosphate Monobasic 0.122g/l (1.018 mM)

Potassium Chloride 0.4g/l (5.366 mM)

Magnesium Sulphate.$7H_2O$ 0.2g/l (0.811 mM)

Dextrose Anhydrous 1.0g/l (5.551 mM)

Sodium Pyruvate 0.3g/l (2.724 mM)

DL-Lactic Acid, Sodium 4.68g/l (41.763 mM)

Calcium Chloride.$2H_2O$ 0.73g/l (4.966 mM)

Sodium Bicarbonate 2.2g/l (26.187 mM)

Sodium Chloride ~5.0g/l (85.558 mM)

EGTA – 2.28g/l (5.994 mM)

Prepared as for standard sEBSS. 0.3% (w/v) BSA was added on day of experiment.

M medium

137mM Sodium Chloride

2.5mM Potassium Chloride

20mM 4-(2-hydroxyethyl)-1-piperazineethanesulfonic acid (HEPES)

10mM Glucose

Immunoprecipitation (IP) buffer

150mM Sodium Chloride

20mM Tris-HCL pH 7.4

2mM DTT

1% (v/v) Triton X-100

10% (v/v) protease inhibitor cocktail and 1mM AEBSF hydrochloride were added on day of experiment.

Tris buffered saline supplemented with Tween-20 (TTBS)

150mM Sodium Chloride

20mM Tris-HCL (pH 7.8)

0.1% (v/v) Tween-20.

For high salt TTBS increase Sodium Chloride concentration to 0.5M.

Phosphate buffered saline (PBS)

One tablet dissolved in 200ml deionised water gives;

10mM phosphate

2.7mM Potassium Chloride

137mM Sodium Chloride

pH is 7.4 at 25°C. To make TPBS supplement with 0.1% or 0.2% (v/v) Triton X-100 as required.

Sodium dodecyl polyacrylamide gel electrophoresis (SDS-PAGE) loading buffer

2% (w/v) SDS

10% (w/v) Glycerol

62.5mM Tris-HCL (pH 6.8)

0.16M Dithiothreitol, dry

0.2% (w/v) Bromophenol blue

APPENDIX II

PUBLICATIONS AND PRESENTATIONS OF RESEARCH

Publications

Nash, K.L., Lefievre, L., Peralta-Arias, R., Morris, J., Morales-Garcia, A., Connolly, T., Costello, S., Kirkman-Brown, J. and Publicover, S.J**.** (2010). Techniques for imaging Ca^{2+} signalling in human sperm. *J Vis Exp* **16**

Costello, S, Michelangeli, F., **Nash, K.,** Lefievre, L., Morris, J., Machado-Oliveira, G., Barratt, C., Kirkman-Brown, J. and Publicover, S. (2009). Ca^{2+} stores in sperm: their identities and functions. *Reprod* **138**, 425-437.

Machado-Oliveira, G., Lefievre, L., Ford, C., Herrero, M.B., Barratt, C., Connoly, T.J., **Nash, K.,** Morales-Garcia, A., Kirkman-Brown, J. and Publicover, S. (2008). Mobilisation of calcium stores and flagella regulation in human sperm by S-nitrosylation: a role for nitric oxide synthesised in the female tract. *Development* **135**, 3677-3686.

Conference presentations and posters

Gordon conference, Fertilization & Activation of development 2011, Boston, USA

2-APB-sensitive (store-operated type) Ca^{2+} channels mediate rapid and prolonged progesterone-activated Ca^{2+} influx in human sperm. **Katherine Nash**, Linda Lefievre and Stephen Publicover.

Gordon conference, Fertilization & Activation of development 2009, Boston, USA

Intracellular calcium stores and store-operated calcium influx in human spermatozoa. **Katherine Nash**, Linda Lefievre, Aduen Morales-Garcia, Frank Michelangeli and Stephen Publicover.

Does human spermatozoa contain ryanodine receptors? Linda Lefievre, **Katherine Nash,** Gisela Machado-Oliveira, Aduen Morales-Garcia, Frank Michelangeli and Stephen Publicover.

Society for Reproduction and Fertility (SRF) annual conference 2010, Nottingham, UK

STIMulating sperm! **Katherine Nash**, Linda Lefievre and Stephen Publicover.

University of Birmingham, Bioscience symposium 2009 & 2010

STIMulating sperm until they CRAC! **Katherine Nash**, Linda Lefievre and Stephen Publicover.

REFERENCES

Aitken, R.J., Buckingham, D.W. and Irvine, D.S. (1996). The extragenomic action of progesterone on human spermatozoa: evidence for a ubiquitous response that is rapidly down-regulated. *Endocrinology* **137**, 3999-4009.

Ardón, F., Rodríquez-Miranda, E., Beltrán, C., Hernández-Cruz, A. and Darzon, A. (2009). Mitochondrial inhibitors activate influx of external Ca^{2+} in sea urchin sperm. *Biochimica et Biophysica Acta* **1787,** 15-24.

Arienti, G., Carlini, E., and Palmerini, C.A. (1997). Fusion of human sperm to prostasomes at acidic pH. *J Membr Biol* **155,** 89-94.

Arienti, G., Carlini, E., Nicolucci, A., Cosmi, F and Palmerini, C.A. (1999). The motility of spermatozoa as influenced by prostasomes at various pH levels. *Biol Cell* **91**, 51-54.

Arienti, G., Carlini, E., Saccardi, C., and Palmerini, C.A. (2004). Role of human prostasomes in the activation of spermatozoa. *J Cell Mol Med* **8,** 77-84.

Arnoult, C., Cardullo, R.A., Lemos, J.R. and Florman, H.M. (1996). Activation of mouse sperm T-type Ca2+ channels by adhesion to the egg zona pellucida. *Proc Natl Acad Sci U S A* **93**, 13004-13009.

Arnoult, C., Kazam, I.G., Visconti, P.E., Kopf, G.S., Villaz, M. and Florman, H.M. (1999). Control of the low voltage-activated calcium channel of mouse sperm by egg ZP3 and by membrane hyperpolarization during capacitation. *Proc Natl Acad Sci U S A* **96**, 6757-6762.

Austin, C. R. (1951). Observations on the penetration of the sperm into the mammalian egg. *Aust J Scient Res* **4**, 581.

Avidan, N., Tamary, H., Dgany, O., Cattan, D., Pariente, A., Thulliez, M., Borot, N., Moati, L. And Beckman, J.S. (2003). CATSPER2, a human autosomal nonsyndromic male infertility gene. *Eur J Hum Genet* **11**, 497-502.

Awouters, F., Niemegeers, J.E. and Janssen, P.A.J. (1983). Pharmacology of antidiarrheal drugs. *Ann Rev Pharmacol Toxicol* **23**, 279-301

Baartscheer, A., Schumacher, C.A., Coronel, R. and Fiolet, J.W. (2011). The driving force of the Na/Ca-Exchanger during metabolic inhibition. *Front Physiol* **2**, 10.

Baba, Y., Hayashi, K., Fujii, Y., Mizushima, A., Watarai, H., Wakamori, M., Numaga, T., Mori, Y., Lino, M., Hikida, M. And Kurosaki, T. (2006). Coupling of STIM1 to store-operated Ca2+ entry through its constitutive and inducible movement in the endoplasmic reticulum. *Proc Natl Acad U S A* **103**, 16704-16709.

Babcock, D.F., First, N.L. and Lardy, H.A. (1975). Transport mechanism for succinate and phosphate localized in the plasma membrane of bovine spermatozoa. *J Biol Chem* **250**, 6488-6495.

Bailey, J. L. and Storey, B. T. (1994). Calcium influx into mouse spermatozoa activated by solublised mouse zona pellucida, monitored with the calcium fluorescent indicator, fluo-3. Inhibition of the influx by three inhibitors of the zona pellucida induced acrosome reaction: tyrphostin A48, pertussis toxin, and 3-quinuclidinyl benzilate. *Reprod* **39**, 297-308.

Baird, D.T. (1999). Folliculogenesis and Gonadotrophins. *in*: Gonadotrophins and fertility in women. Sereno Fertility Series, Vol 3 (ed. E. Y. Adashi, D. T. Baird and P. G. Crosignani), pp. 1-10. Rome, Christengraf.

Bajpai, M., Fiedler, S.E., Huang, Z., Vijayaraghavan, S., Olson, G.E., Livera, G., Conti, M. and Carr, D.W. (2006). AKAP3 selectively binds PDE4A isoforms in bovine spermatozoa. *Biol Reprod* **74**, 109-118.

Baldi, E., Luconi, M., Muratori, M., Marchiani, S., Tamburrino, L. and Forti, G. (2009). Nongenomic activation of spermatozoa by steroid hormones: facts and fictions. *Mol Cell Endocrinol* **308,** 39–46.

Barratt, C.L.R. (1995). Spermatogenesis. in *Gametes: The Spermatozoon* (ed. J.G. Grudzinskas and J.L. Yovich), pp 250-268. Cambridge, UK: Cambridge University Press.

Barratt, C.L.R. and Kirkman-Brown, J.C. (2006). Man-made versus female-made environment-will the real capacitation please stand up? *Hum Reprod Update* **12**, 1-2.

Bedford, J. M. and Yanagimachi, R. (1992). Initiation of sperm motility after mating

in the rat and hamster. *J Androl* **13**, 444–449.

Bedu-Addo, K., Lefievre, L., Moseley, F.L., Barratt, C.L. and Publicover, S.J. (2005). Bicarbonate and bovine serum albumin reversibly 'switch' capacitation-induced events in human spermatozoa. *Mol Hum Reprod* **11**, 683-691.

Bedu-Addo, K., Barratt, C.L., Kirkman-Brown, J.C. and Publicover, S.J. (2007). Patterns of [Ca2+](i) mobilization and cell response in human spermatozoa exposed to progesterone. *Dev Biol* **302**, 324-332.

Berridge, M.J. (1993). Inositol trisphosphate and calcium signaling. *Nature* **28**, 315-325.

Berridge, M.J., Lipp, P. and Bootman, M.D. (2000). The versatility and universality of calcium signaling. *Nat Rev Mol Cell Biol* **1**, 11-21.

Berrios, J., Osses, N., Opazo, C., Arenas, G., Mercado, L., Benos, D.J., Reyes, J.G. (1998). Intracellular Ca2+ homeostasis in rat round spermatids. *Biol Cell* **90**, 391-398.

Bianchi, K., Rimessi, A., Prandini, A., Szabadkai, G. and Rizzuto. (2004). Calcium and mitochondria: mechanisms and functions of a troubled relationship. *Biochim Biophys Acta* **1742**, 119-131.

Biel, M. (2008). Cyclic nucleotide-regulated cation channels. *J Biol Chem* **284**, 9017-9021.

Bigelow, J. L., Dunson, D.B., Stanford, J.B., Ecochard, R., Gnoth, C. and Colombo, B. (2004). Mucus observations in the fertile window: a better predictor of conception than timing of intercourse. *Hum Reprod* **19**, 889-892.

Bird, G.S. and Putney, J.W. (2006). Capacitative calcium entry supports calcium oscillations in human embryonic kidney cells. *J Physiol* **562**, 697-706.

Bird, G.S., Hwang, S.Y., Smyth, J.T., Fukushima, M., Boyles, R.R. and Putney, J.W. (2009). STIM1 is a calcium sensor specialised for digital signaling. *Curr Biol* **19**, 1724-1729.

Blackmore, P.F. (1993). Thapsigargin elevates and potentiates the ability of progesterone to increase intracellular free calcium in human sperm: possible role of perinuclear calcium. *Cell Calcium* **14,** 53-60.

Bolotina, V.M. (2008). Orai, STIM1 and iPLA2beta: a view from a different perspective. *J Physiol* **586**, 3035-3042.

Bootman, M.D., Lipp, P. and Berridge, M.J. (2001). The organisation and functions of local Ca(2+) signals. *J Cell Sci* **114**, 2213-2222.

Bradley, M.P. and Forrester, I.T. (1980). A sodium-calcium exchange mechanism in plasma membrane vesicles isolated from ram sperm flagella. *FEBS Lett* **121,** 15-18.

Brandman, O., Liou, J., Park, W.S. and Meyer, T. (2007). STIM2 is a feedback regulator that stabilizes basal cytosolic and endoplasmic reticulum Ca2+ levels. *Cell* **131,** 1327-1339.

Braun, F.J., Broad, L.M., Armstrong, D.L. and Putney, J.W. (2001). Stable activation of single Ca^{2+} release-activated Ca^{2+} channels in divalent cation-free solutions. *J Biol Chem* **276**, 1063-1070.

Brewer, L., Corzett, M. and Balhorn., R (2002). Condensation of DNA by spermatid basic nuclear proteins. *J Biol Chem* **277**, 38895-38900.

Brown, J.S. (2009). Effects of bisphenol-A and other endocrine disruptors compared with abnormalities of schizophrenia: an endocrine-disruption theory of schizophrenia. *Schizophr Bull* **35**, 256-78.

Bryant, C.E., Tomlinson, A., Mitchell, J.A., Thiemermann, C. and Willoughby, D. A. (1995) Nitric oxide synthase in the rat fallopian tube is regulated during the oestrous cycle. *J Endocrinol* **146,** 149-157.

Burden, H.P., Holmes, C.H., Persad, R., and Whittington, K. (2005). Prostasomes – their effects on human male reproduction and fertility. *Human Reprod Update* **12,** 283-292.

Burkman, L.J. (1986). Temporal pattern of hyperactivation-like motility in human spermatozoa. *Biol Reprod* **34,** 226.

Burkman, L.J. (1995). Human sperm motility and fertilization. in *Gametes: The Spermatozoon* (ed. J.G. Grudzinskas and J.L. Yovich), pp122-139. Cambridge, UK: Cambridge University Press.

Cahalan, M. (2009). STIMulating store-operated Ca2+ entry. *Nat Cell Biol* **11**, 669-677.

Cai, X. (2007). Molecular evolution and functional divergence of the Ca(2+) sensor protein in store-operated Ca(2+) entry: stromal interaction molecule. *PLoS ONE* **2**, e609.

Calloway, N., Vig, M., Kinet, J. P., Holowka, D., Baird, B. (2009). Molecular clustering of STIM1 with Orai1/CRACM1 at the plasma membrane depends dynamically on depletion of Ca2+ stores and on electrostatic interactions. *Mol Biol Cell* **20**, 389-399.

Calogero, A.E., Hall, J., Fishel, S., Green, S., Hunter, A. and D'Agata. (1996). Effects of y-aminobutyric acid on human sperm motility and hyperactivation. *Mol Hum Reprod* **2,** 733-738.

Calogero, A.E., Burrello, N., Ferrara, E., Hall, J., Fishel, S., D'Agata, R. (1999). Gamma-aminobutyric acid (GABA) A and B receptors mediate the stimulatory effects of GABA on the human sperm acrosome reaction: interaction with progesterone. *Fertil steril* **71**, 930-936.

Carafoli, E. and Brini, M. (2000). Calcium pumps: structural basis for and mechanism of calcium transmembrane transport. *Curr Opin Chem Biol* **4,** 152-161.

Carballada, R. and Esponda, P. (1997). Fate and distribution of seminal plasma proteins in the genital tract of the female rat after natural mating. *J Reprod Fertil* **109**, 325-335.

Carlini, E., Palmerini, C. A., Cosmi, E.V., and Arienti, G. (1997). Fusion of sperm with prostasomes: Effects on membrane fluidity. *Arch Biochem Biophys* **343**, 6-12.

Carlson, A.E., Westenbroek, R.E., Quill, T., Ren, D., Clapham, D.E., Hille, B., Garbers, D. L. and Babcock, D. F. (2003). CatSper1 required for evoked Ca^{2+} entry and control of flagellar function in sperm. *Proc Natl Acad Sci USA* **100,** 14864-14868.

Carlson, A.E., Quill, T.A., Westenbroek, R.E., Schuh, S.M., Hille, B. and Babcock, D.F. (2005). Identical phenotypes of CatSper1 and Catsper2 null sperm. *J Biol Chem* **16**, 32238-32244.

Carrell, D.T., Middleton, R.G., Peterson, C. M., Jones, K.P., Urry, R.L. (1993). Role of the cumulus in the selection of morphologically normal sperm and induction of the acrosome reaction during human in vitro fertilization. *Arch Androl* **31**, 133-137.

Carrera, A. (1994). The Major Fibrous Sheath Polypeptide of Mouse Sperm: Structural and Functional Similarities to the A-kinase Anchoring Proteins. *Dev Biol* **165**, 272-284.

Castellano, L.E., Treviño, C.L., Rodríguez, D., Serrano, C.J., Pacheco, J., Tsutsumi, V., Felix, R. and Darszon A. (2003). Transient receptor potential (TRPC) channels in human sperm: expression, cellular localization and involvement in the regulation of flagellar motility. *FEBS Lett* **541,** 69-74.

Catterall, W.A. (2000). Structure and regulation of voltage-gated Ca^{2+} channels. *Ann Rev Cell Dev Biol* **16**, 521-555.

Chang, M.C. (1951). Fertilizing capacity of spermatozoa deposited into the fallopian tubes. *Nature* **168**, 697-698.

Chen, M.S., Tung, K.S., Coonrod, S.A., Takahashi, Y., Bigler, D., Chang, A., Yamashita, Y., Kincade, P.W., Herr, J.C and White, J.M. (1999). Role of the integrin-associated protein CD9 in binding between sperm ADAM 2 and the egg integrin alpha6beta1: implications for murine fertilization. *Pro Natl Acad Sci U S A* **96**, 11830–11835

Chen, Y., Cann, M., Litvin, T.N., Iourgenko, V., Sinclair, M.L., Levin, L.R. and Buck, J. (2000). Soluble adenylyl cyclase as an evolutionary conserved bicarbonate sensor. *Science* **289**, 625-628.

Chiarella, P., Puglisi, R., Sorrentino, V., Boitani, C. and Stefanini, M. (2004). Ryanodine receptors are expressed and functionally active in mouse spermatogenic cells and their inhibition interferes with spermatogonial differentiation. *J Cell Sci* **15**, 4127-4134.

Chung, M.K., Lee, H., Mizuno, A., Suzuki, M. and Caterina, M.J. (2004). 2-aminoethoxydiphenyl borate activates and sensitizes the heat-gated ion channel TRPV3. *J Neurosci* **24,** 5177-5182.

Clermont, Y. and Rambourg, A. (1978). Evolution of the endoplasmic reticulum during rat spermiogenesis. *Am J Anat* **151**, 191-212.

Coffey, D. (1995). What is the prostate and what is its function? in: *Handbook of Andrology* (ed. B. Robaire, J. L. Pryor and J. M. Trasler), pp.21-4. Lawrence, Kans: Allen Press Inc.

Collins, S.R. and Meyer, T. (2011). Evolutionary origins of STIM1 and STIM2 within ancient Ca2+ signaling systems. *Trends Cell Biol* **21,** 202-211.

Cooper, T.G. (2004). Cytoplasmic droplets: the good, the bad or just confusing? *Hum Repro* **20**, 9-11.

Correia, J.N., Conner, S.J. and Kirkman-Brown, J.C. (2007). Non-genomic steroid actions in human spermatozoa. "Persistant ticking from a laden environment". *Semin Reprod Med* **25**, 208-219.

Costello, S, Michelangeli, F., Nash, K., Lefievre, L., Morris, J., Machado-Oliveira, G., Barratt, C., Kirkman-Brown, J. and Publicover, S. (2009). Ca2+-stores in sperm: their identities and functions. *Reprod* **138**, 425-437.

Cross, N.L. (1996). Effect of cholesterol and other sterols on human sperm acrosomal responsiveness. *Mol Reprod Dev* **45**, 212-217.

Cross, N.L., and Mahasreshti, P. (1997). Prostasome fraction of human seminal plasma prevents sperm from becoming acrosomally responsive to the agonist progesterone. *Arch Androl* **39**, 39-44.

Curry, M.R. and Watson, P.F. (1999). Sperm structure and function. in *Gametes: The Spermatozoon* (ed. J.G. Grudzinskas and J.L. Yovich), pp 45-70. Cambridge, UK: Cambridge University Press.

Dadoune, J.P. (2003). Expression of mammalian spermatozoal nucleoproteins. *Microsc Res Tech* **61**, 56-75.

Daly, J.W., Lueders, J., Padgett, W.L., Shin, Y. And Gusovsky, F. (1995). Maitotoxin-elicited calcium influx in cultured cells: effect of calcium-channel blockers. *Biochem Pharmacol* **50**, 1187-1197.

DeHaven, W.I., Smyth, J.T, Boyles, R.R. and Putney, J.W. (2007). Calcium inhibition and calcium potentiation of Orai1, Orai2, and Orai3 calcium release-activated calcium channels. *J Biol Chem* **282**, 17548-17556.

DeHaven, W.I., Smyth, J.T., Boyles, R.R., Bird, G.S. and Putney, J,W. (2008). Complex actions of 2-aminoethyldiphenyl borate on store-operated calcium entry. *J Biol Chem* **283**, 19265-19273.

de Lamirande, E. and Gagnon, C. (1992). Reactive oxygen species and human spermatozoa. II. Depletion of adenosine triphosphate plays an important role in the inhibition of sperm motility. *J Androl* **13,** 379-386.

de Lamirande, E., Leclerc, P. and Gagnon, C. (1997). Capacitation as a regulatory event that primes spermatozoa for the acrosome reaction and fertilization. *Mol Hum Reprod* **3**, 175-194.

de Lamirande, E. and Gagnon, C. (1998). Paradoxical effect of reagents for sulfhydryl and

disulfide groups on human sperm capacitation and superoxide production. *Free Radic Biol Med* **25**, 803-817.

Demarco, I.A., Espinosa, F., Edwards, J., Sosnik, J., De La Vega-Beltran, J.L., Hockensmith, J.W., Kopf, G.S., Darszon, A. and Visconti, P.E. (2003). Involvement of a Na+/HCO3− cotransporter in mouse sperm capacitation. *J Biol Chem* **278**, 7001–7009.

De Meis., L. And Vianna, A.L. (1979). Energy interconversion by the Ca2+-dependent ATPase of the sarcoplasmic reticulum. *Annu Rev Biochem* **48**, 275-292.

Deng, X., Wang, Y., Zhou, Y., Soboloff, J. and Gill, D.L. (2009). STIM and Orai: Dynamic intermembrane coupling to control cellular calcium signals. *J Biol Chem* **284**, 22501-22505.

de Vries, K.J., Wiedmer, T, Sims, P.J. and Gadella, B.M. (2003). Caspase-independent exposure of aminophospholipids and tyrosine phosphorylation in bicarbonate responsive human sperm cells. *Biol Reprod* **68**, 2122-2134

de Ziegler, D., Bulletti, C., Fanchin, R., Epiney M. and Brioschi P.A. (2001). Contractility of the nonpregnant uterus: the follicular phase. *Ann N Y acad Sci* **943**, 172-184.

Docampo, R. and Moreno, S.N. (1999). Acidocalcisome: A novel Ca2+ storage compartment in trypanosomatids and apicomplexan parasites. *Parasitol Today* **15**, 443-448.

Dragileva, E., Rubinstein, S. and Breitbart, H. (1999). Intracellular Ca^{2+}-Mg^{2+} -ATPase regulates calcium influx and acrosomal exocytosis in bull and ram spermatozoa. *Biol Reprod* **61**, 1226-1234.

Dube, C., Tardif, S., Leclerc, P. and Bailey, J.L. (2003). The importance of calcium in the appearance of p32, a boar sperm tyrosine phosphorylation during in vitro capacitation. *J Androl* **24**, 727-733.

Eddy, E.M., Toshimori, K. and O'Brien, D.A. (2003). Fibrous sheath of mammalian spermatozoa. *Microsc Res Tech* **61**, 103-115.

Ekerhovd, E., Brannstrom, M., Alexandersson, M. and Norstrom, A. (1997). Evidence for nitric oxide mediation of contractile activity in isolated strips of the human Fallopian tube. *Hum Reprod* **12,** 301-305.

Eisenbach, M. (1999). Sperm chemotaxis. *Rev Reprod* **4**, 56-66.

Espino, J., Mediero, M., Lozano, G. M., Bejarano, I., Ortiz, A., Garcia, J. F., Pariente, J. A. and Rodriguez, A. B. (2009). Reduced levels of intracellular calcium releasing in spermatozoa from asthenozoospermic patients. *Reprod Biol Endocinol* **6**, 7-11.

Esposito, G., Jaiswal, B.S., Xie, F., Krajnc-Franken, M.A.M., Robben, T.J.A.A., Strik, A.M., Kuil, C., Philipisen, R.L.A., van Duin, M., Conti, M. and Gossen, J.A. (2004). Mice deficient for soluble adenylyl cyclase are infertile because of a severe sperm-motility defect. *Proc Natl Acad Sci USA* **101**, 2993–2998.

Eu, J. P., Xu, L., Stamler, J. S. and Meissner, G. (1999). Regulation of ryanodine receptors by reactive nitrogen species. *Biochem Pharmacol*. **57**, 1079-1084.

Evans, J.P and Florman, H.M. (2002). The state of the union: the cell biology of fertilization. *Nat Cell Biol* **4**, s57-63.

Fabiani, R., Johansson, L., Lundkvist, O., and Ronquist, G. (1994). Enhanced recruitment of motile spermatozoa by prostasome inclusion in swim-up medium. *Hum Repro Update* **12**, 283-292.

Falsetti, C., Baldi, E., Krausz, C., Casano, R., Failli, P., Forti, G. (1993). Decreased responsiveness to progesterone of spermatozoa in oligozoospermic patients. *J Androl* **14**, 17-22.

Feske, S., Gwack, Y., Prakriya, M., Srikanth, S., Puppel, S.H., Tanasa, B., Hogan, P.G., Lewis, R.S., Daly, M. and Rao, A. (2006). A mutation in Orai1 causes immune deficiency by abrogating CRAC channel function. *Nature* **441**, 179.

Fischer, A. (2007). Human primary immunodeficiency diseases. *Immunity* **27,** 835-845.

Florman, H.M., Tombes, R.M., First, N.L. and Babcock, D.F. (1989). An adhesion-associated agonist from the zona pellucida activates G protein-promoted elevations of internal Ca2+ and pH that mediate mammalian sperm acrosomal exocytosis. *Dev Biol* **135**, 133-46.

Franca, L.R, Parreira, G.G., Gates, R.J. and Russell, L.D. (1998). Hormonal regulation of spermatogenesis in the hypophysectomized rat: quantitation of germ-cell population and effect of elimination of residual testosterone after long-term hypophysectomy. *J Androl* **19**, 335-342.

Franklin, L.E. (1968). Formation of the redundant nuclear envelope in monkey spermatids. *Anat Rec* **161**, 149-162.

Frenette, G., Lessard, C., and Sullivan, R. (2002). Selected proteins of prostasome like particles from epididymal cauda fluid are transferred to epididymal caput spermatozoa in bull. *Biol Reprod* **67**, 308-313.

Frischauf, I., Schindl, R., Derler, I., Bergsmann, J., Fahrner, M. and Romanin, C. (2008). The STIM/Orai coupling machinery. *Channels* **2**, 261-268.

Gadella, B.M. and Harrison, R.A.P. (2000). The capacitating agent bicarbonate induces protein kinase A-dependent changes in phospholipid transbilayer behavior in the sperm plasma membrane, *Development* **127**, 2407–2420.

Gadella, B.M. and van Gestel, R.A. (2004). Bicarbonate and its role in mammalian sperm

function. *Animal Repro Sci* **82-83**, 307-319.

Gadella, B.M and Visconti, P.E. (2006). Regulation of capacitation. in *The Sperm Cell* (ed. C. DeJonge and C. Barratt), pp 134-170. Cambridge, UK: Cambridge University Press.

Gakamsky, A., Armon, L. And Eisenbach, M. (2009). Behavioral response of human spermatozoa to a concentration jump of chemoattractants or intracellular cyclic nucleotides. *Hum Reprod* **24**, 1153-1163.

Galantino-Homer, H.L., Florman, H.M., Storey, B.T., Dobrinski, I. and Kopt, G.S. (2004). Bovine sperm capacitation: assessment of phosphodiesterase activity and intracellular alkinisation on capacitation-associated protein tyrosine phosphorylation. *Mol Reprod Dev* **67**, 487-500.

Garban, H. J., Marquez-Garban, D. C., Piedras, R. J., Ignarro, L. J. (2005). Rapid Nitric Oxide-Mediated S-Nitrosylation of Estrogen Receptor: Regulation of Estrogen-Dependent Gene Transcription. *Nat Acad Sci U S A* **102**, 2632-2636.

Garcia, M.A. and Meizel, S. (1999). Progesterone-mediated calcium influx and acrosome reaction of human spermatozoa: pharmacological invcestigation of T-type calcium channels. *Biol Reprod* **60**, 102-109.

Gavrilescu L.C. and Van Etten R.A. (2007). Production of replication-defective retrovirus by transient transfection of 293T cells. *J Vis Exp* **10**, 550.

Gerasimenko, O.V., Gerasimenko, J.V., Tepikin, A.V. and Petersen, O.H. (1995). ATP-dependent accumulation and inositol trisphosphate or cyclic ADP-ribose-mediated release of Ca^{2+} from the nuclear envelope. *Cell* **80**, 439-444.

Giannini, G., Conti, A., Mammarella, S., Scrobogna, M. and Sorrentino, V. (1995). The ryanodine receptor/calcium channel genes are widely and differentially expressed in murine brain and peripheral tissues. *J Cell Biol* **128**, 893-904.

Glover, T.B., Barratt, C.L.R., Tyler, J.P.P. and Hennessey, J.F. (1990). Human male fertility and semen analysis. London, UK: Academic Press.

Gonzalez-Martinez, M.T., Galindo, B.E., de De La Toore, L., Zapata, O., Rodriquez, E., Florman, H.M. and Darszon, A. (2001). A sustained increase in intracellular Ca^{2+} is required for the acrosome reaction in sea urchin sperm. *Dev Biol* **236,** 220-229.

Gosden, R.G., and Telfer, E. (1987). Scaling of follicular sizes in mammalian ovaries. *J Zool* **211**, 157-168.

Gosden, R.G., and Bownes, M. (1995). Molecular and cellular aspects of oocyte development. in Gametes The Oocyte (ed J. G. Grudzinskas and J.L. Yovich), pp23-53. Cambridge, UK: Cambridge University Press.

Graham, S.J.L., Dziadek, M.A. and Johnstone, L.S. (2011). A cytosolic STIM2 pre-protein created by signal peptide inefficiency activates Orai1 in a store independent manner. *J Biol Chem* **286**, 16174-16185.

Grigoriev, I., Montenegro Gouveia, S., van de Vaart, B., Demmers, J. and Akhmanova, A. (2008) STIM1 is a MT-plus-end-tracking protein involved in remodeling of the ER. *Curr Biol* **18**, 177–182.

Groden, D.L., Guan, Z. and Stokes, B.T. (1991). Determination of Fura-2 dissociation constants following adjustment of the apparent Ca-EGTA association constant for temperature and ionic strength. *Cell Calcium* **12**, 279-287.

Gunter, T.E., Buntinas, L., Sparagna, R., Eliseev, R. and Gunter, K. (2000) Mitochondrial calcium transport: mechanisms and functions. *Cell Calcium* **28**, 285-296.

Gunteski-Hamblin, A.M., Clarke, D.M. and Shull, G.E. (1992). Molecular cloning and

tissue distribution of alternatively spliced mRNAs encoding possible mammalian homologues of the yeast secretory pathway calcium pump. *Biochem* **31**, 7600-7608.

Gwack, Y., Srikanth, S., Feske, S., Cruz-Guiloty, F., Oh-hora, M., Neems, D.S, Hogan, P.G, Rao, A. (2007). Biochemical and functional characterization of Orai proteins. *J Biol Chem* **282**, 1623-1643.

Hakamata, Y., Nishimura, S., Nakai, J., Nakashima, Y., Kita, T. and Imoto, K. (1994). Involvement of the brain type ryanodine receptor in T-cell proliferation. *FEBS Lett* **352**, 206-210.

Hanson, F.W. and Overstreet, J.W. (1981). The interaction of human spermatozoa with cervical mucus in vivo. *Am J Obstet Gynecol* **15**, 173-178.

Harper, J.L., Shin, Y. and Daly, J.W. (1997). Loperamide: a positive modulator for store-operated calcium channels. *Proc Natl Acad Sci U S A* **94**, 14912-14917.

Harper, J.L. and Daly, J.W. (1999). Inhibitors of store-operated calcium channels: imidazoles, phenothiazines, and other tricyclics. *Drug Dev Res* **47**, 107-117.

Harper, C.V., Kirkman-Brown, J. Barratt, C.L. and Publicover, S.J. (2003). Encoding of progesterone stimulus intensity by intracellular [Ca^{2+}] ([Ca^{2+}]$_i$) in human spermatozoa. *Biochem J* **372**, 407-417.

Harper, C.V., Barratt, C.L.R., Publicover, S.J. (2004). Stimulation of Human Spermatozoa with progesterone gradients to stimulate approach to the oocyte. *J Biol Chem* **279**, 46315-46325.

Harper, C.V., Wootton, L., Michelangeli, F., Lefievre, L., Barratt, C. and S.J. Publicover. (2005). Secretory pathway Ca2+-ATPase (SPCA1) Ca2+ pumps, not SERCAs, regulate complex [Ca2+]i signals in human spermatozoa. *J Cell Sci* **118**, 1673-1685.

Harrison, R.A.P. and Miller, N.G.A. (2000). cAMP-dependent protein kinase control of plasma membrane lipid architecture in boar sperm. *Mol Reprod Dev* **55**, 220–228.

Harrison, R.A.P. and Gadella, B.M. (2005). Bicarbonate-induced membrane processing in sperm capacitation. *Theriogenology* **63**, 342–351.

Hess, K.C., Jones, B.H., Marquez, B., Chen, Y., Ord, T.S., Kamenetsky, M., Miyamoto, C., Zippin, J.H., Kopf, G.S., Suarez, S.S. et al. (2005). The soluble adenylyl cyclase in sperm mediates multiple signalling events required for fertilization. *Dev Cell* **9**, 249-259.

Ho, H.C. and Suarez, S.S. (2001). An inositol 1,4,5-trisphosphate receptor-gated intracellular Ca^{2+} store is involved in regulating sperm hyperactivated motility. *Biol Reprod* **65**, 1606-1615.

Ho, H.C. and Suarez, S.S. (2003). Characterization of the intracellular calcium store at the base of the sperm flagellum that regulates hyperactivated motility. *Biol Reprod* **65**, 1606-1615.

Hu, Z., Gu, Q., Wang, C., Colton, C.K., Tang, J., Kinoshita-Kawada, M., Lee, L.Y., Wood, J.D., and Zhu, M.X. (2004). 2-Aminoethoxydiphenyl borate is a common activator of TRPV1, TRPV2 and TRPV3. *J Biol Chem* **279**, 35741-35748.

Huang, G.N., Zeng, W., Kim, J.Y., Yuan, J.P., Han, L., Muallem, S. and Worley, P.F. (2006). STIM1 carboxyl-terminus activates native SOC, I(crac) and TRPC1 channels. *Nat Cell Biol* **8**, 1003-1010.

Hu, H., Grandl, J., Bandell, M., Petrus, M., and Patapoutian, A. (2009) Two amino acid residues determine 2-APB sensitivity of the ion channels TRPV3 and TRPV4. *Proc Natl Acad Sci U S A* **106**, 1626-1631.

Hunter, R.H.F. (1981). Sperm transport and reservoirs in the pig oviduct in relation to the time of ovulation. *J Reprod Fertil* **63**, 109-117.

Huszar, G., and Vigue, L. (1993). Incomplete development of human spermatozoa is associated with increased creatine phosphokinase concentrations and abnormal head morphology. *Mol Reprod Dev* **34**, 292-298.

Inoue, N., Ikawa, M., Isotani, A. and Okabe, M. (2005). The immunoglobulin superfamily protein Izumo is required for sperm to fuse with eggs. *Nature* **434**, 234-238.

Iwai, M., Michikawa, T., Bosanac, I., Ikura, M. and Mikoshiba, K. (2007). Molecular basis of the isoform-specific ligand-binding affinity of inositol 1,4,5-trisphosphate receptors. *J Biol Chem* **282,** 12755-12764.

Jacobson, G. and Karsnas, P. (1990). Important parameters in semi-dry electrphoretic transfer. *Electrophoresis* **11**, 46-52.

Jagannathan, S., Publicover, S.J. and Barratt, C.L. (2002). Voltage-operated calcium channels in male germ cells. *Reprod* **123**, 203-215.

Jaiswal, B.S., Tur-Kaspa, I., Dor, J., Mashiach, S. Eisenbach, M. (1999). Human sperm chemotaxis: is progesterone a chemoattractant? *Biol Reprod* **60**, 1314-1319.

Jimenez-Gonzalez, C., Michelangeli, F., Harper, C.V., Barratt, C.L. and Publicover, S.J. (2006). Calcium signaling in human spermatozoa: a specialized 'toolkit' of channels, transporters and stores. **12,** 253-267.

Jin, J., Jin, N., Zheng, H., Ro, S., Tafolla, D., Sanders, K.M., Yan, W. (2007). Catsper3 and Catsper4 are essential for sperm hyperactivated motility and male fertility in the mouse. *Biol Reprod* **77**, 37-44.

Johnson, M. H., Everitt, B. J. (1995). Testicular function. in *Essential Reproduction,* pp 45-54. Oxford, UK: Blackwell Science Ltd.

Jouaville, L.S., Ichas, F. and Mazat, J.P. (1998). Modulation of cell calcium signals by mitochondria. *Mol Cell Biochem* **184**, 371-376.

Jow, W.W., Steckel, J., Schlegel, P.N., Magid, M.S. and Goldstein, M. (1993). Motile sperm in human testis biopsy specimens. *J Androl* **14**, 194-198.

Jungnickel, M.K., Marrero, H., Birnbaumer, L., Lemos, J.R. and Florman, H.M. (2001). Trp2 regulates entry of Ca^{2+} into mouse sperm triggered by egg ZP3. *Nat Cell Biol* **3**, 499-502.

Juvin, V., Penna, A., Chemin, J., Lin, Y.L., and Rassendren, F.A. (2007). Pharmacological characterization and molecular determinants of the activation of transient receptor potential V2 channel orthologs by 2-aminoethoxydiphenyl borate. *Mol Pharmacol* **72**, 1258-1268.

Katz, D.F., Drobnis, E.Z. and Overstreet, J.W. (1989). Factors regulating mammalian sperm migration through the female reproductive tract and oocyte vestments. *Gamete Res* **22**, 443-469.

Katz, D.F., Morales, P., Samuels, S.J. and Overstreet, J.W. (1990). Mechanisms of filtration of morphologically abnormal human sperm by cervical mucus. *Fertil Steril* **54**, 513-516.

Katz, D.F., Slade, D.A. and Nakajima, S.T. (1997). Analysis of preovulatory changes in cervical mucus hydration and sperm penetrability. *Adv Contracept* **13,** 143-151.

Kaupp, U.B. and Seifert, R. (2002). Cyclic nucleotide-gated ion channels. *Physiol Rev* **82,** 769-824

Kaupp, U.B., Kashikar, N.D. and Weyand, I. (2008). Mechanisms of sperm chemotaxis. *Annu Rev Physiol* **70**, 93-117.

Kilic, F., Kashikar, N.D., Schmidt, R., Alvarez, L., Weyand, I., Wiesner, B., Goodwin, N., Hagen, V. and Kaupp, U.B. (2009). Caged progesterone: a new tool for studying rapid nongenomic actions of progesterone. *Arch Gynecol Obstet* **281**, 933-938.

Kingston R.E., Chen C.A. and Okayama H. (1999). Calcium phosphate transfection. *Curr Prot Immunol* **10**, 10-13.

Kirkman-Brown, J.C., Bray, C., Stewart, P.M., Barratt, C.L. and Publicover, S.J. (2000). Biphasic elevation of [Ca(2+)](i) in individual human spermatozoa exposed to progesterone. *Dev Biol* **222**, 326-35.

Kirkman-Brown, J.C., Punt, E.L., Barratt, C.L. and Publicover, **S.J.** (2002). Zona pellucida and progesterone-induced Ca^{2+} signaling and acrosome reaction in human spermatozoa. *J Androl* **23**, 306-315.

Kirkman-Brown, J.C. and Smith, D.J. (2011). Sperm motility: is viscosity fundamental to progress? *Mol Hum Reprod* **8**, 539-544.

Kiselvov, K., Xu, X., Mozhayeva, G., Kuo, T., Pessah, L., Mignery, G., Zhu, X., Birnbaumer, L. and Muallem, S. (1998). Functional interaction between InsP3 receptors and store-operated Htrp3 channels. *Nature* **396**, 478-482.

Kuroda, Y., Kaneko, S., Yoshimura, Y., Nozawa, S. and Mikoshiba, K. (1999). Are there inositol 1,4,5-triphosphate (IP3) receptors in human sperm? *Life Sci* **65**, 135-143.

Launikonis, B.S. and Rios, E. (2007). Store-operated Ca2+ entry during intracellular Ca2+ release in mammalian skeletal muscle. *J Physiol* **15,** 81-97.

Lawson, C., Dorval, V., Goupil, S. and Leclerc, P. (2007). Identification and localization of SERCA 2 isoforms in mammalian sperm. *Mol Hum Reprod* **13**, 307-316.

Lawson, C., Goupil, S. and Leclerc, P. (2008). Increased activity of the human sperm tyrosine kinase SRC by the cAMP-dependent pathway in the presence of Calcium. *Biol Reprod* **79**, 657-666.

Leclerc, P., de Lamirande, E. And Gagnon, C. (1996). Cyclic adenosine 3',5'monophosphate-dependent regulation of protein tryrosine phosphorylation in relation to human sperm capacitation and motility. *Biol Reprod* **55**, 684-93.

Lee, H.C. (2006). Structure and enzymatic functions of human CD38. *Mol Med* **12,** 317-323.

Lefievre, L., De Lamirande, E., Gagnon, C. (2000). The cyclic GMP-specific phosphodiesterase inhibitor, sildenafil, stimulates human sperm motility and capacitation but not acrosome reaction. *J Androl* **21**, 929-937.

Lefievre., L, Conner, S.J., Salpekar, A., Olufowobi, O., Ashton, P., Pavlovic, B., Lenton, W., Afnan, M., Brewis, I.A., Monk, M., Hughes, D.C. and Barratt, C.L. (2004). Four zona pellucida glycoproteins are expressed in the human. *Hum Reprod* **19**, 1580-1586.

Lefievre, L., Chen, Y., Conner, S. J., Scott, J., Publicover, S., Ford, W., Barratt, C.L.R. (2007). Human Spermatozoa Contain multiple Targets for Protein S-Nitrosylation: An alternative Mechanism of the Modulation of Sperm Function by Nitric Oxide? *Proteomics* **7,** 3066-3084.

Le Naour, F., Rubinstein, E., Jasmin, C., Prenant, M. and Boucheix, C. (2000). Severely reduced female fertility in CD9-deficient mice. *Science* **287**, 319-321.

Lewis, R.S. (2007). The molecular choreography of a store-operated calcium channel. *Nature* **446**, 284-287.

Li, L. and Moore, P.K. (2007). An overview of the biological significance of endogenous gases: new roles for old molecules. *Biochem Soc Trans* **35**, 1138-1141.

Liou, J., Kim, M.L., Heo, W.D., Jones, J.T., Myers, J.W., Ferrell, J.E. and Meyer, T. (2005). STIM is a Ca^{2+} sensor essential for Ca^{2+} store depletion triggered Ca^{2+} influx. *Curr Biol* **15**, 1235.

Liou, J., Fivaz, M., Inoue, T and Meyer, T. (2007). Live-cell imaging reveals sequential oligomerization and local plasma membrane targeting of stromal interaction molecule 1 after Ca^{2+} store depletion. *Proc Natl Acad Sci U S A* **104**, 9301-9306.

Lis, A., Peinelt, C., Beck, A., Parvez, S., Monteilh-Zoller, M., Fleig, A. and Penner, R. (2007). CRACM1, CRACM2, and CRACM3 are store-operated Ca2+ channels with distinct functional properties. *Curr Biol* **17**, 794-800.

Lishko, P.V., Botchkina, I.L. and Kirichok, Y. (2011). Progesterone activates the principal Ca2+ channel of human sperm. *Nature* **471**, 387-391.

Litvin, T.N., Kamenetsky, M., Zarifyan, A., Buck, J. and Levin, L.R. (2003). Kinetic properties of "soluble" adenylyl cyclase. Synergism between calcium and bicarbonate. *J. Biol. Chem*. **278**, 15922–15926.

Lobley, A., Pierron, V., Reynolds, L., Allen, L. And Michalovich, D. (2003). Identification of human and mouse CatSper3 and CatSper4 gebes: characterisation of a common interaction domain and evidence for expression in testis. *Reprod Biol Endocrinol* **1**, 53.

Luik, R.M., Wang, B., Prakriya, M., Wu, M.M. and Lewis, R.S. (2008). Oligomerization of STIM1 couples ER calcium depletion to CRAC channel activation. *Nature* **454**, 538-542.

Ma, H.T., Patterson, R.L., van Rossum, D.B., Birnbaumer, L., Mikoshiba, K. and Gill, D.L. (2000). Requirement of the inositol triphosphate receptor for activation of store-operated Ca^{2+} channels. *Science* **287**, 1647-1651.

Ma, H. T., Venkatachalam, K., Li, H.S., Montell, C., Kurosaki, T., Patterson, R.L., and Gill, D. L. (2001*).* Assessment of the role of the inositol 1,4,5-trisphosphate receptor in the activation of transient receptor potential channels and store-operated Ca2+ entry channels. *J Biol Chem* **276,** 18888-18896.

Maccarrone, M., Barboni, B., Paradisi, A., Bernabo, N., Gasperi, V., Pistilli, M.G., Fezza, F., Lucidi, P., and Mattioli, M. (2005). Characterisation of the endocannabinoid system in boar spermatozoa and implications for sperm capacitation and acrosome reaction. *J Cell Sci* **118**, 4393-4404

Machado-Oliveira, G., Lefievre, L., Ford, C., Herrero, M.B., Barratt, C., Connolly, T.J., Nash, K., Morales-Garcia, A., Kirkman-Brown, J. and Publicover, S.J. (2008). Mobilisation of Ca2+ stores and flagellar regulation in human sperm by S-nitrosylation: a role for NO synthesised in the female reproductive tract. *Development* **135**, 3677-3686.

Manji, S.S., Parker, N.J., Williams, R.T., van Stekelenburg, L., Pearson, R.B., Dziadek, M. and Smith, P.J. (2000). STIM1: a novel phosphoprotein located at the cell surface. *Biochim Biophys Acta* **1481**, 147-155.

Marquez, B. and Suarez, S.S. (2007). Bovine sperm hyperactivation is promoted by alkaline-stimulated Ca^{2+} influx. *Biol Reprod* **76,** 660-665.

Martínez-López, P., Santi, C.M., Treviño, C.L., Ocampo-Gutierrez, A.Y., Acevedo, J.J., Alisio, A. (2009). Mouse sperm K+ currents stimulated by pH and cAMP possibly coded by Slo3 channels. *Biochem Biophys Res Commum* **381**, 204-209.

McCormack, J.G., Halestrap, R.M. and Denton. (1990). Role of calcium ions in regulation of mammalian intramitochondrial metabolism. *Physiol Rev* **70**, 391-425.

McLachlan, R.I. (2000). The endocrine control of spermatogenesis. *Bailleres Best Prat Res Clin Endocrinol Metab* **14**, 345-362.

Meistrich, M.L., Mohapatra, B., Shirley, C.R. and Zhoa, M. (2003). Roles of transition nuclear proteins in spermiogenesis. *Chromosoma* **111**, 483-488.

Meizel, S. and Turner, K.O. (1993). Effects of polyamine biosynthesis inhibitors on the progesterone-initiated increase in intracellular free Ca2+ and acrosome reactions in human sperm. *Mol Reprod Dev* **34**, 457-465.

Meizel, S. (1995). Initiation of human sperm acrosome reaction by progesterone. in: Human sperm acrosome reaction (ed. P. Fenichel and J. Parinaud), pp. 205-22. Serono Symposia, Norwell, MA.

Mercer, J.C., Dehaven, W.I., Smyth, J.T., Wedel, B., Boyles R.R., Bird, G.S. and Putney, J.W. (2006). Large store-operated calcium selective currents due to co-expression of Orai1 or Orai2 with the intracellular calcium sensor, Stim1. *J Biol chem* **281**, 24979-24990.

Michelangeli, F., Mezna, M., Tovey, S. and Sayers, L.G. (1995). Pharmacological modulators of the inositol 1,4,5-trisphosphate receptor. *Neuropharmacology* **34**, 1111-1122.

Michelangeli, F., Ogunbayo, O.A. and Wootton, L.L. (2005). A plethora of interacting organellar Ca2+ stores. *Curr Opin Cell Biol* **17**, 135-140.

Mignen, O., Thompson, J.L., Shuttleworth, T.J. (2008). Orai1 subunit stoichiometry of the mammalian CRAC channel pore. *J Physiol* **586**, 419-425.

Mignen, O., Thompson, J.L., Shuttleworth, T.J. (2009). The molecular architecture of the arachidonate-regulated Ca2+-selective ARC channel is a pentameric assembly of Orai1 and Orai3 subunits. *J Physiol*, ahead of print.

Miraglia, E., Rullo, M.L., Bosia, A., Massobrio, M., Revelli, A. and Ghigo, D. (2007). Stimulation of the nitric oxide/cyclic guanosine monophosphate signaling pathway elicits human sperm chemotaxis in vitro. *Fertil Steril* **87**, 1059-1063.

Mitchell, D.R. (2007). The evolution of eukaryotic cilia and flagella as motile and sensory organelles. *Adv Exp Med Bio* **607,** 130-140.

Moore, H.D.M., Hartman, T.D., Pryor, J.P. (1983). Development of the oocyte penetrating capacity of spermatozoa in the human epididymis. *Int J Androl* **6**, 310-318

Moore, H.D.M. (1995). Post-testicular sperm maturation and transport in the excurrent ducts. in *Gametes: The Spermatozoon* (ed. J.G. Grudzinskas and J.L. Yovich), pp 140-157. Cambridge, UK: Cambridge University Press.

Morales, P., Roco, M. and Vigil, P. (1993). Human cervical mucus: relationship between biochemical characteristics and ability to allow migration of spermatozoa. *Hum Reprod* **8,** 78–83.

Morozumi, K., Shikano, T., Miyazaki, S. and Yangimachi, R. (2006). Simultaneous removal of sperm plasma membrane and acrosome before intracytoplasmic sperm injection improves oocyte activation/embryonic development. *Proc Natl Acad Sci U S A* **103**, 17661-17666.

Mortimer, D. (1994). Practical Laboratory Andrology. Oxford, UK: Oxford University Press.

Mortimer, S.T. and Swan, M.A. (1995) Variable kinematics of capacitating human spermatozoa. *Hum Reprod* **10**, 3178-3182.

Moss, S.B. and Gerton, G.L. (2001). A-Kinase Anchor Proteins in Endocrine Systems and Reproduction. *TEM* **10**, 434-440.

Motta, P.M., Makabe, S., Naguro, T., Correr, S. (1994). Oocyte follicle cells association during development of human ovarian follicle. A study by high resolution scanning and transmission electron microscopy. *Arch Histol Cytol* **57**, 369-394.

Motta, P.M., Nottola, S.A., Pereda, J., Croxatto, H.B., and Familiari, G. (1995). Ultrastructure of human cumulus oophorus: a transmission electron microscopic study on oviductal oocytes and fertilized eggs. *Hum Reprod* **10**, 2361-2367.

Muik, M., Frischauf, I., Derler, I., Fahrner, M., Bergsmann, J., Eder, P., Schindl, R., Hesch, C., Polzinger, B., Fritsch, R., Kahr, H., Madl, J., Gruber, H., Groschner, K. and Romanin, C. (2008). Dynamic coupling of the putative coiled-coil domain of Orai1 with STIM1 mediates Orai1 channel activation. *J Biol Chem* **283**, 8014-8022.

Munace, M.J., Quintero, I., Caille, A.M., Ghersevich, S. and Berta, C.L. (2006). Comparative concentrations of steroid hormones and proteins in human peri-ovulatory peritoneal and follicular fluids. *Reprod Biomed Online* **13**, 202-207.

Muratori, M., Luconi, M., Marchiani, S., Forti, G., and Baldi, E. (2009). Molecular markers of sperm functions. *Int J Androl* **32**, 25-45.

Naaby-Hansen, S., Wolkowicz, M.J., Klotz, K., Bush, L.A., Westbrook, V.A., Shibahara, H., Shetty. J., Coonrod, S.A., Reddi, P.P., Shannon, J. *et al.* (2001). Colocalization of the inositol 1,4,5-triphosphate receptor and calreticulin in the equatorial segment and in membrane bound vesicles in the cytoplasmic droplet of human spermatozoa. *Mol Hum Reprod* **7**, 923-933.

Nash, K.L., Lefievre, L., Peralta-Arias, R., Morris, J., Morales-Garcia, A., Connolly, T., Costello, S., Kirkman-Brown, J. and Publicover, S.J. (2010). Techniques for imaging Ca^{2+} signaling in human sperm. *J Vis Exp* **16.**

Neeper, M.P., Liu, Y., Hutchinson, T.L., Wang, Y., Flores, C.M., and Qin, N. (2007). Activation properties of heterologously expressed mammalian TRPV2: evidence for species dependence. *J Biol Chem* **282**, 15894-15902

Nottola, S.A., Macchiarelli, G., Familiari, G., Stallone, T., Sathananthan, A.H, Motta, P.M. (1998). Egg-sperm interactions in humans: ultrastructural aspects. *Ital J And Embryol* **103**, 85-101.

Oko, R.J., Costerton, J.W. and Coulter, G.H. (1976). An ultrastructural study of the head region of bovine spermatozoa. *Can J Zool* **54**, 1326-1340.

Oko, R., Hermo, L., Chan, P.T., Fazel, A. and Bergeron, J.J. (1993). The cytoplasmic droplet of rat epididymal spermatozoa contains saccular elements with Golgi characteristics**.** *J Cell Biol* **123**, 809-821

Oko, R.J. (1995). Developmental expression and possible role of perinuclear theca proteins in mammalian spermatozoa. *Reprod Fertil Dev* **7**, 777-797.

Okunade, G.W., Miller, M.L., Pyne, G.J., Sutliff, R.L., O'Connor, K.T., Neumann, J.C., Andringa, A., Miler, D.A., Prasad, V., Doetschman, T., Paul, R.J. and Shull, G. E. (2004). Targeted ablation of plasma membrane Ca^{2+}-ATPase (PMCA) 1 and 4 indicates a major housekeeping function for PMCA1 and a critical role in hyperactivated sperm motility and male fertility for PMCA4. *J Biol Chem* **279,** 33742-33750.

O'Toole, C.M., Arnoult, C., Darszon, A., Steinhardt, R.A. and Florman, H.M. (2000). Ca^{2+} entry through store-operated channels in mouse sperm is initiated by egg ZP3 and drives the acrosome reaction. *Mol Biol Cell* **11**, 1571-1584.

Osheroff J.E., Visconti, P.E., Valenzuela, J.P., Travis A.J., Alvarez, J. and Kopf, G.S. (1999). Regulation of human sperm capacitation by a cholesterol efflux stimulated signal transduction pathway leading to protein kinase A mediated up-regulation of protein tyrosine phosphorylation. *Mol Hum Reprod* **5**, 1017-1026.

Osman, R.A., Andria, Jones, A.D., and Meizel, S. (1989). Steroid induced exocytosis: the human sperm acrosome reaction. *Biochem Biophys Res Commum* **160**, 828-833.

O'Toole, C.M., Arnoult, C., Darzon, A., Steinhardt, R.A. and Florman, H.M. (2000). Ca^{2+} entry through store-operated channels in mouse sperm is initiated by egg ZP3 and drives the acrosome reaction. *Mol Bio Cell* **11** 1571-1584.

Otsu, K., Willard, H.F., Khanna, V.K., Zorzato, F., Green, N.M. and MacLennan, D.H. (1990). Molecular cloning of cDNA encoding the Ca^{2+} release channel (ryanodine receptor) of rabbit cardiac muscle sarcoplasmic reticulum. *J Biol Chem* **265**,13472-13483.

Parekh, A.B., Fleig, A. and Penner, R. (1997). The store-operated calcium current I(CRAC): nonlinear activation by InsP3 and dissociation from calcium release. *Cell* **13**, 973-980.

Parekh, A.B., and Putney, J.W. (2005). Store-operated calcium channels. *Physiol Rev* **85**, 757-810.

Parish, J.J., Susko-Parrish, J.L. and First, N.L. (1989). Capacitation of bovine sperm by heparin: inhibitory effect of glucose and role of intracellular pH. *Biol Reprod* **41**, 683-699.

Park, J.Y., Ahn, H.J., Gu, J.G., Lee, K.H., Kim, J.S., Kang, H.W. and Lee, J.H. (2003). Molecular identification of Ca2+ channels in human sperm. *Exp Mol Med* **35**, 285-292.

Park, C.Y., Hoover, P.J., Mullins, F.M., Bachhawat, P., Covington, E.D., Raunser, S., Walz, T., Garcia, K.C., Dolmetsch, R.E. and Lewis, R.S. (2009). STIM1 clusters and activates CRAC channels via direct binding of a cytosolic domain to Orai1. *Cell* **136**, 876-890.

Park, K.H., Kim, B.J., Kang, J., Nam, T.S, Lim, M.L., Kim, H.T., Park, J.K., Kim, Y.G., Chae, S.W., Kim, U.H. (2011). Ca2+ signaling tools acquired from prostasome are required for progesterone-induced sperm motility. *Sci Signal* **4**, 1-10.

Parvez, S., Beck, A., Peinelt, C., Soboloff, J., Lis, A., Monteilh-Zoller, M., Gill, D.L., Fleig, A. and Penner, R. (2008). STIM2 protein mediates distinct store-dependent and store-independent modes of CRAC channel activation. *FASEB J* **22**, 752-761.

Peier, A.M., Reeve, A.J., Andersson, D.A., Moqrich, A., Earley, T.J., Hergarden, A.C., Story, G.M., Colley, S., Hogenesch, J.B., McIntyre, P., Bevan, S. and Patapoutian, A. (2002). A heat-sensitive TRP channel expressed in karatinocytes. (2002) *Science* **296**, 2046-2049.

Penna, A., Demuro, A., Yeromin, A.V., Zhang, S.L, Safina, O., Parker, I., Cahalan, M.D. (2008). The CRAC channel consists of a tetramer formed by Stim-induced dimerization of Orai dimers. *Nature* **456**, 116-120.

Poliakov, A., Spilmam, M., Dokland, T., Amling C. L., Moble, J. A. (2009). Structural heterogeneity and protein composition of exosome-like vesicles (prostasomes) in human semen. *Prostate* **69**, 159-167.

Prakriya, M. and Lewis, R.S. (2001). Potentiation and inhibition of Ca(2+) release-activated Ca (2+) channels by 2-aminoethyldiphenyl borate (2-APB) occurs independently of IP(3) receptors. *Physiol* **536**, 3-19.

Prakriya, M., Feske, S., Gwack, Y., Srikanth, S., Rao, A., Hogan, P.G. (2006). Orai1 is an essential pore subunit of the CRAC channel. *Nature* **442**, 230-233.

Prasad, V., Okunade, G.W., Miller, M.L. and Shull, G.E. (2004). Phenotypes of SERCA and PMCA knockout mice. *Biochem Biophys Res Commun* 322, 1192-1203.

Protty, M.B., Watkins, N.A., Colombo, D., Thomas, S.G., Heath, V.L., Herbert, J., Bicknell, R., Senis, Y.A., Ashman, L.K., Berditchevski, F., Ouwehand, W.H., Watson, S.P., and Tomlinson, M.G. (2008) Identification of Tspan9 as a novel platelet tetraspanin and the collagen receptor GPVI as a component of tetraspanin microdomains. *Biochem J* **417**, 391-400.

Publicover, S.J., Harper, C.V. and Barratt, C. (2007). $[Ca^{2+}]_i$ signalling in sperm – making the most of what you've got. *Nat Cell Biol* **9**, 235-242.

Putney, J.W., Broad, L.M., Braun, F.J., Lievremont, J.P. and Bird, G.S. (2001). Mechanisms of capacitative calcium entry. *J Cell Sci* **114**, 2223-2229.

Qi, H., Moran, M.M, Navarro, B., Chong, J.A., Krapivinsky, G., Krapivinsky, L., Kirichok, Y., Ramsey, I.S., Quill, T.A., Clapham, D.E. (2007). All four CatSper ion channels proteins are required for male fertility and sperm cell hyperactivated motility. *Proc Natl Acad U S A* **104**, 1219-1223.

Quill, T.A., Ren, D., Clapham, D.E. and Garbers, D.L. (2001). A voltage-gated ion channel expressed specifically in spermatozoa. *Proc Natl Acad Sci U S A* **23**, 12527–12531.

Quill, T.A., Sugden, S.A., Rossi, K.L., Doolittle, L.K., Hammer, R.E. and Gabers, D. L. (2003). Hyperactivated sperm motility driven by CatSper2 is required for fertilization. *Proc Natl Acad Sci U S A* **25**, 14869-14874.

Rathi, R., Colenbrander, B., Bevers, M.M. and Gadella, B.M. (2001). Evaluation of in vitro capacitation of stallion spermatozoa. *Biol Reprod* **65**, 462-470.

Reeves, J.P. and Hale, C.C. (1984). The stoichiometry of the cardiac sodium-calcium exchange system. *J Biol Chem* **259**, 77333-7739.

Ren, D., Navarro, B., Perez, G., Jackson, A.C., Hsu, S., Shi, Q., Tilly, J.L. and Clapham, D.E. (2001). A sperm ion channel required for sperm motility and male fertility. *Nature* **413**, 603-609.

Retamal, M.A., Cortes, C.J., Reuss, L., Bennett, M.V., Saez, J.C. (2006). S-nitrosylation and Permeation through Connexin 43 Hemichannels in Astrocytes: Induction by Oxidant Stress and Reversal by Reducing Agents. *Pro Nat Acad Sci U S A* **103**, 4475-4480.

Revelli, A., Ghigo, D., Moffa, F., Massobrio, M., Tur-Kaspa, L. (2002).Guanylate cyclase activity and sperm function. *Endocrine Reviews* **23**, 484-494.

Roberts, M.L, Scouten, W.H. and Nyquist, S.E. (1976). Isolation and characterization of the cytoplasmic droplet in the rat. *Biol Reprod* **14**, 421-424

Roberts, S.J. (1986). Veterinary Obstetrics and Genital Diseases, 3rd edn. Stephen Roberts, Woodstock, VT.

Rockwell, P.L. and Storey, B.T. (2000). Kinetics of onset of mouse sperm acrosome reaction induced by solubilized zona pellucida: fluorimetric determination of loss of pH gradient between acrosomal lumen and medium monitored by dapoxyl (2-aminoethyl) sulfonamide and of intracellular Ca(2+) changes monitored by fluo-3. *Mol Reprod Dev* **55**, 335-349.

Rodriguez-Martinez, H., Ekstedt, E. and Einarsson, S. (1990). Acidification of epididymal fluid in the boar. *Int J Androl* **13**, 238-243.

Rodriguez-Martinez, H., Saravia, F., Wallgren, M., Tienthai, P., Johannisson, A., Vazquez, J.M. (2005). Boar spermatozoa in the oviduct. *Theriogenology* **63**, 514-535.

Roldan, E.R. and Murase, T. (1994). Polyphosphoinositide-derived diacylglycerol stimulates the hydrolysis of phosphatidylcholine by phospholipase C during exocytosis of the ram sperm acrosome. Effect is not mediated by protein kinase C. *J Biol Chem* **23**, 23583-23589.

Roldan, E.R. and Shi, Q.X. (2007). Sperm phospholipases and acrosomal exocytosis. *Front Biosci* **1**, 89-104.

Roos, J., DiGregorio, P.J., Yeromin, A.V., Ohlsen, K., Lioudyno, M., Zhang, S., Safina, O., Kozak, J.A. Wagner, S.L., Cahalan, M.D., Velicelebi, G., Stauderman, K.A. (2005). STIM1, an essential and conserved component of store-operated Ca2+ channel function. *J Cell Biol* **169**, 435-445.

Ronquist, G., and Brody, I. (1985). The prostasome its secretion and function in man. *Biochim Biophys Acta* **822**, 203-218.

Rossato, M., Di Virgilio F., Rizzuto R., Galeazzi C. and Foresta C. (2001). Intracellular calcium store depletion and acrosome reaction in human spermatozoa: role of calcium and plasma membrane potential. *Mol Hum Repro* **7,** 119-128.

Rowley, M. J., Teshima and F., Heller, C. G. (1970). Duration of transit of spermatozoa through the human male ductular system. *Fertil Steril* **21**, 390-396.

Rubinstein, E., Ziyyat, A., Prenant, M., Wrobel, E., Wolf, J.P., Levy, S., Le Naour, F. and Boucheix, C. (2006). Reduced fertility of female mice lacking CD81. *Dev Biol* **290**, 351-358.

Rufo, G.A., Schoff, P.K. and Lardy, H. A. (1984) Regulation of calcium content in bovine spermatozoa. *J.Biol Chem **259***, 2547-2552.

Salicioni, A.M., Platt, M.D., Wertheimer, E,V., Arcelay, E., Allaire, A., Sosnik, J. and Visconti, P.E. (2007). Signaling pathways involved in sperm capacitation. Soc *Reprod Fertil Suppl* **65**, 245-259.

San Agustin, J.T. and Witman, G.B. (1994). Role of cAMP in the reactivation of demembranated ram spermatozoa. *Cell Motil Cytoskeleton* **27**, 206-218.

Santella, L. and Kyozuka, K. (1997). Effects of 1-methyladenine on nuclear Ca^{2+} transients and meiosis resumption in starfish oocytes are mimicked by the nuclear injection of inositol 1,4,5-trisphosphate and cADP-ribose. *Cell Calcium* **22,** 11-20.

Sbracia, M., Sayme, N., Grasso, J., Vigue, L., and Huszar, G. (1996). Sperm function and choice of preparation media: comparison of Percoll and Accudenz discontinuous density gradients. *J Androl* **17**, 61-67.

Schindl, R., Bergsmann, J., Frischauf, I., Derler, I., Fahrner, M., Muik, M., Fritsch, R., Groschner, K. and Romanin, C. (2008). 2-aminoethoxydiphenyl borate alters selectivity of Orai3 channels by increasing their pore size. *J Biol Chem* **283**, 20261-20267

Shadan, S., James, P.S., Howes, E.A. and Jones, R. (2004). Cholesterol efflux alters lipid raft stability and distribution during capacitation of boar spermatozoa. *Biol Reprod* **71**, 253-265.

Shalet, S. (2009). Normal testicular function and spermatogenesis. *Pediatr Blood Cancer* **53**, 285-288.

Shin, D.M. and Muallem, S. (2008) Skeletal muscle dressed in SOCs. *Nat Cell Biol* **10**, 639-641.

Shriver, D.A., Rosenthale, M.E., Mckenzie, B.E., Weintraub, H.S. and McGuire, J.L. (1981). Loperamide. *Pharmacol Biochem Prop Drug Sub* **3**, 461-476.

Shuttleworth, T.J. and Migen, O. (2003). Calcium entry and the control of calcium oscillations. *Biochem Soc Trans* **31**, 916-919.

Si, Y. and Olds-Clarke, P. (2000). Evidence for the involvement of calmodulin in mouse sperm capacitation. *Biol Reprod* **62**, 1231-1239.

Skalhegg, B.S., Huang, Y., Su, T., Idzerda, R.L., McKnight, G.S. and Burton, K.A. (2002). Mutation of the Calpha subunit of PKA leads to growth retardation and sperm dysfunction. *Mol Endocrinol* **16**, 630-639.

Smyth, J.T., Dehaven W.I., Jones, B.F., Mercer, J.C., Trebak, M., Vazquez, G. and Putney, J.W. (2006). Emerging perspectives in store-operated Ca2+ entry: roles of Orai, Stim and TRP. *Biochim Biophys Acta* **11**, 1147-1160.

Smyth, J.T., Dehaven W.I., Bird, G.S. and Putney, J.W. (2008). Ca2+-store-dependent and –independent reversal of Stim1 localization and function. *J Cell Sci* **121**, 762-772.

Soboloff, J., Spassova, M. and Hewavitharana, T. (2006) STIM2 is an inhibitor of STIM1-mediated store-operated Ca2+ entry. *Curr Biol* 2006 **16**, 1465-1470.

Sobrero, A.J. and MacLeod, J. (1962). The immediate postcoital test. *Fertil Steril* **13**, 184-189.

Stamboulian, S., Moutin, M.J., Treves, S., Pochon, N., Grunwald, D., Zorzato, F., De Waard, M., Ronjat, M. And Arnoult, C. (2005). Junctate, an inositol 1,4,5-triphosphate receptor associated protein, is present in rodent sperm and binds TRPC2 and TRPC5 but not TRPC1 channels. *Dev Biol* **286**, 326-337.

Stathopulos, P.B., Zheng, L. and Ikura, M. (2009). Stromal interaction molecule (STIM) 1 and STIM2 calcium sensing regions exhibit distinct unfolding and oligomerization kinetics. *J Biol Chem* **284**, 728-732.

Stathopulos, P.B., Zheng, L. Li, G.Y., Plevin, M.J. and Ikura, M. (2008). Structural and mechanistic insights into STIM1-mediated initiation of store-operated calcium entry. *Cell* **135**, 110-122.

Stauss, C.R., Votta, T.J. and Surez, S.S. (1995). Sperm motility hyperactivation facilitates penetration of the hamster zona pellucida. *Biol Reprod* **53**, 1280-1285.

Stiber, J., Hawkins, A., Zhang, Z.S., Wang, S., Burch, J., Graham, V., Ward, C.C., Seth, M., Finch, E., Malouf, N. et al. (2008). STIM1 signalling controls store-operated calcium entry required for development and contractile function in skeletal muscle. *Nat Cell Biol* **10**, 688-697.

Storey, B.T. and Keyhani, E. (1973). Interaction of calcium ion with the mitochondria of rabbit spermatozoa. *FEBS Lett* **37**, 33-36.

Stowers, L., Holy, T.E., Meister, M., Dulac, C. and Koentges, G. (2002). Loss of sex discrimination and male-male aggression in mice deficient for TRP2. *Science* **295**, 1493-1500.

Strunker, T., Goodwin, N., Brenker, C., Kashikar, N.D., Weyand, I., Seifert, R. and Kaupp, U.B. (2011). The CatSper channel mediates progesterone-induced Ca2+ influx in human sperm. *Nature* **471**, 382-386.

Su, Y.H. and Vacquier, V.D. (2002). A flagella K^+ dependent Na^+/Ca^{2+} exchanger keeps Ca^{2+} low in sea urchin spermatozoa. *Proc Natl Acad Sci USA* **99**, 6743-6748.

Suarez, S.S. and Oliphant, G. (1982) The interaction of rabbit spermatozoa and serum complement proteins. *Biol Reprod* **27**, 473–483.

Suarez, S.S. and Osman, R.A. (1987). Initiation of hyperactivated flagella bending in mouse sperm within the female reproductive tract. *Biol Reprod* **36**, 1191-1198.

Suarez, S.S. and Dai, X. (1992). Hyperactivation enhances mouse sperm capacity for penetrating viscoelastic media. *Biol Reprod* **46**, 686-691.

Suarez, S.S., Ho, H.C. (2003). Hyperactivation of Mammalian Sperm. *Cell and Mol Biol* **49**, 351-356.

Suarez, S.S. and Pacey, A.A. (2006**).** Sperm transport in the female reproductive tract. *Hum Repro Update* **12**, 23-37.

Suarez, S.S. (2008). Control of hyperactivation in sperm. *Hum Repro Update* **14**, 467-457.

Sugawara, H., Kurosaki, M., Takata, M. And Kurosaki, T. (1997). Genetic evidence for involvement of type 1, type 2 and type 3 inositol 1,4,5-trisphosphate receptors in signal transduction through the B-cell antigen receptor. *EMBO* **16,** 3078-3088.

Sutovsky, P., Mandahar, G. and Schatten, G. (1999). Biogenesis of the centrosome during mammalian gametogenesis and fertilization. *Protoplasma* **206**, 249-262.

Sutovsky, P. and Mandahar, G. (2006). Mammalian spermatogenesis and sperm structure: anatomical and compartmental analysis. in *The Sperm Cell: Production, Maturation, Fertilization and Regeneration* (ed. C. de Jonge and C. Barratt), pp1-30. Cambridge, UK: Cambridge University Press.

Taylor, C.W., Genazzani, A.A. and Morris, S.A. (1999). Expression of inositol trisphosphate receptors. *Cell calcium* **26**, 237-251.

Tesarik, J. and Mendoza, C. (1993). Insights into the function of a sperm-surface progesterone receptor: evidence of ligand-induced receptor aggregation and the implication of proteolysis. *Exp Cell Res* **205,** 111-117.

Teves, M.E., Barbano, F., Guidobaldi, H.A., Sanchez, R., Miska, W. and Giojalas, L.C. (2006). Progesterone at the picomolar range is a chemoattractant for mammalian spermatozoa. *Fertil Steril* **86**, 745-749.

Therien, I., Soubeyrand, S. and Manjunath, **P**. (1997). Major proteins of bovine seminal plasma modulate sperm capacitation by high-density lipoprotein. *Biol Reprod* **57,** 1080-1088.

Tienthai, P., Johannisson, A. and Rodriguez-Martinez, H. (2004). Sperm capacitation in the porcine oviduct. *Anim Reprod Sci* **80**, 131–146.

Tomes, C.N., McMaster, C.R. and Saling, P.M. (1996). Activation of mouse sperm

phosphatidylinositol-4,5 bisphosphate-phospholipase C by zona pellucida is modulated by tyrosine phosphorylation. *Mol Reprod Dev* **43**, 196-204.

Toshimori, K., Higashi, R. and Oura, C. (1985). Distribution of intramembranous particles and filipin-sterol complexes in mouse sperm membranes: polyene antibiotic filipin treatment. *Am J Anat* **174**, 455-470.

Toshimori, K., Tanii, I., Araki, S. and Oura, C. (1992). Characterisation of the antigen ercognized by a monoclonal antibody MN9: unique transport pathway to the equatorial segment of sperm head during spermiogenesis. *Cell Tissue Res* **270**, 459-468.

Tovey, S.C., Godfrey, R.E., Hughes, P.J., Mezna, M., Minchin, S.D., Mikoshiba, K. and Michelangeli, F. (1997). Identification and characterization of inositol 1,4,5-trisphosphate receptors in rat testis. *Cell Calcium* **21**, 311-319.

Travis, A.J. and Kopf, G.S. (2002). The role of cholesterol efflux in regulating the fertilization potential of mammalian spermatozoa*, J Clin Invest* **110**, 731-736.

Trevino, C.L., Santi, C.M., Beltran, C., Hernandez-Cruz, A., Darszon, A. and Lomeli, H.. (1998). Localisation of inositol trisphosphate and ryanodine receptors during mouse spermatogenesis: possible functional implications, **6**, 159-172.

Trevino, C.L., Serrano, C.J., Beltran, C., Felix, R. and Darszon, A. (2001). Identification of mouse trp homologues and lipid rafts from spermatogenic cells and sperm. *FEBS Lett* **509,** 119-125.

Tulsiani, D.R., Zeng, H.T. and Abou-Haila, A. (2007). Biology of sperm capacitation: evidence for multiple signalling pathways. *Soc Reprod Fertil Suppl* **63**, 257-272.

Turner, R.M. (2006). Moving to the beat: a review of mammalian sperm motility regulation. *Reprod Fertil Dev* **18,** 25-38.

Verkleij, A.J., Zwaal, R.F., Roelofsen, B., Comfurius, P., Kastelijn, D., van Deenen, L.L. (1973). The asymmetric distribution of phospholipids in the human red cell membrane. A combined study using phospholipases and freeze-etch electron microscopy. *Biochim Biophys Acta* **323**, 178-193.

Vig, M., Peinelt, C., Beck, A., Koomoa, D.L., Rabah, D., Koblan-Huberson, M., Kraft, S., Turner, H., Fleig, A., Penner, R. and Kinet, J.P. (2006). CRACM1 is a plasma membrane protein essential for store-operated Ca2+ entry. *Science* **312**, 1220-1223.

Vijayaraghava, S. and Hoskins, D. (1990). Changes in the mitochondrial calcium influx and efflux properties are responsible for the decline in sperm calcium during epididymal maturation. *Mol Reprod Dev* **25**, 186-194.

Visconti, P.E. (2009). Understanding the molecular basis of sperm capacitation through kinase design. *Proc Natl Acad U S A* **106,** 667-668.

Visconti, P.E., Galantino-Homer, H., Moore, G.D., Bailey, J.L., Ning, X., Fornes, M. and Kopf, G.S. (1998). The molecular basis of sperm capacitation. *J Androl* **19**, 242-248.

Visconti, P.E., Moore, G.D., Bailey, J.L., Leclerc, P., Connors, S.A., Pan, D., Olds-Clarke, P. and Kopf, G.S. (1995). Capacitation of mouse spermatozoa. II. Protein tyrosine phosphorylation and capacitation are regulated by a cAMP-dependent pathway. *Development* **121**, 1139-1150.

Visconti, P.E., Ning, X., Fornes, M.W., Alvarez, J.G, Stein, P., Connors, S.A and Kopf, G.S. (1999). Cholesterol efflux-mediated signal transduction in mammalian sperm: cholesterol release signals an increase in protein tyrosine phosphorylation during mouse sperm capacitation. *Dev Biol* **214**, 429-443.

Visconti, P.E., Westbrook, V.A., Chertilhin, O., Demarco, I., Sleight, S. and Diekman, A.B. (2002). Novel signalling pathways involved in sperm acquisition of fertilizing capacity.

J Reprod Immunol **53**, 133-150.

Walensky, L.D. and Snyder, S.H. (1995). Inositol 1,4,5-trisphosphate receptors selectively localized to the acrosomes of mammalian sperm. *J Cell Biol* **130**, 857-869.

Wang, D., King, S.M., Quill, T.A., Doolittle, L.K. and Garbers, D.L. (2003). A new sperm-specific Na+/H+ exchanger required for sperm motility and fertility. *Nat Cell Biol* **5**, 1117–1122.

Wang, G., Moniri, N.H., Ozawa, K., Stamler, J.S., Daaka, Y. (2006). Nitric Oxide Regulates Endocytosis by S-Nitrosylation of Dynamin. *Pro Natl Acad Sci U S A* **103**, 1295-1300.

Wang, Y., Deng, X., Zhou, Y., Hendron, E., Mancarella, S., Ritchie, M.F, Tang, X. D., Baba, Y., Kurosakl, T., Morl, Y., Soboloff, J. and Gill, D.L. (2009). STIM protein coupling in the activation of Orai channels. *Pro Natl Acad Sci U S A* **106,** 7391-7396,

Ward, C.R., Storey, B.T. and Kopf, G.S. (1994). Selective activation of Gi1 and Gi2 in mouse sperm by the zona pellucida, the egg's extracellular matrix. *J Biol Chem* **269**, 13254-8.

Wassarman, P.M., Jovine, L. And Litscher, E.S. (2001). A profile of fertilization in mammals. *Nat Cell Biol* **3**, 59-64.

Weber, C.R., Piacentino, V., Margulies, K.B., Bers, D.M. and Houser, S.R. (2002). Calcium influx via I(NCX) is favoured in failing human ventricular myocytes. *Ann N Y Acad Sci* **976**, 478-479.

Wennemuth, G., Babcock, D.F. and Hille, B. (2003). Calcium clearance mechanisms of mouse sperm. *J Gen Physiol* **122**, 115-128.

Wictome, M., Henderson, Lee, A.G. and East, J.M. (1992). Mechanism of inhibition of the calcium pump of sarcoplasmic reticulum by thapsigargin. *Biochem J* **283**, 525-529.

Williams, K.M. and Ford, W.C. (2003). Effects of Ca-ATPase inhibitors on the intracellular calcium activity and motility of human spermatozoa. *Int J Androl* **26** 366-375.

Wissenback, U., Schroth, G., Philipp, S. and Flockerzi, V. (1998). Structure and mRNA expression of a bovine trp homologue related to mammalian trp2 transcripts. *FEBS Lett* **429**, 61-66.

Wu, M.M., Buchanan, J., Luik, R.M., Lewis, R.S. (2006). Ca2+ store depletion causes STIM1 to accumulate in ER regions closely associated with the plasma membrane. *J Cell Biol* **174**, 803-813.

Wuytack, F., Raeymaekers, L. And Missiaen, L. (2003). PMR1/SPCA Ca2+ pumps and the role of the Golgi apparatus as a Ca2+ store. *Pflugers Arch* **446**, 148-153.

Xia, J., Reigada, D., Mitchell, C.H. and Ren, D. (2007). CATSPER channel-mediated Ca2+ entry into mouse sperm triggers a tail-to-head propagation. *Biol Reprod* **77**, 551-559.

Xia, J. and Ren, D. (2009). The BSA-induced Ca2+ influx during sperm capacitation is CATSPER channel-dependent. *Reprod Biol Endocrinol* **27**, 119-128.

Xu, L., Cohn, A.H. and Meissner, G. (1993) Ryanodine sensitive calcium release channel from left ventricle, septum, and atrium of canine heart. *Cardiovasc Res* **27**, 1815-1819.

Xu, P., Lu, J., Li, Z., Yu, X., Chen, L. and Xu, T. (2006). Aggregation of STIM1 underneath the plasma membrane induces clustering of Orai1. *Biochem Biophys Res Commun* **350**, 969-976.

Yamano., S., Yamazaki, J., Irahara, M., Tokumara, A., Nakagawa, K., and Saito, H. (2004). Human spermatozoa capacitated with progesterone or a long incubation show accelerated internalization by an alkyl ether lysophospholipid. *Fertil Steril* **81**, 605-610.

Yang, Y. and Losclazo, J. (2005). S-nitrosoprotein formation and localization in endothelial cells. *Proc Natl Acad Sci U S A* **102**, 117-122.

Yanagimachi, R. (1994). Fertility of mammalian spermatozoa: its development and relativity. *Zygote* **2**, 271-272.

Yeromin, A.V., Zhang, S.L., Jiang, W., Yu, Y., Safina, O. and Cahalan, M.D. (2006). Molecular identification of the CRAC channel by altered ion selectivity in a mutant of Orai. *Nature* **443**, 226-229.

Yoshida, M., Ishikawa, M., Izumi, H., De Santis, R. and Morisawa, M. (2003). Store-operated calcium channel regulates the chemotactic behavior of ascidian sperm. *Proc Natl Acad U S A* **100** 149-154.

Yu, Y., Xu, W., Yi, Y.J., Sutovsky, P. and Oko, R. (2006). The extracellular protein coat of the inner acrosomal membrane is involved in zona pellucida binding and penetration during fertilization: Characterization of its most prominent polypeptide (IAM38). *Dev Biol* **1**, 32-43.

Yuan, J.P., Zeng, W., Dorwart, M.R., Choi, Y.J., Worley, P.F. and Muallem, S. (2009). SOAR and the polybasic STIM1 domains gate and regulate Orai channels. *Nat Cell Biol* **11,** 337-343.

Yudin, A.I., Hanson, F.W. and Katz, D.F. (1989). Human cervical mucus and its interaction with sperm : a fine-structural view. *Biol Reprod* **40**, 661-671.

Zalk, R., Lehnart, S.E. and Marks, A.R. (2007). Modulation of the ryanodine receptor and intracellular calcium. *Annu Rev Biochem* **76**, 367-385.

Zanetti, N. and Mayorga, L.S. (2009). Acrosomal swelling and membrane docking are required for hybrid vesicle formation during the human sperm acrosome reaction. *Biol Reprod* **81**, 396-405.

Zeng, Y., Clark, E.N. and Florman, H.M. (1995). Sperm membrane potential: hyperpolarization during capacitation regulates zona pellucida dependent acrosomal secretion. *Dev Biol* **171**, 554-563.

Zhang, S.L., Yu, Y., Roos, J., et al. (2005). STIM1 is a Ca^{2+} sensor that activates CRAC channels and migrates from the Ca^{2+} store to the plasma membrane. *Nature* **437**, 902-905.

Zhang, S.L., Yeromin, A.V., Zhang, X.H., Yu, Y., Safrina, O., Penna, A., Roos, J., Stauderman, K.A. And Cahalan, M.D. (2006). Genome-wide RNAi screen of Ca(2+) influx identifies genes that regulate Ca(2+) release-activated Ca(2+) channel activity. *Proc Natl Acad Sci U S A* **24**, 9357-9362.